

Modularity of Gridshells

An application to the modular segmentation of
timber geodesic gridshell domes

Master Thesis
Ilse van der Zwet

Delft University of Technology

This page intentionally left blank.

Modularity of Gridshells

An application to the modular segmentation of
timber geodesic gridshell domes

Master Thesis

by

Ilse van der Zwet

to obtain the degree of Master of Science
at the Delft University of Technology.

June, 2025

Faculty of Civil Engineering and Geosciences, Delft

Student number:	4698940	
Thesis committee:	Dr. F. Kavoura,	TU Delft, chair
	Dr. R. Oval,	TU Delft, 1st supervisor
	Dr.ir. H.R. Schipper,	TU Delft, 2nd supervisor
	Ir. J.R. de Jong,	ABT bv., company supervisor

Cover: Taiyuan Botanical Garden (©CreatAR)

This page intentionally left blank.

Preface

This thesis marks the conclusion of my master's degree in Civil Engineering at Delft University of Technology. Within the Structural Engineering track, I explored various aspects of the field, from structural design and material behaviour to sustainability and innovative construction methods. Over the past year, I delved into the world of gridshells and modularity.

Throughout my studies, I became fascinated by complex aesthetically building structures. The idea of designing such structures and tackling the challenges they present has always excited me. What makes this field even more rewarding is the possibility to contribute to a more environmentally responsible future. This thesis reflects both of these interests. It allowed me to explore the aesthetic and structural complexity of gridshells, while investigating how modularity and timber construction can support circularity and sustainability. The chance to make even a small contribution to a better environment, while working on a topic that truly inspires me, made working on this thesis an enjoyable experience.

This study would not have been possible without the support of my thesis committee. First of all, I would like to thank Robin for providing a topic that made me excited from the very beginning, and for all the valuable discussions throughout the process. I also truly appreciate your understanding of my circumstances and the flexibility around my planning. Next, I would like to thank Jorn for offering me the opportunity to conduct my thesis at ABT. Your understanding while I worked mostly from home, along with your insightful input during the design process, were of great value. I also want to thank Florentia and Roel for their constructive feedback and critical perspective during our progress meetings, which helped me refine my thesis further.

Finally, I am grateful to my family and friends for their ongoing support throughout my studies. Especially in the final years, their encouragement and reassurance meant a great deal to me.

This journey has been both challenging and rewarding, and I am grateful for everything I have learned. I am excited to carry these experiences with me into the future.

*Ilse van der Zwet
Delft, June 2025*

Abstract

Given the importance of modularity in structural design, understanding the performance of modular shell structures is essential for improving both circularity and construction efficiency in spatial structures. To enhance sustainability and aesthetics, timber gridshells can be used to integrate sustainable building materials with complex pattern topologies. Modularity not only contributes to circularity of building materials, but also eases assembly, reducing both cost and construction time. By investigating different segmentation strategies, their impact on structural behaviour and buildability can be identified. This knowledge supports the optimisation of modular gridshells, leading to more efficient construction solutions.

This research aims to explore optimal segmentation strategies for timber gridshells, considering structural behaviour, element reusability and the efficiency of production, assembly and transport. A timber geodesic gridshell dome serves as a case study, but the findings contribute to modularity of gridshells in general. The main research question is: **How can the modular segmentation of timber gridshells be designed to optimise their structural and construction efficiency?**

For this research a method is developed to generate modular gridshells and optimise their design by evaluating both structural performance and construction efficiency. The modular designs consist of pinned splice joints that longitudinally connect two beams of different modules. Various modular designs are created by defining the location of these intermodular joints, thereby determining the overall modular geometry in the structure. A structural analysis – including Finite Element Analysis (FEA) and cross sectional optimisation – gives understanding of the structural behaviour and the required material use. A construction analysis - focusing on quantity and variability of elements, joints and transport - provides insight into reusability and efficiency of production, assembly and transport. These two analyses are used to assess the overall performance of each design. A multi-objective comparative analysis is conducted to identify the most favourable designs based on project goals and stakeholder preferences.

Findings show that this modular approach improves assembly efficiency and the reusability of elements. It is particularly advantageous to choose a modular gridshell over a classic one when the primary design objective is reusability. However, certain drawbacks are also identified. The modular segmentation method negatively affects structural performance and increases material usage, primarily due to the use of pinned splice joints, which reduce overall stability. Additionally, applying modularity results in lower production and transport efficiency.

The results further indicate that larger modules improve structural stability and reduce the required material, due to fewer splice joints. Larger modules also result in higher assembly efficiency and reusability. However, increasing module sizes may exceed maximum transport size limits. It could also lead to a higher number of module types, reducing production and assembly efficiency. Furthermore, the module shape significantly influences the number of splice joints, underlining the importance of careful geometric consideration to minimise joint quantity. Additionally, increasing the rotational stiffness of splice joints could improve the structural performance and reduce the material usage.

In conclusion, it is crucial to consider project objectives and stakeholder interests in the structural design of a gridshell, in order to evaluate whether a modular design can achieve the desired overall performance more effectively than a classic gridshell. Moreover, this research concludes that modular gridshell designs perform best when:

- Module sizes are maximised within transport constraints;
- Module shapes are designed to minimise the number of splice joints;
- An increase in module size comes with a minimisation of number of module types.

In addition to these key design principles, suggestions for further research are proposed. It is suggested to assess the impact of rotational stiffness in splice joints on structural performance of a modular grid-shell in more detail, including focussing on assembly efficiency and demountability of joints. Besides this, it is proposed to explore whether this modular approach is suitable for various other grid patterns, shapes and variable materials. Furthermore, research on the potential of bending active beams instead of bending inactive beams, could contribute to the structural efficiency. Finally, alternative approaches for modular segmentation of gridshells should be explored, in which optimal modular shapes, such as triangles, are considered, together with their joint and assembly complexity.

Contents

Preface	ii
Abstract	iii
1 Introduction	1
1.1 Context	1
1.2 Problem statement	1
1.3 Research aim	2
1.4 Objectives and research questions	2
1.5 Scope	2
1.6 Thesis outline	3
2 Literature Review	4
2.1 Design aspects	4
2.2 Structural behaviour	5
3 Research Methodology	6
3.1 Methodological approach	6
3.2 Data collection	6
3.3 Preliminary study	9
3.4 Design of modular geodesic gridshell	9
3.5 Structural analysis	9
3.6 Construction analysis	9
3.7 Multi-objective comparative analysis	10
3.8 Validation of constraints	11
3.9 Evaluation	11
3.10 Material specific aspects	11
4 Preliminary study: Classic Geodesic Gridshell	12
4.1 Geometry of geodesic gridshell	12
4.2 Classic Geodesic Gridshell	13
4.3 Structural analysis	14
4.4 Construction analysis	22
4.5 Findings and discussion	23
5 Modular Geodesic Gridshell	24
5.1 Generation of modules	24
5.2 Modular designs	25
5.3 Structural analysis	29
5.4 Construction analysis	36
5.5 Multi-objective comparative analysis	37
5.6 Validation	44
5.7 Findings and discussion	44
6 Modular Geodesic Gridshell with Denser Grid	48
6.1 Preliminary study	48
6.2 Modular designs	49
6.3 Structural analysis	50
6.4 Construction analysis	55
6.5 Multi-objective comparative analysis	56
6.6 Validation	59
6.7 Findings and discussion	59

7 Discussion	61
7.1 Structural performance	61
7.2 Classic versus modular gridshells	62
7.3 Modular designs	63
7.4 Design selection	63
7.5 Grid density	64
8 Conclusion and Recommendations	67
8.1 Conclusion	67
8.2 Research limitations	69
8.3 Design recommendations	69
8.4 Recommendations for further research	69
References	71
A FEA results: Geodesic Gridshell	73
A.1 Assumptions and input	73
A.2 Numerical results	94
A.3 Axial stress & displacement plots	96
A.4 Results bar charts	114
A.5 Utilisation results after cross section optimisation	120
B FEA results: Geodesic Gridshell with Denser Grid	121
B.1 Assumptions and input	121
B.2 Numerical results	136
B.3 Axial stress & displacement plots	138
B.4 Results bar charts	144
B.5 Utilisation results after cross section optimisation	152
C ULS & SLS verification	153
C.1 ULS verification	153
C.2 SLS verification	157
D Transport analysis: Geodesic Gridshell	159
D.1 Preliminary Study: Classic Geodesic Gridshell	159
D.2 Design Option 1	160
D.3 Design Option 2	160
D.4 Design Option 3	161
D.5 Design Option 4	161
D.6 Design Option 5	161
D.7 Design Option 6	162
D.8 Design Option 7	163
D.9 Design Option 8	163
E Transport analysis: Geodesic Gridshell with Denser Grid	165
E.1 Preliminary Study: Classic Geodesic Gridshell	165
E.2 Design Option 1	166
E.3 Design Option 2	167
F Discarded Design Options: Geodesic Gridshell	168
F.1 Design Option 9	168
F.2 Design Option 10	168
F.3 Design Option 11	169
F.4 Design Option 12	169
F.5 Design Option 13	169
F.6 Design Option 14	170

List of Figures

3.1	Research methodology overview	7
4.1	Geodesic gridshell	12
4.2	Geodesic gridshell model	13
4.3	Geometric formation of structure, perspective view	13
4.4	Classic geodesic gridshell	14
4.5	Local coordinate system timber elements	14
4.6	Beam orientation	15
4.7	Pressure coefficients (Nederlands Normalisatie-instituut, 2011a)	16
4.8	Snow coefficients (Nederlands Normalisatie-instituut, 2019)	17
4.9	Linear elements in curved beams	19
4.10	Classic Geodesic Gridshell: FEA results, front view (20 m span, C30, 200x175 mm)	20
4.11	Classic Geodesic Gridshell: First buckling mode (ULS, 20 m span, C30, 200x175 mm)	21
5.1	Joint configuration	24
5.2	Joint with steel bolts and angled slotted-in steel plates (BASS joint) (Shu et al., 2020)	25
5.3	Hinged ridge joint with dowelled steel plate, end plate and hinge pin (Crocetti, 2016)	25
5.4	Geodesic Gridshell: Design Option 1	26
5.5	Geodesic Gridshell: Design Option 2	26
5.6	Geodesic Gridshell: Design Option 3	27
5.7	Geodesic Gridshell: Design Option 4	27
5.8	Geodesic Gridshell: Design Option 5	28
5.9	Geodesic Gridshell: Design Option 6	28
5.10	Geodesic Gridshell: Design Option 7	28
5.11	Geodesic Gridshell: Design Option 8	29
5.12	Joint orientation	29
5.13	Geodesic Gridshell: Displacement utilisation results (SLS, 20 m span, C30, 200x175 mm)	30
5.14	Geodesic Gridshell: cross-section utilisation results (ULS, 20 m span, C30, 200x175 mm)	30
5.15	Geodesic Gridshell: First buckling mode (ULS, 20 m span, C30, 200x175 mm)	31
5.16	Geodesic Gridshell: Buckling factor results (ULS, 20 m span, C30, 200x175 mm)	32
5.17	Geodesic Gridshell: Axial stress (ULS, 20 m span, C30, 200x175 mm)	33
5.18	Geodesic Gridshell: Normal forces diagram (ULS, 20 m span, C30, 200x175 mm)	34
5.19	Forces in a spherical dome due to self-weight (Hoogenboom, 2023)	34
5.20	Geodesic Gridshell: Material (20 m span)	35
5.21	Geodesic Gridshell: Construction analysis	37
5.22	Geodesic Gridshell: Comparative analysis	39
5.23	Geodesic Gridshell: Comparative analysis per design	40
5.24	Geodesic Gridshell: Design Option 4 and 8, front view	46
6.1	Geodesic gridshell with Denser Grid model	48
6.2	Benchmark: Classic geodesic gridshell with denser grid	49
6.3	Geodesic Gridshell with Denser Grid: Design Option 1	50
6.4	Geodesic Gridshell with Denser Grid: Design Option 2	50
6.5	Geodesic Gridshell with Denser Grid: Displacement utilisation (SLS, 20 m span, C30, 150x125 mm)	51
6.6	Geodesic Gridshell with Denser Grid: cross-section utilisation results (ULS, 20 m span, C30, 150x125 mm)	51
6.7	Geodesic Gridshell with Denser Grid: First buckling mode (ULS, 20 m span, C30, 150x125 mm)	52

6.8 Geodesic Gridshell with Denser Grid: Buckling factor results (ULS, 20 m span, C30, 150x125 mm)	53
6.9 Geodesic Gridshell with Denser Grid: Axial stress (ULS, 20 m span, C30, 150x125 mm)	53
6.10 Geodesic Gridshell with Denser Grid: Normal forces diagram (ULS, 20 m span, C30, 150x125 mm)	54
6.11 Geodesic Gridshell with Denser Grid: Material (20 m span)	55
6.12 Geodesic Gridshell with Denser Grid: Construction analysis	55
6.13 Geodesic Gridshell with Denser Grid: Comparative analysis	58
7.1 Geodesic Gridshell: Design Option 5	64
7.2 Geodesic Gridshell with Denser Grid: Design Option 2	64
7.3 Geodesic gridshells with different grid densities	64
7.4 Multi-Objective Comparative Analysis, radar charts	66
A.1 Geodesic gridshell top view	74
A.2 Geodesic gridshell front view	74
A.3 Classic Geodesic Gridshell: Axial stress (ULS, 20 m span, C30, 200x175 mm)	96
A.4 Classic Geodesic Gridshell: Displacement (SLS, 20 m span, C30, 200x175 mm)	97
A.5 Geodesic Gridshell: Axial stress, Design Option 1 (ULS, 20 m span, C30, 200x175 mm)	98
A.6 Geodesic Gridshell: Displacement, Design Option 1 (SLS, 20 m span, C30, 200x175 mm)	99
A.7 Geodesic Gridshell: Axial stress, Design Option 2 (ULS, 20 m span, C30, 200x175 mm)	100
A.8 Geodesic Gridshell: Displacement, Design Option 2 (SLS, 20 m span, C30, 200x175 mm)	101
A.9 Geodesic Gridshell: Axial stress, Design Option 3 (ULS, 20 m span, C30, 200x175 mm)	102
A.10 Geodesic Gridshell: Displacement, Design Option 3 (SLS, 20 m span, C30, 200x175 mm)	103
A.11 Geodesic Gridshell: Axial stress, Design Option 4 (ULS, 20 m span, C30, 200x175 mm)	104
A.12 Geodesic Gridshell: Displacement, Design Option 4 (SLS, 20 m span, C30, 200x175 mm)	105
A.13 Geodesic Gridshell: Axial stress, Design Option 5 (ULS, 20 m span, C30, 200x175 mm)	106
A.14 Geodesic Gridshell: Displacement, Design Option 5 (SLS, 20 m span, C30, 200x175 mm)	107
A.15 Geodesic Gridshell: Axial stress, Design Option 6 (ULS, 20 m span, C30, 200x175 mm)	108
A.16 Geodesic Gridshell: Displacement, Design Option 6 (SLS, 20 m span, C30, 200x175 mm)	109
A.17 Geodesic Gridshell: Axial stress, Design Option 7 (ULS, 20 m span, C30, 200x175 mm)	110
A.18 Geodesic Gridshell: Displacement, Design Option 7 (SLS, 20 m span, C30, 200x175 mm)	111
A.19 Geodesic Gridshell: Axial stress, Design Option 8 (ULS, 20 m span, C30, 200x175 mm)	112
A.20 Geodesic Gridshell: Displacement, Design Option 8 (SLS, 20 m span, C30, 200x175 mm)	113
A.21 Geodesic Gridshell: Reaction force results (Qualitative, 20 m span, C30, 200x175 mm)	114
A.22 Geodesic Gridshell: Nodal displacement results (SLS, 20 m span, C30, 200x175 mm)	114
A.23 Geodesic Gridshell: Beam displacement results (SLS, 20 m span, C30, 200x175 mm)	115
A.24 Geodesic Gridshell: Deformation energy results (Qualitative, 20 m span, C30, 200x175 mm)	115
A.25 Geodesic Gridshell: Axial-total deformation energy ratio results (Qualitative, 20 m span, C30, 200x175 mm)	115
A.26 Geodesic Gridshell: Stress results (ULS, 20 m span, C30, 200x175 mm)	116
A.27 Cross section normal force results: Geodesic Gridshell (ULS, 20 m span, C30, 200x175 mm)	116
A.28 Geodesic Gridshell: Cross section shear force results (ULS, 20 m span, C30, 200x175 mm)	116
A.29 Geodesic Gridshell: Cross section torsional moment results (ULS, 20 m span, C30, 200x175 mm)	117
A.30 Geodesic Gridshell: Cross section y-axis bending moment results (ULS, 20 m span, C30, 200x175 mm)	117
A.31 Geodesic Gridshell: Cross section z-axis bending moment results (ULS, 20 m span, C30, 200x175 mm)	117
A.32 Geodesic Gridshell: Nodal normal force, pinned joints results (ULS, 20 m span, C30, 200x175 mm)	118
A.33 Geodesic Gridshell: Nodal shear force, pinned joints results (ULS, 20 m span, C30, 200x175 mm)	118

A.34 Geodesic Gridshell: Nodal bending moment, pinned joints results (ULS, 20 m span, C30, 200x175 mm)	118
A.35 Geodesic Gridshell: Nodal normal force. rigid joints results (ULS, 20 m span, C30, 200x175 mm)	119
A.36 Geodesic Gridshell: Nodal shear force, rigid joints results (ULS, 20 m span, C30, 200x175 mm)	119
A.37 Geodesic Gridshell: Nodal bending moment, rigid joints results (ULS, 20 m span, C30, 200x175 mm)	119
B.1 Geodesic Gridshell with Denser Grid top view	121
B.2 Geodesic Gridshell with Denser Grid front view	122
B.3 Classic Geodesic Gridshell with Denser Grid: Axial stress (ULS, 20 m span, C30, 150x125 mm)	138
B.4 Classic Geodesic Gridshell with Denser Grid: Displacement (SLS, 20 m span, C30, 150x125 mm)	139
B.5 Geodesic Gridshell with Denser Grid: Axial stress, Design Option 1 (ULS, 20 m span, C30, 150x125 mm)	140
B.6 Geodesic Gridshell with Denser Grid: Displacement, Design Option 1 (SLS, 20 m span, C30, 150x125 mm)	141
B.7 Geodesic Gridshell with Denser Grid: Axial stress, Design Option 2 (ULS, 20 m span, C30, 150x125 mm)	142
B.8 Geodesic Gridshell with Denser Grid: Displacement, Design Option 2 (SLS, 20 m span, C30, 150x125 mm)	143
B.9 Geodesic Gridshell with Denser Grid: Reaction force results (Qualitative, 20 m span, C30, 150x125 mm)	144
B.10 Geodesic Gridshell with Denser Grid: Nodal displacement results (SLS, 20 m span, C30, 150x125 mm)	144
B.11 Geodesic Gridshell with Denser Grid: Beam displacement results (SLS, 20 m span, C30, 150x125 mm)	145
B.12 Geodesic Gridshell with Denser Grid: Deformation energy results (Qualitative, 20 m span, C30, 150x125 mm)	145
B.13 Geodesic Gridshell with Denser Grid: Axial-total deformation energy ratio results (Qualitative, 20 m span, C30, 150x125 mm)	146
B.14 Geodesic Gridshell with Denser Grid: Stress results (ULS, 20 m span, C30, 150x125 mm)	146
B.15 Geodesic Gridshell with Denser Grid: Cross section normal force results (ULS, 20 m span, C30, 150x125 mm)	147
B.16 Geodesic Gridshell with Denser Grid: Cross section shear force results (ULS, 20 m span, C30, 150x125 mm)	147
B.17 Geodesic Gridshell with Denser Grid: Cross section torsional moment results (ULS, 20 m span, C30, 150x125 mm)	148
B.18 Geodesic Gridshell with Denser Grid: Cross section y-axis bending moment results (ULS, 20 m span, C30, 150x125 mm)	148
B.19 Geodesic Gridshell with Denser Grid: Cross section z-axis bending moment results (ULS, 20 m span, C30, 150x125 mm)	149
B.20 Geodesic Gridshell with Denser Grid: Nodal normal force, pinned joints results (ULS, 20 m span, C30, 150x125 mm)	149
B.21 Geodesic Gridshell with Denser Grid: Nodal shear force, pinned joints results (ULS, 20 m span, C30, 150x125 mm)	150
B.22 Geodesic Gridshell with Denser Grid: Nodal bending moment, pinned joints results (ULS, 20 m span, C30, 150x125 mm)	150
B.23 Geodesic Gridshell with Denser Grid: Nodal normal force. rigid joints results (ULS, 20 m span, C30, 150x125 mm)	151
B.24 Geodesic Gridshell with Denser Grid: Nodal shear force, rigid joints results (ULS, 20 m span, C30, 150x125 mm)	151
B.25 Geodesic Gridshell with Denser Grid: Nodal bending moment, rigid joints results (ULS, 20 m span, C30, 150x125 mm)	152

F.1	Geodesic Gridshell: Design Option 9	168
F.2	Geodesic Gridshell: Design Option 10	168
F.3	Geodesic Gridshell: Design Option 11	169
F.4	Geodesic Gridshell: Design Option 12	169
F.5	Geodesic Gridshell: Design Option 13	169
F.6	Geodesic Gridshell: Design Option 14	170

List of Tables

4.1	Results load combinations	18
4.2	Classic Geodesic Gridshell: Structural analysis results (ULS, 20 m span)	22
4.3	Classic Geodesic Gridshell: Construction analysis results	23
5.1	Geodesic Gridshell: Required cross-sections (20 m span)	35
5.2	Splice joint rotational stiffness variation results, Design Option 5 (ULS, 20 m span, C30)	36
5.3	Geodesic Gridshell: Construction analysis	36
5.4	Geodesic Gridshell: Structural and construction results	38
5.5	Geodesic Gridshell: Multi-objective scores	38
5.6	Weight distribution: Cost	41
5.7	Geodesic Gridshell: Objective function ranking Cost	41
5.8	Weight distribution: Sustainability	42
5.9	Geodesic Gridshell Objective function ranking Sustainability	42
5.10	Weight distribution: Time	42
5.11	Geodesic Gridshell: Objective function ranking Time	43
5.12	Weight distribution: Cost + Sustainability	43
5.13	Geodesic Gridshell: Objective function ranking Cost + Sustainability	43
5.14	Relative change C_o : Classic geodesic gridshell to modular geodesic gridshell	44
5.15	Material impact $\epsilon_{m,o}$: Classic geodesic gridshell to modular geodesic gridshell	44
6.1	Classic Geodesic Gridshell with Denser Grid: Construction analysis results	49
6.2	Geodesic Gridshell with Denser Grid: Required cross-sections (20 m span)	54
6.3	Geodesic Gridshell with Denser Grid: Construction analysis	55
6.4	Geodesic Gridshell with Denser Grid: Structural and construction results	56
6.5	Geodesic Gridshell with Denser Grid: Multi-objective scores	57
6.6	Geodesic Gridshell with Denser Grid: Objective function ranking Cost	58
6.7	Geodesic Gridshell with Denser Grid: Objective function ranking Sustainability	59
6.8	Geodesic Gridshell with Denser Grid: Objective function ranking Time	59
6.9	Geodesic Gridshell with Denser Grid: Objective function ranking Cost + Sustainability	59
7.1	Relative changes when choosing modularity over classic design	62
A.1	Geodesic gridshell: Node coordinates, Classic	75
A.2	Geodesic gridshell: Node coordinates, Design Option 1 (1/2)	76
A.3	Geodesic gridshell: Node coordinates, Design Option 1 (2/2)	77
A.4	Geodesic gridshell: Node coordinates, Design Option 2 (1/2)	78
A.5	Geodesic gridshell: Node coordinates, Design Option 2 (2/2)	79
A.6	Geodesic gridshell: Node coordinates, Design Option 3 (1/2)	80
A.7	Geodesic gridshell: Node coordinates, Design Option 3 (2/2)	81
A.8	Geodesic gridshell: Node coordinates, Design Option 4 (1/2)	82
A.9	Geodesic gridshell: Node coordinates, Design Option 4 (2/2)	83
A.10	Geodesic gridshell: Node coordinates, Design Option 5 (1/2)	84
A.11	Geodesic gridshell: Node coordinates, Design Option 5 (2/2)	85
A.12	Geodesic gridshell: Node coordinates, Design Option 6 (1/2)	86
A.13	Geodesic gridshell: Node coordinates, Design Option 6 (2/2)	87
A.14	Geodesic gridshell: Node coordinates, Design Option 7 (1/2)	88
A.15	Geodesic gridshell: Node coordinates, Design Option 7 (2/2)	89
A.16	Geodesic gridshell: Node coordinates, Design Option 8 (1/2)	90
A.17	Geodesic gridshell: Node coordinates, Design Option 8 (2/2)	91

A.18	Strength properties C30 timber	92
A.19	Geodesic Gridshell: Support coordinates	92
A.20	Geodesic Gridshell: Support conditions	92
A.21	Classic Geodesic Gridshell: Joint conditions, pinned nodes	93
A.22	Modular Geodesic Gridshell: Joint conditions, rigid nodes	93
A.23	Modular Geodesic Gridshell: Joint conditions, splice joints	93
A.24	Geodesic Gridshell: FEA results (1/2) (20 m span, C30, 200x175 mm)	94
A.25	Geodesic Gridshell: FEA results (2/2) (20 m span, C30, 200x175 mm)	95
A.26	Geodesic Gridshell: FEA utilisation results after cross section optimisation (20 m span)	120
B.1	Geodesic Gridshell with Denser Grid: Node coordinates, Classic (1/2)	123
B.2	Geodesic Gridshell with Denser Grid: Node coordinates, Classic (2/2)	124
B.3	Geodesic Gridshell with Denser Grid: Node coordinates, Design Option 1 (1/4)	125
B.4	Geodesic Gridshell with Denser Grid: Node coordinates, Design Option 1 (2/4)	126
B.5	Geodesic Gridshell with Denser Grid: Node coordinates, Design Option 1 (3/4)	127
B.6	Geodesic Gridshell with Denser Grid: Node coordinates, Design Option 1 (4/4)	128
B.7	Geodesic Gridshell with Denser Grid: Node coordinates, Design Option 2 (1/5)	129
B.8	Geodesic Gridshell with Denser Grid: Node coordinates, Design Option 2 (2/5)	130
B.9	Geodesic Gridshell with Denser Grid: Node coordinates, Design Option 2 (3/5)	131
B.10	Geodesic Gridshell with Denser Grid: Node coordinates, Design Option 2 (4/5)	132
B.11	Geodesic Gridshell with Denser Grid: Node coordinates, Design Option 2 (5/5)	133
B.12	Geodesic Gridshell with Denser Grid: Support coordinates	135
B.13	Geodesic Gridshell with Denser Grid: FEA results (1/2) (20 m span, C30, 150x125 mm)	136
B.14	Geodesic Gridshell with Denser Grid: FEA results (2/2) (20 m span, C30, 150x125 mm)	137
B.15	Geodesic Gridshell with Denser Grid: FEA utilisation results after cross section optimisation (20 m span)	152
C.1	Classic Geodesic Gridshell: Cross-sectional properties	153
C.2	Strength properties C30 timber	153
C.3	Classic Geodesic Gridshell: Resulting forces	154
C.4	Classic Geodesic Gridshell: Resulting displacement	157
D.1	Classic Geodesic Gridshell: Transport sizes	159
D.2	Classic Geodesic Gridshell: Transport truck capacity	159
D.3	Classic Geodesic Gridshell: Transport arrangement	159
D.4	Geodesic Gridshell: Transport sizes, Design Option 1	160
D.5	Geodesic Gridshell: Transport truck capacity, Design Option 1	160
D.6	Geodesic Gridshell: Transport arrangement, Design Option 1	160
D.7	Geodesic Gridshell: Transport sizes, Design Option 2	160
D.8	Geodesic Gridshell: Transport truck capacity, Design Option 2	160
D.9	Geodesic Gridshell: Transport arrangement, Design Option 2	161
D.10	Geodesic Gridshell: Transport sizes, Design Option 3	161
D.11	Geodesic Gridshell: Transport sizes, Design Option 4	161
D.12	Geodesic Gridshell: Transport sizes, Design Option 5	161
D.13	Geodesic Gridshell: Transport truck capacity, Design Option 5	162
D.14	Geodesic Gridshell: Transport arrangement, Design Option 5	162
D.15	Geodesic Gridshell: Transport sizes, Design Option 6	162
D.16	Geodesic Gridshell: Transport truck capacity, Design Option 6	162
D.17	Geodesic Gridshell: Transport arrangement, Design Option 6	162
D.18	Geodesic Gridshell: Transport sizes, Design Option 7	163
D.19	Geodesic Gridshell: Transport truck capacity, Design Option 7	163
D.20	Geodesic Gridshell: Transport arrangement, Design Option 7	163
D.21	Geodesic Gridshell: Transport sizes, Design Option 8	163
D.22	Geodesic Gridshell: Transport truck capacity, Design Option 8	164
D.23	Geodesic Gridshell: Transport arrangement, Design Option 8	164
E.1	Classic Geodesic Gridshell with Denser Grid: Transport sizes	165

E.2	Classic Geodesic Gridshell with Denser Grid: Transport truck capacity	166
E.3	Classic Geodesic Gridshell with Denser Grid: Transport arrangement	166
E.4	Geodesic Gridshell with Denser Grid: Transport sizes, Design Option 1	166
E.5	Geodesic Gridshell with Denser Grid: Transport sizes, Design Option 2	167
E.6	Geodesic Gridshell with Denser Grid: Transport truck capacity, Design Option 2	167
E.7	Geodesic Gridshell with Denser Grid: Transport arrangement, Design Option 2	167

Introduction

1.1. Context

Given the importance of modularity in structural design, understanding the behaviour of modular structures is essential for contributing to a circular building environment and improving the efficiency of construction. Modularity improves the demountability of structures, which positively contributes to the reusability of elements and circularity of materials. Also, by using prefabricated modules, the assembly of structures is simplified, saving both cost and time. Implementation of modularity in shell structures is a rising topic and given the essence of using sustainable building materials, maximising the use of timber as a structural building material in combination with modularity in shell structures is essential. Timber gridshells can enhance the building aesthetics, using complex pattern topologies as a structure.

The Timber Lazo gridshell dome project of de Mingo García and Martín (2021) is an example of this and focuses on the structural behaviour of timber shell crafts, like *Carpintería de lo blanco*. Their project investigates how the timber crafts can serve as a structural element, beyond their traditional ornamental use.

According to Wang et al. (2024), stability is the main design criterion for gridshells, as a single-layer gridshell is mostly based on compression and therefore susceptible to global buckling. The stability of a gridshell is dependent on multiple aspects, such as the joint rotational stiffness (Tomei, 2023) and the boundary conditions (Tomei, 2023; Venuti & Bruno, 2018). Besides this, the geometry also influences the structural behaviour (López et al., 2007; Wan et al., 2024), for example the angles between members and the slenderness of members, but also parameters such as the normal curvature, geodesic curvature and geodesic torsion (Schling & Barthel, 2020; Wan et al., 2024), which describe the type of shell structure, i.e. geodesic, pseudo-geodesic or asymptotic. Another type of shell structure is a reciprocal frame structure, where short members rest on each other, causing shear forces (Popovic Larsen, 2014).

Gridshells can be built modularly of timber elements. Possible shapes of the gridshell are influenced by the load path and the structural behaviour. Consequently, design aspects such as the geometry, the boundary conditions, the shape of the modules and the design of both the joints within the modules, along with their semi-rigid stiffness, and the hinges between the different modules influence the design of the structure.

Another important aspect of a gridshell is its feasibility for construction and its financial feasibility. Repetition of building elements plays a significant role in simplifying the fabrication process of building parts and to save costs and time (Schling & Barthel, 2020). In timber gridshells, repetition could be implemented in multiple ways, for example by minimising the number of different joints within modules by designing the modules in such a way that the variety in joint stiffness is minimised. Besides the design of joints, repetition of the timber members could also be a design goal. This could be done by minimising the variety in dimensions of members.

Besides using a sustainable material for gridshells, the amount of material use in the design of a gridshell is important to consider. Additionally, circularity is another important sustainability aspect, which can be described by the demountability and reusability of elements.

1.2. Problem statement

The construction of timber gridshells is complex, due to their doubly-curved geometry (Koronaki et al., 2020). Additionally, using an intricate pattern into the gridshell's geometry further increases this

complexity. However, modularity can simplify the construction process, thus saving both costs and time.

Optimising construction efficiency by minimising the number of prefabricated modular elements that need to be constructed on-site, as well as optimising feasibility to assemble the gridshell with little temporary support are other ways of saving costs and time. From a sustainability perspective, it is beneficial to consider the reusability of structural elements, which is mainly affected by the demountability of joints. Additionally, the ability to efficiently transport the prefabricated modules, which is determined by the ability to stack the modules efficiently, is another important sustainability and financial aspect.

Exploring different segmentation strategies could lead to different distributions of weak joints versus stiff joints across a gridshell, thereby affecting its structural behaviour and consequently the design of the modules with respect to aspects such as the joint stiffness and the timber cross-sections. However, limited possibilities for segmenting the gridshell into modules are investigated and the impact of different module segmentations on the structural behaviour of a timber gridshell remains unexplored.

1.3. Research aim

The research gap leads to the aim of this research, which is to investigate the best possibilities for segmenting a timber gridshell into modules, while considering the structural behaviour, the reusability of elements and the efficiency of production, assembly and transport. Aiming to use a bottom-up approach, this research uses a geodesic timber gridshell as a case study, with the potential for application to gridshells in general, such as the Timber Lazo Gridshell or steel gridshells.

1.4. Objectives and research questions

The aim of this research is supported by the following objectives:

- Evaluating the potential of modular design to enhance the economic and environmental sustainability of timber gridshell construction;
- Assessing the impact of modular segmentation on the structural performance and construction efficiency of timber gridshells;
- Evaluating modular timber gridshell designs through a multi-objective analysis of structural performance, sustainability, and construction efficiency.

These objectives lead to the following main research question of this thesis:

How can the modular segmentation of timber gridshells be designed to optimise their structural and construction efficiency?

To answer the main research question, the following subquestions are formulated:

1. What are the key aspects of the structural design of a timber gridshell?
2. What parameters mainly influence the structural behaviour of a timber gridshell, and how?
3. How can a modular gridshell be generated in terms of the geometrical design of modules and the allocation of joints?
4. How does the design of modular segmentation influence the structural performance of a timber gridshell?
5. How can modular segmentations be designed to optimise the structural performance and maximise the reusability of elements, as well as the efficiency of production, assembly and transport?

1.5. Scope

This research aims to find the most optimal modular design of a timber geodesic gridshell, while considering structural performance, reusability of elements, as well as the efficiency of production, assembly and transport.

Given that the gridshell modules are fabricated off-site and assembled on-site, the transport efficiency aspect focuses on maximising the use of transportation volume by efficiently stacking the modules. The reusability aspect focuses on the ability to deconstruct the structure, which affects the ability

to reuse the elements. The production and assembly aspects concern the efficiency with which the off-site fabricated modules can be produced and assembled on-site. Additionally, it considers the assembly efficiency and its feasibility to assemble the gridshell with as little support as possible.

To mainly focus on how to segment the structure into modules and its effect on multiple aspects, the scope of this research is also defined by constraints. The design of a modular gridshell is based on roughly three aspects: the analytical shape of the structure, the pattern topology and the module segmentation. In this research the only variable of these three aspects is the module segmentation, meaning that the gridshell's shape and pattern are constrained. The study focuses on a hemispherical shape. A geodesic pattern topology is used, based on triangular shapes.

Moreover, as mentioned above, the number of different joints and cross-sections is constrained. This research considers two types of joints: a joint with stiffness, which could be glued or a combination of bolts and screws, and a hinge, which is used in the intersections between modules. Additionally, the cross-sectional variation is constrained and it is preferred to use a single cross-section for all timber elements in one modular design.

In addition to these constraints, several aspects are variable during the design and optimisation process, based on the structural behaviour of the different segmentations. These variables include the dimension and shape of the modules, the distribution of the different joint types together with their stiffnesses, and the cross-section of the timber elements. In subsection 3.2.2 these parameters and their implementation in the optimisation are discussed further.

This research is an application to gridshells, more specifically to timber geodesic gridshells. However, this research contributes to the modular and circular design of shells and spatial structures in general.

1.6. Thesis outline

This thesis is structured into several chapters. In chapter 2, a literature review is provided, focusing on construction aspects and structural behaviour relevant to timber gridshells. The research methodology is outlined in chapter 3.

The application of the research is presented in chapter 4, chapter 5 and chapter 6. A preliminary study of a geodesic gridshell is introduced in chapter 4, followed by the modular segmentation in chapter 5. Next, chapter 6 investigates a geodesic gridshell with a denser grid.

The results and findings are discussed in chapter 7. Finally, in chapter 8 the conclusions of the research are presented, along with research limitations and recommendations for design and further research.

2

Literature Review

This chapter presents a review of existing literature on gridshells and modular structures. It examines key design considerations, key aspects that influence the structural behaviour of gridshells and strategies for optimising modular designs.

2.1. Design aspects

Designing a gridshell includes multiple key considerations. Various factors influence the structural behaviour, material usage, construction feasibility, financial feasibility, and sustainability of the structure. This section gives an overview of the most important aspects to consider when designing a gridshell.

Stability

As mentioned in section 1.1, the stability is a crucial aspect (Wang et al., 2024). Since stability can be the determining factor in design, it is important to consider the effect of joint rotational stiffness (Tomei, 2023). Joints can be hinged, semi-rigid or rigid, largely influencing the global stability of the structure. Additionally, boundary conditions play an important role in buckling behaviour and can be either stiffened or non-stiffened. Stability and other main factors affecting the structural behaviour are further discussed in section 2.2.

Geometry

Geometry of the gridshell is another important aspect. The grid consists of beams, which have specific lengths, curvatures and torsion, as well as the nodes, where the beams intersect at different angles (Schling & Barthel, 2020). Together, these elements form the mesh of the grid.

One approach to defining the grid's geometry is through geodesic technology. Geodesic domes are created by subdividing a spherical surface into smaller shapes, typically triangles, based on an icosahedron (Stasi, 2022). Geodesic curves follow the shortest path between two points on the structure's surface (Schling et al., 2017). According to Stasi (2022), designing the mesh in a repetitive pattern improves structural efficiency, simplifies production and improves aesthetics.

The shape and curvature of the gridshell's surface are also crucial geometrical considerations (Schling & Barthel, 2020). These factors affect both the structural performance of and the aesthetics.

Bending active or bending inactive

The type of gridshell significantly affects its properties and structural behaviour. The structure can be classified as either bending active or bending inactive. A bending active gridshell consists of initially straight beams that are elastically deformed to achieve the desired curvature (Roig et al., 2022). In such structures, the primary loads arise from the bending stresses that occur during construction, where the beams are actively bent (Roig et al., 2022).

In contrast, bending inactive gridshells use beams that do not require deformation to achieve their final shape (Collins & Cosgrove, 2016). These beams can be either curved or straight.

Modularity

Incorporating modularity in structures can significantly improve construction and financial feasibility. Regarding modularity in gridshells, Kuda and Petříčková (2021) suggest that the default network of a modular gridshell should be based on triangular modules, as they improve stability and allow for more design flexibility. However, they also note that triangular modules can result in complex joints designs. Therefore, when considering modular gridshells, it is important to consider the effect on joint complexity on the overall feasibility of the structure.

2.2. Structural behaviour

The structural behaviour of gridshells is influenced by numerous factors. This section discusses the main factors influencing the behaviour of gridshells identified in literature.

In a research on the effect of joint stiffness on optimising design strategies for gridshells, Tomei (2023) found that the susceptibility to global buckling of a gridshell is primarily related to the global stiffness of the gridshell, which is mainly determined by the joint stiffness, the boundary conditions and the presence of imperfections. Similarly, Venuti and Bruno (2018) and Venuti (2021) state that the joint stiffness, the boundary conditions and the geometrical and mechanical imperfections are the main factors influencing the buckling behaviour. They specify that the boundary stiffness depends on the moment of inertia and the area of elements, both being cross-sectional properties. Additionally, they say that the Gaussian curvature and the grid topology affect the behaviour.

Research specifically focussed on timber gridshells that are cable-braced, conducted by Wang et al. (2024) explores different influences on the structural behaviour. They state that the stability is the main design criterion, since a single-layer gridshell is a compression-based system and therefore particularly susceptible to global buckling. They observed that improving the boundary stiffness and joint stiffness positively influences the system's stability. Additionally, they noted that imperfections reduce the global stability and that the positive imperfections are always less advantageous than the negative imperfections.

López et al. (2007) investigated the buckling loads of semi-rigidly jointed single-layer latticed domes and explained that buckling can appear in various ways, including member buckling, node instability, line instability and general instability. They observed that dome geometry, member slenderness, joint rigidity and load hypothesis influence the structural behaviour of a single-layer spherical dome. According to Schling and Barthel (2020), important geometric parameters include node angles (intersection angles, normal angles, geodesic angles and torsion angles), edge parameters (edge length, normal curvature, geodesic curvature and geodesic torsion) and face parameters (the face shape, gaussian curvature and planarity).

Wan et al. (2024) studied the influence of three parameters on the structural behaviour of an asymptotic geodesic hybrid timber gridshell and concluded that a non-polar array layout arrangement negatively influences the behaviour. They also found that the rotational stiffness of the joints has minimal impact on the structural behaviour, indicating that the joints do not have to be rigid. Lastly, they concluded that the support condition has a crucial role in the force transfer and stiffness.

Based on this literature, the main factors affecting the structural behaviour of a gridshell are the:

- Joint stiffness;
- Boundary conditions/stiffness;
- Imperfections;
- Slenderness of members;
- cross-sectional properties: moment of inertia, area;
- Geometry: node angles, member lengths, (gaussian) curvature, geodesic torsion, face shape, planarity;
- Grid topology;
- Load conditions.

3

Research Methodology

This research aims to design and optimise the modular segmentation of timber gridshells, while considering the structural behaviour, the reusability of elements, as well as the efficiency of production, assembly and transport. This chapter discusses the methodology of this research, based on the research questions outlined in chapter 1.

3.1. Methodological approach

This section provides an overview of the methodological approach and the software that is used in this study. The approach is applied to a timber geodesic gridshell, which means that the structure's pattern is only made out of triangles. The research serves as a guide for other gridshells, for example, the Timber Lazo Gridshell, the structure of which has a more complex pattern, or gridshells made out of other materials.

3.1.1. Overview

Figure 3.1 shows the process of investigating the optimal module segmentation. The process begins with data collection and analysis on a classic geodesic gridshell, which serves as a reference structure. After this, different modular segmentation options are designed. Subsequently, multiple analyses are applied to the classic geodesic gridshell and the design options, followed by a multi-objective comparative analysis, which selects the most optimal design. The following paragraphs discuss the details of the methodology.

3.1.2. Software

To execute this approach, software able to parameterise and optimise the design of the gridshell is required. Grasshopper® (McNeel & Associates, 2024) and Karamba3D (Preisinger, 2013), running within the Rhino® (McNeel & Associates, 2024) environment, is used for this purpose.

3.2. Data collection

First of all, data is collected, serving as an input for the design and optimisation. The data consists of two parts, data that is constrained and data that is variable. The latter consists of the parameters in the optimisation. Both are discussed below.

3.2.1. Constraints

As discussed in section 1.5, this research has some constraints, which also serve as an input for the design and optimisation. First of all, several constraints are made regarding the design of the gridshell. Secondly, some constraints are made based on the performance and execution of the structure. All constraints are discussed below.

Analytical shape and geometry

The structure's shape is a hemisphere, with a constrained radius. The span is therefore also constrained. Additionally, the pattern topology is constrained. It is based on triangular shapes, which all have the same dimensions.

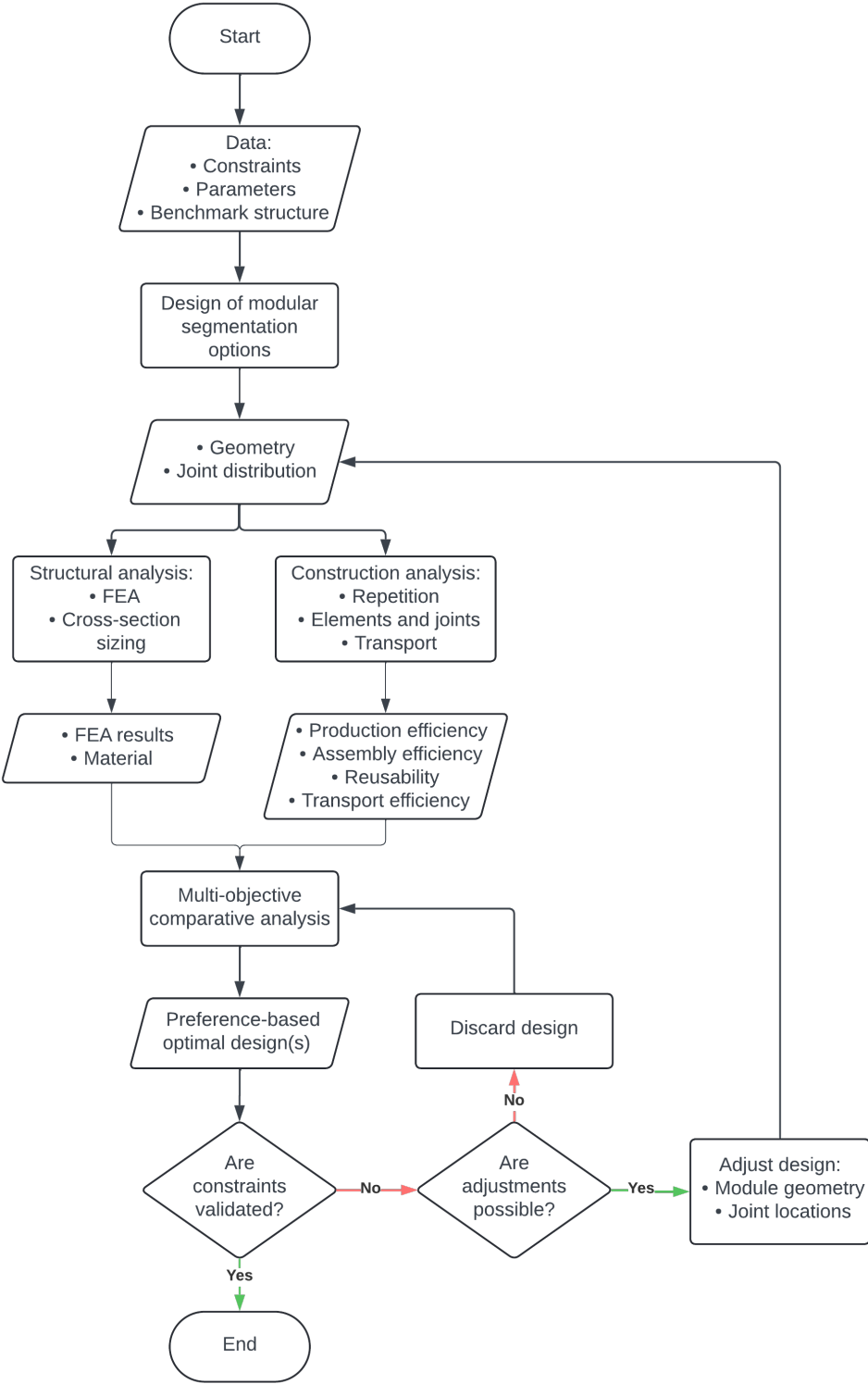


Figure 3.1: Research methodology overview

Joint types

Another constraint is the number of different joints that can be used in the gridshell. Hinges, with zero rotational stiffness in one direction serve as inter-module joints, to connect all modules together. The intra-module joints, which are present within modules, are infinitely rigid.

Single cross-section

To completely focus on the effect of different modular segmentations on the performance of a structure, only one cross-section for the timber elements is used across the entire structure. However the cross-section can vary between different design options, depending on their structural performance.

Structural performance

The utilisation of the gridshell's strength should be lower than 1, as well as the utilisation of the stability and deflections.

Transportation

Regarding the transportation of the structure, the module size is constrained to a maximum to ensure that the bounding box of each module fits within a lorry. Additionally, the maximum dimensions of the stacked modules must also fit within a lorry's dimensions.

3.2.2. Parameters

In addition to the constraints, the optimisation process includes several parameters that are variable and are adjusted to achieve the best outcome of the optimisation. section 2.2 discusses the main factors that influence a gridshell's structural behaviour. Several of these are not used as a parameter, as explained below.

First of all, the boundary stiffness of a gridshell is an important aspect. Since the modules are connected through hinges, the boundaries of the modules are automatically pinned as well. This also holds for the boundary of the outer modules in the gridshell. The boundary conditions are therefore not parameters in the optimisation.

Imperfections are not entirely controllable by the design. They can occur from material flaws or during fabrication and assembly. Since imperfections are a result of the design process and not controllable, they cannot be used as parameters.

The next aspect is the slenderness of the members, which depends on the member length (influenced by the grid topology), member's boundary conditions (joint stiffness) and cross-sectional properties. Since the slenderness is a result of these parameters, it is not an individual parameter.

The geometry of the structure (i.e. node angles, member lengths, curvature, torsion, face shape and planarity) also affects the structural behaviour. However, as discussed in subsection 3.2.1, these geometry aspects are constrained.

Lastly, the load conditions depend on external effects, such as design regulations, weather conditions and seismic conditions. Additionally it depends on the structure's design, such as the self weight, the slope affecting the water and snow runoff. Therefore, load conditions cannot be parameterised directly in the optimisation.

The parameters that are considered variable are the following:

Modular shape and location of joints

Moreover, because this research focuses on the segmentation of the gridshell and the module design, the shape of the modules are variable. The design could contain a single shape that is applied to all modules, but it could also contain multiple module shapes.

Consequently, the location of the hinges in the structure, which serve as inter-module joints, is a parameter. These locations depend on the modular shapes and the locations of the modules.

cross-section

Cross-sectional properties are significant as they influence the slenderness and therefore the buckling behaviour of the elements. Initially, the cross-section of the reference structure is used to perform the structural analysis. Subsequently, the cross-section is optimised, depending on the structural performance of the design.

3.3. Preliminary study

Before the initial design for the modular segmentation is made, a classic geodesic gridshell is analysed as a preliminary study. The classic geodesic gridshell consists of only separate beams, connected together through hinges in all nodes of the gridshell. A structural and construction analysis is performed on the classic geodesic gridshell as explained in section 3.5 and section 3.6.

3.4. Design of modular geodesic gridshell

After collecting the data and performing the preliminary study, the next step of the methodology is the design of multiple modular segmentation options. The design consists of the two following things.

First of all, the structure is segmented into modules. This is done by selecting specific shapes for the faces of the modules and fitting these faces onto the structure, in this case a hemisphere, which divide the structure into the modules.

Second of all, based on the modular shapes and their locations on the hemisphere, the distribution of joints is determined. The inter-module connections consist of hinges with zero stiffness. On the other hand, the intra-module connections have infinite stiffness.

The outputs of this step are the geometry of the module segmentation and the distribution of the different joints. Using these outcomes, the structural and construction analysis is performed on the designs in the same way as on the preliminary study.

3.5. Structural analysis

The first step of the structural analysis is the Finite Element Analysis (FEA). To perform the FEA, assumptions are made, loads are defined and a mesh convergence analysis is performed to determine the sufficient number of finite elements.

The required cross-section of the timber members is determined to make the design as economically feasible and sustainable as possible. Simultaneously with minimising the cross-sectional area, the constraints regarding structural performance are validated.

The outputs of this steps are the FEA results and the required cross-section sizes. The dimensions or strength class that are used, influence the material usage of the structure.

3.6. Construction analysis

The purpose of the construction analysis is to determine the efficiency of the design in the execution phase. During the analysis, the designs are evaluated on the following aspects.

The first part of the construction analysis is to determine the production repetition rate of the modules. The number of module types in the structure determines the production repetition rate. When a structure has no modules, this number is set to 0. A high number of module types means a low repetition rate. A low repetition rate means higher production time and costs due to the number of designs that need to be made to produce the modules.

In addition, the assembly repetition rate is determined. Again, the number of element types determines the repetition rate. When a structure has no modules, this number is equal to the number of beam types. The assembly repetition rate influences the assembly costs, as the construction equipment has to be adapted for each different element.

The second part is to determine the total number of modular elements or, if no modules are used, individual beams. The number of elements affects the cost of assembly, because a larger number of elements means that more scaffolding is needed to support the modules and the assembly time is longer. Because the assembly costs are affected by both scaffolding and time, this aspect counts twice. The number of elements also affects the reusability of the elements and therefore the circularity of the structure. A larger number of elements means higher deconstruction costs, which means that the elements are less likely to be reused.

The third part is to assess the number of beam ends that have to be connected on-site. This specific number is assessed because besides the effect of the number of joints on-site on the assembly time and assembly costs, the number of beams through one of these nodes also increases the assembly time and costs. Therefore the total number of beams ends and module ends to be joined on-site is determined.

The final part is to assess the transportation of the elements, which affects both the costs and sustainability. Using maximum transport dimensions, the number of trucks is determined by stacking the elements. A larger number of trucks means higher transport costs and is less sustainable. If special transport is needed instead of general transport, costs will also increase.

3.7. Multi-objective comparative analysis

The multi-objective comparative analysis compares the designs based on five objectives: material, production, assembly, reusability and transport. This is done by scoring each objective and using an objective function.

3.7.1. Scoring objectives

The results of the structural and construction analysis are scored from 0 to 1, where 0 represents the best possible outcome, such as no material use or no trucks, and 1 represents the worst outcome among all designs. The goal is to minimise the scores to achieve the most optimal design.

An aspect of a particular design is scored by dividing the value of the design in that aspect, x , by the highest value across all designs in that aspect, D :

$$\text{Score} = \frac{x}{\max(D)} \quad (3.1)$$

The scores for the five objectives are determined by taking the average value of the scores in that category.

3.7.2. Objective function

To evaluate each design alternative, an objective function is used, combining the objectives of the comparative analysis. This leads to the following objective function:

$$F = \omega_m F_m + \omega_p F_p + \omega_a F_a + \omega_r F_r + \omega_t F_t \quad (3.2)$$

F_m , F_p , F_a , F_r and F_t are the terms of respectively material, production, assembly, reusability and transport and ω_m , ω_p , ω_a , ω_r and ω_t are the corresponding weights.

The weights can be based on the importance of each goal. In practice, the weights that are assigned to each term are based on the interest of stakeholders and the goals of a project. A sensitivity analysis is applied to assess the influence of different weight distributions.

The result of the multi-objective comparative analysis is a preference-based optimal design or multiple designs.

3.7.3. Material impact analysis

In order to evaluate the relationship between material usage and the different objectives, a material impact analysis is conducted. This analysis evaluates how sensitive the amount of required material is to changes in the other four design objectives: production efficiency, assembly efficiency, reusability and transport efficiency.

The analysis investigates how a 1% change in each of these objectives influences the required material use. These effects are examined by comparing the classic gridshell to the modular gridshells.

The evaluation is carried out by first calculating the relative change, $C_{o,ij}$, in the score of objective o between two designs i and j , using Equation 3.3. The objective o could be material (m), production (p), assembly (a), reusability (r) or transport (t).

Next, the material impact for each objective is calculated by dividing the relative change in material (m) by the relative change in one of the other four objectives (p , a , r or t), as shown in Equation 3.4. This value is then multiplied by 100 to express the result as a percentage.

The material impact, $\epsilon_{m,o}^{ij}$, represents the percentage change between designs i and j in material usage resulting from a 1% change in one of the four other objectives: production efficiency, assembly efficiency, reusability or transport efficiency.

$$C_{o,ij} = \frac{F_{o,j} - F_{o,i}}{F_{o,i}} \quad (3.3)$$

$$\epsilon_{m,o}^{ij} = \frac{C_{m,ij}}{C_{o,ij}} \cdot 100\% \quad (3.4)$$

3.8. Validation of constraints

After selecting the optimal designs, the constraints that are discussed in subsection 3.2.1, are validated. First of all, this consists of the geometrical constraints and the constraints regarding the number of different joints, which are taken into account from the beginning on and should therefore give a positive outcome. Secondly, the constraints regarding the structural performance have to be validated, which means that the strength, the stability and the deflections are verified. Additionally, the constraints regarding the maximum element dimensions have to be validated, to ensure transport feasibility.

If the constraints cannot be met for a certain design, the geometry of the module and the joint locations should be adjusted if possible. If adjustments are not an option, for example, because they would result in a design that already exists, the design is discarded, and the multi-objective comparative analysis can be repeated.

Once the constraints are met, the segmentation and final design(s) of the modules can be completed.

3.9. Evaluation

The final part of this research involves evaluating the design possibilities related to the research objectives. This includes evaluating the structural performance, material use, reusability of elements, and efficiency of production, assembly and transport.

3.10. Material specific aspects

This study focuses specifically on a timber gridshell. However, as suggested by the title, the proposed method is applicable to gridshells in general, constructed from a range of materials. When using materials other than timber, several aspects should be taken into account.

Firstly, in terms of geometry, the structure in this study uses curved beams. It must be considered whether the chosen material is suitable for the application of curved beams. Cross-sectional dimensions and strength classifications will also vary between materials.

The joint configuration of the gridshell is also influenced by the material choice. This study assumes either fully rigid or pinned joints, with an option to increase the joint stiffness. It is important to note that joint design is material dependent, and therefore their stiffness as well. In timber structures, joint design can also affect the required cross-section sizes, which may differ significantly for other materials. Therefore, if a study would include specific joint configurations, these factors must be considered.

The structural analysis is also influenced by the selected material. In particular, Ultimate Limit State (ULS) and Serviceability Limit State (SLS) checks based on Eurocode standards will differ. It is essential to apply the correct material specific Eurocode.

Besides these considerations, other parts of the research remain consistent when applying different materials. The grid topology and the shape of the modules are generally material independent, provided that the structure remains stable. Furthermore, both the construction analysis and the multi-objective comparative analysis remain similar.

The methodology proposed in this study can also be used to compare gridshells made from different materials. In such cases, the construction analysis should be expanded to include cost considerations and climate impact. These could account for material usage, production efficiency, and reusability, thereby enabling a more comprehensive comparison.

4

Preliminary study: Classic Geodesic Gridshell

The research is applied to a timber geodesic gridshell, shown in Figure 4.1. The grid of this structure is based on a triangular geodesic pattern. The geometry is further discussed in section 4.1. This chapter discusses the preliminary study on a classic geodesic gridshell, as discussed in section 3.3. This gridshell is used as a benchmark for the comparison of different designs.

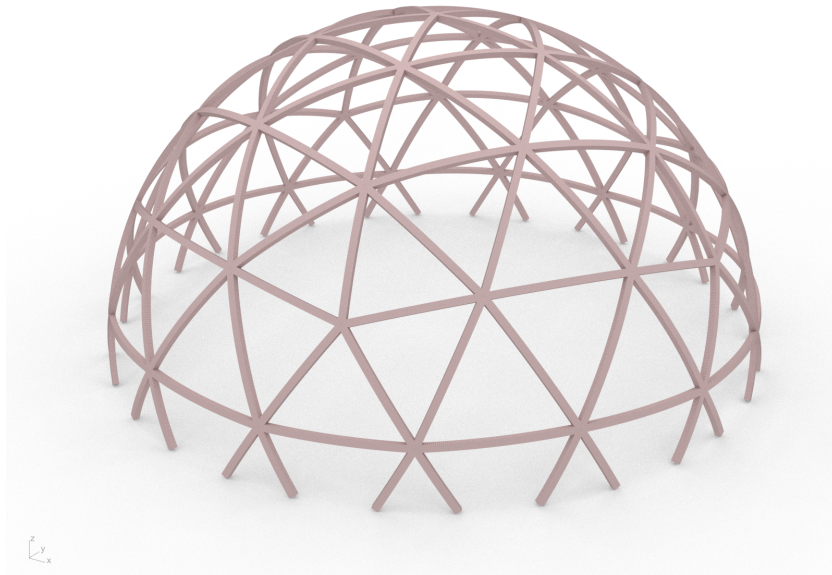


Figure 4.1: Geodesic gridshell

4.1. Geometry of geodesic gridshell

Figure 4.2 shows the curves of the geodesic gridshell in Grasshopper. The gridshell is formed using a base triangle, shown in Figure 4.2a. The base triangle is divided into nine equal triangles. Using Grasshopper, it is first projected onto a icosahedron, as shown in Figure 4.3a and Figure 4.3b. Subsequently, the curves on the icosahedron are projected onto a sphere, with a radius of 10 m, as visualised in Figure 4.3c and Figure 4.3d. This results in beams that are curved. The sphere is cut in half to form a hemisphere, as presented in Figure 4.2b and Figure 4.2c.

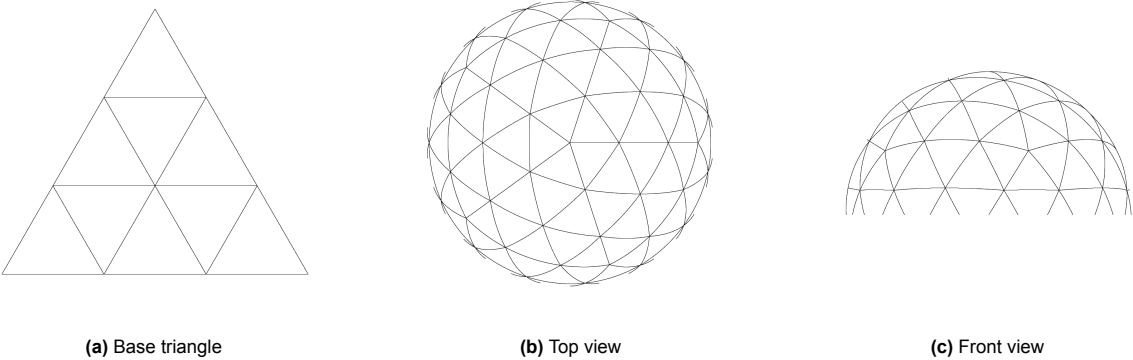


Figure 4.2: Geodesic gridshell model

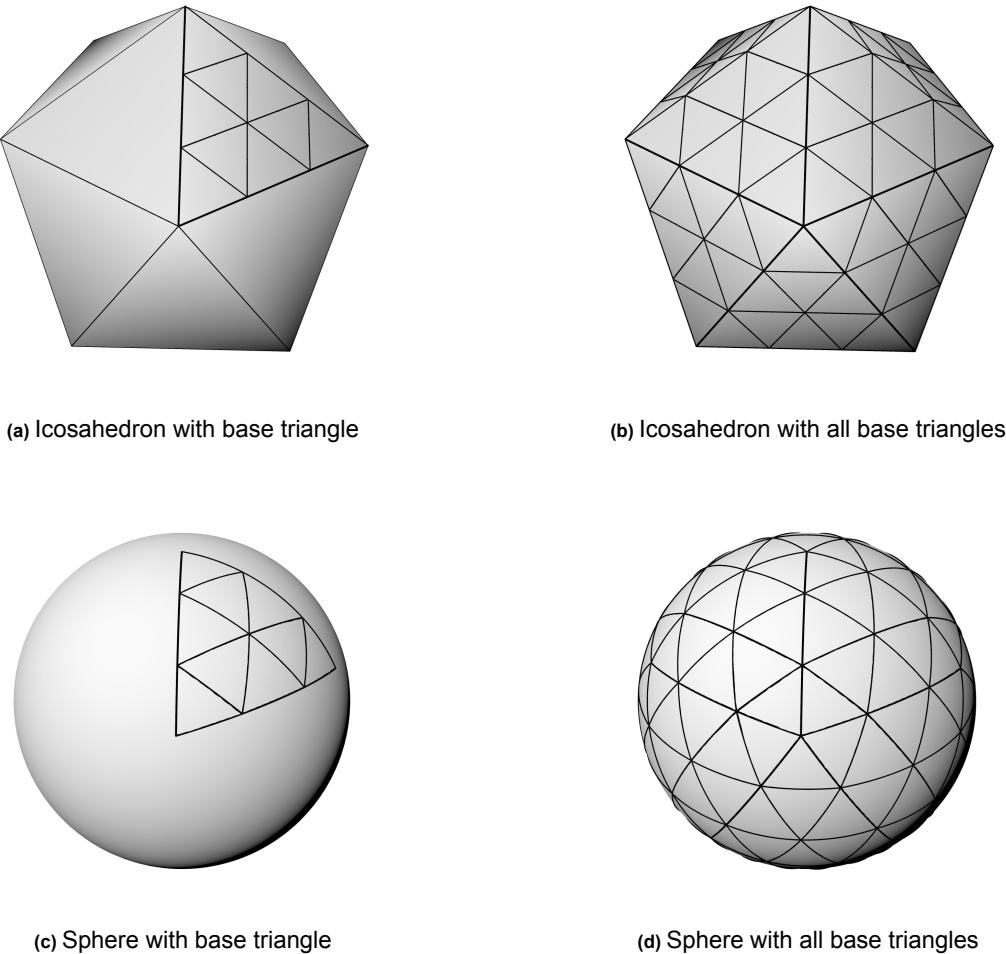


Figure 4.3: Geometric formation of structure, perspective view

4.2. Classic Geodesic Gridshell

The classic geodesic gridshell, which consists only of separate beams connected by hinges at all nodes, serves as a reference against which the different modular designs can be compared. The structure is shown in Figure 4.4.

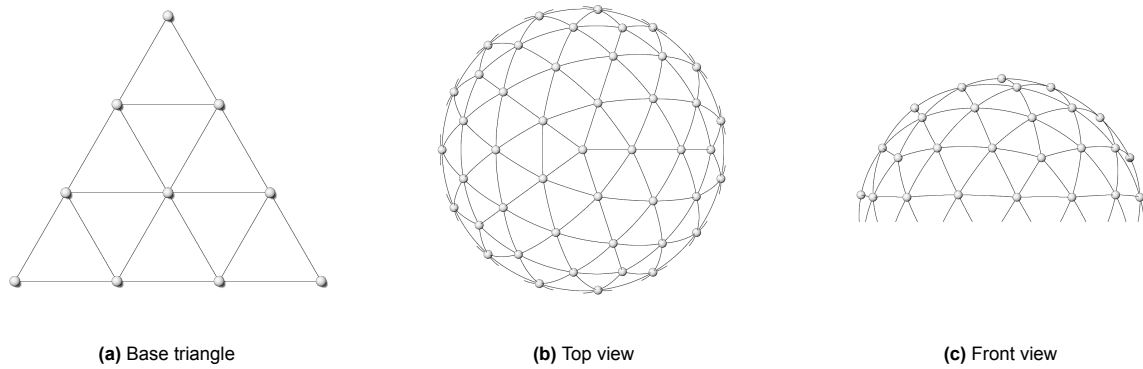


Figure 4.4: Classic geodesic gridshell

4.3. Structural analysis

To compare the differences in structural behaviour, the designs are analysed using an Finite Element Analysis (FEA) in Karamba3d (Preisinger, 2013). This section discusses the data and assumptions of the FEA, the loads and load combinations that are applied in the analysis, the mesh convergence analysis, the cross-section sizing and the joint stiffness analysis.

4.3.1. Data and assumptions

A number of assumptions were made as inputs to the model in order to perform the structural analysis. This section discusses the assumptions and the data that has been used in the structural analysis.

The geodesic dome has a radius of 10 m. The density of the grid is formed by the projection of a 5 m radius icosahedron onto a 10 m radius sphere. The triangular faces of the icosahedron consist of the base triangle as shown in Figure 4.2a.

The local coordinate system of the timber elements is shown in Figure 4.5. In the local coordinate system, the x-axis is aligned with the longitudinal direction of the beam. The y- and z-axes are oriented perpendicular to the beam, with the y-axis lying in-plane of spherical surface and the z-axis oriented out-of-plane. This means that the beams are curved around the y-axis.

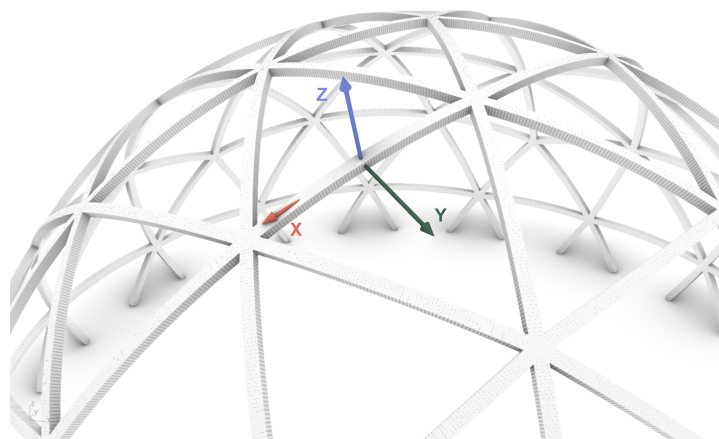


Figure 4.5: Local coordinate system timber elements

In the local coordinate system the beams are oriented as shown in Figure 4.6. The beam width is oriented the y-direction and the beam height is oriented in the z-direction.

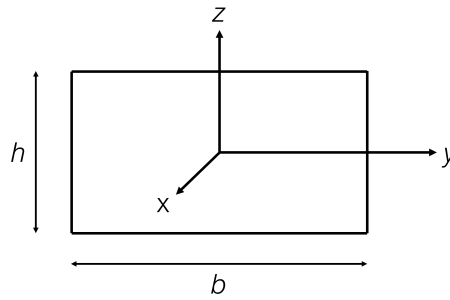


Figure 4.6: Beam orientation

In the classic geodesic gridshell, one type of joints is considered. The beams are connected to each other in the nodes with hinges, having zero rotational stiffness in y-direction. The rotation of the connections is fixed in x-, and z-direction.

Additionally, pinned supports with zero rotational stiffness in all directions are used to support the structure in x, y and z direction.

The members are made of solid sawn timber, which means that a material safety factor of $\gamma_M = 1.3$ is applied, according to Eurocode 5 (Nederlands Normalisatie-instituut, 2011b). All beams in the structure have the same cross-section.

4.3.2. Loads

Several load cases are analysed, each forming part of different load combinations. These load cases and combinations are selected to ensure the structure is thoroughly analysed. Although not all loads from the Eurocode are applied, the selected loads are based on the Eurocode. Each load case and combination is discussed in detail in the following sections.

Self-weight

The first load case to act on the structure is the self-weight, G . It acts on the structure in the negative z-direction.

Wind load

Secondly, a wind load, Q_{wind} , is applied to the structure based on Eurocode 1 (Nederlands Normalisatie-instituut, 2011a). The wind load consists of internal and external pressures acting in the local z-direction of the beams. The internal and external pressure coefficients are multiplied by the peak velocity pressure to obtain the external and internal wind force, described by the following equations. To obtain the total wind load, the internal wind load is subtracted from the external wind load.

$$w_e = q_p \cdot c_{pe} \quad (4.1)$$

$$w_i = q_p \cdot c_{pi} \quad (4.2)$$

For the peak velocity pressure, q_p , it is assumed that the structure is located on the coast in wind zone I. This gives a peak velocity pressure of 1.58 kN/m^2 for a structure of 10 m height. The external wind pressure is based on Figure 4.7a. $h = 0$, so the values of $c_{pe,10}$ at locations A, B and C are equal to 0.8, -1.2 and 0.0 respectively.

As it is not possible to apply non-linear variable distributed loads in Karamba3D, the structure is divided into a mesh, with a continuous distributed pressure acting on each part of the mesh, approximating the non-linear distributed pressure in the figure.

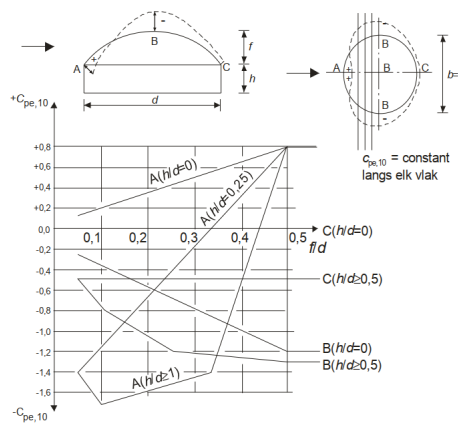
The internal pressure coefficient, c_{pi} is based on Figure 4.7b. To calculate μ , the ratio of the area of openings with $c_{pe,10} \leq 0.0$ and the total area of openings is determined. This ratio can also be calculated from the area where $c_{pe,10}$ is negative in Figure 4.7a and the total area of the hemisphere. This is done as follows, where α is the angle to the point where the external pressure line between A and B in Figure 4.7a is zero:

$$A_{hemisphere} = \frac{1}{2} \cdot 4\pi R^2 \tag{4.3}$$

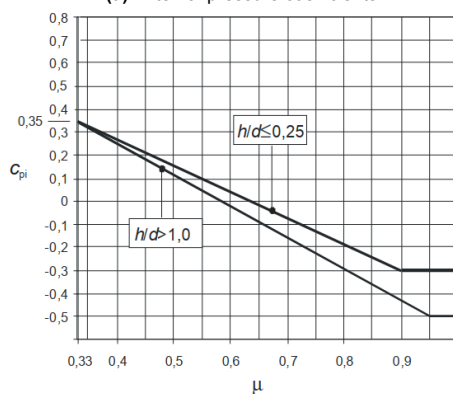
$$\begin{aligned} A_\alpha &= \frac{1}{2} \cdot 2\pi R^2 (1 - \cos(\alpha)) \\ &= \frac{1}{2} \cdot 2\pi R^2 \left(1 - \frac{\sqrt{2}}{2}\right) \end{aligned} \tag{4.4}$$

$$\begin{aligned} \mu &= \frac{\sum \text{Area of openings with } c_{pe,10} \leq 0.0}{\sum \text{Area of all openings}} \\ &= \frac{\frac{1}{2} \cdot 4\pi R^2 - \frac{1}{2} \cdot 2\pi R^2 \left(1 - \frac{\sqrt{2}}{2}\right)}{\frac{1}{2} \cdot 4\pi R^2} \\ &= \frac{2 - \left(1 - \frac{\sqrt{2}}{2}\right)}{2} \\ &= \frac{1}{2} + \frac{\sqrt{2}}{4} = 0.85 \end{aligned} \tag{4.5}$$

This gives a value of -0.25 for c_{pi} as read from the graph in Figure 4.7b.



(a) External pressure coefficients



(b) Internal pressure coefficients

Figure 4.7: Pressure coefficients (Nederlands Normalisatie-instituut, 2011a)

Snow load

The snow load is applied to the structure based on Eurocode 1 (Nederlands Normalisatie-instituut, 2019). The snow load is determined using the following formula:

$$s = \mu_i \cdot C_e \cdot C_t \cdot s_k \tag{4.6}$$

Both C_e and C_t are equal to 1.0 and $s_k = 0.7 \text{ kN/m}^2$ in the Netherlands. μ_i is determined according to Figure 4.8. For cylindrical roofs, the snow load is divided into two load cases, $Q_{snow,1}$ and $Q_{snow,2}$. For the first snow load case μ_i is equal to 0.8. For the second load case it holds that for $\beta \leq 60^\circ$, $\mu_4 = 0.2 + 10 \cdot \frac{h}{b}$ with a maximum value of 2.0. In this case b is twice as large as h and therefore $h/b = 0.5$. This gives a value of 5.2 and therefore the maximum value of 2.0 is used for μ_4 . The length, l_s , over which the snow load acts, is determined as follows:

$$l_s = 2 \cdot \sin(60^\circ) \cdot R = 2 \cdot \frac{\sqrt{3}}{2} \cdot R = \sqrt{3} \cdot R \quad (4.7)$$

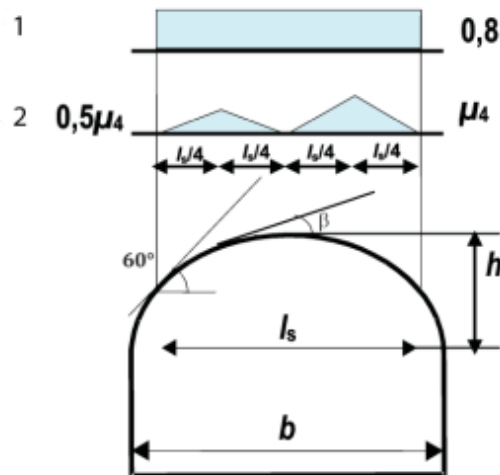


Figure 4.8: Snow coefficients (Nederlands Normalisatie-instituut, 2019)

Point load

A point load, F is applied to the structure at the centre of the dome. The point load could be, for example, a person at the top of the structure during maintenance or repair. The applied value for this load is 1 kN.

Load combinations

The categories into which load combinations are divided are Ultimate Limit State (ULS) load combinations, Serviceability Limit State (SLS) load combinations and Qualitative load combinations. The load factors are based on the consequence class of the structure. It is assumed that this structure is categorised in CC2, which refers to normal consequence according to Eurocode 0 (Nederlands Normalisatie-instituut, 2015).

The ULS load combinations are used for the stresses, cross-section forces, nodal forces, and the stability. The ULS load combinations are as follows:

Only self-weight: $1.35G$

Wind load leading, unfavourable: $1.2G + 1.5Q_{wind}$

Wind load leading, favourable: $0.9G + 1.5Q_{wind}$

Snow load leading, case 1: $1.2G + 1.5Q_{snow,1}$

Snow load leading, case 2: $1.2G + 1.5Q_{snow,2}$

Point load leading: $1.2G + 1.5F$

The SLS load combinations are used for the nodal displacements and beam displacements. The SLS load combinations are as follows:

Only self-weight: $1.0G$

Wind load leading: $1.0G + 1.0Q_{wind}$

Snow load leading, case 1: $1.0G + 1.0Q_{snow,1}$
 Snow load leading, case 2: $1.0G + 1.0Q_{snow,2}$
 Point load leading: $1.0G + 1.0F$

The Qualitative load combinations are used for a qualitative review of the results regarding the reaction forces and deformation energy. The Qualitative load combinations are as follows:

Only self-weight: $1.0G$
 Wind load leading: $1.0G + 1.0Q_{wind}$
 Snow load leading, case 1: $1.0G + 1.0Q_{snow,1}$
 Snow load leading, case 2: $1.0G + 1.0Q_{snow,2}$
 Point load leading: $1.0G + 1.0F$

The different load combinations are used for different result types, as shown in Table 4.1.

Table 4.1: Results load combinations

Result	Load combination
Reaction force	Qualitative
Displacement	SLS
Deformation energy	Qualitative
Stress	ULS
cross-section force	ULS
Nodal force	ULS
Buckling factor	ULS

4.3.3. Mesh convergence analysis

To perform the finite element analysis the curved beams in the structure have to be divided into linear elements. The sufficient number of linear elements has been determined through a mesh convergence analysis. The mesh convergence analysis consists of a loop that increases the number of segments and performs the structural analysis with every step. Every time, it reviews the increase or decrease in the results of the cross-section forces, the displacements and the deformation energy. The loop ends when the relative change in these results, described by the formula below, is smaller than 0.01, meaning that the percentage change is lower than 1%. F_n is the force, displacement or energy at the n^{th} step in the loop.

$$\text{Relative change} = \frac{|F_n - F_{n-1}|}{|F_{n-1}|} < 0.01 \quad (4.8)$$

The mesh convergence analysis has been performed for the ULS, SLS and Quantitative load combinations. This analysis has determined that each beam in the dome should be divided into 42 elements, based on the dimensions and mesh density described in subsection 4.3.1. To simplify future analyses when beam lengths change, due to adjustments in mesh density or dome radius, this value of 42 elements is converted into a standard length.

This value of 42 changes if the beam lengths change, for example due to changing the overall dimensions of the structure. Therefore, this value is translated into a general value that can be used in different cases. The average beam length of the gridshell, calculated under the given assumptions, is divided by 42. This gives an average element length of 0.046513 m. This value is rounded to two significant numbers and can be used as a standard element length. If the dimensions of the structure change, the average beam length of the structure can be divided by the standard element length, 0.047 m. The result is then rounded to determine the updated number of elements for each beam.

Figure 4.9 shows the linear beam elements in detail in the Karamba3D model.

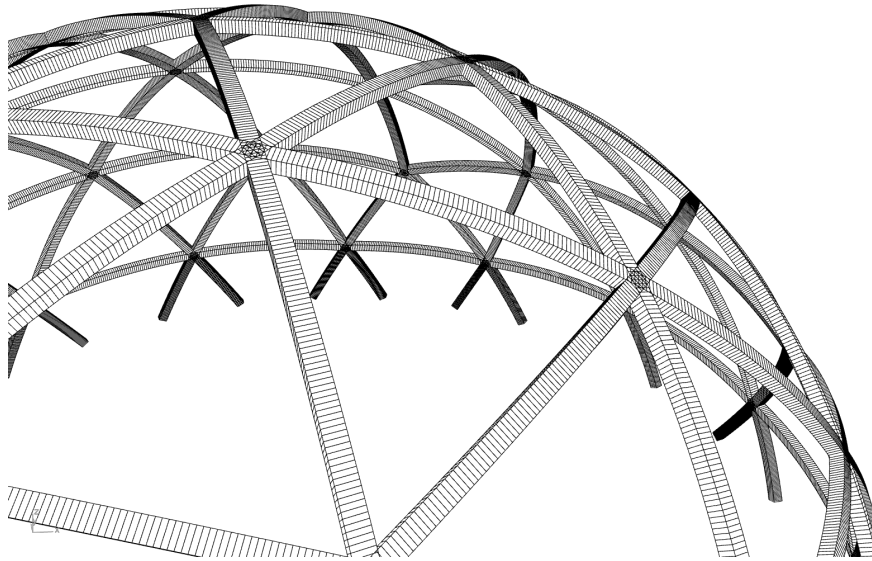


Figure 4.9: Linear elements in curved beams

4.3.4. FEA results

This section presents the results of the structural analysis. The Finite Element Analysis “ is based on a cross-section with a width of 200 mm, a height of 175 mm and a strength class of C30. This represents the optimised cross-section, which will be discussed in subsection 4.3.7.

Figure 4.10 shows a front view of the axial stresses and displacements in the structure. The maximum axial stresses and displacements occur under the ULS load combination where the second snow load case is leading ($1.2G + 1.5Q_{snow,2}$). The top view of these results are presented in section A.3. Compression has negative values and is represented by the red colour, while tension is positive and is shown in blue. A combination of compression and tension in one beam means the presence of bending. The numerical results of the finite element analysis are presented in section A.2.

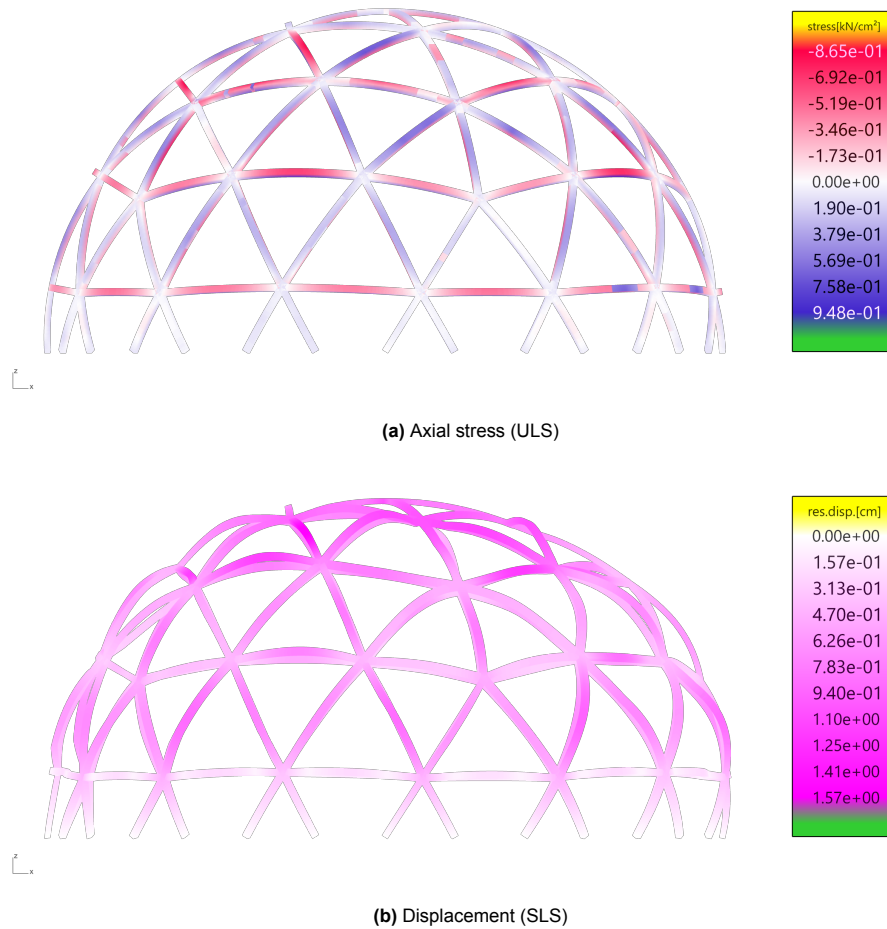


Figure 4.10: Classic Geodesic Gridshell: FEA results, front view (20 m span, C30, 200x175 mm)

4.3.5. Global stability

The global stability of the structure is assessed through its buckling modes, which are identified using a second order analysis in Karamba3D. Its results are used to determine the buckling modes and corresponding buckling load factors via the *Buckling Modes* component.

Figure 4.11 shows the first buckling mode of the classic geodesic gridshell. It can be observed that one beam and one node in the structure are critical for buckling. The location of this beam, slightly to the right side of the structure, is probably caused by the wind forces, that are not equally distributed over the area of the structure, as discussed in subsection 4.3.2.

The buckling load factors indicate how much the second order normal forces would need to increase before the structure becomes unstable. Using the *Buckling Modes* component, the buckling factor of the most critical buckling mode, is determined. A structure is considered to have sufficient global stability if this buckling factor is greater than 1.

For the classic geodesic gridshell, the buckling factor of the first and most critical buckling mode is equal to 14.19, as shown in section A.2. This means that the structure would become unstable if the loads are increased by a factor of 14.19.

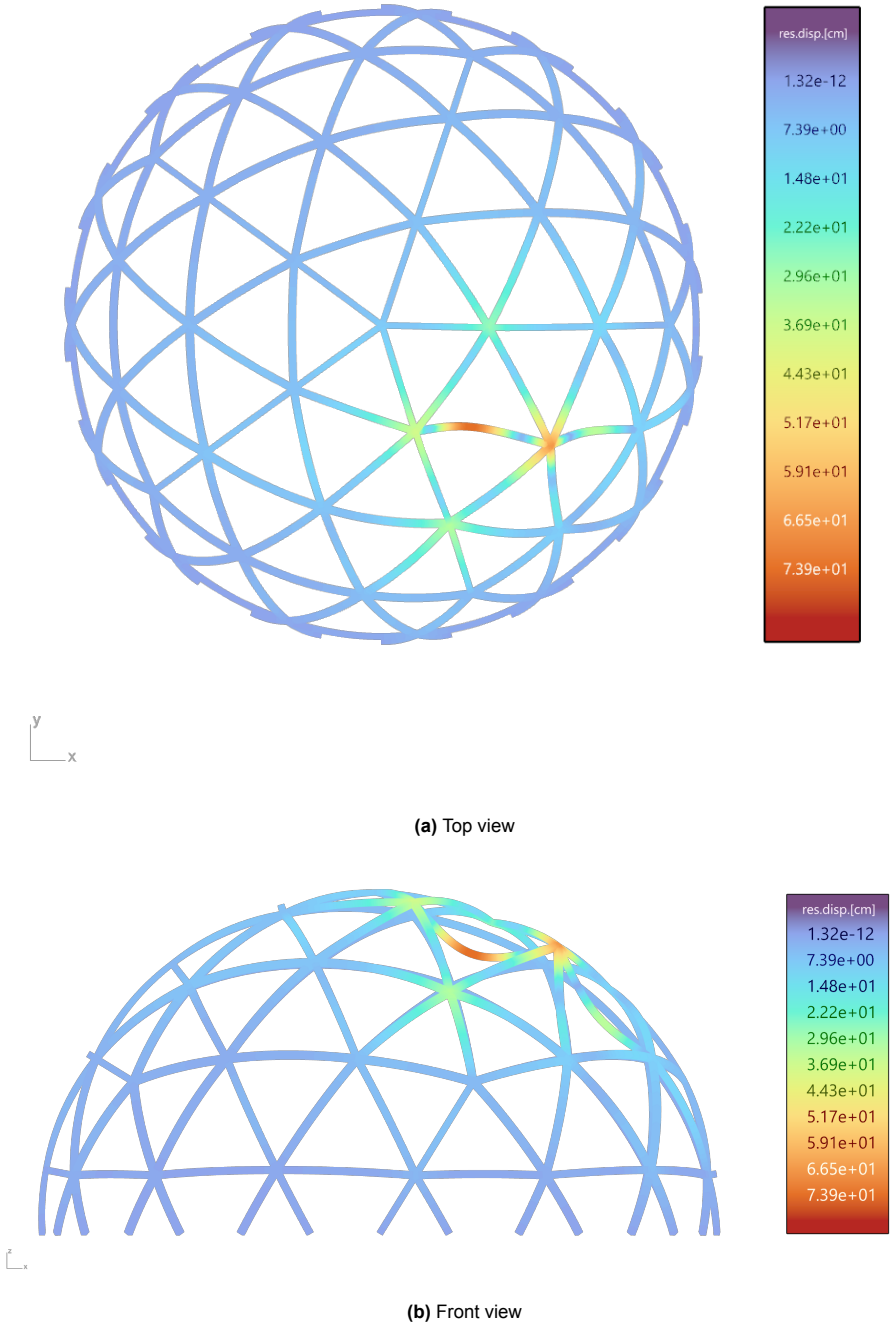


Figure 4.11: Classic Geodesic Gridshell: First buckling mode (ULS, 20 m span, C30, 200x175 mm)

4.3.6. ULS and SLS verification

The verification of both the ultimate limit state (ULS) and the serviceability limit state (SLS) is carried out in accordance with Eurocode 5 (Nederlands Normalisatie-instituut, 2011b). Appendix C provides the calculations for this verification.

4.3.7. Cross-section sizing

Cross-section sizing has been first conducted on the classic geodesic gridshell to establish a basis for comparison with other designs. This approach allows all designs to be evaluated against the classic geodesic gridshell as a benchmark and in relation with each other using the same cross-section.

The analysis is performed by verifying the structure in both ULS and SLS according to Eurocode 5 (Nederlands Normalisatie-instituut, 2011b), as discussed in subsection 4.3.6. The results of these verifications indicated that buckling is the critical failure mechanism. Therefore, the required cross-section is determined by adjusting its dimensions rather than altering the timber strength class.

A strength class of C30 is used and the dimensions are optimised by testing the following widths and heights: 100 mm, 125 mm, 175 mm, 200 mm, 225 mm, 250 mm. The final required cross-section has a width of 200 mm, a height of 175 mm and a strength class of C30.

4.3.8. Results

The total results of the structural analysis of the classic geodesic gridshell are given in Table 4.2.

Table 4.2: Classic Geodesic Gridshell: Structural analysis results (ULS, 20 m span)

Beam element length	0.047 m
Buckling factor	14.19
Cross section	200x175 mm
Strength class	C30

4.4. Construction analysis

In order to compare the differences in the efficiency of the designs in the execution phase, the construction analysis focuses on the repetition of elements, the number of elements and joints to be constructed on-site and the transport, as explained in section 3.6. In this section the construction analysis is applied to the preliminary study.

Firstly, the the number of elements is determined. For the classic geodesic gridshell, which has no modules, the number of individual beams is counted. Secondly, the number of module types is identified, which is equal to zero in the case of the classic geodesic gridshell. In addition, the number of element types for assembly is determined, which is equal to the number of beam types in the case of the classic geodesic gridshell. This value is determined by measuring the beam lengths in Grasshopper. Besides, the number of beam ends to be joined on-site is determined. In this case, this is equal to the number of beams multiplied by two, minus the number of supports in the structure.

4.4.1. Transport

The final part of the construction analysis is the transport of the building elements to the construction site. The maximum transport dimensions are 12 x 2.55 x 4 m for regular transport and 12 x 4.5 x 4 m for special transport (Jonkeren, 2023). In order to assess the transport of the elements, in this case individual beams, the bounding box and stackability of the elements are determined.

First, the dimensions of the bounding box of the curves in Grasshopper are determined for each element. Then 200 mm is added to each dimension of the bounding box to allow for the cross-section. Using these dimensions, the elements are tested to the maximum transport dimensions.

If the individual elements have sufficient dimensions to be transported, the stackability of the elements is determined. The maximum number of elements on top of each other and side by side is determined based on the maximum transport dimensions. The elements are stacked and placed side by side with a space of 350 mm between the curves. This includes 200 mm for the cross-section and 150 mm for a protective layer. 200 mm is added in every dimension to allow for the cross-section of the bottom and top elements. Elements are rotated if this results to a more efficient way of transport.

Using the number of elements per type and the maximum number of elements that can be stacked and transported side by side, the minimum number of trucks is determined by combining the different elements in trucks. The results are given in Appendix D, section D.1.

4.4.2. Results

The total results of the construction analysis of the classic geodesic gridshell are given in Table 4.3.

Table 4.3: Classic Geodesic Gridshell: Construction analysis results

No. of elements (beams)	150
No. of module types	0
No. of element types	6
No. of on-site joined beam ends	270
No. of trucks	3

4.5. Findings and discussion

The results of the preliminary study provide a benchmark for the following parts of the research.

The structural analysis results in forces, displacements, energy and utilisations. The SLS utilisations are relatively low compared to the ULS utilisations, which means that deflection and displacement are not dominant. Looking at the deformation energy, it can be concluded that the bending is an important mechanism for the force distribution as the bending energy is relatively high compared to the axial energy. From the ULS utilisations, local stability appears to be the dominant aspect. In particular flexural buckling plays an important role.

The construction analysis results in the number of individual elements, the number of modular element types, the number of on-site joined beam ends and the number of trucks. In this case, the elements in the structure are the individual beams. This results in a relatively high number of elements, and this number is expected to be much lower in the case of a modular geodesic gridshell. Also the number of on-site joined beam ends is relatively high due to the individual beams. These are the main reasons for using modular elements instead of individual beams.

Modular Geodesic Gridshell

The second step in the application is the modular segmentation of the structure. Several design options are created. This chapter discusses the eight designs and their analysis. They are compared with the multi-objective comparative analysis.

5.1. Generation of modules

The first step is to explore how a modular gridshell can be generated, focusing on the geometric design of the modules and the placement of joints within the structure.

As discussed in section 2.1, triangular shaped modules can result in complex joint configurations, which in turn affect the overall feasibility of the structure (Kuda & Petříčková, 2021). Incorporating such shapes into a geodesic dome leads to joints composed of multiple sub-joints. A schematic representation of this concept is shown in Figure 5.1a. In the figure, different colours represent distinct modules, each containing intra-module joints at the corners. These modules and their intra-module joints are prefabricated off site. They are then assembled on-site via inter-module joints, shown as black circles, meaning that both intra- and inter-module joints converge at a single node.

To make on-site construction more efficient, the process described above can be simplified. One alternative is to use beam-to-beam connections to simplify on-site assembly, as illustrated in Figure 5.1b. In this research, these connections in which two beams are joined longitudinally, are called *splice joints*¹. The intra-module joints, connecting beams within a module, are positioned at the nodes, represented by the small blue and red hexagons in the figure. This reduces joint complexity: the connection of six beams at a single node can be prefabricated, while the inter-module joints required on-site are kept as simple as possible.

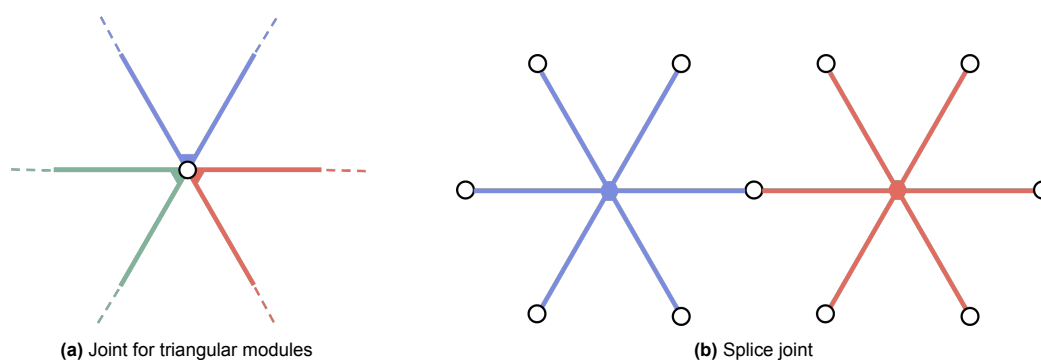


Figure 5.1: Joint configuration

For this study, it is assumed that the inter-module splice joints are pinned in one direction and the intra-module joints are considered infinitely rigid. The splice joints are placed at the midpoints of triangle sides, creating two separate beams instead of one continuous one. This segmentation results in hexagonal and pentagonal - where five beams meet at a node - modules, as shown in Figure 5.1b.

¹The term *splice joints* typically refers to connections that join timber elements along their length, with the contact plane oriented parallel or diagonal to the elements, and capable of transferring bending moments (Karolak et al., 2020). In this research, however, the term *splice joints* refers more broadly to any longitudinal connection between two elements, regardless of the joint geometry or its ability to transfer moments.

A possible joint design of the intra-module rigid joints is shown in Figure 5.2. This is the so-called BASS joint (Bolted Angled Slotted-in Steel plates), a bolted connection specifically developed for small to medium-sized timber dome structures, as proposed by Shu et al. (2020).

The hinged splice joints can also be constructed using slotted-in steel plates, secured with dowels or bolts. An example of this type of connection, using an end plate and a steel hinge, is illustrated in Figure 5.3 (Crocetti, 2016).

Various modular design configurations can be generated by adjusting the positions of splice joints within the base triangle. Where no splice joint is placed, the beam remains continuous rather than split into two connected segments.

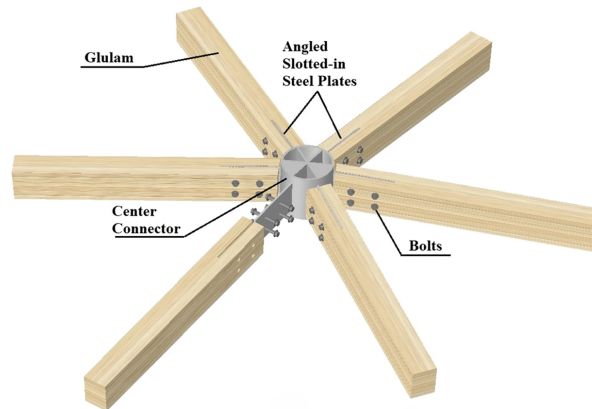


Figure 5.2: Joint with steel bolts and angled slotted-in steel plates (BASS joint) (Shu et al., 2020)

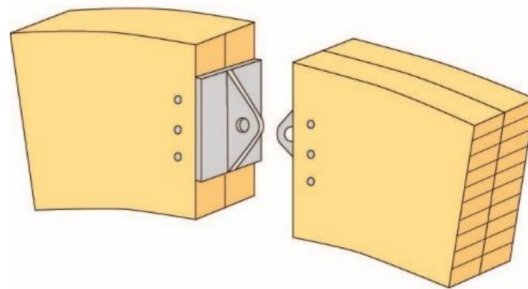


Figure 5.3: Hinged ridge joint with dowelled steel plate, end plate and hinge pin (Crocetti, 2016)

5.2. Modular designs

This section discusses the different design options and the data and assumptions used. Eight design options are considered for the modular segmentation of the structure, which are designed using the method described in section 5.1. Discarded designs are presented in Appendix F.

5.2.1. Design Option 1

The first design option considers splice joints at all possible locations, as shown in Figure 5.4. This results in the modules presented by the coloured lines. First of all, a module is formed in the centre of the base triangle, represented by the light blue lines. The second module types is formed at the sides of the base triangle, shown by the dark blue and green lines. These modules all consist of six beams connected in the centre of a hexagon. The bottom of the structure consists of both the light blue module type and the dark blue and green module type. Finally, a module is formed in each corner of the base triangle, visualised by the red lines. This module has only five beams which are rigidly connected in the centre of a pentagon.

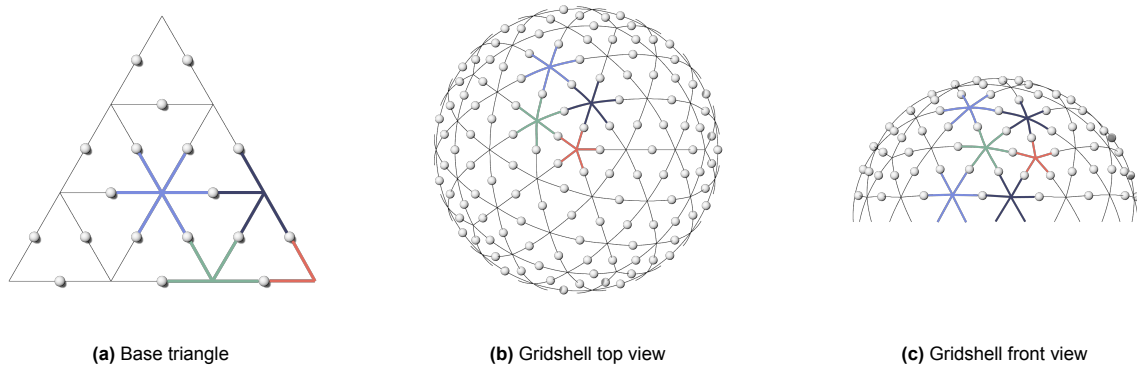


Figure 5.4: Geodesic Gridshell: Design Option 1

5.2.2. Design Option 2

The second design option leaves out one splice joint per side of the base triangle, as shown in Figure 5.5. The first module is again formed in the centre of the base triangle and consists of six beams that are rigidly connected in the centre of a hexagon, as shown by the light blue lines. Secondly, a module is formed on all sides of the base triangle. Unlike Design Option 1, the two modules on each side are now connected by a continuous beam, forming a larger module, shown by the purple and green lines. As in Design Option 1, a module is formed in each corner of the base triangle, resulting in a module made out of five beams that are rigidly connected in the centre of a pentagon, visualised by the red lines. The bottom of the structure consists of the light blue module type and the same dark blue module from Design Option 1.

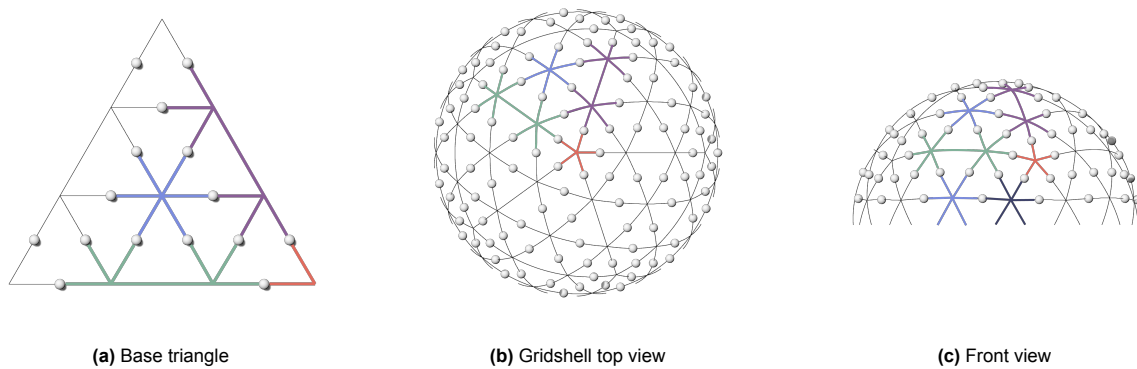


Figure 5.5: Geodesic Gridshell: Design Option 2

5.2.3. Design Option 3

The third design option leaves out three splice joints in each corner of the base triangle, as shown in Figure 5.6. As in Design Options 1 and 2, the first module is formed in the centre of the base triangle and consists of six beams that are rigidly connected in the centre of a hexagon, as shown by the light blue lines. The next module is formed by each corner of the base triangle. The beams of the small triangle in the corners of the base triangle are now continuous. This results in a pentagonal module, as shown by the dark blue lines. At the bottom of the structure, this dark blue module is alternated with the light blue module.

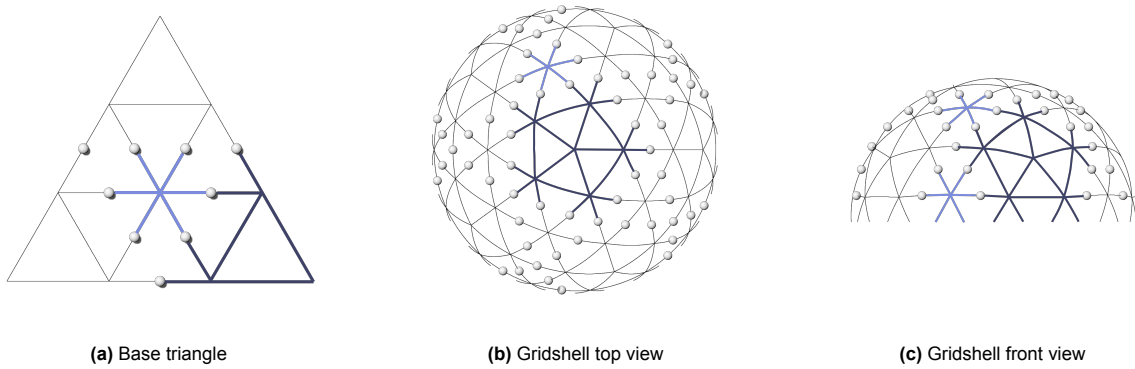


Figure 5.6: Geodesic Gridshell: Design Option 3

5.2.4. Design Option 4

Figure 5.7a shows the base triangle on which Design Option 4 is based. However, some adjustments are made after applying the base triangle, as certain points did not fully align with the intended pattern. Figure 5.7 shows the final design of Option 4.

The design contains two module types from the earlier design options. The red module appears in each corner of the base triangle and consists of five beams connected at the centre. Additionally, the design includes relatively large, triangular shaped modules, represented in the figure by the light blue and green lines. At the bottom, the light blue and green module types are alternated with the dark blue ones, which are the same dark blue modules as in Design Option 1 and 2.

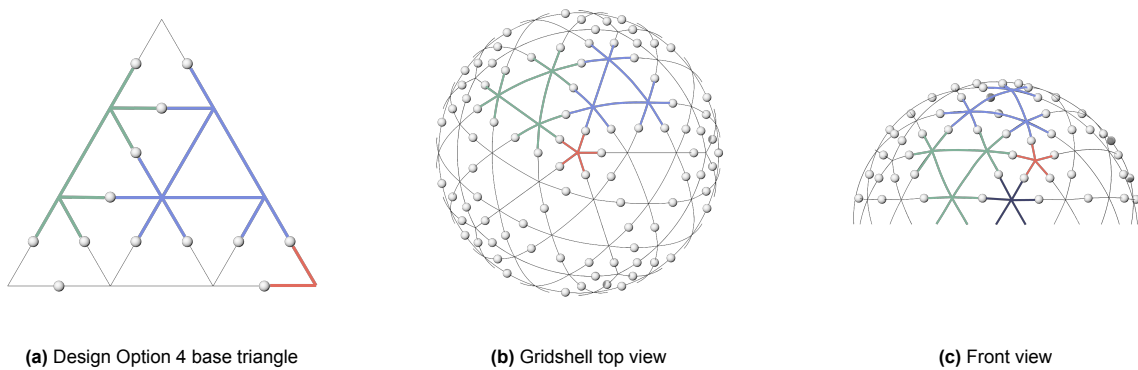


Figure 5.7: Geodesic Gridshell: Design Option 4

5.2.5. Design Option 5

Figure 5.8 shows Design Option 5. It is largely similar to Option 2, as it is also based on the same base triangle and includes the light blue, red, purple and green modules. However, some changes have been made at the bottom of the structure. While Design Option 2 only consists of light blue modules at the bottom, Design Option 5 alternates these with the purple modules, located below the red ones.

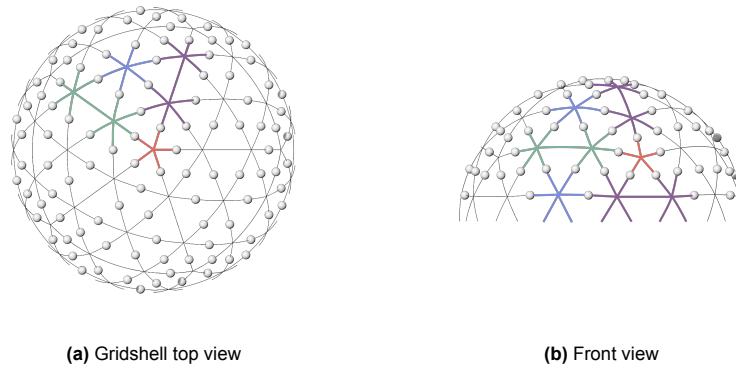


Figure 5.8: Geodesic Gridshell: Design Option 5

5.2.6. Design Option 6

Figure 5.9 illustrates Design Option 6, which is similar to Design Option 5. The difference is that the light blue modules at the bottom are now expanded, forming the pink modules. These are alternated with the dark blue modules from previous Design Options 1, 2 and 4.

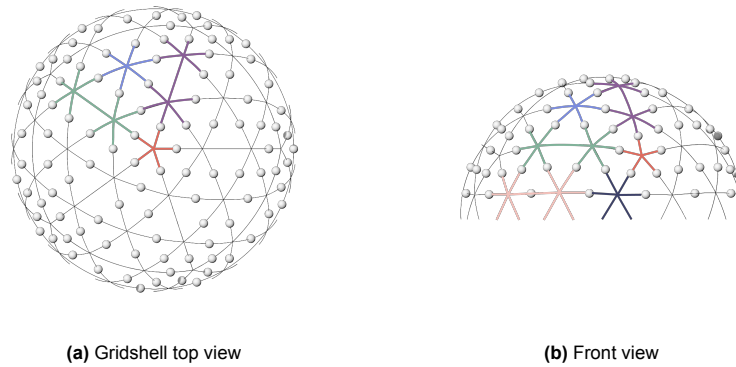


Figure 5.9: Geodesic Gridshell: Design Option 6

5.2.7. Design Option 7

Figure 5.10 shows Design Option 7, which is similar to Options 5 and 6. Like these design options, it is based on the base triangle of Option 2 and includes the light blue, red, purple and green modules. In this design, the pink module of Design Option 6 is expanded to one side, creating in even larger modules at the bottom, that are no longer alternated with the light blue modules. These bottom modules are shown in dark blue.

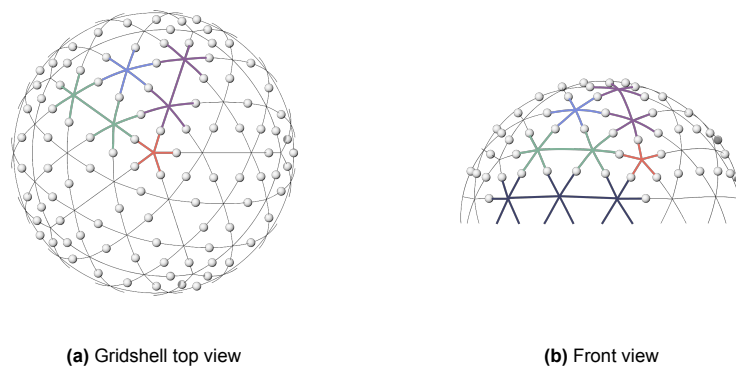


Figure 5.10: Geodesic Gridshell: Design Option 7

5.2.8. Design Option 8

In Design Option 8, even more splice joints are removed compared to Design Option 7. Figure 5.11 shows that the red, light blue, green and dark blue module from Option 7 are retained in this design. However, some of the purple and green modules are expanded downwards, now incorporating some of the red modules of the previous designs. This creates the modules visualised by the purple lines.

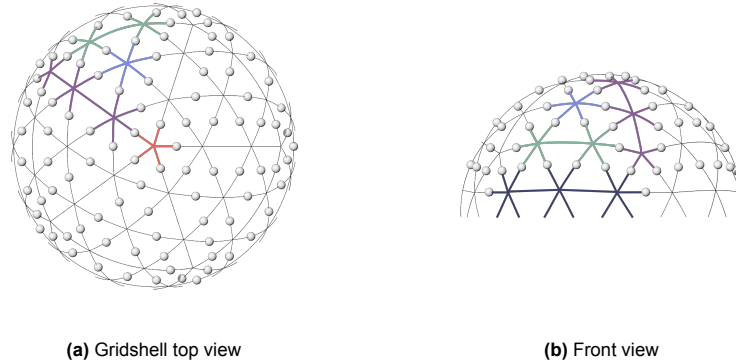


Figure 5.11: Geodesic Gridshell: Design Option 8

5.3. Structural analysis

This section presents the results of the structural analysis, including the FEA results and the required cross-section sizes.

5.3.1. Data and assumptions

The assumptions as inputs of the structural analysis are similar as discussed in subsection 4.3.1.

However, now two types of joints are considered. Firstly, the intra-module joints are the joints that connect the beams within a module, which are assumed to be infinitely rigid in all directions. Secondly, the inter-module joints connect the different modules to each other. These connections are so called splice joints, which are assumed to be pinned and have zero rotational stiffness in y-direction. Their rotation is fixed in x- and z-direction. Their orientation is visualised in Figure 4.6. Pinned supports with zero stiffness in all directions are used to support the structure in x, y and z direction.

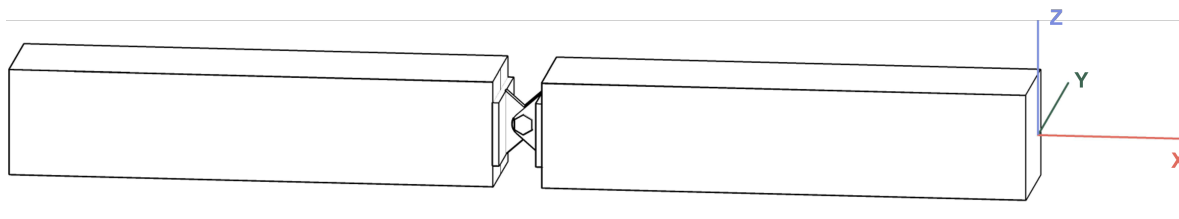


Figure 5.12: Joint orientation

As explained in subsection 4.3.3, to model the curvature in the beams, they are divided into multiple straight elements with a length of 0.047 m.

The FEA is first performed on all design options using the reference cross-section of the classic geodesic gridshell, determined in the preliminary study. This cross-section has a width of 200 mm, a height of 175 mm and a strength class of C30, as discussed in subsection 4.3.7. After collecting all FEA results based on this cross-section, the required cross-section is determined for all designs.

5.3.2. FEA results

The FEA results are presented in Appendix A. These results of the modular designs are based on C30 timber with a 200x175mm cross-section, which is the required cross-section of the classic geodesic gridshell. This is also why utilisations may be too high, resulting in a failing structure.

This appendix consist of both numerical results (section A.2) and stress and displacement diagrams (section A.3).

The ULS and SLS utilisations are based on Eurocode 5 (Nederlands Normalisatie-instituut, 2011b). The calculations that have been performed for the utilisations are described in Appendix C.

To compare the results of the preliminary study and all design options, Figure 5.13 and Figure 5.14 show bar charts of both SLS and ULS utilisations. section A.4 contains bar charts of all FEA results.

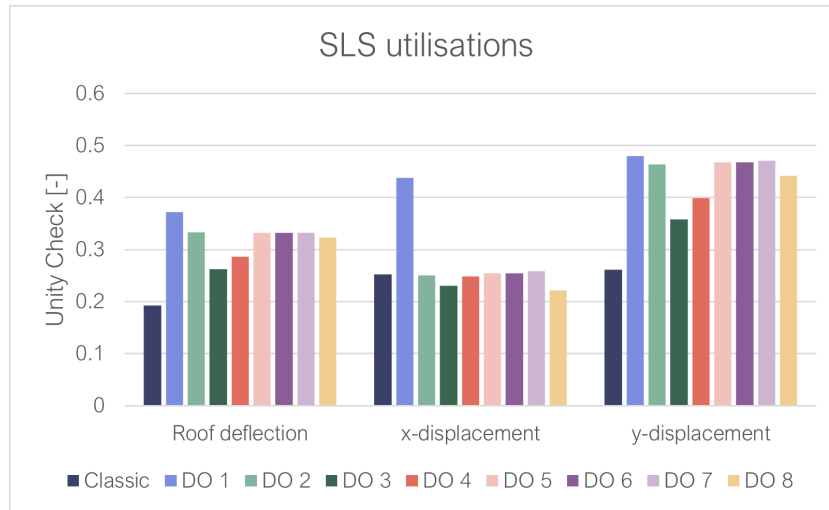


Figure 5.13: Geodesic Gridshell: Displacement utilisation results (SLS, 20 m span, C30, 200x175 mm)

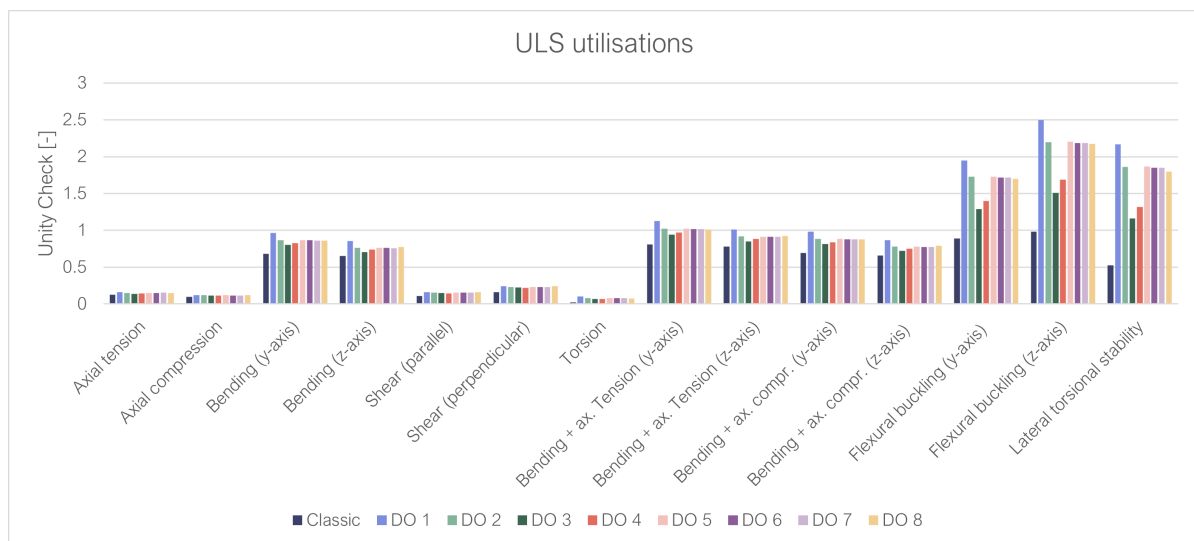


Figure 5.14: Geodesic Gridshell: cross-section utilisation results (ULS, 20 m span, C30, 200x175 mm)

5.3.3. Global stability

The global stability of the structure is assessed through its buckling modes, which are identified using a second order analysis in Karamba3D, as discussed in subsection 4.3.5. Figure 5.15 compares the first buckling mode of the modular geodesic gridshell - Design Option 5, shown on the right - with that of the classic geodesic gridshell - shown on the left.

It can be observed that, in both cases, the most critical buckling occurs at the same beam. However, the maximum displacement in the modular design's first buckling mode is significantly larger than that of the classic gridshell. This difference is mainly due to the presence of splice joints halfway along the beams in the modular design.

The plots for the modular gridshell also reveal that, in addition to the most critical beam, several other beams exhibit relatively large displacements at their midpoints due to buckling. In contrast, the classic gridshell shows fewer such critical locations. Based on this comparison, it can be concluded that the modular gridshell is globally less stable than the classic gridshell.

Additionally, in the classic gridshell, one of the nodes experiences a relatively large displacement, whereas the nodes in the modular gridshell remain more stable. This is because the classic gridshell uses pinned nodes, while the modular gridshell contains rigid connections in the nodes.

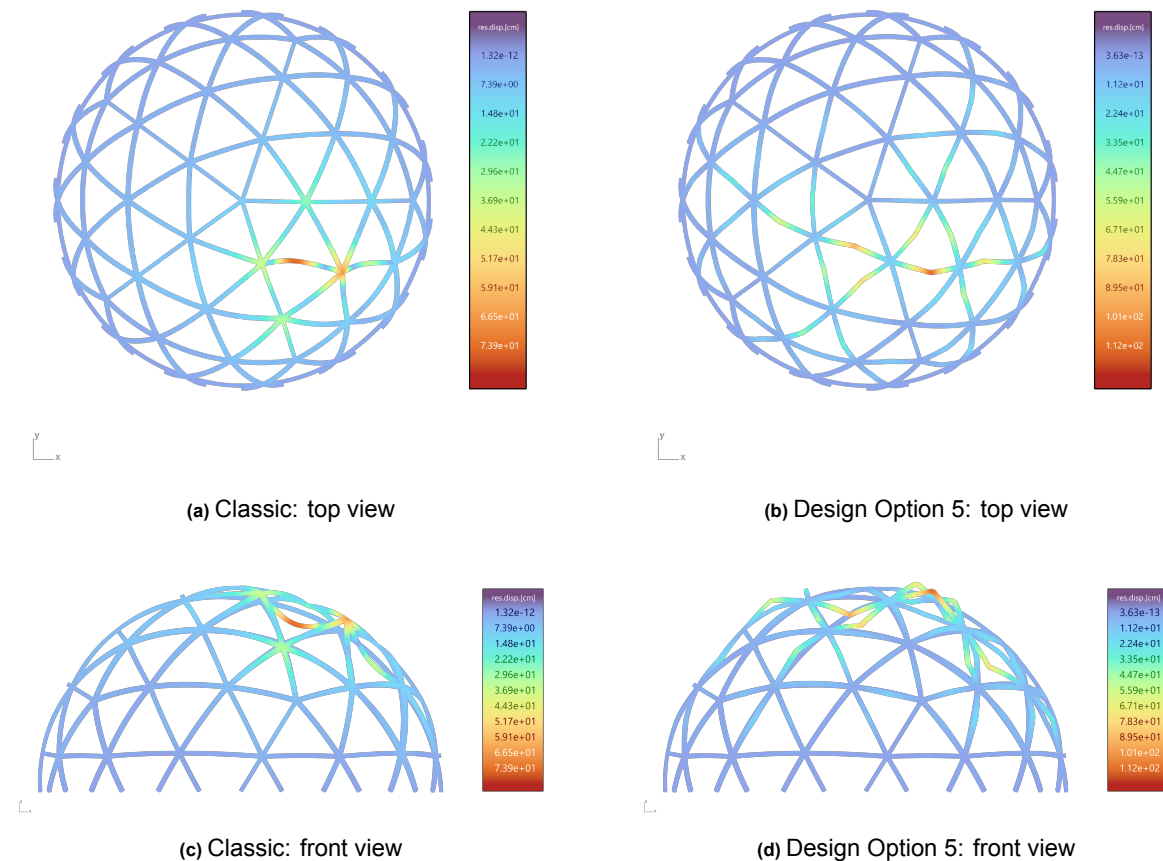


Figure 5.15: Geodesic Gridshell: First buckling mode (ULS, 20 m span, C30, 200x175 mm)

As explained in subsection 4.3.5, the buckling load factors of the first buckling mode determine the global stability of the structure. The graph in Figure 5.16 shows the buckling load factors of the different modular design options in comparison with the classic geodesic gridshell. The buckling factors of all design options are bigger than 1, meaning that the structures have sufficient global stability.

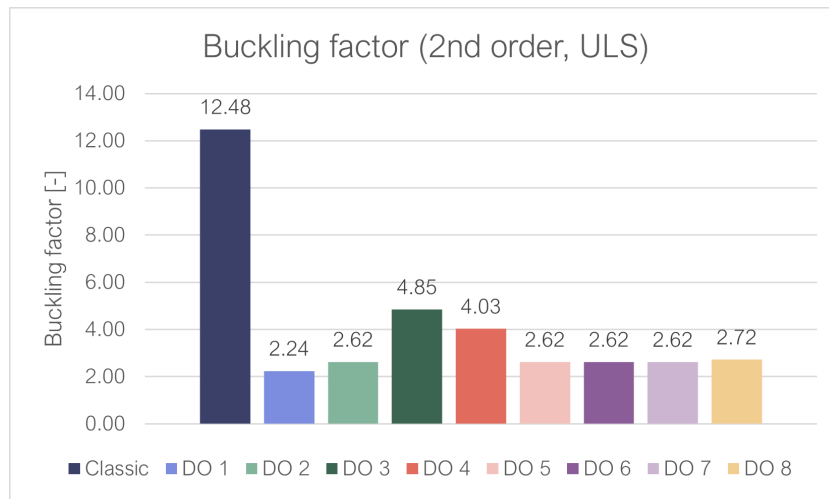


Figure 5.16: Geodesic Gridshell: Buckling factor results (ULS, 20 m span, C30, 200x175 mm)

5.3.4. Force distribution

Figure 5.17 presents the axial stress diagrams for both the classic geodesic gridshell and the modular geodesic gridshell, illustrating Design Option 5 for the latter. In both structures the maximum axial stresses occur under the ULS load combination where the second snow load case is leading ($1.2G + 1.5Q_{snow,2}$). A comparison between the two structures reveals noticeable differences in how the forces are distributed.

Firstly, Figure 5.17a and Figure 5.17c show that in the classic gridshell, the areas of highest stress are located slightly away from the nodes. This can be attributed to the lack of rotational stiffness in the nodes. Since the nodes are hinged, they do not transfer any bending moments, which means no axial stresses due to bending occur at those points. The stresses at the nodes are instead caused by normal and shear forces.

A similar explanation applies to the low stress levels observed halfway along the beams in the modular gridshell, as shown in Figure 5.17b and Figure 5.17d. At these points, splice joints are present, and because they are hinged, they also do not transfer bending moments, resulting in lower stress concentrations.

In contrast to the classic gridshell, the nodes of the modular gridshell do transfer bending moments due to their assumed infinite stiffness. This leads to increased axial stresses near the nodes, as a result of the higher bending moments.

Additionally, in areas of the modular gridshell where the beams are continuous in Design Option 5, where no splice joints are located halfway along the beam span, axial stresses are higher. This is because the full beam span is capable of transferring bending moments.

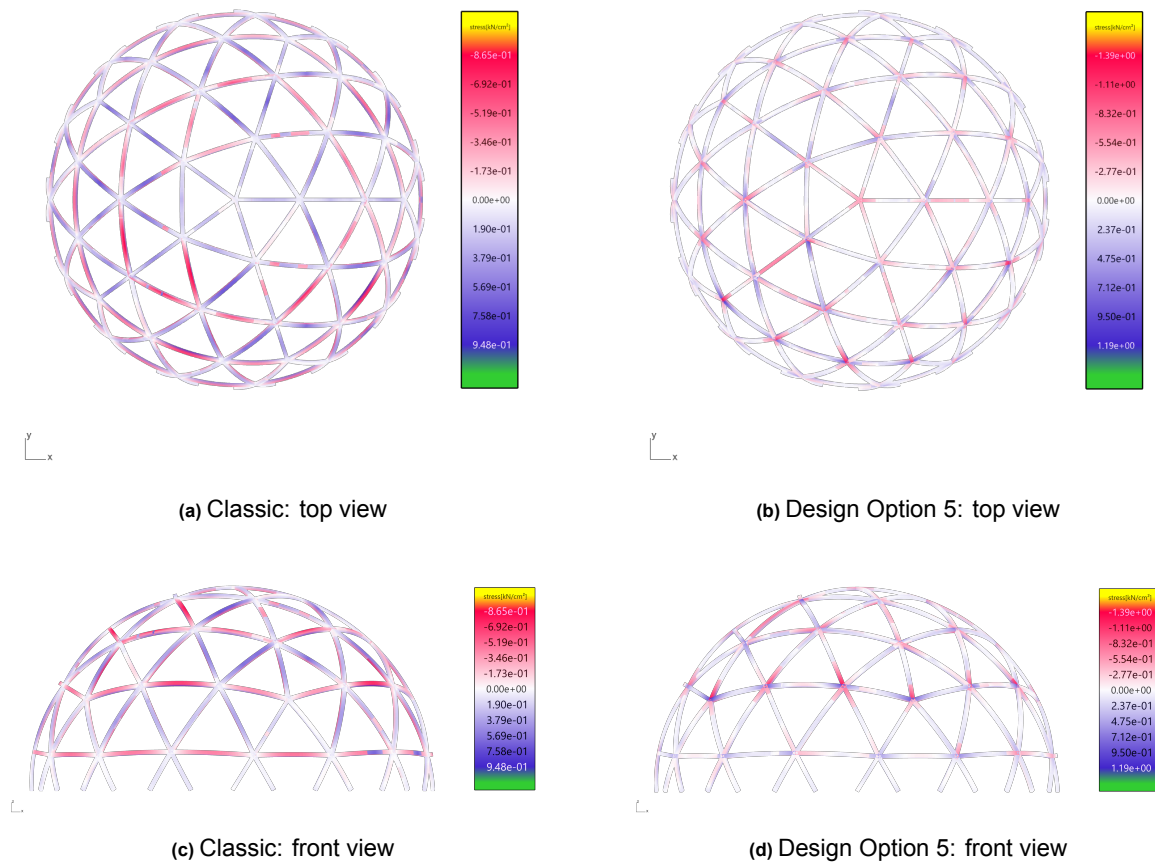


Figure 5.17: Geodesic Gridshell: Axial stress (ULS, 20 m span, C30, 200x175 mm)

Figure 5.18 shows the normal force diagrams of both structures. Compression forces are represented by orange areas and tension forces are shown by blue areas. Also the maximum normal forces occur under the ULS load combination where the second snow load case is leading ($1.2G + 1.5Q_{snow,2}$).

In a spherical dome, the bottom hoop forces are tensile, while the top hoop forces are compressive, as shown in Figure 5.19 (Hoogenboom, 2023).

Figure 5.18 shows that in this case, the bottom two hoops contain tensile normal forces, while the top hoops are mostly compressive. All other beams serve as columns, containing compressive normal forces as well.

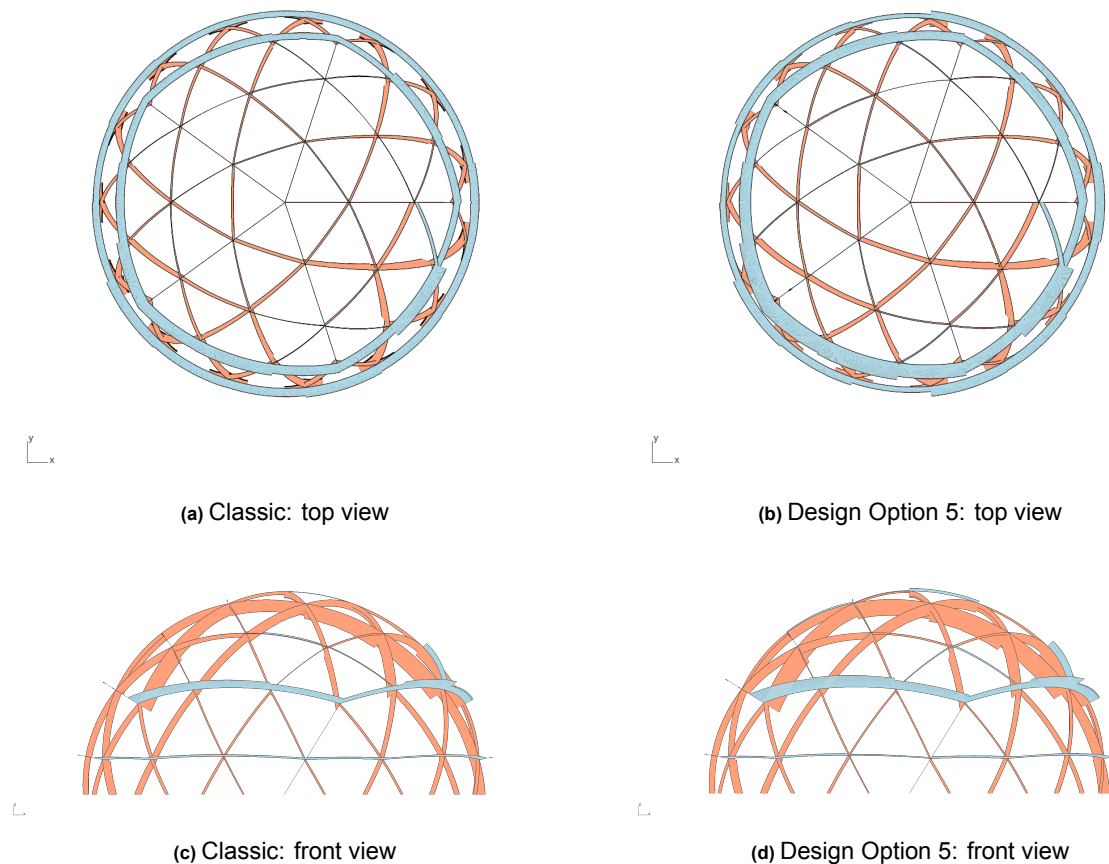


Figure 5.18: Geodesic Gridshell: Normal forces diagram (ULS, 20 m span, C30, 200x175 mm)

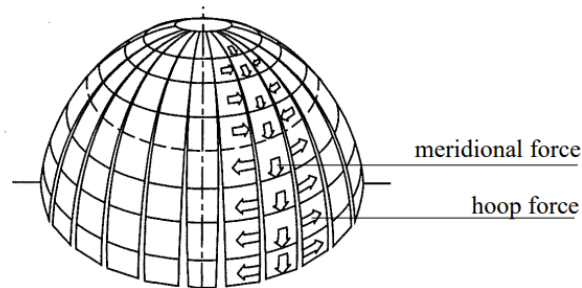


Figure 5.19: Forces in a spherical dome due to self-weight (Hoogenboom, 2023)

5.3.5. Cross-section sizing

After analysing the results of the FEA using the cross-section of 200x175 mm as a benchmark, the required cross-section sizes of all design options are determined to satisfy strength and stability requirements.

To determine the required cross-sections, both the strength class and dimensions can be adjusted. As concluded in the preliminary study, buckling is the leading design aspect in this case. As a result, the optimisation focuses on selecting the smallest dimensions that still meet the required structural performance. The final selected cross-sections are those with sufficient utilisation while maintaining the smallest possible dimensions.

The results are listed in Table 5.1. Table A.26 in Appendix A contains the SLS and ULS utilisations of all designs after the cross-section are adjusted to their required sizes.

To compare the material mass of the designs, the mass per m^2 of covered area is calculated. Table 5.1 contains these results and Figure 5.20 shows a comparison of the mass per m^2 of covered area.

Table 5.1: Geodesic Gridshell: Required cross-sections (20 m span)

Design	Strength class	Dimensions [mm]	Mass/area [kg/m^2]
Classic geodesic gridshell	C30	200x175	27.5
Design Option 1	C30	250x250	49.2
Design Option 2	C30	250x225	44.2
Design Option 3	C30	225x200	35.4
Design Option 4	C30	225x225	39.8
Design Option 5	C30	250x225	44.2
Design Option 6	C30	250x225	44.2
Design Option 7	C30	250x225	44.2
Design Option 8	C30	250x225	44.2

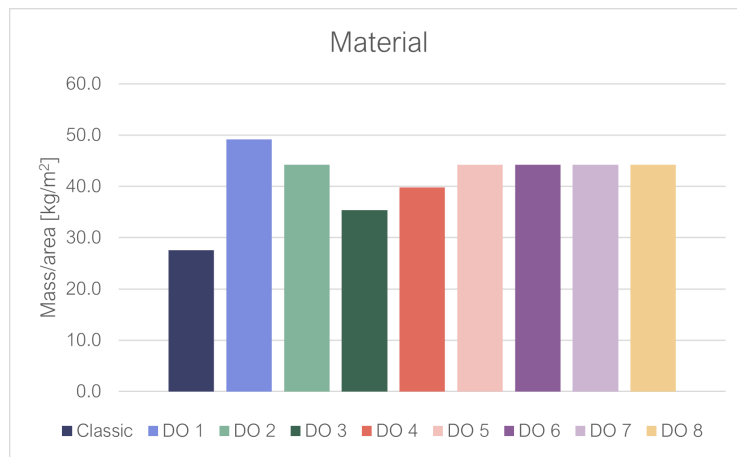


Figure 5.20: Geodesic Gridshell: Material (20 m span)

5.3.6. Joint stiffness

As shown in subsection 5.3.5 the modular designs require significantly more material than the classic gridshell. In subsection 5.3.3, it is observed that the first buckling mode of the modular gridshell showed large displacement at the midpoints of beams, where splice joints are located. Since buckling is the critical failure mode, increasing rotational stiffness at splice joints could enhance overall stability and potentially reduce the material use.

This section explores the effect of increasing joint stiffness at the splice joints in a modular gridshell. A structural analysis is performed on Design Option 5 once again, incorporating additional rotational stiffness at the splice joints.

Assumptions

Joint stiffness varies depending on the type of joint used. To demonstrate the influence of adding low, moderate and high stiffness to the splice joints, the analysis includes rotational stiffness around the y -axis ($k_{\phi,y}$) of 10 kNm/rad , 100 kNm/rad and 500 kNm/rad . Since the ULS is the governing load combination, only ULS load combinations are considered. All other assumptions remain unchanged.

Results

The results after cross-section sizing are presented in Table 5.2.

Table 5.2: Splice joint rotational stiffness variation results, Design Option 5 (ULS, 20 m span, C30)

$k_{\phi,y}$ [kNm/rad]	$k_{\phi,y} = 0$	$k_{\phi,y} = 10$	$k_{\phi,y} = 100$	$k_{\phi,y} = 500$
Cross-section [mm]	250x225	250x225	225x200	200x175
Material [kg/m ²]	44.2	44.2	35.4	27.5
Buckling factor	6.62	6.95	7.40	12.21

5.4. Construction analysis

This section presents the results of the construction analysis. The number of elements, the number of module types, the number of element types, the number of beam ends that have to be connected on-site and the number of trucks are identified. The number of module and element types is the same in the modular geodesic gridshell. This value is determined by measuring the total beam length of every module.

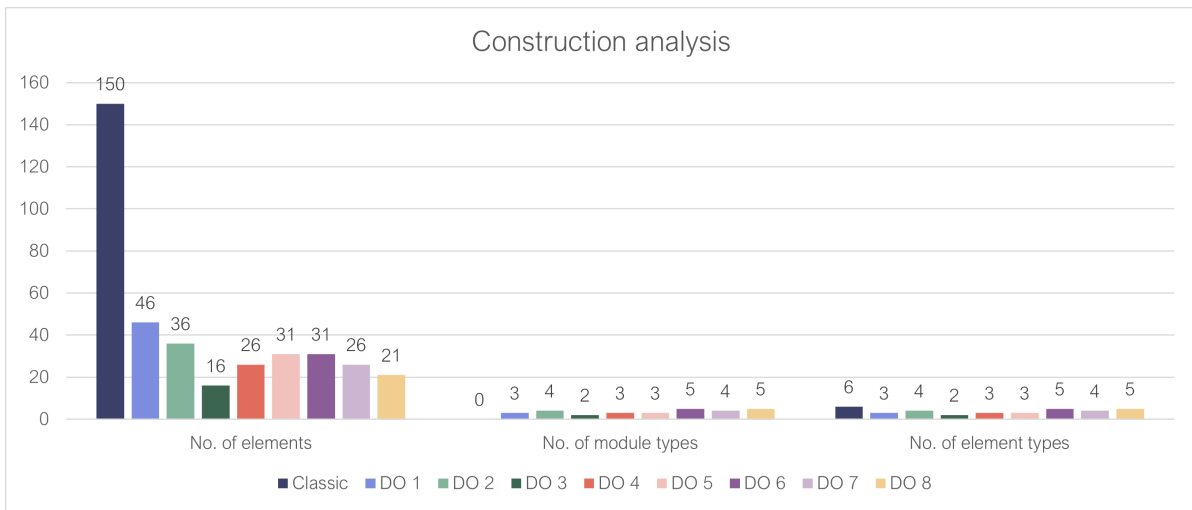
Appendix D contains the transport analysis results, including the transport bounding box of all modules, and for all design options the number of trucks.

The results of the construction analysis are given in Table 5.3. To compare the results of the preliminary study and the design options, Figure 5.21 shows a bar chart of the results per category.

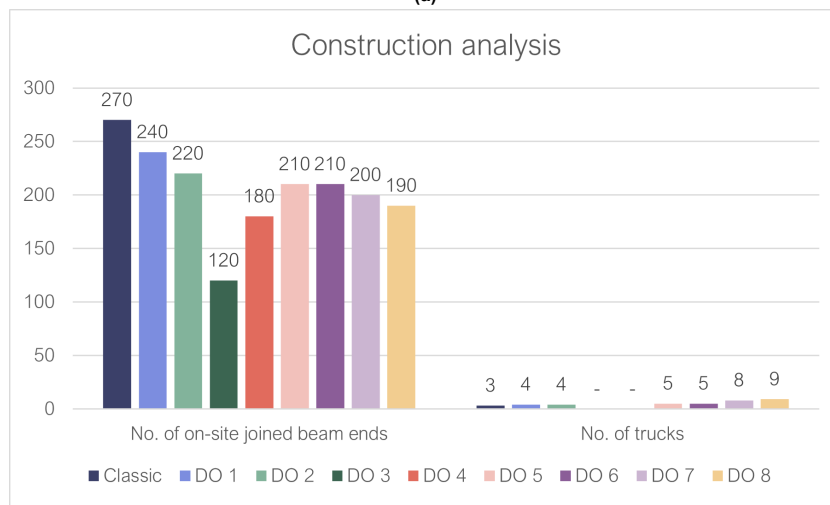
Table 5.3: Geodesic Gridshell: Construction analysis

	Classic	DO 1	DO 2	DO 3	DO 4	DO 5	DO 6	DO 7	DO 8
No. of elements	150	46	36	16	26	31	31	26	21
No. of module types	0	3	4	2	3	3	5	4	5
No. of element types	6	3	4	2	3	3	5	4	5
No. of on-site joined beam ends	270	240	220	120	120	210	210	200	190
No. of trucks	3	4	4	- ²	- ²	5	5	8	9

²No transport possible



(a)



(b)

Figure 5.21: Geodesic Gridshell: Construction analysis

5.5. Multi-objective comparative analysis

Using the results of both the structural and construction analysis, the designs can be compared through a multi-objective comparative analysis. The results are categorised into five categories, as discussed in section 3.6, with an overview provided in Table 5.4.

5.5.1. Scoring objectives

To compare the results across all categories, scores ranging from 0 to 1 are assigned, as explained in section 3.7. Table 5.5 presents the scores for each aspect, along with the the total scores per category, which are determined by averaging all scores within that category. In the assembly category, the number of elements is weighted twice due its impact on both scaffolding requirements and assembly time.

Table 5.4: Geodesic Gridshell: Structural and construction results

	Classic	DO 1	DO 2	DO 3	DO 4	DO 5	DO 6	DO 7	DO 8
Material									
Mass/area [kg/m ²]	27.5	49.2	44.2	35.4	39.8	44.2	44.2	44.2	44.2
Production									
No. of module types	0	3	4	2	3	3	5	4	5
Assembly									
No. of element types	6	3	4	2	3	3	5	4	5
No. of elements (x2)	150	46	36	16	26	31	31	26	21
No. of on-site joined beam ends	270	240	220	120	180	210	210	200	190
Reusability									
No. of elements	150	46	36	16	26	31	31	26	21
Transport									
No. of trucks	3	4	4	-	-	5	5	8	9

Table 5.5: Geodesic Gridshell: Multi-objective scores

	Classic	DO 1	DO 2	DO 3	DO 4	DO 5	DO 6	DO 7	DO 8
Material									
Mass per area	0.56	1.00	0.90	0.72	0.81	0.90	0.90	0.90	0.90
Total	0.56	1.00	0.90	0.72	0.81	0.90	0.90	0.90	0.90
Production									
Module types	0.00	0.60	0.80	0.40	0.60	0.60	1.00	0.80	1.00
Total	0.00	0.60	0.80	0.40	0.60	0.60	1.00	0.80	1.00
Assembly									
Element types	1.00	0.50	0.67	0.33	0.50	0.50	0.83	0.67	0.83
Elements (x2)	1.00	0.31	0.24	0.11	0.17	0.21	0.21	0.17	0.14
On-site joined beam ends	1.00	0.89	0.81	0.44	0.67	0.78	0.78	0.74	0.70
Total	1.00	0.50	0.49	0.25	0.38	0.42	0.51	0.44	0.45
Reusability									
Elements	1.00	0.31	0.24	0.11	0.17	0.21	0.21	0.17	0.14
Total	1.00	0.31	0.24	0.11	0.17	0.21	0.21	0.17	0.14
Transport									
Trucks	0.33	0.44	0.44	-	-	0.56	0.56	0.89	1.00
Total	0.33	0.44	0.44	-	-	0.56	0.56	0.89	1.00

Figure 5.22 shows a radar chart illustrating the scores per category, showing how the designs perform relative to each other. However, it is important to note that this chart does not include weights, even though different categories may have varying impacts on cost, time and sustainability. For example, production is influenced only by the number of module types, which affects the production costs, whereas assembly is affected by the number of elements element types and on-site joined beam ends, impacting both scaffolding requirements and assembly time.

Therefore, the best design cannot be selected purely based on the number of categories in which it scores highest. A well balanced trade-off between the different categories should be considered to determine the most suitable design(s).

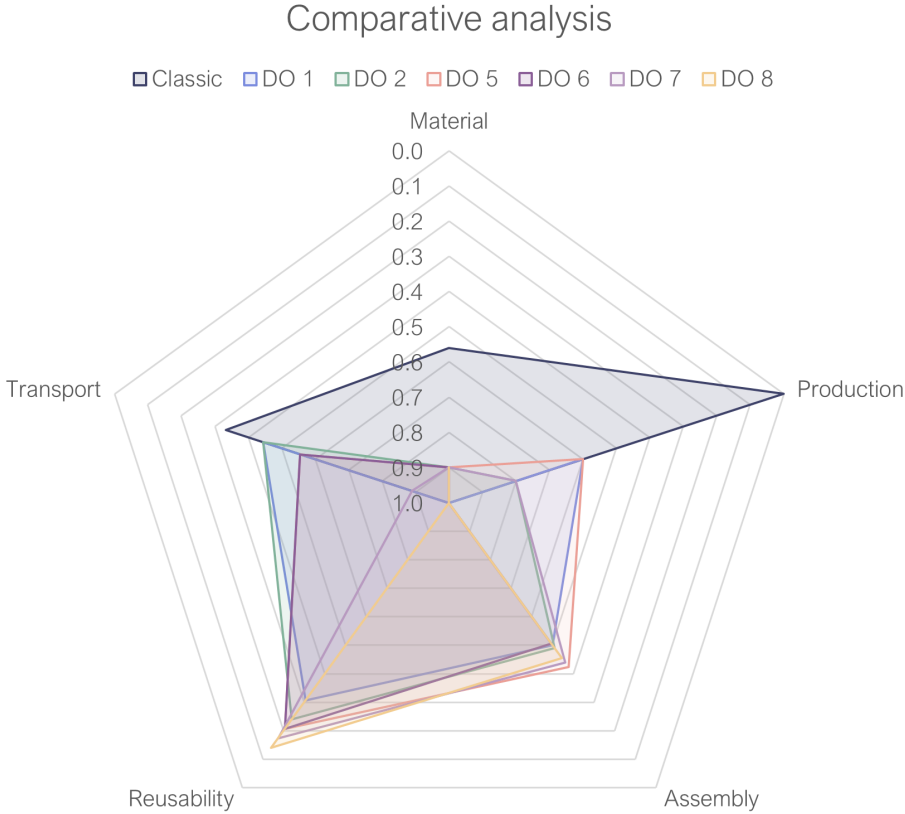
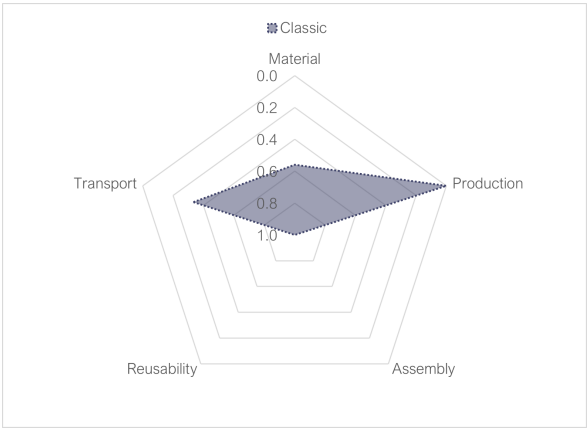
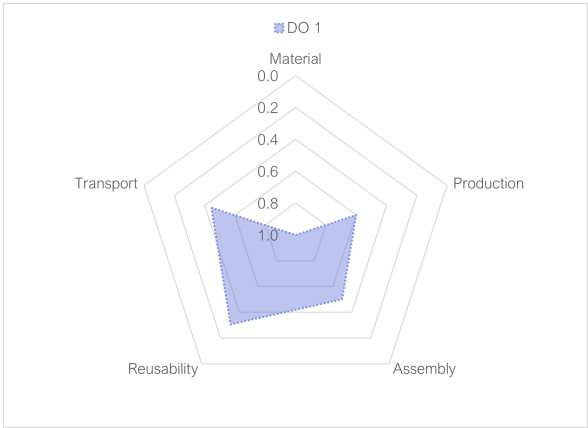


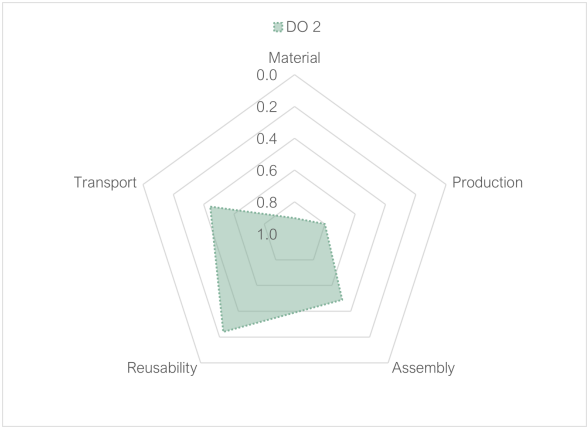
Figure 5.22: Geodesic Gridshell: Comparative analysis



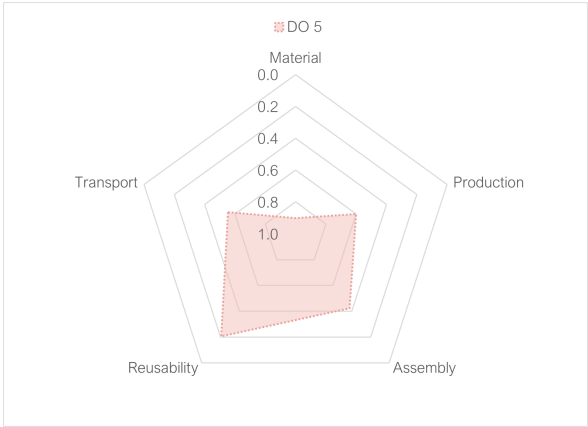
(a) Classic Geodesic Gridshell



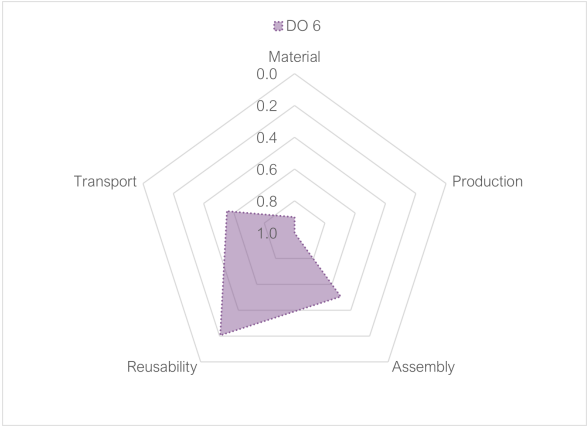
(b) Design Option 1



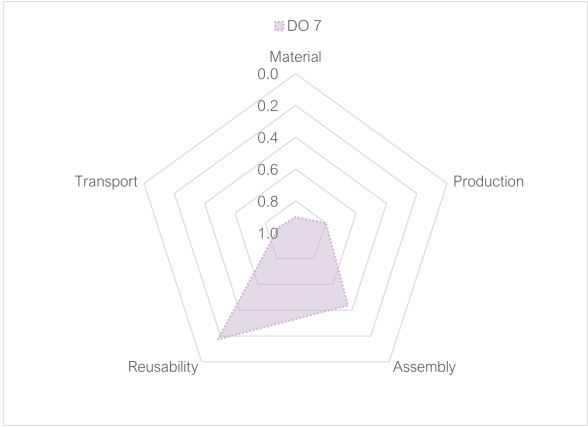
(c) Design Option 2



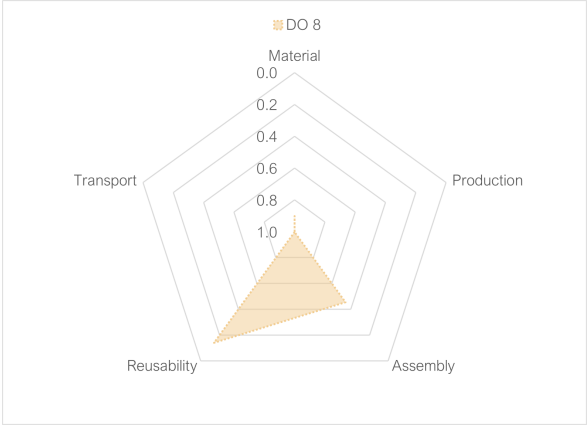
(d) Design Option 5



(e) Design Option 6



(f) Design Option 7



(g) Design Option 8

Figure 5.23: Geodesic Gridshell: Comparative analysis per design

5.5.2. Objective function

As previously mentioned, achieving a well balanced trade-off between different objectives is essential to identifying the most suitable designs. One possible approach is to combine the results of different objectives using an objective function, as explained in subsection 3.7.2. However, this is not strictly necessary for making a decision.

The weights in the objective function allow stakeholders' interests to be incorporated. A total of 100 points can be distributed across the different objectives, representing the percentage contribution of each one.

For the timber geodesic gridshell, multiple hypothetical weight distributions are considered. This also serves as a sensitivity analysis to determine whether different stakeholder interests influence the outcome. The distributions focus on cost, sustainability and time.

Cost

The first weight distribution prioritises cost before and during construction, rather than sustainability, time, or other specific interests, as shown in Table 5.6. The weight assigned to reusability is low since it only affects costs after the structure's service life. Transport has a slightly higher weight, as its impact on costs is minimal. Material and production have moderately higher weights because they contribute more significantly to overall expenses. Assembly, however, is assigned nearly four times the weight of material and production, as discussed in section 3.6, due to its influence on costs in four distinct ways. The final results of the objective function are shown in Table 5.7, showing that for Design Option 5, the objective function is minimised.

Table 5.6: Weight distribution: Cost

Objective	Weight
Material	15 %
Production	15 %
Assembly	55 %
Reusability	5 %
Transport	10 %

Table 5.7: Geodesic Gridshell: Objective function ranking Cost

Ranking	Design	Objective function
1	Design Option 5	0.52
2	Design Option 1	0.58
3	Design Option 2	0.58
4	Design Option 7	0.59
5	Design Option 6	0.63
6	Design Option 8	0.64
7	Classic geodesic gridshell	0.72
8	Design Option 3	-
9	Design Option 4	-

Sustainability

The second weight distribution prioritises sustainability, including circularity, as shown in Table 5.8. The weights assigned to production and assembly are low, as they have little impact on the structure's overall sustainability and circularity. Transport has a slightly higher weight, as its contribution to carbon emissions is relatively small. In contrast, material and reusability receive significantly higher weights due to their large influence on sustainability and circularity. The final results of the objective function are shown in Table 5.9, showing that for Design Option 5, the objective function is minimised.

Table 5.8: Weight distribution: Sustainability

Objective	Weight
Material	35 %
Production	5 %
Assembly	5 %
Reusability	40 %
Transport	15 %

Table 5.9: Geodesic Gridshell Objective function ranking Sustainability

Ranking	Design	Objective function
1	Design Option 5	0.53
2	Design Option 2	0.54
3	Design Option 6	0.56
4	Design Option 7	0.58
5	Design Option 8	0.59
6	Design Option 1	0.59
7	Classic geodesic gridshell	0.70
8	Design Option 3	-
9	Design Option 4	-

Time

The third weight distribution prioritises time, as shown in Table 5.10. Material, reusability, and transport are assigned low weights as they have little to no impact on the overall construction time. Production has a higher weight due to its significant influence on the construction time. However, assembly is given more than twice the weight of production, as it affects time in two distinct ways, as explained in section 3.6. The final results of the objective function are shown in Table 5.11, showing that for Design Option 5, the objective function is minimised.

Table 5.10: Weight distribution: Time

Objective	Weight
Material	5 %
Production	25 %
Assembly	60 %
Reusability	5 %
Transport	5 %

Table 5.11: Geodesic Gridshell: Objective function ranking Time

Ranking	Design	Objective function
1	Design Option 5	0.49
2	Design Option 1	0.54
3	Design Option 7	0.56
4	Design Option 2	0.57
5	Design Option 8	0.62
6	Design Option 6	0.64
7	Classic geodesic gridshell	0.69
8	Design Option 3	-
9	Design Option 4	-

Cost + Sustainability

The final weight distribution prioritises both cost and sustainability, with a primary focus on money, as shown in Table 5.12. Reusability and transport are assigned relatively low weights. While reusability contributes to sustainability in terms of circularity, it does not impact cost, and transport has little effect on either aspect. Production receives a slightly higher weight due to its moderate influence on cost. Material is assigned an even higher weight, as it affects both financial and sustainability considerations. However, assembly is given the largest weight, as it influences cost in multiple distinct ways. The final results of the objective function are presented in Table 5.13, showing that for Design Option 5, the objective function is minimised.

Table 5.12: Weight distribution: Cost + Sustainability

Objective	Weight
Material	20 %
Production	15 %
Assembly	45 %
Reusability	10 %
Transport	10 %

Table 5.13: Geodesic Gridshell: Objective function ranking Cost + Sustainability

Ranking	Design	Objective function
1	Design Option 5	0.54
2	Design Option 2	0.59
3	Design Option 1	0.59
4	Design Option 7	0.60
5	Design Option 6	0.63
6	Design Option 8	0.65
7	Classic geodesic gridshell	0.70
8	Design Option 3	-
9	Design Option 4	-

5.5.3. Material impact analysis

The material impact analysis is carried out to examine how production efficiency, assembly efficiency, reusability and transport efficiency affect material usage, as outlined in subsection 3.7.3. Specifically, it

investigates how material usage changes when a modular gridshell is chosen instead of a classic one.

Using the multi-objective scores in Table 5.5, the relative changes, C_m , C_p , C_a , C_r and C_t , between the classic gridshell and each modular design option are calculated using Equation 5.1. In this context, *modular* refers to any of the eight design options, 1 through 8.

$$C_o = \frac{F_{o,modular} - F_{o,classic}}{F_{o,classic}} \quad (5.1)$$

Table 5.14: Relative change C_o : Classic geodesic gridshell to modular geodesic gridshell

	Classic	DO 1	DO 2	DO 3	DO 4	DO 5	DO 6	DO 7	DO 8
C_m	-	0.786	0.607	0.286	0.446	0.607	0.607	0.607	0.607
C_p	-	-	-	-	-	-	-	-	-
C_a	-	-0.500	-0.510	-0.750	-0.620	-0.580	-0.490	-0.560	-0.550
C_r	-	-0.690	-0.760	-0.830	-0.830	-0.790	-0.790	-0.830	-0.860
C_t	-	0.333	0.333	-	-	0.697	0.697	1.697	2.030

Table 5.15: Material impact $\epsilon_{m,o}$: Classic geodesic gridshell to modular geodesic gridshell

	Classic	DO 1	DO 2	DO 3	DO 4	DO 5	DO 6	DO 7	DO 8	Average
$\epsilon_{m,p}$	-	-	-	-	-	-	-	-	-	-
$\epsilon_{m,a}$	-	-1.57%	-1.19%	-0.38%	-0.72%	-1.05%	-1.24%	-1.08%	-1.10%	-1.04%
$\epsilon_{m,r}$	-	-1.14%	-0.80%	-0.34%	-0.54%	-0.77%	-0.77%	-0.73%	-0.71%	-0.72%
$\epsilon_{m,t}$	-	2.36%	1.82%	-	-	0.87%	0.87%	0.36%	0.30%	1.10%

The relative change in production efficiency, C_p , cannot be calculated because the classic gridshell received a score of 0 for production.

These results highlight the trade-offs involved in choosing a modular design over a classic one. On average, material usage increases by 1.04% for every 1% decrease in assembly costs. Additionally, a 1% increase in reusability leads to a 0.72% increase in material usage. Finally, a 1% improvement in transport efficiency results in an average decrease of 1.10% in material usage.

5.6. Validation

In this section, the constraints discussed in subsection 3.2.1 are validated as described in section 3.8. The constraints are validated for all viable design options. Design Options 3 and 4 have already been classified as non-viable in the transport analysis, due to their element sizes.

First of all, the number of different joints is constrained to two. The intra-module joints are infinitely rigid and the inter-module joints are pinned in one direction. In addition, all beams in the structure have the same cross-section. These are all verified using the Eurocode and have utilisations below 1. Finally, transportation of the elements is possible, considering the maximum transport dimensions of a truck.

Therefore, the constraints are validated for all viable design options: Design Options 1, 2, 5, 6, 7 and 8.

5.7. Findings and discussion

The multi-objective comparative analysis provides a comprehensive overview of the performance of each design. This performance is based on the results of both the structural and construction analysis. This section discusses all results of this chapter.

5.7.1. Structural analysis

The structural analysis and its results indicate that the classic geodesic gridshell has the most optimal structural performance and therefore the best material efficiency. Both the ULS and SLS utilisations are relatively low and the buckling factor is relatively high compared to the designs of the modular gridshell. This can be explained by the locations of hinges in the structure. In the classic gridshell, hinges are located only at the nodes, with continuous beams spanning between them.

In contrast, the modular gridshell designs consist of rigid connections at the nodes but also include splice joints halfway along some of the beams. These interruptions reduce the overall stability of the structure, both locally and globally, resulting in lower structural performance.

The number of beam ends joined on-site in modular designs specifically also has a significant impact on the material use. These beam ends are connected using splice joints. An increase in splice joints, and consequently in on-site joined beam ends, generally corresponds with an increase in material use. For instance, Option 3 has relatively few splice joints and low material use, whereas other options with a greater number of splice joints or on-site joined beam ends require more material. Although the material use does not increase consistently with each added joint, it never decreases when the number of splice joints rises. This can be explained by the zero stiffness of the splice joints. These pinned joints negatively contribute to the overall stiffness of the structure, which leads to reduced stability. As a result, additional material is required to ensure the stability of the structure. This further supports the conclusion that designs with fewer splice joints have more favourable structural behaviour.

A comparison of material usage across various designs reveals that a lower number of elements does not necessarily lead to lower material use. For instance, while Options 3 and 4 have both a low number of elements and low material use, Options 7 and 8 use significantly more material, despite having a similar number of elements. This is due to the influence of the splice joints on structural efficiency. As previously discussed, the number of splice joints is affected not only by the number of elements but also by the shape of the modules. Consequently, both the structural behaviour and the material usage are influenced by these factors.

An exploration of the influence of rotational stiffness at splice joints compares four different stiffness values. The analysis shows that increasing rotational stiffness improves global stability, as demonstrated by a higher buckling factor. In addition, the results indicate that sufficiently high rotational joint stiffness can reduce the required cross-sectional dimensions.

5.7.2. Construction analysis

The results of the construction analysis indicate that the number of on-site joined beam ends does not directly correlate with the number of elements. For instance, Options 4 and 7 both consist of 26 elements, yet differ by 20 in the number of on-site joined beam ends. A similar contrast is observed when comparing Options 4 and 8. Although Option 4 has more elements, it contains fewer beam ends that have to be connected on-site.

This arises from the varying shapes of the modules. While the total number of elements is influenced by the size of the modular elements, the number of on-site joined beam ends is affected by both the size and the shape of these elements.

Figure 5.24 illustrates this point. The green module in Design Option 4 is the same size as the dark blue module in Design Option 8. However, their shapes differ significantly. The hexagonal sections of the modules connect in different ways, resulting in a varying number of on-site joints. In the green module of Option 4, there are three locations where the beams are continuous and do not contain splice joints, whereas in the dark blue module of Option 8, only two beams are continuous.

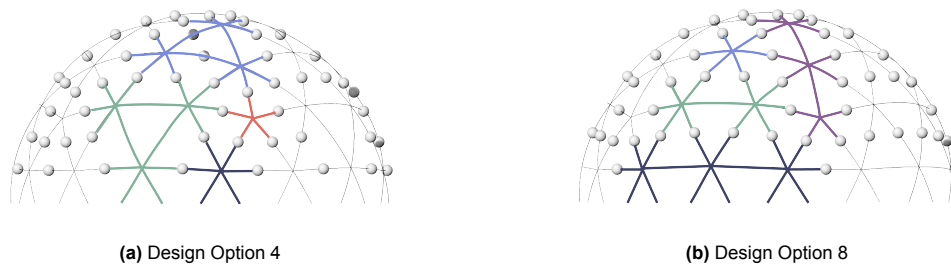


Figure 5.24: Geodesic Gridshell: Design Option 4 and 8, front view

5.7.3. Comparative analysis

The comparative analysis shows that opting for a modular gridshell over a classic one significantly reduces assembly costs and improves the reusability. In particular, modular designs with larger modules score well in reusability, which can be explained by the lower number of joints when modular elements are larger. However, the same does not apply to assembly, because that is also affected by the number of on-site joined beam ends and the number of element types.

However, modular gridshells require more trucks for transport, as their elements occupy more unused space. Specifically, modular designs with fewer, larger modules use more transport capacity. In some cases, for example in Options 2 and 3, the module dimensions even exceed transport limits.

In terms of production, the classic gridshell performs better than modular designs. This is caused by the number of module types, which is equal to zero, meaning that no production costs arise for assembling the beams into modules.

From the construction analysis, it is already clear that Design Options 3 and 4 are not viable for this structure. The elements in both designs are too large to be transported.

Nevertheless, both designs perform well across the remaining objectives. In terms of material efficiency, they score relatively high compared to other modular designs. This is primarily due to the use of large modules, which results in large areas without splice joints. This improves the both the local and global stability in the structure.

Furthermore, these designs get high results in the production and assembly categories. This is partly due to the limited variety of module types and the reduced number of on-site joints, particularly in Design Option 3. Additionally, the larger module sizes mean fewer individual elements are required, which significantly benefits the assembly process.

The radar charts in Figure 5.23 show that Options 7 and 8 perform unsuccessfully in three out of five categories: material, production and transport. The relatively large elements result in a high number of required trucks. However, the shape of these large elements is not sufficiently efficient to achieve a small number of on-site joined beam ends, and therefore does not improve either structural performance or material use. In addition, the high number of module types in these options adversely affects the production costs.

The classic gridshell and modular Design Option 6 also perform less favourably, each scoring low in two categories. The classic gridshell underperforms in assembly and reusability, primarily due to the use of individual beams, which results in a large number of separate elements. This limitation highlights one of the key motivations for introducing modularity in gridshell structures.

Option 6 performs poorly in terms of material use and production. The high number of splice joints reduces the structural efficiency, as previously discussed, leading to increased material use. Furthermore, the design incorporates a large variety of module types, which negatively impacts production efficiency.

In contrast, the most promising designs are Options 1, 2 and 5. Although Option 1 performs worst in material use, its performance in the other categories is comparable to Option 5. The increased material usage - and corresponding reduction in structural efficiency - is primarily due to the high number of splice joints. In this design, all potential splice joint locations are used, resulting in the maximum number of hinges.

Options 2 and 5 show comparable performance, which can be attributed to the similar designs: Option 5 is derived from Option 2. Nevertheless, Option 2 scores slightly higher in transport due to its

greater number of relatively small elements, whereas Option 5 achieves a better score in production as a result of its higher number of module types.

Based on the radar chart comparison, Options 5, 2, and 1 appear to be the most favourable designs. However, the final choice depends on stakeholder priorities and the intended use of the structure.

Focusing on the results of the objective function, Option 5 is consistently identified as the most preferred design across all weighting distributions applied in this study.

This outcome appears reasonable when considering the performance of this design across the various objectives. Option 5 performs well in terms of production and assembly, and achieves moderate scores in material use, reusability, and transport. While Options 3 and 4 perform better in most categories, which is mainly due to the use of large modules, as previously discussed, these designs are not viable due to transport limitations. Therefore, Option 5 presents a suitable alternative. The modules in this design are large enough to avoid a relatively low structural performance, yet small enough for transport.

In contrast, the use of even larger modules, as seen in Options 6, 7, and 8, results in an increased number of module and element types, which significantly reduces efficiency in both production and assembly. Moreover, the structural performance of these designs does not improve sufficiently to allow for a reduction in material usage.

Therefore, among all evaluated options, Design Option 5 scores highest in the objective function.

However, the rankings of the other options vary significantly depending on the applied weightings in the objective function. This indicates that the outcome of the objective function is highly sensitive to the specific interests and priorities of stakeholders. This result is not unexpected, as varying stakeholder priorities are likely to favour different objectives, and individual designs may perform very differently depending on which criteria are given greater importance.

However, across the various weight distributions, the classic geodesic gridshell receives consistently low rankings. This highlights the potential of modularity in gridshells.

The material impact analysis shows that improving the assembly efficiency and the reusability by opting for a modular design rather than a classic gridshell, requires an increase in material usage. Specifically, material consumption must increase by a similar proportion as the gain in assembly efficiency. An increase in assembly of 1% requires an increase in material of approximately 1%. However, to improve reusability, the necessary increase in material volume is smaller than the relative improvement in reusability. An increase in reusability of 1% only requires increase in material usage of 0.7%

Conversely, the transport efficiency generally decreases when a modular gridshell is chosen over a classic one. More precisely, when transport efficiency improves, the material usage decreases, though by a slightly greater proportion.

In conclusion, Design Option 5 is identified as the most favourable design overall. Furthermore, this study highlights that the outcome of the objective function is highly sensitive to the specific interests of stakeholders.

Design Options 3 and 4 could also be promising options, if the overall dimensions of the structure were smaller and transport was not a limiting factor.

The findings also indicate that well performing designs typically have relatively large modules, provided that they remain within feasible transport limits. However, it is important to note that increasing module sizes may lead to a more different element types, which in turn can reduce production and assembly efficiency.

6

Modular Geodesic Gridshell with Denser Grid

To demonstrate that the approach outlined in chapter 4 and chapter 5 can also be applied to gridshells with different properties, this chapter describes how the research method is applied to a timber geodesic gridshell with a denser grid. First, the preliminary study is discussed, followed by two designs for the modular geodesic gridshell.

The gridshell with a denser grid is formed by a base triangle, shown in Figure 6.1a, which is subdivided into 25 smaller triangles. The radius of the dome remains unchanged from the original structure and is still 10 metres. Figure 6.1b and Figure 6.1c present the top view and front view of the gridshell, respectively.

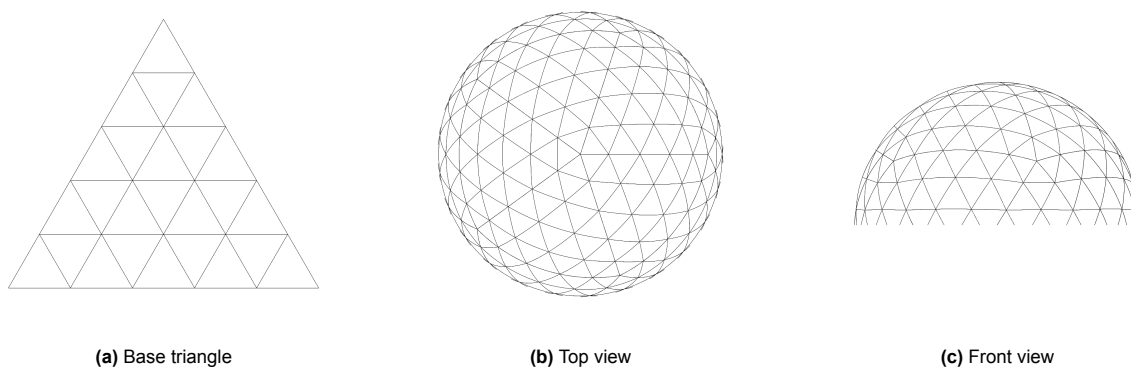


Figure 6.1: Geodesic gridshell with Denser Grid model

6.1. Preliminary study

This section presents the preliminary study of the gridshell with a denser grid, which is used as a benchmark for comparing different modular designs.

6.1.1. Classic Geodesic Gridshell with Denser Grid

The classic geodesic gridshell, composed solely of individual beams connected by hinges at each node, serves as a reference structure for evaluating the various modular designs. This structure is illustrated in Figure 4.4.

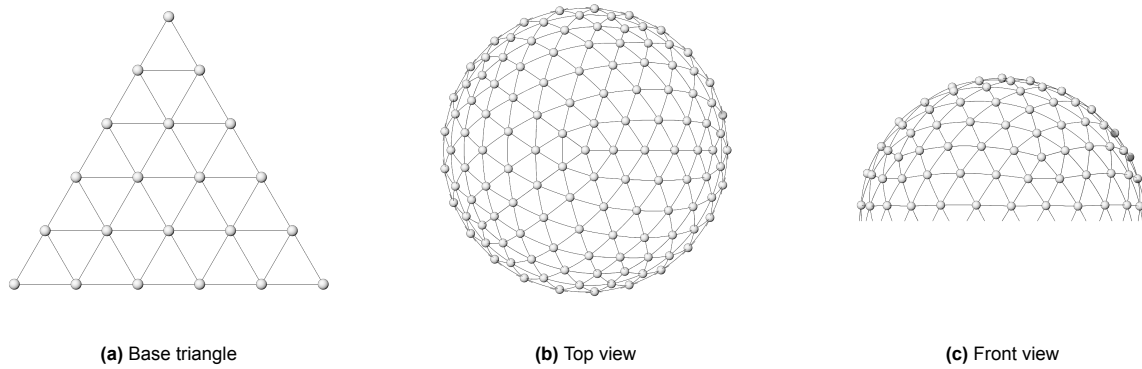


Figure 6.2: Benchmark: Classic geodesic gridshell with denser grid

6.1.2. Structural analysis

The finite element analysis is carried out in the same way as described in chapter 4. The model uses the same standard element length of 0.047 metres.

Cross-section sizing of the classic geodesic gridshell has resulted in a beam width of 150 mm, a height of 125 mm and a strength class of C30. The numerical results from the FEA are provided in section B.2. The axial stress and displacement diagrams can be found in section B.3.

6.1.3. Construction analysis

The construction analysis is also carried out in the same manner as previously described. The results for the classic geodesic gridshell with a denser grid are summarised in Table 6.1.

Table 6.1: Classic Geodesic Gridshell with Denser Grid: Construction analysis results

No. of elements (beams)	400
No. of module types	0
No. of element types	14
No. of on-site joined beam ends	750
No. of trucks	2

6.1.4. Findings and discussion

The preliminary study of the geodesic gridshell with a denser grid serves as a benchmark for evaluating the modular segmentation of the structure. The results of this study support the findings from the earlier research, discussed in section 4.5.

Firstly, the structural analysis results in low SLS utilisations, indicating that deflection and displacement are not dominant. Instead, ULS utilisations indicate once again that flexural buckling is the dominant failure mode. The ratio between the axial and bending deformation energy confirms that the bending energy is relatively high compared to the axial energy.

The construction analysis supports the key motivation behind developing a modular gridshell rather than a classic one. Specifically, it highlights that the classic gridshell contains a significantly larger number of elements due to the use of individual beams.

6.2. Modular designs

For the modular geodesic gridshell with a denser grid, two design options are developed. This section discusses the different design options. The structure is divided into modules using the same method as described in chapter 5.

6.2.1. Design Option 1

Figure 6.3a shows the base triangle used for this design. It consists of triangular shaped modules, which are based on the modules of Design Option 4 of the previous study (subsection 5.2.4). After projecting

the base triangle onto the hemisphere, some adjustments were made to achieve the intended pattern. Figure 6.3 shows the final design of Option 1.

The design contains of the red module, which is formed in each corner of the base triangle. It is the same red module as in the previous study and consists of five beams rigidly connected in the centre of a pentagon. In addition, the design includes triangular shaped modules represented by the light blue, green, dark blue and purple lines.

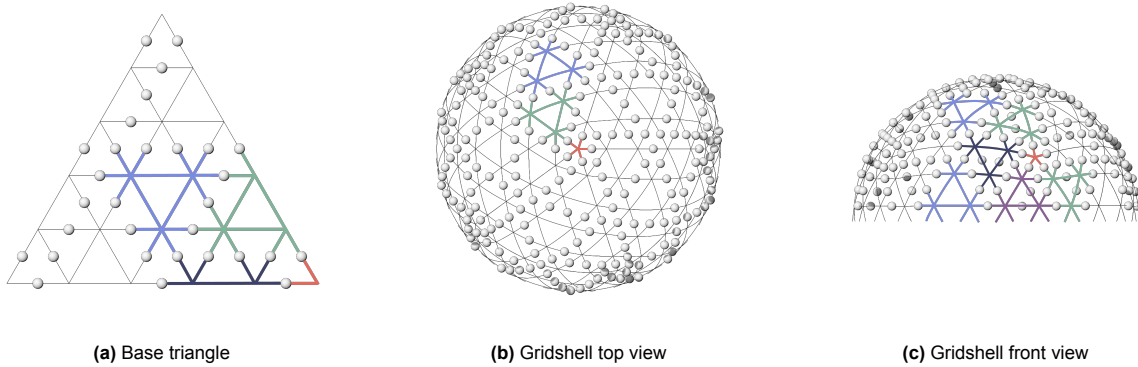


Figure 6.3: Geodesic Gridshell with Denser Grid: Design Option 1

6.2.2. Design Option 2

The second design is based on the module shapes from Design Option 2 of the previous study. Figure 6.4a presents the base triangle on which this structure is based. After projecting the base triangle onto the hemisphere, some adjustments were made to achieve the intended pattern. The final structure of Option 2 is shown in Figure 6.4.

The design also includes the red module, which is formed in each corner of the base triangle. Additionally, it consists of modules made from six beams, rigidly connected in the centre of a hexagon, represented by the light blue lines. These modules are similar to the light blue modules in the previous study. Another type of module appears twice along each side of the base triangle and twice within it. These are indicated by the green, dark blue and purple lines, and are also based on the modules from Design Option 2 of the previous study.

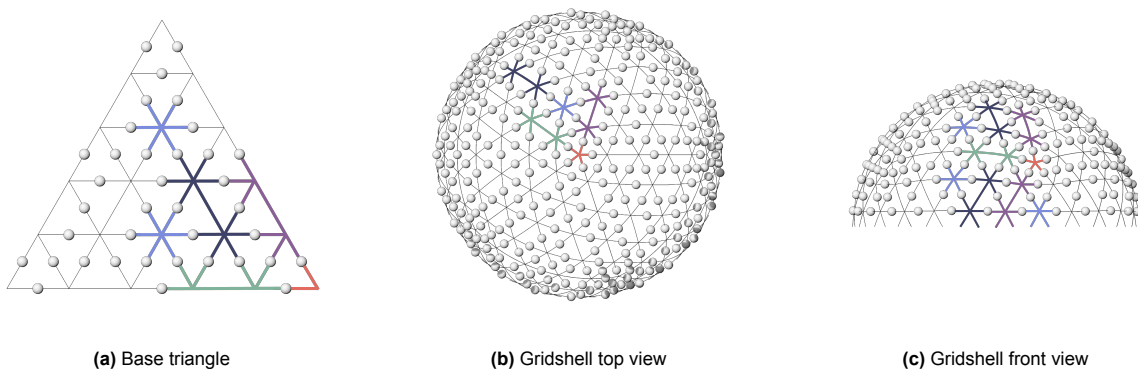


Figure 6.4: Geodesic Gridshell with Denser Grid: Design Option 2

6.3. Structural analysis

This section discusses the results of the structural analysis, which is performed in the same way as described in section 4.3 and section 5.3.

6.3.1. FEA results

The finite element analysis is performed on all design options using the reference cross-section with a width of 150 mm, a height of 125 mm and a strength class of C30.

The numerical FEA results and the ULS and SLS utilisation are presented in section B.2. Plots of axial stresses and displacements in the structure are shown in section B.3.

To compare the results of the preliminary study and all design options, Figure 6.5 and Figure 6.6 show bar charts of both SLS and ULS utilisations. section B.4 contains bar charts of all FEA results.



Figure 6.5: Geodesic Gridshell with Denser Grid: Displacement utilisation (SLS, 20 m span, C30, 150x125 mm)

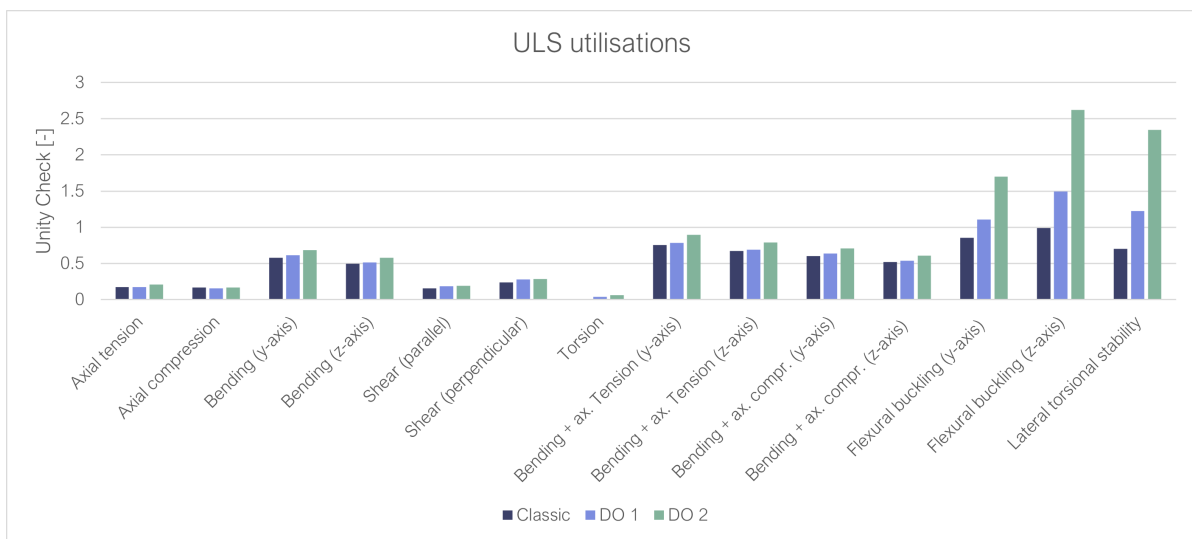


Figure 6.6: Geodesic Gridshell with Denser Grid: cross-section utilisation results (ULS, 20 m span, C30, 150x125 mm)

6.3.2. Global stability

The global stability is determined by both the first buckling modes, shown in Figure 6.7, and the buckling factors, presented in Figure 6.8.

Figure 6.7b and Figure 6.7d present the buckling mode of a modular gridshell, specifically Design Option 2. The buckling mode is similar to the modular gridshell of chapter 5 (Figure 5.15).

However, Figure 6.7a and Figure 5.15c show that the buckling mode of the classic gridshell with a denser grid is different to the one with a less dense grid, as shown in Figure 5.15. The first buckling mode occurs in a different load combination, in this case the load combination where the point load in

the centre of the dome is governing.

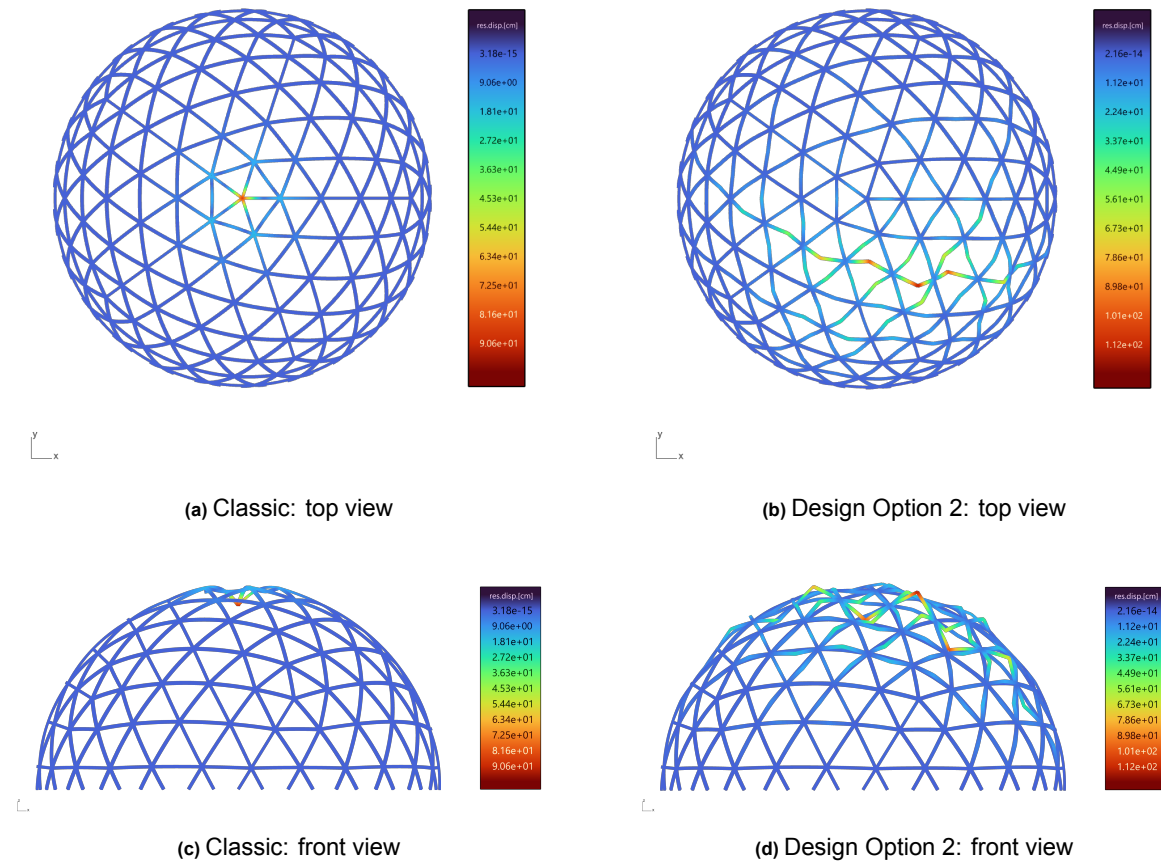


Figure 6.7: Geodesic Gridshell with Denser Grid: First buckling mode (ULS, 20 m span, C30, 150x125 mm)

The graph in Figure 6.8 shows the buckling load factors of the modular design options in comparison with the classic geodesic gridshell.

The buckling factors of both design options are bigger than 1, meaning that the structures have sufficient global stability.

6.3.3. Force distribution

Figure 6.9 shows the axial stress diagrams for the gridshell with a denser grid, comparing the classic gridshell with modular Design Option 2. Similar to the gridshell of chapter 5, the maximum axial stresses occur under the ULS load combination where the second snow load case is leading ($1.2G + 1.5Q_{snow,2}$).

The same differences as discussed in subsection 5.3.4 are noticeable. In the classic gridshell, high stresses occur slightly away from the nodes, as the nodes are hinged and do not take any bending moments. The nodes of the modular gridshell do transfer high axial stresses, as these nodes are rigid and consist of bending moments.

The same thing occurs at the hinges present in the modular gridshell. These do not transfer bending moments, resulting in lower axial stresses at these locations.

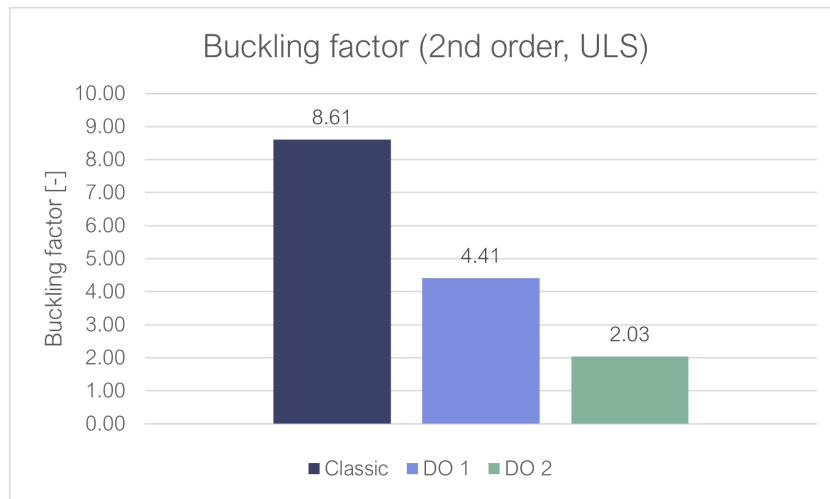


Figure 6.8: Geodesic Gridshell with Denser Grid: Buckling factor results (ULS, 20 m span, C30, 150x125 mm)

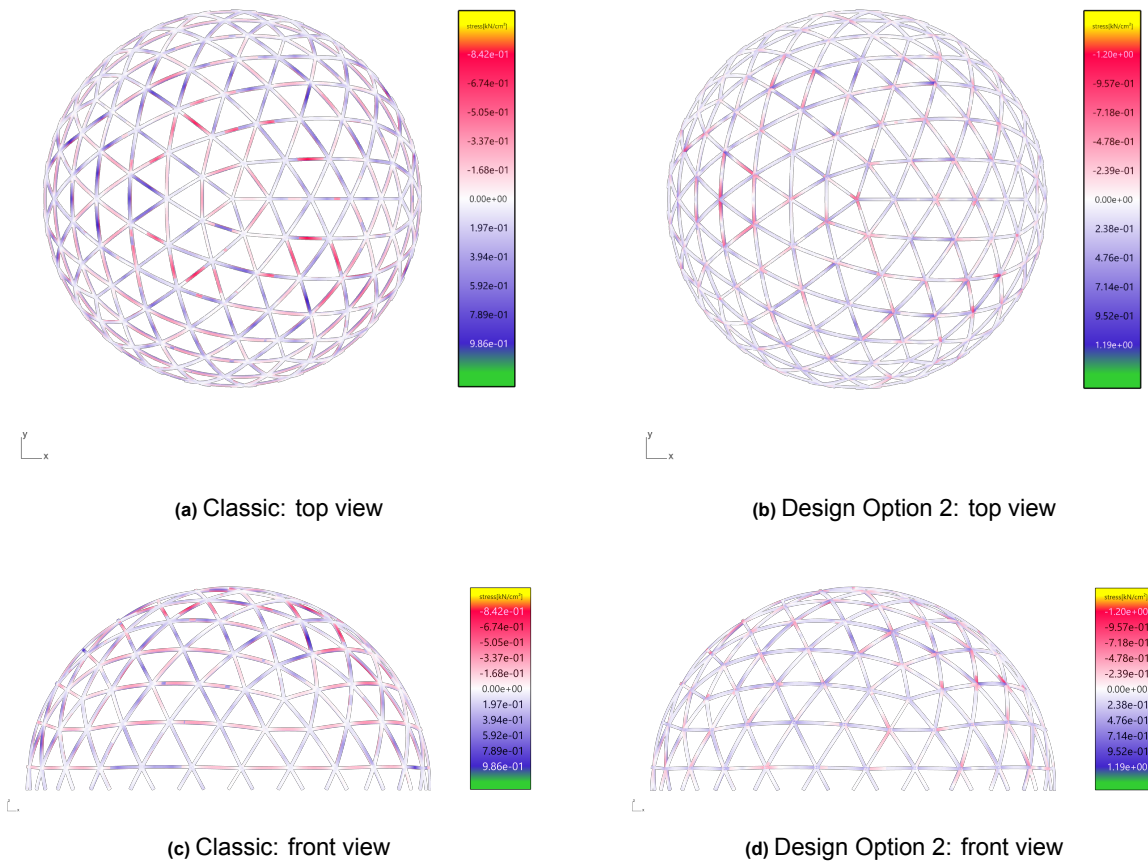


Figure 6.9: Geodesic Gridshell with Denser Grid: Axial stress (ULS, 20 m span, C30, 150x125 mm)

Figure 6.10 shows the normal force diagram of the classic gridshell and the modular gridshell, specifically Design Option 2. Again, the maximum normal forces occur under the ULS load combination where the second snow load case is leading ($1.2G + 1.5Q_{snow,2}$). Similar to Figure 5.18, it shows the tensile hoops in the bottom, shown by the blue normal forces, and the compression hoops in the top of the structures, shown by the orange normal forces.

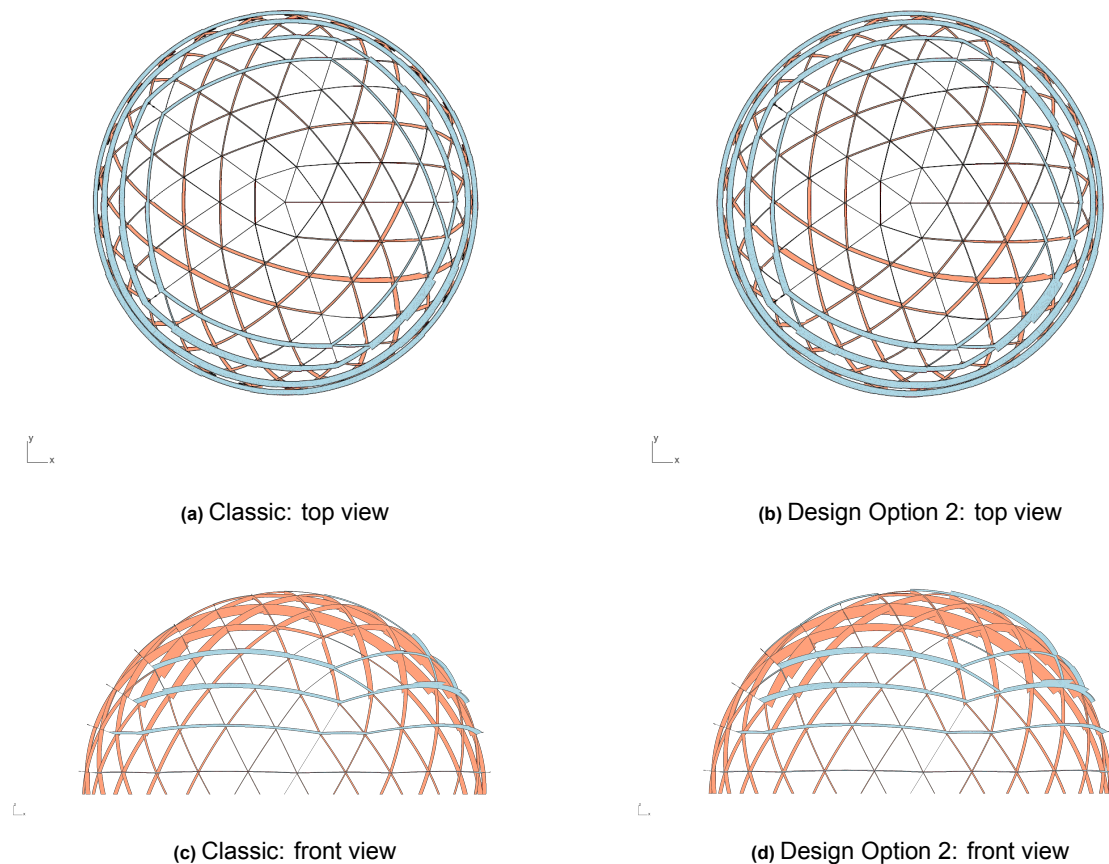


Figure 6.10: Geodesic Gridshell with Denser Grid: Normal forces diagram (ULS, 20 m span, C30, 150x125 mm)

6.3.4. Cross-section sizing

After using the cross-section of 150x125 mm as a benchmark, the required cross-section sizes of the design options are determined to satisfy strength and stability requirements, as explained in subsection 5.3.5.

Table 6.2 contains the results of the cross-section sizing, including the required cross-sections and the mass per m^2 of covered area. Table B.15 in Appendix B contains the SLS and ULS utilisations of all designs after the cross-section is adjusted. Figure 6.11 shows a comparison of the material use between all designs.

Table 6.2: Geodesic Gridshell with Denser Grid: Required cross-sections (20 m span)

Design	Strength class	Dimensions [mm]	Mass/area [kg/m^2]
Classic geodesic gridshell	C30	150x125	24.7
Design Option 1	C30	150x150	29.6
Design Option 2	C30	175x175	40.4

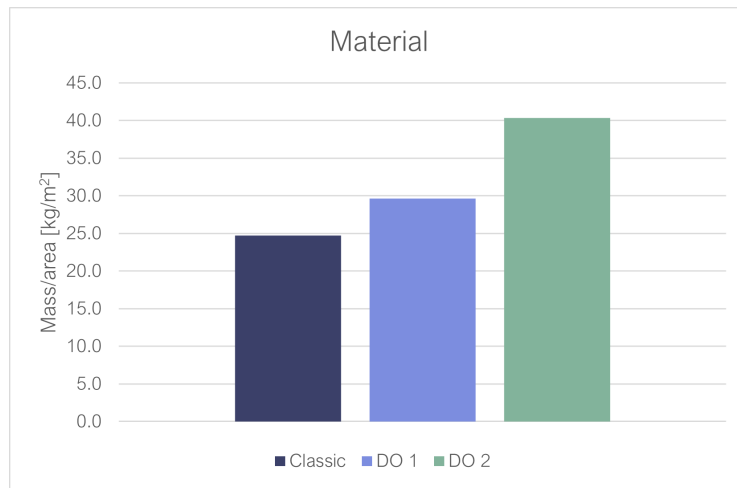


Figure 6.11: Geodesic Gridshell with Denser Grid: Material (20 m span)

6.4. Construction analysis

This section presents the results of the construction analysis, which is carried out in the same way as described in section 5.4.

Appendix E contains the transport analysis results, including the transport bounding box of all modules, and for all design options the number of trucks.

The results of the construction analysis are given in Table 6.3 and Figure 6.12 shows a bar chart of the results per category.

Table 6.3: Geodesic Gridshell with Denser Grid: Construction analysis

	Classic	DO 1	DO 2
No. of elements	400	46	76
No. of module types	0	3	5
No. of element types	14	3	5
No. of on-site joined beam ends	126	230	300
No. of trucks	2	- ¹	3

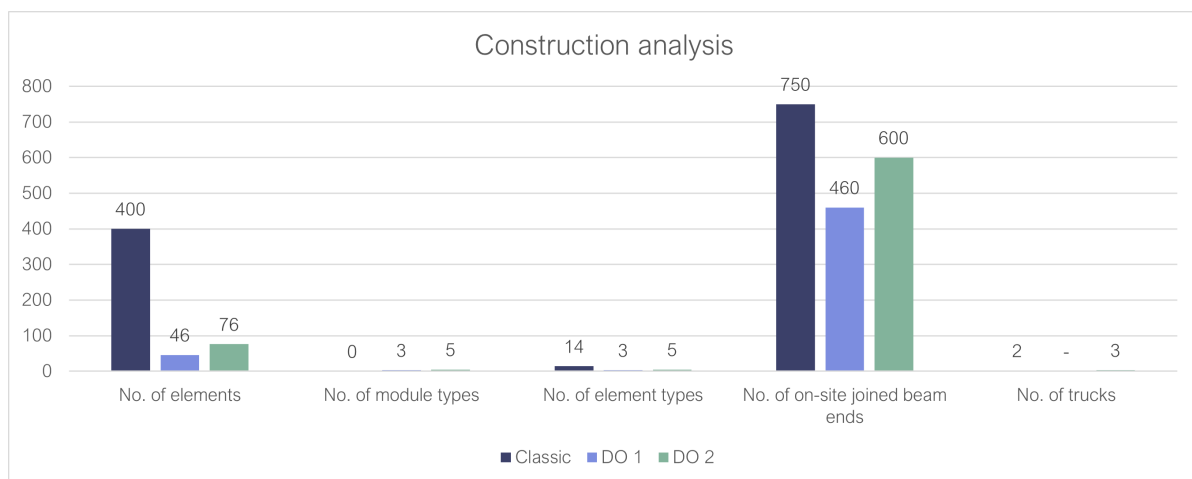


Figure 6.12: Geodesic Gridshell with Denser Grid: Construction analysis

¹No transport possible

6.5. Multi-objective comparative analysis

The multi-objective comparative analysis is carried out in the same way as described in section 5.5.

6.5.1. Scoring objectives

Table 6.4 gives an overview of the results of the structural and construction analysis. Table 6.5 presents the scores for each aspect, along with the total scores per category. Figure 6.13 shows a radar chart illustrating the scores per category, showing how the designs perform relative to each other.

Table 6.4: Geodesic Gridshell with Denser Grid: Structural and construction results

	Classic	DO 1	DO 2
Material			
Mass/area [kg/m ²]	24.7	29.6	40.4
Production			
No. of module types	0	3	5
Assembly			
No. of element types	14	3	5
No. of elements (x2)	400	46	76
No. of on-site joined beam ends	750	460	600
Reusability			
No. of elements	400	46	76
Transport			
No. of trucks	2	-	3

Table 6.5: Geodesic Gridshell with Denser Grid: Multi-objective scores

	Classic	DO 1	DO 2
Material			
Mass per area	0.61	0.73	1.00
Total	0.61	0.73	1.00
Production			
Module types	0.00	0.60	1.00
Total	0.00	0.60	1.00
Assembly			
Element types	1.00	0.21	0.36
Elements (x2)	1.00	0.12	0.19
On-site joined beam ends	1.00	0.61	0.80
Total	1.00	0.26	0.38
Reusability			
Elements	1.00	0.12	0.19
Total	1.00	0.12	0.19
Transport			
Trucks	0.67	-	1.00
Total	0.67	-	1.00

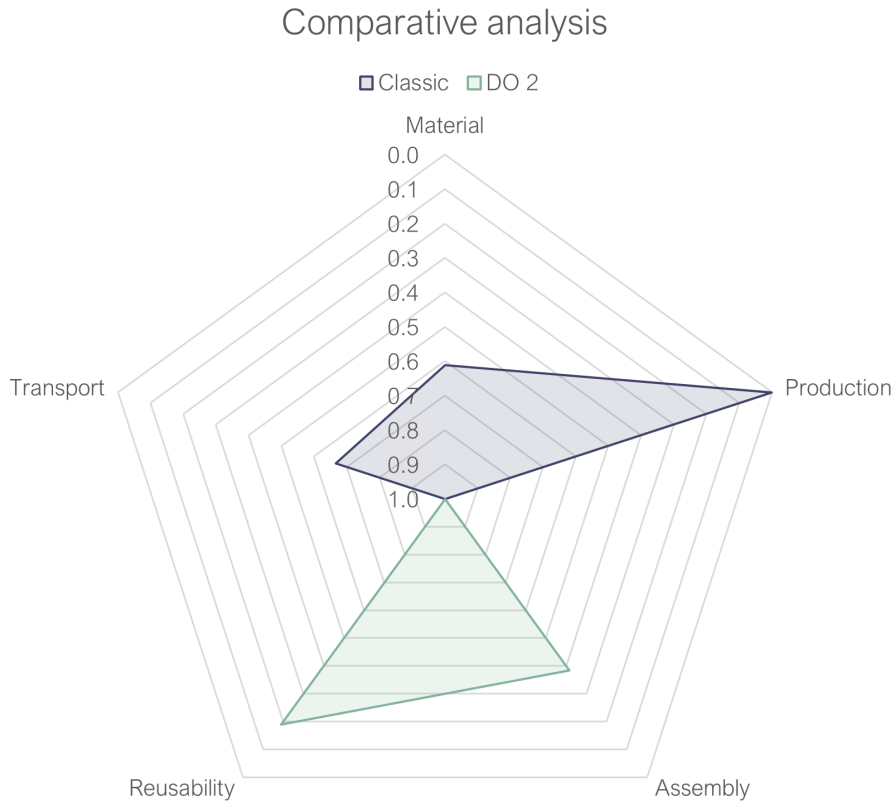


Figure 6.13: Geodesic Gridshell with Denser Grid: Comparative analysis

6.5.2. Objective function

This section provides the results of the objective function. The same weight distributions, focussing on cost, sustainability and time, described in subsection 5.5.2, are applied to the geodesic gridshell with a denser grid.

Cost

Table 6.6 shows the results of the objective function in which the weight distribution prioritises cost. It shows that for Design Option 2, the objective function is minimised.

Table 6.6: Geodesic Gridshell with Denser Grid: Objective function ranking Cost

Ranking	Design	Objective function
1	Design Option 2	0.62
2	Classic geodesic gridshell	0.76
3	Design Option 1	-

Sustainability

Table 6.7 shows the results of the objective function in which the weight distribution prioritises sustainability. It shows that for Design Option 2, the objective function is minimised.

Table 6.7: Geodesic Gridshell with Denser Grid: Objective function ranking Sustainability

Ranking	Design	Objective function
1	Design Option 2	0.65
2	Classic geodesic gridshell	0.76
3	Design Option 1	-

Time

Table 6.8 shows the results of the objective function in which the weight distribution prioritises time. It shows that for Design Option 2, the objective function is minimised.

Table 6.8: Geodesic Gridshell with Denser Grid: Objective function ranking Time

Ranking	Design	Objective function
1	Design Option 2	0.59
2	Classic geodesic gridshell	0.71
3	Design Option 1	-

Cost + Sustainability

Table 6.9 shows the results of the objective function in which the weight distribution prioritises a combination of cost and sustainability. It shows that for Design Option 2, the objective function is minimised.

Table 6.9: Geodesic Gridshell with Denser Grid: Objective function ranking Cost + Sustainability

Ranking	Design	Objective function
1	Design Option 2	0.64
2	Classic geodesic gridshell	0.74
3	Design Option 1	-

6.6. Validation

This section validates the constraints of the designs, as discussed in subsection 3.2.1 and section 3.8. Design Option 1 is already identified as non-viable by the transport analysis, due to the large element sizes.

For Design Option 2 all constraints can be validated. The number of different joints, which is equal to two, is correct. Also the number of different cross-sections in the structure is equal to the constrained value of one, and all beams have strength, stability and displacement utilisations below 1. The constraints regarding transport sizes are also validated by the transport analysis.

Therefore, all constraints of Design Option 2 are validated.

6.7. Findings and discussion

The earlier study presented in chapter 5 concludes that the classic geodesic gridshell offers the best structural performance and the lowest material use. This finding is confirmed in the current study, focusing on the gridshell with a denser grid. Once again, the classic gridshell has the most favourable structural behaviour and the most efficient material use, while the modular alternatives perform less effectively in these areas.

The findings in chapter 5 also highlights that choosing a modular gridshell over a classic one, leads to significant improvements in both assembly efficiency and reusability. This is confirmed in the current study, as shown in Table 6.5 and Figure 6.13. Modular designs continue to perform strongly in these two aspects.

However, as previously observed, modular gridshells perform less well in terms of transport and production. One of the modular options in this study is not even feasible from a transport perspective.

Regarding production, the classic gridshell again stands out, because it does not require the production of modules, resulting in no module production costs.

The construction analysis indicates early on that Design Option 1 is not suitable for this structure. Due to the size of its modules, the elements are too large to be transported. Despite this limitation, the design performs relatively well across all other criteria, suggesting it could still be a viable option for structures with an even denser grid, where the size of the modules could be less critical.

Figure 6.13 suggests that the decision between the classic gridshell and modular Design Option 2 is highly dependent on the specific priorities of the project and its stakeholders.

The objective function offers additional insight into this comparison. Design Option 2 achieves the highest scores across all weight distributions. Nevertheless, except under the sustainability focused weighting, the classic gridshell follows closely behind.

However, as noted in chapter 5, when sustainability is prioritised, a modular gridshell is a more suitable choice than a classic gridshell. This is confirmed by the results of the sustainability ranking in subsection 6.5.2, where the classic gridshell scores significantly lower than the modular design alternative.

In conclusion, while modular Design Option 2 emerges as the most preferable choice overall based on the objective function, the classic gridshell remains a promising alternative, particularly in scenarios where material use, transport efficiency and production efficiency are prioritised.

Given the limited scope of this study, which examines only two design alternatives, it would be beneficial to include a broader range of design options in future research of this structure. Based on the findings in chapter 5, it is recommended that these designs incorporate large modules, provided that they remain within transport constraints. Additionally, further development of Design Option 2 is encouraged. Creating and evaluating variations of this design may lead to improved overall performance.

7

Discussion

This chapter reflects on the key findings presented throughout the study. The previous chapters provide insights into structural behaviour, construction efficiency, and overall design performance of different gridshell designs. By comparing various modular design options through structural analyses, construction analyses and multi-objective evaluations, a deeper understanding has been gained of how modularity affects the overall feasibility and performance of a geodesic gridshell.

The discussion is divided into five main sections. First, the structural performance of classic and modular gridshells is discussed. Next, the performance of modular designs is compared to classic gridshells. Subsequently, the differences between modular design alternatives are observed. Next, the process of selecting the most suitable design is explored, with a focus on the sensitivity of the objective function to stakeholder priorities. Finally, the impact of grid density on structural and construction aspects is examined, comparing results across the two case studies.

Together, these discussions help putting the findings into perspective.

7.1. Structural performance

The structural analyses presented in chapter 4, chapter 5 and chapter 6 provide insight into the structural behaviour of various timber geodesic gridshell designs. These analyses allow for a comparison of the structural performance between classic geodesic gridshells and modular alternatives, as well as among the different modular designs themselves.

Firstly, the results of the Finite Element Analysis (FEA) offer a general understanding of the structural behaviour of the gridshells. The analysis, carried out for both the Ultimate Limit State (ULS) and Serviceability Limit State (SLS), reveals that the ULS checks are governing. Specifically, flexure buckling is identified as the critical failure mode in both the classic and the modular timber geodesic domes.

Cross-section sizing, conducted as part of the structural analysis, further illustrates the performance differences between the designs. In both chapter 5 and chapter 6 it is found, based on material usage and overall stability, that classic geodesic gridshells have the most favourable structural performance. These structures require the least amount of material and demonstrate relatively high buckling factors. Based on these findings, it can be stated that the method used in this study for the design of modular gridshells does not positively contribute to the structural behaviour.

This performance difference can be attributed to the differences in joint configuration. The classic gridshells consist of only pinned joints at the nodes, locations where multiple beams meet, resulting in uninterrupted, continuous beams in between these nodes. Conversely, in modular gridshells, certain beams are divided into two equal segments and joined using pinned splice joints, while the nodes themselves are rigidly connected. These mid-span interruptions reduce the overall stability of the structure, thereby leading to less desirable structural behaviour.

Therefore, it is important to evaluate whether opting for a modular gridshell over a classic one offers sufficient improvements in other aspects, such as assembly and reusability. These considerations depend on preferences and interests of stakeholders and can be explored through the multi-objective comparative analysis.

Furthermore, the study in chapter 5 indicates that among the modular designs, those with relatively large modules have a higher structural performance than those with smaller modules. This finding is

supported by both reduced material requirements and higher buckling factors. The improved performance of larger modules can be explained by the greater uninterrupted spans they allow, due to the reduced number of splice joints, thus maintaining more beam continuity.

As discussed earlier, the pinned splice joints in the modular gridshell have a negative effect on the overall structural performance. Because the splice joints are pinned, large rotations are possible, reducing the stability. A study on the effect of rotational stiffness at these joints shows that increasing rotational stiffness enhances the overall stability of the structure. A sufficiently high level of rotational stiffness can also reduce the amount of material required.

Based on these four observations, four key findings can be drawn. Pinned splice joints negatively affect the overall stability of gridshells, which means that this method of segmenting gridshells into modules negatively affects the structural performance. Because of this, modular gridshells generally require more material than classic ones, and this material demand increases with smaller modules due to the higher number of splice joints. However, the increase in material usage can be limited by increasing the rotational stiffness at splice joints. In addition, using larger modules, and thus fewer splice joints, improves both local and global stability.

7.2. Classic versus modular gridshells

The multi-objective comparative analyses presented in chapter 5 and chapter 6 provide a comprehensive comparison between all design alternatives. This section first summarises the key findings from the comparison between classic and modular gridshells.

As discussed previously, the use of material increases significantly when opting for a modular gridshell over a classic one. This can be assigned to the modular approach used in this study. In addition, production efficiency declines due to the higher manufacturing costs resulting from prefabricating modular elements instead of individual beams. Transport efficiency is also reduced, primarily because modular elements do not utilise space in transport as effectively.

However, introducing modularity to gridshells also leads to improvements in performance. Firstly, assembly efficiency increases as fewer elements are required on-site and fewer beam ends have to be connected on-site. The reusability of elements improves likewise, which is again attributed to the reduced number of structural components. Furthermore, the application of the objective function in the multi-objective comparative analysis demonstrates that choosing a modular gridshell over a classic one consistently improves the sustainability of the structure. This is mainly the result of a lower number of elements, which improves both the demountability of the structure and the circularity of the materials.

To quantify the advantages of adopting a modular approach for a gridshell structure over a classic design, the relative changes across key performance objectives are considered. As shown in Table 7.1, these differences are based on a comparison between the classic gridshell and the most favourable modular design, Design Option 5, using the data presented in Table 5.14.

Table 7.1: Relative changes when choosing modularity over classic design

Objective	Relative difference
Material efficiency	-61%
Production efficiency	-
Assembly efficiency	+58%
Reusability	+79%
Transport efficiency	-70%

The material impact analysis focuses specifically on the relative increase in material usage when improving other objectives through the use of modularity. It is found that increasing assembly efficiency by 1% requires an almost equivalent relative increase in material usage. Conversely, improving reusability by 1% results in a proportionally smaller material increase, namely 0.7%.

The overall trade-offs show that applying modularity brings both advantages and drawbacks, depending on the specific goals of the project. It is therefore important to accurately consider the interests of all stakeholders. Based on the findings described above, it can be stated that applying modularity to gridshells is particularly beneficial when the primary objective is to maximise the reusability of elements. Although improving assembly efficiency requires a relatively higher material increase, modular designs always offer a combination of improved assembly efficiency and reusability.

7.3. Modular designs

Having compared classic and modular gridshells, the discussion now turns to the differences among the modular designs themselves.

As discussed earlier, designs with larger modules show higher local and global stability along with lower SLS and ULS utilisations. As a result, these designs require less material than those with smaller modules.

In addition, larger modules lead to improved assembly efficiency and higher reusability. This is primarily due to the reduced number of elements in the structure, the same reason why modular gridshells perform better in these aspects than classic ones, as discussed previously.

However, increasing module sizes can result in greater variety of module types within the structure, which in turn reduces both production and assembly efficiency. Designs that limit the variation of module types and reduce the number of splice joints are likely to perform better in terms of production and assembly. Therefore, when increasing module sizes, it is essential to assess different alternatives to ensure minimal variation in modular elements. Moreover, it is important to stay within the transport limitations when increasing module sizes.

The comparison also shows that the number of splice joints does not directly correspond to the number of elements. Fewer modular elements in a design does not necessarily mean fewer splice joints or improved stability. This is because the number of splice joints also depends on the shape of the modules. Therefore, it is important to consider the module shapes and their effect on the overall joint configuration within the structure.

From these findings, three key aspects of a well performing modular design can be identified:

- Module sizes are maximised, while remaining within transport limits;
- Module shapes are designed to minimise the number of splice joints;
- Increasing module size is done with minimal variation in module types.

7.4. Design selection

To determine the most suitable design among all alternatives, the objective function serves as a helpful decision-making tool. However, its outcome is highly sensitive to stakeholder interests and project-specific goals. Although the first-ranked design remains consistent, the sensitivity of the objective function becomes evident in the lower-ranked options, where the ranking significantly varies depending on the weighting.

Despite this sensitivity, in both chapter 5 and chapter 6 a clear preference is observed regardless of the different weightings applied to the objective function.

For the gridshell analysed in chapter 5, Design Option 5 is identified as the most favourable design, shown in Figure 7.1. This design consists of medium sized modules that balance structural performance with transport limitations.

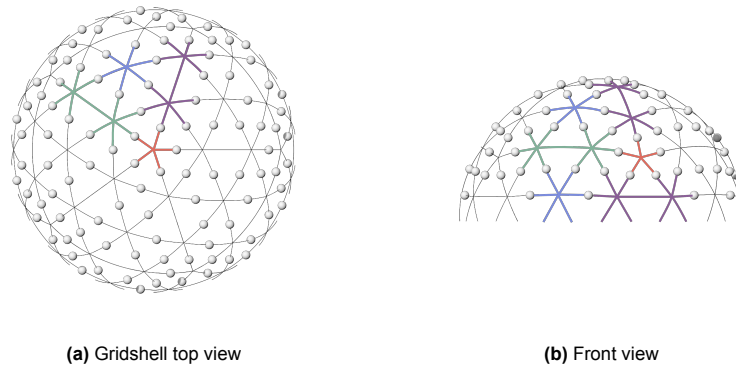


Figure 7.1: Geodesic Gridshell: Design Option 5

In the case of the denser geodesic gridshell in chapter 6, only two design options are evaluated, resulting in a considerably narrower scope. Nonetheless, the findings confirmed those of chapter 5. Design Option 2, shown in Figure 7.2, appears to be the preferred design, primarily due to transport limitations that made Design Option 1 unviable.

That said, the limited scope of chapter 6 must be considered. Including a wider range of design options or refining Design Option 2 further could potentially lead to different outcomes.

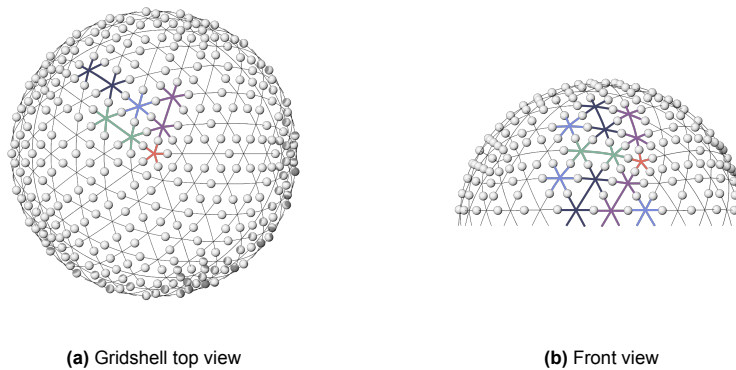


Figure 7.2: Geodesic Gridshell with Denser Grid: Design Option 2

7.5. Grid density

This section compares the differences between the two grid densities. Figure 7.3 shows the two gridshells analysed in this study, with the one from chapter 6 featuring a denser grid than the gridshell in chapter 5.

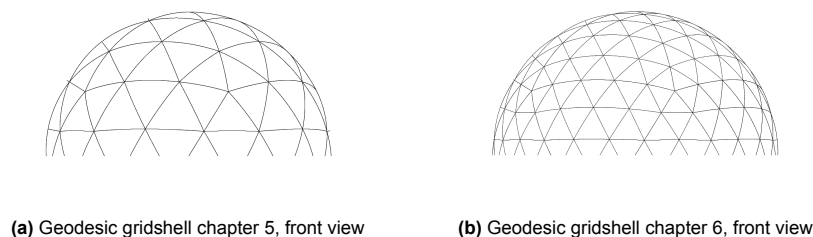


Figure 7.3: Geodesic gridshells with different grid densities

Structural analyses reveal notable differences in structural behaviour. In both the classic and modular designs, the denser gridshell requires significantly smaller cross-sections. It also contains less total

material, despite having more elements. This is explained by the denser grid's greater total beam length and shorter distances between nodes, reducing span lengths of beams. These shorter spans lead to smaller bending moments and a more efficient force distribution. As a result, the beams in the denser gridshell are locally more stable.

In contrast, the classic version of the denser gridshell is globally less stable than the less dense gridshell. The buckling factor of the gridshell in chapter 5 is almost 1.5 times higher than the denser one. This reduced global stability is likely caused by the higher number of pinned nodes in the denser design, which makes the structure less form fixed. However, since local stability is the governing factor, it ultimately determines the required material use.

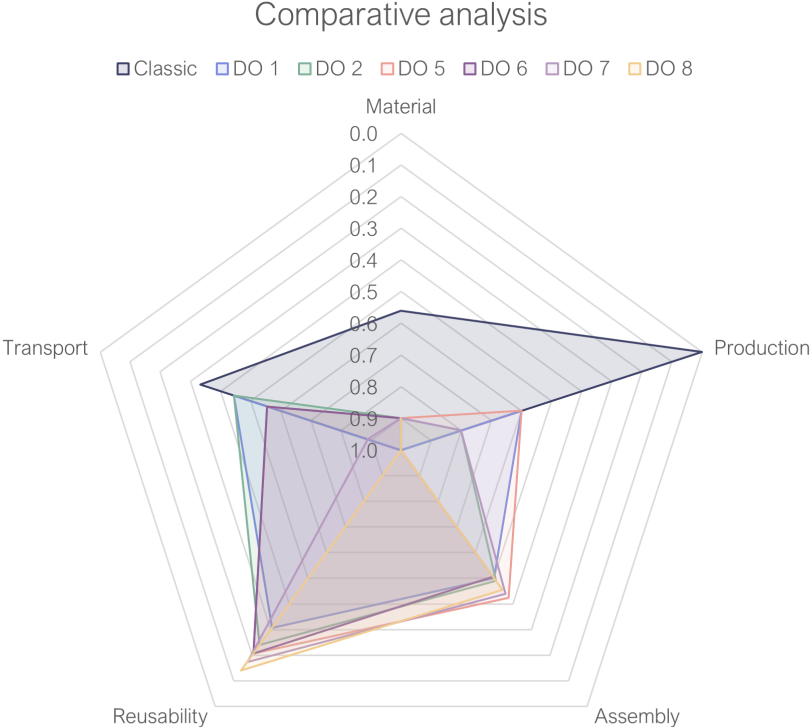
For the modular versions, no significant differences in global stability are observed between the two grid densities. The buckling factors are similar, which is likely due to the use of rigid joints in the modular designs, in contrast to the pinned nodes of the classic designs.

In summary, the denser gridshell has a better local performance and requires significantly less material due to more efficient force distribution. Although the classic version of the denser gridshell is globally less stable, local behaviour is governing, resulting in significantly lower material use.

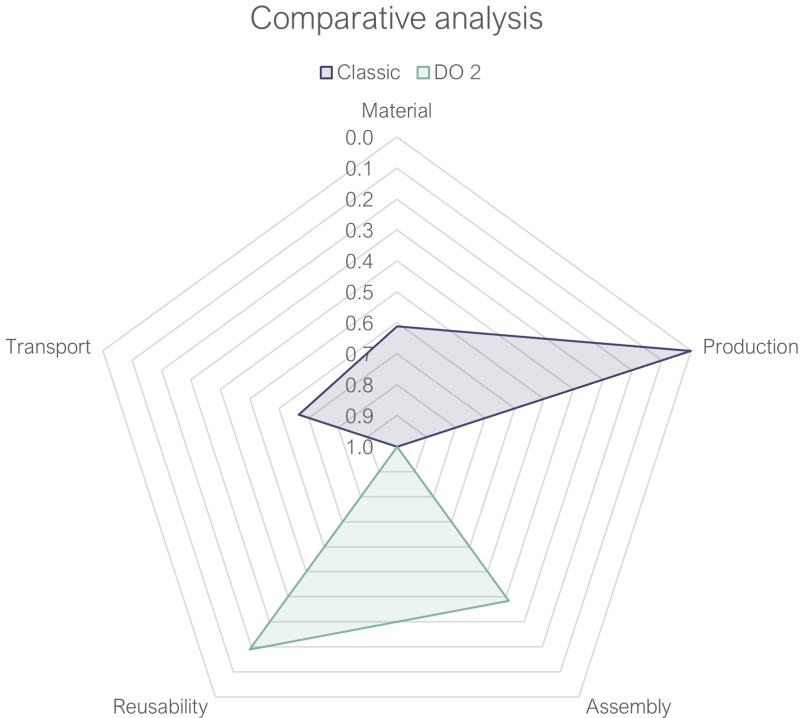
The construction analyses also reveal differences. A direct comparison between the modular gridshells is not possible due to the limited number of design options in chapter 6. However, for the classic versions, the denser gridshell includes significantly more elements and on-site joined beams. This is a result of applying a denser mesh over the same dome span, leading to more beams and, in turn, more joints. Additionally, the number of beam types is higher, due to the larger number of beams within the base triangle (see Figure 6.2a).

Lastly, the multi-objective comparison results are discussed. Figure 7.4 shows the radar charts of the comparative analysis for both grid densities. The classic gridshells produce similar radar chart shapes. Furthermore, the radar chart of Design Option 2 in chapter 6 is similar to those of Design Options 7 and 8 in chapter 5.

The objective function from chapter 6 also reveals that for the denser grid, the classic gridshell becomes a good alternative to Design Option 2 when prioritising cost, time, or a combination of cost and sustainability. However, it performs less favourably when sustainability is considered independently. In contrast, the results from chapter 5 show that, for the less dense grid, the classic gridshell scores considerably lower than the top modular option. This inconsistency is likely due to the limited number of design alternatives evaluated in chapter 6.



(a) Geodesic Gridshell chapter 5



(b) Geodesic Gridshell chapter 6

Figure 7.4: Multi-Objective Comparative Analysis, radar charts



Conclusion and Recommendations

This research aims to answer the following main research question: **How can the modular segmentation of timber gridshells be designed to optimise their structural and construction efficiency?**

The research has been divided into five sub questions to answer the main research question:

1. What are the key aspects of the structural design of a timber gridshell?
2. What parameters mainly influence the structural behaviour of a timber gridshell, and how?
3. How can a modular gridshell be generated in terms of the geometrical design of modules and the allocation of joints?
4. How does the design of modular segmentation influence the structural performance of a timber gridshell?
5. How can modular segmentations be designed to optimise the structural performance and maximise the reusability of elements, as well as the efficiency of production, assembly and transport?

This chapter provides an overview of the research conclusions based on these questions. From this, the final conclusion is drawn to answer the main research question. Lastly, the limitations of the study are discussed along with design recommendations and recommendations for further research.

8.1. Conclusion

From the literature review, it can be concluded that there are several key aspects and parameters influencing the design of timber gridshells. These aspects influence the structural behaviour, material usage, construction feasibility, financial feasibility and sustainability of the structure.

Stability is the primary design criterion for gridshells, which makes the consideration of rotational stiffness in joints essential. The geometry of both the surface and the grid significantly influences structural performance and aesthetics. Grid related aspects include beam length, curvature, torsion, and node angles, while surface geometry includes overall shape and curvature. An important distinction is the type of gridshell in terms of bending. Bending active beams are elastically deformed into shape, while bending inactive beams are initially curved or straight and do not undergo deformation before construction. Incorporating modularity can improve construction and financial aspects. However, complexity of joints resulting from the implementation of modularity, plays a critical role in determining the overall feasibility of the structure.

The main parameters that affect the structural behaviour of timber gridshells include: joint stiffness, boundary conditions, imperfections, slenderness of members, cross-sectional properties, geometry, grid topology and load conditions. These parameters primarily influence the structure's susceptibility to both global and local buckling.

This research has developed a method to generate modular gridshells, taking into account both geometric design of modules and configuration of joints. A distinction is made between rigid intra-module joints, which connect beams within a module, and pinned inter-module joints, which connect modules to one another. The intra-module joints are located at all structural nodes, while the inter-module joints are splice joints that longitudinally join two beams. The exact location of the splice joints determines the geometry of the resulting modules, as illustrated in Figure 5.1b.

The method determines the overall joint configuration by manually selecting the splice joint locations on either the base triangle of the gridshell or on the overall structure. Beam continuity is maintained

between nodes where no splice joint is placed.

In terms of structural performance, it is found that local flexural buckling is the dominant failure mode. The modular segmentation method negatively affects structural performance due to the presence of pinned splice joints, which reduce overall stability. Consequently, modular gridshells typically require more material than classic gridshells. However, the research also shows that increase in material usage can be limited by increasing the rotational stiffness of the splice joints. This highlights the importance of exploring whether the modular design offers enough benefits in other building aspects, such as construction or reusability, to align with stakeholder priorities.

Additionally, it is found that increasing the module sizes improves structural performance, primarily because it reduces the number of beam interruptions. Therefore, modular gridshells with larger modules generally require less material than those with smaller modules.

This research has also developed a method for optimising modular gridshell design by considering not only structural performance, but also the reusability of elements and the efficiency of production, assembly and transport.

Once the study parameters and constraints are set, multiple modular design options are generated. Structural performance is assessed using Finite Element Analysis (FEA) and cross-section sizing, determining the required material for each design. Construction performance is evaluated through factors such as the repetition of modules, number of elements, joints that have to be assembled on-site, and transport feasibility.

These assessments result in indicators for production, assembly and transport efficiency, as well as reusability. Subsequently, the multi-objective comparative analysis assigns scores to each design across five categories: material, production efficiency, assembly efficiency, reusability and transport efficiency. This allows for a clear comparison of qualities across different design options. An objective function is introduced to help incorporate stakeholder interests and project goals into the decision making process to select the most suitable designs.

Finally, the method is applied to a timber geodesic gridshell dome with two different grid densities as a case study. From this application, it can be concluded that the use of modularity in this manner has both advantages and disadvantages. While it improves the assembly efficiency and reusability by 58% and 79% respectively, it has a negative impact on material usage. Material usage increases by 61% when opting for a modular gridshell over a classic one. In addition, both production and transport efficiency decline when modularity is applied to a gridshell. Production efficiency decreases by an unknown number, as the production of individual beams is not considered in this research. Transport efficiency decreases by 70% when modularity is used.

It is found that choosing a modular design over a classic one using this approach for modularity, is particularly beneficial when reusability is the primary design objective, as the required relative increase in material is only 70% of the relative reusability gain. It is therefore important to align the design strategy with stakeholder priorities.

Furthermore, it can be concluded that modular designs perform best when module sizes are maximised, while still staying within transport constraints. Structural performance and construction efficiency also benefit when module shapes are designed to minimise the number of splice joints, and when module sizes are increased with minimal variation in module types.

In the application to the geodesic gridshell with a less dense grid, the most favourable design is Design Option 5. In the application with the denser grid, Design Option 2 is the most suitable. However, the latter case study has a more limited scope, which may have affected its outcome.

Comparing the two different grid densities shows that the denser modular gridshell requires less material due to improved structural performance. In addition, the multi-objective comparative analysis shows results that are similar between the different case studies.

The approach of this research uses a timber geodesic gridshell dome as a case study, but has the potential to be applied to gridshells in general.

In conclusion, this research demonstrates that while modular segmentation introduces structural challenges, it can significantly improve other aspects of gridshell construction, particularly assembly and reusability. The developed method supports a design approach that helps to balance structural effi-

ciency with construction efficiency, guided by project specific priorities and stakeholder goals.

8.2. Research limitations

The application of this research is limited to a timber gridshell with a specific grid topology, shape and span. While the developed method can serve as a framework for studying modular gridshells more broadly, this study does not extend to gridshells constructed from alternative materials or featuring different grid topologies, shapes or spans.

Moreover, the analysis is based on a single set of boundary conditions and joint stiffnesses. In particular, the assumption of zero stiffness in the splice joints is a limitation of this study. A small analysis of the effect of joint stiffness in modular designs already shows that incorporating splice joints with rotational stiffness could improve the structural performance. It can also reduce the amount of material required, and simplify joint designs, thereby improving the overall performance.

Additionally, this research explores only one specific approach to modular segmentation. While gridshells can be modularly segmented in various ways, the method presented here represents just one of many possible strategies. That said, the conclusions drawn apply only to this particular segmentation approach and may not directly translate to other methods of modularity.

The application of the method to the geodesic gridshell with a denser grid has a narrower scope. This case study explores only two design options, in contrast to the eight considered for the less dense grid. The denser grid case study is primarily included to demonstrate how the approach can be used for different geometries. However, due to the limited amount of design options, it is not possible to make a direct comparison between the outcomes of the two gridshell configurations.

8.3. Design recommendations

Based on the findings of this research, several recommendations can be made for the design of modular gridshells. A well performing design should focus on the following aspects:

- Maximising module sizes, while remaining within transport constraints;
- Shaping modules to minimise the number of splice joints;
- Limiting the variation in module types when increasing module sizes.

In addition, iterating the design process contributes significantly to the quality of the final outcome. This involves eliminating design options that prove unviable in an early stage, as well as developing alternatives based on the most promising designs for subsequent iterations.

Optionally, integration of lateral supports between beams could improve both the local and global stability of the structure. A potential solution for this is the use of glass, as this is a promising structural material. It could serve both as a structural support and as a facade element to enclose the gridshell.

However, in the current case studies, the weak axis of the beams lies perpendicular to the spherical surface. To enable the glass to effectively contribute to structural stability, the cross-section should be rotated such that the strong axis is oriented perpendicular to the surface, and the weak axis aligns with the direction of the lateral supports.

8.4. Recommendations for further research

Based on the limitations identified in this research, several directions for further study are recommended.

Firstly, this study demonstrates that using pinned splice joints as inter-module connections negatively affects the structural performance of the gridshell. It also shows that increasing the rotational stiffness of splice joints could improve the structural performance and reduce material usage. Since the rotational stiffness of joints significantly influences structural behaviour, it is recommended that future research explores in more detail how introducing rotational stiffness in these joints affects the behaviour of a modular gridshell. Moreover, as joint stiffness has a direct effect on the joint design itself, further research could explore how different joint stiffnesses influence assembly efficiency and demountability.

Secondly, it would be valuable to investigate whether this modular method is suitable for gridshells with different grid patterns or shapes. This includes gridshells with different grid topologies, such as the Timber Lazo gridshell dome, or alternative shapes. For instance, it could be examined how the current geodesic dome could be adapted into a canopy with a rectangular footprint, while maintaining spherical curvature and geometry of the geodesic dome. Such investigations could offer valuable insights into the adaptability of the method. Also, expanding this research to include the comparison of different building materials could give valuable insights in material efficiency in modular gridshells. This could be done by including material costs and carbon emission.

Future work could explore the use of bending-active beams instead of bending inactive ones. Bending active beams include a pre-stress from their curvature, which could affect stability. Investigating this alternative may provide a better understanding of how pre-stressed elements can improve the performance of modular timber gridshells.

Finally, a different approach to the modular segmentation itself could be investigated. It is found in literature that triangular modules are mentioned as a preferred shape due to their structural benefits. However, these require more complex joints and on-site assembly. Further research could investigate the performance and feasibility of triangular modules.

References

- AirSain. (n.d.). Luchtvochtigheid in Nederland en België. <https://www.airsain.nl/kenniscentrum/luchtvochtigheid-in-nederland-en-belgie/#:~:text=De%20gemiddelde%20luchtvochtigheid%20buiten%20in,relatieve%20luchtvochtigheid%20boven%2085%25%20gemeten.>
- Collins, M., & Cosgrove, T. (2016). *A review of the state of the art of timber gridshell design and construction* (tech. rep.). <https://hdl.handle.net/10344/5192>
- Crocetti, R. (2016). Large-Span Timber Structures. <https://doi.org/10.11159/icsenm16.124>
- de Mingo García, J., & Martín, Á. M. (2021). Strapwork Wooden Domes: History, Design and Proposed Development with Spherical Geometry and the Rules of the Trade as a Basis. *Journal of Traditional Building, Architecture and Urbanism*, 290–304.
- Hoogenboom, P. (2023). Notes on Shell Structures.
- Jonkeren, O. (2023). *Kostenkengetallen voor het goederenvervoer 2023* (tech. rep.). Kennisinstituut voor Mobiliteitsbeleid (KiM).
- Karolak, A., Jasieńko, J., & Raszczuk, K. (2020). Historical scarf and splice carpentry joints: state of the art. *Heritage Science*, 8(1), 105. <https://doi.org/10.1186/s40494-020-00448-2>
- Koninklijk Nederlands Normalisatie-instituut. (2019). Nationale bijlage bij NEN-EN 1990+A1:2006+A1:2006/C2:2019 Eurocode: Grondslagen van het constructief ontwerp.
- Koronaki, A., Shepherd, P., & Evernden, M. (2020). Rationalization of freeform space-frame structures: Reducing variability in the joints. *International Journal of Architectural Computing*, 18(1), 84–99. <https://doi.org/10.1177/1478077119894881>
- Kuda, D., & Petříčková, M. (2021). Modular Timber Gridshells. *Journal of Sustainable Architecture and Civil Engineering*, 28(1), 72–79. <https://doi.org/10.5755/j01.sace.28.1.27617>
- López, A., Puente, I., & Serna, M. A. (2007). Direct evaluation of the buckling loads of semi-rigidly jointed single-layer latticed domes under symmetric loading. *Engineering Structures*, 29(1), 101–109. <https://doi.org/10.1016/j.engstruct.2006.04.008>
- McNeel, R., & Associates. (2024). Rhinoceros.
- Nederlands Normalisatie-instituut. (2011a). Eurocode 1: Belastingen op constructies - Deel 1-4: Algemene belastingen - Windbelasting.
- Nederlands Normalisatie-instituut. (2011b). Eurocode 5: Ontwerp en berekening van houtconstructies - Deel 1-1: Algemeen - Gemeenschappelijke regels en regels voor gebouwen.
- Nederlands Normalisatie-instituut. (2015). Eurocode: Grondslagen voor het constructief ontwerp.
- Nederlands Normalisatie-instituut. (2019). Eurocode 1: Belastingen op constructies – Deel 1-3: Algemene belastingen – Sneeuwbelasting.
- Popovic Larsen, O. (2014). Reciprocal Frame (RF) Structures: Real and Exploratory. *Nexus Network Journal*, 16(1), 119–134. <https://doi.org/10.1007/s00004-014-0181-0>
- Preisinger, C. (2013). Linking Structure and Parametric Geometry. *Architectural Design*, 83(2), 110–113. <https://doi.org/10.1002/ad.1564>
- Roig, A., Lara-Bocanegra, A. J., Xavier, J., & Majano-Majano, A. (2022). Design Framework for Selection of Grid Topology and Rectangular Cross-Section Size of Elastic Timber Gridshells Using Genetic Optimisation. *Applied Sciences*, 13(1), 63. <https://doi.org/10.3390/app13010063>
- Schling, E., & Barthel, R. (2020). Repetitive Structures. In *Impact: Design with all senses* (pp. 360–375). Springer International Publishing. https://doi.org/10.1007/978-3-030-29829-6_{ }29
- Schling, E., Hitrec, D., Schikore, J., & Barthel, R. (2017). Design and Construction of the Asymptotic Pavilion. <http://www.lt.ar.tum.xn--dehttp-u46c/www.fa.uni-lj.si>
- Shu, Z., Li, Z., He, M., Chen, F., Hu, C., & Liang, F. (2020). Bolted joints for small and medium reticulated timber domes: experimental study, numerical simulation, and design strength estimation. *Archives of Civil and Mechanical Engineering*, 20(3), 73. <https://doi.org/10.1007/s43452-020-00073-7>
- Stasi, G. (2022). From Geometry to Reality: Designing Geodesic Structures. https://doi.org/10.1007/978-3-030-99116-6_{ }7

- Tomei, V. (2023). The effect of joint stiffness on optimization design strategies for gridshells: The role of rigid, semi-rigid and hinged joints. *Structures*, 48, 147–158. <https://doi.org/10.1016/j.istruc.2022.12.096>
- Venuti, F. (2021). Influence of pattern anisotropy on the structural behaviour of free-edge single-layer gridshells. *Curved and Layered Structures*, 8(1), 119–129. <https://doi.org/10.1515/cls-2021-0011>
- Venuti, F., & Bruno, L. (2018). Influence of in-plane and out-of-plane stiffness on the stability of free-edge gridshells: A parametric analysis. *Thin-Walled Structures*, 131, 755–768. <https://doi.org/10.1016/j.tws.2018.07.019>
- Wan, Z., D'Acunto, P., & Schling, E. (2024). Structural behaviour of asymptotic geodesic hybrid timber gridshells. *Engineering Structures*, 308, 117918. <https://doi.org/10.1016/j.engstruct.2024.117918>
- Wang, G., Zhang, L., Xu, C., Zhang, S., Zhou, Z., Guo, S., Ji, X., & Lei, H. (2024). Analysis of factors affecting the stability of large-span cable-braced timber gridshells. *Developments in the Built Environment*, 17, 100360. <https://doi.org/10.1016/j.dibe.2024.100360>



FEA results: Geodesic Gridshell

This appendix presents the results of the Finite Element Analysis (FEA) of the geodesic gridshell. First, the assumptions and input of the analysis are discussed in section A.1. The numerical results of the FEA are presented in section A.2, followed by the stress and displacement plots in section A.3. The bar charts in section A.4 visualise the difference in results between all designs. The utilisation results after the cross sections are optimised are presented in section A.5.

A.1. Assumptions and input

This section gives an overview of all assumptions and input of the FEA of the geodesic gridshell.

Software

The software that is used for this FEA is Karamba3D (Preisinger, 2013).

Coordinate system

The global coordinate system of the structure is displayed in Figure A.1 and Figure A.2. The local coordinate system in the beam cross section is shown in Figure 4.5 and Figure 4.6. The z-axis and the beam height are in the direction perpendicular to the spherical surface and the beams are curved around the y-axis.

Element type

The element type of the FEA is beam elements. The curved beams are modelled by dividing them into straight elements with an element length of 0.047 m, as discussed in subsection 4.3.3.

Analysis type

This FEA is performed using both the first and second order analysis. The first order analysis is used for reaction forces, displacements, deformation energy, stresses, cross section forces and nodal forces. The second order analysis is applied to determine the buckling factor and check for stability.

Moreover, Karamba3D assumes linear elastic material behaviour.

Geometry

The geometry of the geodesic gridshell is shown in Figure A.1 and Figure A.2. This geometry is formed as explained in section 4.1. Because the beams have a curvature, they are subdivided in multiple small straight elements with a length of 0.047 m. These elements are rigidly connected to each other. This also explains why the figures consist of many small elements in every single beam.

The hemisphere has a radius of 10 meters. All beams have the same cross section of 200x175 millimeters and strength class C30.

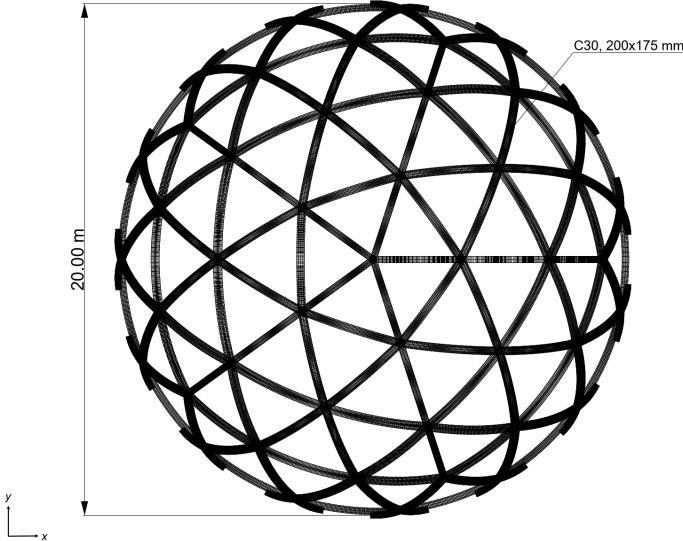


Figure A.1: Geodesic gridshell top view

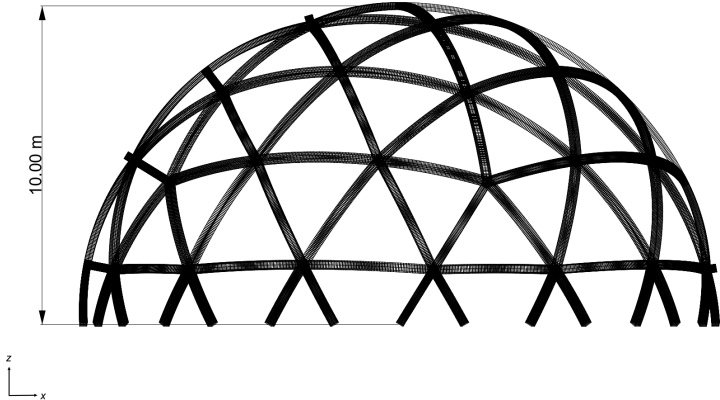


Figure A.2: Geodesic gridshell front view

The coordinates of all nodes are presented in Table A.1 to Table A.17.

Table A.1: Geodesic gridshell: Node coordinates, Classic**Pinned nodes**

	x [m]	y [m]	z [m]
1	0	0	10
2	3.432786	0	9.392336
3	6.865572	0	7.270758
4	8.944272	0	4.472136
5	7.926362	3.264774	5.149179
6	5.554365	6.529547	5.149179
7	2.763932	8.506508	4.472136
8	2.121578	6.529547	7.270758
9	1.060789	3.264774	9.392336
10	4.911235	3.568221	7.946545
11	-0.6556	8.547288	5.149179
12	-4.49358	7.300256	5.149179
13	-7.23607	5.257311	4.472136
14	-5.55437	4.035482	7.270758
15	-2.77718	2.017741	9.392336
16	-1.87593	5.773503	7.946545
17	-8.33155	2.017741	5.149179
18	-8.33155	-2.01774	5.149179
19	-7.23607	-5.25731	4.472136
20	-5.55437	-4.03548	7.270758
21	-2.77718	-2.01774	9.392336
22	-6.07062	0	7.946545
23	-4.49358	-7.30026	5.149179
24	-0.6556	-8.54729	5.149179
25	2.763932	-8.50651	4.472136
26	2.121578	-6.52955	7.270758
27	1.060789	-3.26477	9.392336
28	-1.87593	-5.7735	7.946545
29	5.554365	-6.52955	5.149179
30	7.926362	-3.26477	5.149179
31	4.911235	-3.56822	7.946545
32	4.898761	-8.54729	1.716393
33	9.642755	-2.01774	1.716393
34	7.946545	-5.7735	1.875925
35	9.642755	2.017741	1.716393
36	4.898761	8.547288	1.716393
37	7.946545	5.773503	1.875925
38	1.060789	9.794321	1.716393
39	-6.61515	7.300256	1.716393
40	-3.03531	9.341724	1.875925
41	-8.98715	4.035482	1.716393
42	-8.98715	-4.03548	1.716393
43	-9.82247	0	1.875925
44	-6.61515	-7.30026	1.716393
45	1.060789	-9.79432	1.716393
46	-3.03531	-9.34172	1.875925

Table A.2: Geodesic gridshell: Node coordinates, Design Option 1 (1/2)

Rigid nodes			Splice joints				
	x [m]	y [m]	z [m]		x [m]	y [m]	z [m]
1	0	0	10	1	1.620293	0	9.867859
2	3.432786	0	9.392336	2	5.257311	0	8.506508
3	6.865572	0	7.270758	3	8.101465	0	5.862275
4	8.944272	0	4.472136	4	8.602163	1.54099	4.860879
5	7.926362	3.264774	5.149179	5	6.88191	5	5.257311
6	5.554365	6.529547	5.149179	6	4.123783	7.704951	4.860879
7	2.763932	8.506508	4.472136	7	2.50349	7.704951	5.862275
8	2.121578	6.529547	7.270758	8	1.624598	5	8.506508
9	1.060789	3.264774	9.392336	9	0.500698	1.54099	9.867859
10	4.911235	3.568221	7.946545	10	2.29397	1.666667	9.589574
11	-0.6556	8.547288	5.149179	11	7.551281	1.666667	6.340377
12	-4.49358	7.300256	5.149179	12	3.918568	6.666667	6.340377
13	-7.23607	5.257311	4.472136	13	6.061816	1.742248	7.760088
14	-5.55437	4.035482	7.270758	14	3.530181	5.226745	7.760088
15	-2.77718	2.017741	9.392336	15	4.229907	1.742248	8.892269
16	-1.87593	5.773503	7.946545	16	2.96409	3.484496	8.892269
17	-8.33155	2.017741	5.149179	17	6.627906	3.484496	6.627906
18	-8.33155	-2.01774	5.149179	18	5.362089	5.226745	6.627906
19	-7.23607	-5.25731	4.472136	19	1.192646	8.657335	4.860879
20	-5.55437	-4.03548	7.270758	20	-2.62866	8.09017	5.257311
21	-2.77718	-2.01774	9.392336	21	-6.05353	6.302912	4.860879
22	-6.07062	0	7.946545	22	-6.55422	4.761921	5.862275
23	-4.49358	-7.30026	5.149179	23	-4.25325	3.09017	8.506508
24	-0.6556	-8.54729	5.149179	24	-1.31085	0.952384	9.867859
25	2.763932	-8.50651	4.472136	25	-0.87622	2.696723	9.589574
26	2.121578	-6.52955	7.270758	26	0.74838	7.696723	6.340377
27	1.060789	-3.26477	9.392336	27	-5.12947	5.786893	6.340377
28	-1.87593	-5.7735	7.946545	28	0.216227	6.303513	7.760088
29	5.554365	-6.52955	5.149179	29	-3.88004	4.972554	7.760088
30	7.926362	-3.26477	5.149179	30	-0.34986	4.561265	8.892269
31	4.911235	-3.56822	7.946545	31	-2.398	3.895785	8.892269
32	4.898761	-8.54729	1.716393	32	-1.26582	7.380282	6.627906
33	9.642755	-2.01774	1.716393	33	-3.31395	6.714802	6.627906
34	7.946545	-5.7735	1.875925	34	-7.86507	3.809537	4.860879
35	9.642755	2.017741	1.716393	35	-8.50651	0	5.257311
36	4.898761	8.547288	1.716393	36	-7.86507	-3.80954	4.860879
37	7.946545	5.773503	1.875925	37	-6.55422	-4.76192	5.862275
38	1.060789	9.794321	1.716393	38	-4.25325	-3.09017	8.506508
39	-6.61515	7.300256	1.716393	39	-1.31085	-0.95238	9.867859
40	-3.03531	9.341724	1.875925	40	-2.8355	0	9.589574
41	-8.98715	4.035482	1.716393	41	-7.08876	3.09017	6.340377
42	-8.98715	-4.03548	1.716393	42	-7.08876	-3.09017	6.340377
43	-9.82247	0	1.875925	43	-5.92818	2.153537	7.760088
44	-6.61515	-7.30026	1.716393	44	-5.92818	-2.15354	7.760088
45	1.060789	-9.79432	1.716393	45	-4.44614	1.076769	8.892269
46	-3.03531	-9.34172	1.875925	46	-4.44614	-1.07677	8.892269
				47	-7.41022	1.076769	6.627906
				48	-7.41022	-1.07677	6.627906
				49	-6.05353	-6.30291	4.860879
				50	-2.62866	-8.09017	5.257311

Table A.3: Geodesic gridshell: Node coordinates, Design Option 1 (2/2)

Splice joints				Splice joints			
	x [m]	y [m]	z [m]		x [m]	y [m]	z [m]
51	1.192646	-8.65734	4.860879	101	-5.01223	8.457051	1.831908
52	2.50349	-7.70495	5.862275	102	-8.17452	4.761921	3.240586
53	1.624598	-5	8.506508	103	-7.96498	5.786893	1.752437
54	0.500698	-1.54099	9.867859	104	-8.17452	-4.76192	3.240586
55	-0.87622	-2.69672	9.589574	105	-8.84119	3.09017	3.504874
56	-5.12947	-5.78689	6.340377	106	-8.84119	-3.09017	3.504874
57	0.74838	-7.69672	6.340377	107	-9.24213	-1.07677	3.663817
58	-3.88004	-4.97255	7.760088	108	-9.592	2.153537	1.831908
59	0.216227	-6.30351	7.760088	109	-9.24213	1.076769	3.663817
60	-2.398	-3.89579	8.892269	110	-9.592	-2.15354	1.831908
61	-0.34986	-4.56127	8.892269	111	-7.05492	-6.30291	3.240586
62	-3.31395	-6.7148	6.627906	112	-7.96498	-5.78689	1.752437
63	-1.26582	-7.38028	6.627906	113	2.002792	-9.24594	3.240586
64	4.123783	-7.70495	4.860879	114	-5.67101	-7.45356	3.504874
65	6.88191	-5	5.257311	115	0.206847	-9.36339	3.504874
66	8.602163	-1.54099	4.860879	116	-1.83191	-9.12253	3.663817
67	2.29397	-1.66667	9.589574	117	-5.01223	-8.45705	1.831908
68	3.918568	-6.66667	6.340377	118	-3.88004	-8.45705	3.663817
69	7.551281	-1.66667	6.340377	119	-0.91595	-9.78801	1.831908
70	3.530181	-5.22675	7.760088	120	3.04235	-9.36339	1.752437
71	6.061816	-1.74225	7.760088				
72	2.96409	-3.4845	8.892269				
73	4.229907	-1.74225	8.892269				
74	5.362089	-5.22675	6.627906				
75	6.627906	-3.4845	6.627906				
76	3.814335	-8.65734	3.240586				
77	9.412309	-0.95238	3.240586				
78	8.969032	-2.69672	3.504874				
79	5.33632	-7.69672	3.504874				
80	6.844134	-6.30351	3.663817				
81	8.109951	-4.56127	3.663817				
82	9.025905	-3.89579	1.831908				
83	6.49427	-7.38028	1.831908				
84	9.412309	0.952384	3.240586				
85	3.814335	8.657335	3.240586				
86	8.969032	2.696723	3.504874				
87	5.33632	7.696723	3.504874				
88	6.844134	6.303513	3.663817				
89	9.025905	3.895785	1.831908				
90	8.109951	4.561265	3.663817				
91	6.49427	7.380282	1.831908				
92	9.845251	0	1.752437				
93	2.002792	9.245941	3.240586				
94	3.04235	9.36339	1.752437				
95	-7.05492	6.302912	3.240586				
96	0.206847	9.36339	3.504874				
97	-5.67101	7.45356	3.504874				
98	-3.88004	8.457051	3.663817				
99	-0.91595	9.78801	1.831908				
100	-1.83191	9.12253	3.663817				

Table A.4: Geodesic gridshell: Node coordinates, Design Option 2 (1/2)

Rigid nodes			Splice joints				
	x [m]	y [m]	z [m]		x [m]	y [m]	z [m]
1	0	0	10	1	1.620293	0	9.867859
2	3.432786	0	9.392336	2	8.101465	0	5.862275
3	6.865572	0	7.270758	3	8.602163	1.54099	4.860879
4	8.944272	0	4.472136	4	4.123783	7.704951	4.860879
5	7.926362	3.264774	5.149179	5	2.50349	7.704951	5.862275
6	5.554365	6.529547	5.149179	6	0.500698	1.54099	9.867859
7	2.763932	8.506508	4.472136	7	2.29397	1.666667	9.589574
8	2.121578	6.529547	7.270758	8	7.551281	1.666667	6.340377
9	1.060789	3.264774	9.392336	9	3.918568	6.666667	6.340377
10	4.911235	3.568221	7.946545	10	6.061816	1.742248	7.760088
11	-0.6556	8.547288	5.149179	11	3.530181	5.226745	7.760088
12	-4.49358	7.300256	5.149179	12	4.229907	1.742248	8.892269
13	-7.23607	5.257311	4.472136	13	2.96409	3.484496	8.892269
14	-5.55437	4.035482	7.270758	14	6.627906	3.484496	6.627906
15	-2.77718	2.017741	9.392336	15	5.362089	5.226745	6.627906
16	-1.87593	5.773503	7.946545	16	1.192646	8.657335	4.860879
17	-8.33155	2.017741	5.149179	17	-6.05353	6.302912	4.860879
18	-8.33155	-2.01774	5.149179	18	-6.55422	4.761921	5.862275
19	-7.23607	-5.25731	4.472136	19	-1.31085	0.952384	9.867859
20	-5.55437	-4.03548	7.270758	20	-0.87622	2.696723	9.589574
21	-2.77718	-2.01774	9.392336	21	0.74838	7.696723	6.340377
22	-6.07062	0	7.946545	22	-5.12947	5.786893	6.340377
23	-4.49358	-7.30026	5.149179	23	0.216227	6.303513	7.760088
24	-0.6556	-8.54729	5.149179	24	-3.88004	4.972554	7.760088
25	2.763932	-8.50651	4.472136	25	-0.34986	4.561265	8.892269
26	2.121578	-6.52955	7.270758	26	-2.398	3.895785	8.892269
27	1.060789	-3.26477	9.392336	27	-1.26582	7.380282	6.627906
28	-1.87593	-5.7735	7.946545	28	-3.31395	6.714802	6.627906
29	5.554365	-6.52955	5.149179	29	-7.86507	3.809537	4.860879
30	7.926362	-3.26477	5.149179	30	-7.86507	-3.80954	4.860879
31	4.911235	-3.56822	7.946545	31	-6.55422	-4.76192	5.862275
32	4.898761	-8.54729	1.716393	32	-1.31085	-0.95238	9.867859
33	9.642755	-2.01774	1.716393	33	-2.8355	0	9.589574
34	7.946545	-5.7735	1.875925	34	-7.08876	3.09017	6.340377
35	9.642755	2.017741	1.716393	35	-7.08876	-3.09017	6.340377
36	4.898761	8.547288	1.716393	36	-5.92818	2.153537	7.760088
37	7.946545	5.773503	1.875925	37	-5.92818	-2.15354	7.760088
38	1.060789	9.794321	1.716393	38	-4.44614	1.076769	8.892269
39	-6.61515	7.300256	1.716393	39	-4.44614	-1.07677	8.892269
40	-3.03531	9.341724	1.875925	40	-7.41022	1.076769	6.627906
41	-8.98715	4.035482	1.716393	41	-7.41022	-1.07677	6.627906
42	-8.98715	-4.03548	1.716393	42	-6.05353	-6.30291	4.860879
43	-9.82247	0	1.875925	43	1.192646	-8.65734	4.860879
44	-6.61515	-7.30026	1.716393	44	2.50349	-7.70495	5.862275
45	1.060789	-9.79432	1.716393	45	0.500698	-1.54099	9.867859
46	-3.03531	-9.34172	1.875925	46	-0.87622	-2.69672	9.589574
				47	-5.12947	-5.78689	6.340377
				48	0.74838	-7.69672	6.340377
				49	-3.88004	-4.97255	7.760088
				50	0.216227	-6.30351	7.760088

Table A.5: Geodesic gridshell: Node coordinates, Design Option 2 (2/2)

Splice joints				Splice joints			
	x [m]	y [m]	z [m]		x [m]	y [m]	z [m]
51	-2.398	-3.89579	8.892269	101	-7.05492	-6.30291	3.240586
52	-0.34986	-4.56127	8.892269	102	-7.96498	-5.78689	1.752437
53	-3.31395	-6.7148	6.627906	103	2.002792	-9.24594	3.240586
54	-1.26582	-7.38028	6.627906	104	-5.67101	-7.45356	3.504874
55	4.123783	-7.70495	4.860879	105	0.206847	-9.36339	3.504874
56	8.602163	-1.54099	4.860879	106	-1.83191	-9.12253	3.663817
57	2.29397	-1.66667	9.589574	107	-5.01223	-8.45705	1.831908
58	3.918568	-6.66667	6.340377	108	-3.88004	-8.45705	3.663817
59	7.551281	-1.66667	6.340377	109	-0.91595	-9.78801	1.831908
60	3.530181	-5.22675	7.760088	110	3.04235	-9.36339	1.752437
61	6.061816	-1.74225	7.760088				
62	2.96409	-3.4845	8.892269				
63	4.229907	-1.74225	8.892269				
64	5.362089	-5.22675	6.627906				
65	6.627906	-3.4845	6.627906				
66	3.814335	-8.65734	3.240586				
67	9.412309	-0.95238	3.240586				
68	8.969032	-2.69672	3.504874				
69	5.33632	-7.69672	3.504874				
70	6.844134	-6.30351	3.663817				
71	8.109951	-4.56127	3.663817				
72	9.025905	-3.89579	1.831908				
73	6.49427	-7.38028	1.831908				
74	9.412309	0.952384	3.240586				
75	3.814335	8.657335	3.240586				
76	8.969032	2.696723	3.504874				
77	5.33632	7.696723	3.504874				
78	6.844134	6.303513	3.663817				
79	9.025905	3.895785	1.831908				
80	8.109951	4.561265	3.663817				
81	6.49427	7.380282	1.831908				
82	9.845251	0	1.752437				
83	2.002792	9.245941	3.240586				
84	3.04235	9.36339	1.752437				
85	-7.05492	6.302912	3.240586				
86	0.206847	9.36339	3.504874				
87	-5.67101	7.45356	3.504874				
88	-3.88004	8.457051	3.663817				
89	-0.91595	9.78801	1.831908				
90	-1.83191	9.12253	3.663817				
91	-5.01223	8.457051	1.831908				
92	-8.17452	4.761921	3.240586				
93	-7.96498	5.786893	1.752437				
94	-8.17452	-4.76192	3.240586				
95	-8.84119	3.09017	3.504874				
96	-8.84119	-3.09017	3.504874				
97	-9.24213	-1.07677	3.663817				
98	-9.592	2.153537	1.831908				
99	-9.24213	1.076769	3.663817				
100	-9.592	-2.15354	1.831908				

Table A.6: Geodesic gridshell: Node coordinates, Design Option 3 (1/2)

Rigid nodes			Splice joints				
	x [m]	y [m]	z [m]		x [m]	y [m]	z [m]
1	0	0	10	1	5.257311	0	8.506508
2	3.432786	0	9.392336	2	6.88191	5	5.257311
3	6.865572	0	7.270758	3	1.624598	5	8.506508
4	8.944272	0	4.472136	4	6.061816	1.742248	7.760088
5	7.926362	3.264774	5.149179	5	3.530181	5.226745	7.760088
6	5.554365	6.529547	5.149179	6	4.229907	1.742248	8.892269
7	2.763932	8.506508	4.472136	7	2.96409	3.484496	8.892269
8	2.121578	6.529547	7.270758	8	6.627906	3.484496	6.627906
9	1.060789	3.264774	9.392336	9	5.362089	5.226745	6.627906
10	4.911235	3.568221	7.946545	10	-2.62866	8.09017	5.257311
11	-0.6556	8.547288	5.149179	11	-4.25325	3.09017	8.506508
12	-4.49358	7.300256	5.149179	12	0.216227	6.303513	7.760088
13	-7.23607	5.257311	4.472136	13	-3.88004	4.972554	7.760088
14	-5.55437	4.035482	7.270758	14	-0.34986	4.561265	8.892269
15	-2.77718	2.017741	9.392336	15	-2.398	3.895785	8.892269
16	-1.87593	5.773503	7.946545	16	-1.26582	7.380282	6.627906
17	-8.33155	2.017741	5.149179	17	-3.31395	6.714802	6.627906
18	-8.33155	-2.01774	5.149179	18	-8.50651	0	5.257311
19	-7.23607	-5.25731	4.472136	19	-4.25325	-3.09017	8.506508
20	-5.55437	-4.03548	7.270758	20	-5.92818	2.153537	7.760088
21	-2.77718	-2.01774	9.392336	21	-5.92818	-2.15354	7.760088
22	-6.07062	0	7.946545	22	-4.44614	1.076769	8.892269
23	-4.49358	-7.30026	5.149179	23	-4.44614	-1.07677	8.892269
24	-0.6556	-8.54729	5.149179	24	-7.41022	1.076769	6.627906
25	2.763932	-8.50651	4.472136	25	-7.41022	-1.07677	6.627906
26	2.121578	-6.52955	7.270758	26	-2.62866	-8.09017	5.257311
27	1.060789	-3.26477	9.392336	27	1.624598	-5	8.506508
28	-1.87593	-5.7735	7.946545	28	-3.88004	-4.97255	7.760088
29	5.554365	-6.52955	5.149179	29	0.216227	-6.30351	7.760088
30	7.926362	-3.26477	5.149179	30	-2.398	-3.89579	8.892269
31	4.911235	-3.56822	7.946545	31	-0.34986	-4.56127	8.892269
32	4.898761	-8.54729	1.716393	32	-3.31395	-6.7148	6.627906
33	9.642755	-2.01774	1.716393	33	-1.26582	-7.38028	6.627906
34	7.946545	-5.7735	1.875925	34	6.88191	-5	5.257311
35	9.642755	2.017741	1.716393	35	3.530181	-5.22675	7.760088
36	4.898761	8.547288	1.716393	36	6.061816	-1.74225	7.760088
37	7.946545	5.773503	1.875925	37	2.96409	-3.4845	8.892269
38	1.060789	9.794321	1.716393	38	4.229907	-1.74225	8.892269
39	-6.61515	7.300256	1.716393	39	5.362089	-5.22675	6.627906
40	-3.03531	9.341724	1.875925	40	6.627906	-3.4845	6.627906
41	-8.98715	4.035482	1.716393	41	6.844134	-6.30351	3.663817
42	-8.98715	-4.03548	1.716393	42	8.109951	-4.56127	3.663817
43	-9.82247	0	1.875925	43	9.025905	-3.89579	1.831908
44	-6.61515	-7.30026	1.716393	44	6.49427	-7.38028	1.831908
45	1.060789	-9.79432	1.716393	45	6.844134	6.303513	3.663817
46	-3.03531	-9.34172	1.875925	46	9.025905	3.895785	1.831908
				47	8.109951	4.561265	3.663817
				48	6.49427	7.380282	1.831908
				49	-3.88004	8.457051	3.663817
				50	-0.91595	9.78801	1.831908

Table A.7: Geodesic gridshell: Node coordinates, Design Option 3 (2/2)**Splice joints**

	x [m]	y [m]	z [m]
51	-1.83191	9.12253	3.663817
52	-5.01223	8.457051	1.831908
53	-9.24213	-1.07677	3.663817
54	-9.592	2.153537	1.831908
55	-9.24213	1.076769	3.663817
56	-9.592	-2.15354	1.831908
57	-1.83191	-9.12253	3.663817
58	-5.01223	-8.45705	1.831908
59	-3.88004	-8.45705	3.663817
60	-0.91595	-9.78801	1.831908

Table A.8: Geodesic gridshell: Node coordinates, Design Option 4 (1/2)

Rigid nodes				Splice joints			
	x [m]	y [m]	z [m]		x [m]	y [m]	z [m]
1	0	0	10	1	1.620293	0	9.867859
2	3.432786	0	9.392336	2	8.101465	0	5.862275
3	6.865572	0	7.270758	3	8.602163	1.54099	4.860879
4	8.944272	0	4.472136	4	4.123783	7.704951	4.860879
5	7.926362	3.264774	5.149179	5	2.50349	7.704951	5.862275
6	5.554365	6.529547	5.149179	6	0.500698	1.54099	9.867859
7	2.763932	8.506508	4.472136	7	2.29397	1.666667	9.589574
8	2.121578	6.529547	7.270758	8	7.551281	1.666667	6.340377
9	1.060789	3.264774	9.392336	9	3.918568	6.666667	6.340377
10	4.911235	3.568221	7.946545	10	6.061816	1.742248	7.760088
11	-0.6556	8.547288	5.149179	11	4.229907	1.742248	8.892269
12	-4.49358	7.300256	5.149179	12	6.627906	3.484496	6.627906
13	-7.23607	5.257311	4.472136	13	5.362089	5.226745	6.627906
14	-5.55437	4.035482	7.270758	14	1.192646	8.657335	4.860879
15	-2.77718	2.017741	9.392336	15	-6.05353	6.302912	4.860879
16	-1.87593	5.773503	7.946545	16	-6.55422	4.761921	5.862275
17	-8.33155	2.017741	5.149179	17	-1.31085	0.952384	9.867859
18	-8.33155	-2.01774	5.149179	18	-0.87622	2.696723	9.589574
19	-7.23607	-5.25731	4.472136	19	0.74838	7.696723	6.340377
20	-5.55437	-4.03548	7.270758	20	-5.12947	5.786893	6.340377
21	-2.77718	-2.01774	9.392336	21	0.216227	6.303513	7.760088
22	-6.07062	0	7.946545	22	-0.34986	4.561265	8.892269
23	-4.49358	-7.30026	5.149179	23	-1.26582	7.380282	6.627906
24	-0.6556	-8.54729	5.149179	24	-3.31395	6.714802	6.627906
25	2.763932	-8.50651	4.472136	25	-7.86507	3.809537	4.860879
26	2.121578	-6.52955	7.270758	26	-7.86507	-3.80954	4.860879
27	1.060789	-3.26477	9.392336	27	-6.55422	-4.76192	5.862275
28	-1.87593	-5.7735	7.946545	28	-1.31085	-0.95238	9.867859
29	5.554365	-6.52955	5.149179	29	-2.8355	0	9.589574
30	7.926362	-3.26477	5.149179	30	-7.08876	3.09017	6.340377
31	4.911235	-3.56822	7.946545	31	-7.08876	-3.09017	6.340377
32	4.898761	-8.54729	1.716393	32	-5.92818	2.153537	7.760088
33	9.642755	-2.01774	1.716393	33	-4.44614	1.076769	8.892269
34	7.946545	-5.7735	1.875925	34	-7.41022	1.076769	6.627906
35	9.642755	2.017741	1.716393	35	-7.41022	-1.07677	6.627906
36	4.898761	8.547288	1.716393	36	-6.05353	-6.30291	4.860879
37	7.946545	5.773503	1.875925	37	1.192646	-8.65734	4.860879
38	1.060789	9.794321	1.716393	38	2.50349	-7.70495	5.862275
39	-6.61515	7.300256	1.716393	39	0.500698	-1.54099	9.867859
40	-3.03531	9.341724	1.875925	40	-0.87622	-2.69672	9.589574
41	-8.98715	4.035482	1.716393	41	-5.12947	-5.78689	6.340377
42	-8.98715	-4.03548	1.716393	42	0.74838	-7.69672	6.340377
43	-9.82247	0	1.875925	43	-3.88004	-4.97255	7.760088
44	-6.61515	-7.30026	1.716393	44	-2.398	-3.89579	8.892269
45	1.060789	-9.79432	1.716393	45	-3.31395	-6.7148	6.627906
46	-3.03531	-9.34172	1.875925	46	-1.26582	-7.38028	6.627906
				47	4.123783	-7.70495	4.860879
				48	8.602163	-1.54099	4.860879
				49	2.29397	-1.66667	9.589574
				50	3.918568	-6.66667	6.340377

Table A.9: Geodesic gridshell: Node coordinates, Design Option 4 (2/2)**Splice joints**

	x [m]	y [m]	z [m]
51	7.551281	-1.66667	6.340377
52	3.530181	-5.22675	7.760088
53	2.96409	-3.4845	8.892269
54	5.362089	-5.22675	6.627906
55	6.627906	-3.4845	6.627906
56	3.814335	-8.65734	3.240586
57	9.412309	-0.95238	3.240586
58	8.969032	-2.69672	3.504874
59	5.33632	-7.69672	3.504874
60	9.025905	-3.89579	1.831908
61	6.49427	-7.38028	1.831908
62	9.412309	0.952384	3.240586
63	3.814335	8.657335	3.240586
64	8.969032	2.696723	3.504874
65	5.33632	7.696723	3.504874
66	9.025905	3.895785	1.831908
67	6.49427	7.380282	1.831908
68	9.845251	0	1.752437
69	2.002792	9.245941	3.240586
70	3.04235	9.36339	1.752437
71	-7.05492	6.302912	3.240586
72	0.206847	9.36339	3.504874
73	-5.67101	7.45356	3.504874
74	-0.91595	9.78801	1.831908
75	-5.01223	8.457051	1.831908
76	-8.17452	4.761921	3.240586
77	-7.96498	5.786893	1.752437
78	-8.17452	-4.76192	3.240586
79	-8.84119	3.09017	3.504874
80	-8.84119	-3.09017	3.504874
81	-9.592	2.153537	1.831908
82	-9.592	-2.15354	1.831908
83	-7.05492	-6.30291	3.240586
84	-7.96498	-5.78689	1.752437
85	2.002792	-9.24594	3.240586
86	-5.67101	-7.45356	3.504874
87	0.206847	-9.36339	3.504874
88	-5.01223	-8.45705	1.831908
89	-0.91595	-9.78801	1.831908
90	3.04235	-9.36339	1.752437

Table A.10: Geodesic gridshell: Node coordinates, Design Option 5 (1/2)

Rigid nodes			Splice joints				
	x [m]	y [m]	z [m]		x [m]	y [m]	z [m]
1	0	0	10	1	1.620293	0	9.867859
2	3.432786	0	9.392336	2	8.101465	0	5.862275
3	6.865572	0	7.270758	3	8.602163	1.54099	4.860879
4	8.944272	0	4.472136	4	4.123783	7.704951	4.860879
5	7.926362	3.264774	5.149179	5	2.50349	7.704951	5.862275
6	5.554365	6.529547	5.149179	6	0.500698	1.54099	9.867859
7	2.763932	8.506508	4.472136	7	2.29397	1.666667	9.589574
8	2.121578	6.529547	7.270758	8	7.551281	1.666667	6.340377
9	1.060789	3.264774	9.392336	9	3.918568	6.666667	6.340377
10	4.911235	3.568221	7.946545	10	6.061816	1.742248	7.760088
11	-0.6556	8.547288	5.149179	11	3.530181	5.226745	7.760088
12	-4.49358	7.300256	5.149179	12	4.229907	1.742248	8.892269
13	-7.23607	5.257311	4.472136	13	2.96409	3.484496	8.892269
14	-5.55437	4.035482	7.270758	14	6.627906	3.484496	6.627906
15	-2.77718	2.017741	9.392336	15	5.362089	5.226745	6.627906
16	-1.87593	5.773503	7.946545	16	1.192646	8.657335	4.860879
17	-8.33155	2.017741	5.149179	17	-6.05353	6.302912	4.860879
18	-8.33155	-2.01774	5.149179	18	-6.55422	4.761921	5.862275
19	-7.23607	-5.25731	4.472136	19	-1.31085	0.952384	9.867859
20	-5.55437	-4.03548	7.270758	20	-0.87622	2.696723	9.589574
21	-2.77718	-2.01774	9.392336	21	0.74838	7.696723	6.340377
22	-6.07062	0	7.946545	22	-5.12947	5.786893	6.340377
23	-4.49358	-7.30026	5.149179	23	0.216227	6.303513	7.760088
24	-0.6556	-8.54729	5.149179	24	-3.88004	4.972554	7.760088
25	2.763932	-8.50651	4.472136	25	-0.34986	4.561265	8.892269
26	2.121578	-6.52955	7.270758	26	-2.398	3.895785	8.892269
27	1.060789	-3.26477	9.392336	27	-1.26582	7.380282	6.627906
28	-1.87593	-5.7735	7.946545	28	-3.31395	6.714802	6.627906
29	5.554365	-6.52955	5.149179	29	-7.86507	3.809537	4.860879
30	7.926362	-3.26477	5.149179	30	-7.86507	-3.80954	4.860879
31	4.911235	-3.56822	7.946545	31	-6.55422	-4.76192	5.862275
32	4.898761	-8.54729	1.716393	32	-1.31085	-0.95238	9.867859
33	9.642755	-2.01774	1.716393	33	-2.8355	0	9.589574
34	7.946545	-5.7735	1.875925	34	-7.08876	3.09017	6.340377
35	9.642755	2.017741	1.716393	35	-7.08876	-3.09017	6.340377
36	4.898761	8.547288	1.716393	36	-5.92818	2.153537	7.760088
37	7.946545	5.773503	1.875925	37	-5.92818	-2.15354	7.760088
38	1.060789	9.794321	1.716393	38	-4.44614	1.076769	8.892269
39	-6.61515	7.300256	1.716393	39	-4.44614	-1.07677	8.892269
40	-3.03531	9.341724	1.875925	40	-7.41022	1.076769	6.627906
41	-8.98715	4.035482	1.716393	41	-7.41022	-1.07677	6.627906
42	-8.98715	-4.03548	1.716393	42	-6.05353	-6.30291	4.860879
43	-9.82247	0	1.875925	43	1.192646	-8.65734	4.860879
44	-6.61515	-7.30026	1.716393	44	2.50349	-7.70495	5.862275
45	1.060789	-9.79432	1.716393	45	0.500698	-1.54099	9.867859
46	-3.03531	-9.34172	1.875925	46	-0.87622	-2.69672	9.589574
				47	-5.12947	-5.78689	6.340377
				48	0.74838	-7.69672	6.340377
				49	-3.88004	-4.97255	7.760088
				50	0.216227	-6.30351	7.760088

Table A.11: Geodesic gridshell: Node coordinates, Design Option 5 (2/2)

Splice joints				Splice joints			
	x [m]	y [m]	z [m]		x [m]	y [m]	z [m]
51	-2.398	-3.89579	8.892269	101	0.206847	-9.36339	3.504874
52	-0.34986	-4.56127	8.892269	102	-1.83191	-9.12253	3.663817
53	-3.31395	-6.7148	6.627906	103	-5.01223	-8.45705	1.831908
54	-1.26582	-7.38028	6.627906	104	-3.88004	-8.45705	3.663817
55	4.123783	-7.70495	4.860879	105	-0.91595	-9.78801	1.831908
56	8.602163	-1.54099	4.860879				
57	2.29397	-1.66667	9.589574				
58	3.918568	-6.66667	6.340377				
59	7.551281	-1.66667	6.340377				
60	3.530181	-5.22675	7.760088				
61	6.061816	-1.74225	7.760088				
62	2.96409	-3.4845	8.892269				
63	4.229907	-1.74225	8.892269				
64	5.362089	-5.22675	6.627906				
65	6.627906	-3.4845	6.627906				
66	3.814335	-8.65734	3.240586				
67	9.412309	-0.95238	3.240586				
68	8.969032	-2.69672	3.504874				
69	5.33632	-7.69672	3.504874				
70	6.844134	-6.30351	3.663817				
71	8.109951	-4.56127	3.663817				
72	9.025905	-3.89579	1.831908				
73	6.49427	-7.38028	1.831908				
74	9.412309	0.952384	3.240586				
75	3.814335	8.657335	3.240586				
76	8.969032	2.696723	3.504874				
77	5.33632	7.696723	3.504874				
78	6.844134	6.303513	3.663817				
79	9.025905	3.895785	1.831908				
80	8.109951	4.561265	3.663817				
81	6.49427	7.380282	1.831908				
82	2.002792	9.245941	3.240586				
83	-7.05492	6.302912	3.240586				
84	0.206847	9.36339	3.504874				
85	-5.67101	7.45356	3.504874				
86	-3.88004	8.457051	3.663817				
87	-0.91595	9.78801	1.831908				
88	-1.83191	9.12253	3.663817				
89	-5.01223	8.457051	1.831908				
90	-8.17452	4.761921	3.240586				
91	-8.17452	-4.76192	3.240586				
92	-8.84119	3.09017	3.504874				
93	-8.84119	-3.09017	3.504874				
94	-9.24213	-1.07677	3.663817				
95	-9.592	2.153537	1.831908				
96	-9.24213	1.076769	3.663817				
97	-9.592	-2.15354	1.831908				
98	-7.05492	-6.30291	3.240586				
99	2.002792	-9.24594	3.240586				
100	-5.67101	-7.45356	3.504874				

Table A.12: Geodesic gridshell: Node coordinates, Design Option 6 (1/2)

Rigid nodes			Splice joints				
	x [m]	y [m]	z [m]		x [m]	y [m]	z [m]
1	0	0	10	1	1.620293	0	9.867859
2	3.432786	0	9.392336	2	8.101465	0	5.862275
3	6.865572	0	7.270758	3	8.602163	1.54099	4.860879
4	8.944272	0	4.472136	4	4.123783	7.704951	4.860879
5	7.926362	3.264774	5.149179	5	2.50349	7.704951	5.862275
6	5.554365	6.529547	5.149179	6	0.500698	1.54099	9.867859
7	2.763932	8.506508	4.472136	7	2.29397	1.666667	9.589574
8	2.121578	6.529547	7.270758	8	7.551281	1.666667	6.340377
9	1.060789	3.264774	9.392336	9	3.918568	6.666667	6.340377
10	4.911235	3.568221	7.946545	10	6.061816	1.742248	7.760088
11	-0.6556	8.547288	5.149179	11	3.530181	5.226745	7.760088
12	-4.49358	7.300256	5.149179	12	4.229907	1.742248	8.892269
13	-7.23607	5.257311	4.472136	13	2.96409	3.484496	8.892269
14	-5.55437	4.035482	7.270758	14	6.627906	3.484496	6.627906
15	-2.77718	2.017741	9.392336	15	5.362089	5.226745	6.627906
16	-1.87593	5.773503	7.946545	16	1.192646	8.657335	4.860879
17	-8.33155	2.017741	5.149179	17	-6.05353	6.302912	4.860879
18	-8.33155	-2.01774	5.149179	18	-6.55422	4.761921	5.862275
19	-7.23607	-5.25731	4.472136	19	-1.31085	0.952384	9.867859
20	-5.55437	-4.03548	7.270758	20	-0.87622	2.696723	9.589574
21	-2.77718	-2.01774	9.392336	21	0.74838	7.696723	6.340377
22	-6.07062	0	7.946545	22	-5.12947	5.786893	6.340377
23	-4.49358	-7.30026	5.149179	23	0.216227	6.303513	7.760088
24	-0.6556	-8.54729	5.149179	24	-3.88004	4.972554	7.760088
25	2.763932	-8.50651	4.472136	25	-0.34986	4.561265	8.892269
26	2.121578	-6.52955	7.270758	26	-2.398	3.895785	8.892269
27	1.060789	-3.26477	9.392336	27	-1.26582	7.380282	6.627906
28	-1.87593	-5.7735	7.946545	28	-3.31395	6.714802	6.627906
29	5.554365	-6.52955	5.149179	29	-7.86507	3.809537	4.860879
30	7.926362	-3.26477	5.149179	30	-7.86507	-3.80954	4.860879
31	4.911235	-3.56822	7.946545	31	-6.55422	-4.76192	5.862275
32	4.898761	-8.54729	1.716393	32	-1.31085	-0.95238	9.867859
33	9.642755	-2.01774	1.716393	33	-2.8355	0	9.589574
34	7.946545	-5.7735	1.875925	34	-7.08876	3.09017	6.340377
35	9.642755	2.017741	1.716393	35	-7.08876	-3.09017	6.340377
36	4.898761	8.547288	1.716393	36	-5.92818	2.153537	7.760088
37	7.946545	5.773503	1.875925	37	-5.92818	-2.15354	7.760088
38	1.060789	9.794321	1.716393	38	-4.44614	1.076769	8.892269
39	-6.61515	7.300256	1.716393	39	-4.44614	-1.07677	8.892269
40	-3.03531	9.341724	1.875925	40	-7.41022	1.076769	6.627906
41	-8.98715	4.035482	1.716393	41	-7.41022	-1.07677	6.627906
42	-8.98715	-4.03548	1.716393	42	-6.05353	-6.30291	4.860879
43	-9.82247	0	1.875925	43	1.192646	-8.65734	4.860879
44	-6.61515	-7.30026	1.716393	44	2.50349	-7.70495	5.862275
45	1.060789	-9.79432	1.716393	45	0.500698	-1.54099	9.867859
46	-3.03531	-9.34172	1.875925	46	-0.87622	-2.69672	9.589574
				47	-5.12947	-5.78689	6.340377
				48	0.74838	-7.69672	6.340377
				49	-3.88004	-4.97255	7.760088
				50	0.216227	-6.30351	7.760088

Table A.13: Geodesic gridshell: Node coordinates, Design Option 6 (2/2)

Splice joints				Splice joints			
	x [m]	y [m]	z [m]		x [m]	y [m]	z [m]
51	-2.398	-3.89579	8.892269	101	3.04235	9.36339	1.752437
52	-0.34986	-4.56127	8.892269	102	9.845251	0	1.752437
53	-3.31395	-6.7148	6.627906	103	3.04235	-9.36339	1.752437
54	-1.26582	-7.38028	6.627906	104	-7.96498	-5.78689	1.752437
55	4.123783	-7.70495	4.860879	105	-7.96498	5.786893	1.752437
56	8.602163	-1.54099	4.860879				
57	2.29397	-1.66667	9.589574				
58	3.918568	-6.66667	6.340377				
59	7.551281	-1.66667	6.340377				
60	3.530181	-5.22675	7.760088				
61	6.061816	-1.74225	7.760088				
62	2.96409	-3.4845	8.892269				
63	4.229907	-1.74225	8.892269				
64	5.362089	-5.22675	6.627906				
65	6.627906	-3.4845	6.627906				
66	3.814335	-8.65734	3.240586				
67	9.412309	-0.95238	3.240586				
68	8.969032	-2.69672	3.504874				
69	5.33632	-7.69672	3.504874				
70	6.844134	-6.30351	3.663817				
71	8.109951	-4.56127	3.663817				
72	9.025905	-3.89579	1.831908				
73	9.412309	0.952384	3.240586				
74	3.814335	8.657335	3.240586				
75	8.969032	2.696723	3.504874				
76	5.33632	7.696723	3.504874				
77	6.844134	6.303513	3.663817				
78	8.109951	4.561265	3.663817				
79	6.49427	7.380282	1.831908				
80	2.002792	9.245941	3.240586				
81	-7.05492	6.302912	3.240586				
82	0.206847	9.36339	3.504874				
83	-5.67101	7.45356	3.504874				
84	-3.88004	8.457051	3.663817				
85	-1.83191	9.12253	3.663817				
86	-5.01223	8.457051	1.831908				
87	-8.17452	4.761921	3.240586				
88	-8.17452	-4.76192	3.240586				
89	-8.84119	3.09017	3.504874				
90	-8.84119	-3.09017	3.504874				
91	-9.24213	-1.07677	3.663817				
92	-9.24213	1.076769	3.663817				
93	-9.592	-2.15354	1.831908				
94	-7.05492	-6.30291	3.240586				
95	2.002792	-9.24594	3.240586				
96	-5.67101	-7.45356	3.504874				
97	0.206847	-9.36339	3.504874				
98	-1.83191	-9.12253	3.663817				
99	-3.88004	-8.45705	3.663817				
100	-0.91595	-9.78801	1.831908				

Table A.14: Geodesic gridshell: Node coordinates, Design Option 7 (1/2)

Rigid nodes				Splice joints			
	x [m]	y [m]	z [m]		x [m]	y [m]	z [m]
1	0	0	10	1	1.620293	0	9.867859
2	3.432786	0	9.392336	2	8.101465	0	5.862275
3	6.865572	0	7.270758	3	8.602163	1.54099	4.860879
4	8.944272	0	4.472136	4	4.123783	7.704951	4.860879
5	7.926362	3.264774	5.149179	5	2.50349	7.704951	5.862275
6	5.554365	6.529547	5.149179	6	0.500698	1.54099	9.867859
7	2.763932	8.506508	4.472136	7	2.29397	1.666667	9.589574
8	2.121578	6.529547	7.270758	8	7.551281	1.666667	6.340377
9	1.060789	3.264774	9.392336	9	3.918568	6.666667	6.340377
10	4.911235	3.568221	7.946545	10	6.061816	1.742248	7.760088
11	-0.6556	8.547288	5.149179	11	3.530181	5.226745	7.760088
12	-4.49358	7.300256	5.149179	12	4.229907	1.742248	8.892269
13	-7.23607	5.257311	4.472136	13	2.96409	3.484496	8.892269
14	-5.55437	4.035482	7.270758	14	6.627906	3.484496	6.627906
15	-2.77718	2.017741	9.392336	15	5.362089	5.226745	6.627906
16	-1.87593	5.773503	7.946545	16	1.192646	8.657335	4.860879
17	-8.33155	2.017741	5.149179	17	-6.05353	6.302912	4.860879
18	-8.33155	-2.01774	5.149179	18	-6.55422	4.761921	5.862275
19	-7.23607	-5.25731	4.472136	19	-1.31085	0.952384	9.867859
20	-5.55437	-4.03548	7.270758	20	-0.87622	2.696723	9.589574
21	-2.77718	-2.01774	9.392336	21	0.74838	7.696723	6.340377
22	-6.07062	0	7.946545	22	-5.12947	5.786893	6.340377
23	-4.49358	-7.30026	5.149179	23	0.216227	6.303513	7.760088
24	-0.6556	-8.54729	5.149179	24	-3.88004	4.972554	7.760088
25	2.763932	-8.50651	4.472136	25	-0.34986	4.561265	8.892269
26	2.121578	-6.52955	7.270758	26	-2.398	3.895785	8.892269
27	1.060789	-3.26477	9.392336	27	-1.26582	7.380282	6.627906
28	-1.87593	-5.7735	7.946545	28	-3.31395	6.714802	6.627906
29	5.554365	-6.52955	5.149179	29	-7.86507	3.809537	4.860879
30	7.926362	-3.26477	5.149179	30	-7.86507	-3.80954	4.860879
31	4.911235	-3.56822	7.946545	31	-6.55422	-4.76192	5.862275
32	4.898761	-8.54729	1.716393	32	-1.31085	-0.95238	9.867859
33	9.642755	-2.01774	1.716393	33	-2.8355	0	9.589574
34	7.946545	-5.7735	1.875925	34	-7.08876	3.09017	6.340377
35	9.642755	2.017741	1.716393	35	-7.08876	-3.09017	6.340377
36	4.898761	8.547288	1.716393	36	-5.92818	2.153537	7.760088
37	7.946545	5.773503	1.875925	37	-5.92818	-2.15354	7.760088
38	1.060789	9.794321	1.716393	38	-4.44614	1.076769	8.892269
39	-6.61515	7.300256	1.716393	39	-4.44614	-1.07677	8.892269
40	-3.03531	9.341724	1.875925	40	-7.41022	1.076769	6.627906
41	-8.98715	4.035482	1.716393	41	-7.41022	-1.07677	6.627906
42	-8.98715	-4.03548	1.716393	42	-6.05353	-6.30291	4.860879
43	-9.82247	0	1.875925	43	1.192646	-8.65734	4.860879
44	-6.61515	-7.30026	1.716393	44	2.50349	-7.70495	5.862275
45	1.060789	-9.79432	1.716393	45	0.500698	-1.54099	9.867859
46	-3.03531	-9.34172	1.875925	46	-0.87622	-2.69672	9.589574
				47	-5.12947	-5.78689	6.340377
				48	0.74838	-7.69672	6.340377
				49	-3.88004	-4.97255	7.760088
				50	0.216227	-6.30351	7.760088

Table A.15: Geodesic gridshell: Node coordinates, Design Option 7 (2/2)**Splice joints**

	x [m]	y [m]	z [m]
51	-2.398	-3.89579	8.892269
52	-0.34986	-4.56127	8.892269
53	-3.31395	-6.7148	6.627906
54	-1.26582	-7.38028	6.627906
55	4.123783	-7.70495	4.860879
56	8.602163	-1.54099	4.860879
57	2.29397	-1.66667	9.589574
58	3.918568	-6.66667	6.340377
59	7.551281	-1.66667	6.340377
60	3.530181	-5.22675	7.760088
61	6.061816	-1.74225	7.760088
62	2.96409	-3.4845	8.892269
63	4.229907	-1.74225	8.892269
64	5.362089	-5.22675	6.627906
65	6.627906	-3.4845	6.627906
66	3.814335	-8.65734	3.240586
67	9.412309	-0.95238	3.240586
68	8.969032	-2.69672	3.504874
69	5.33632	-7.69672	3.504874
70	6.844134	-6.30351	3.663817
71	8.109951	-4.56127	3.663817
72	9.412309	0.952384	3.240586
73	3.814335	8.657335	3.240586
74	8.969032	2.696723	3.504874
75	5.33632	7.696723	3.504874
76	6.844134	6.303513	3.663817
77	8.109951	4.561265	3.663817
78	2.002792	9.245941	3.240586
79	-7.05492	6.302912	3.240586
80	0.206847	9.36339	3.504874
81	-5.67101	7.45356	3.504874
82	-3.88004	8.457051	3.663817
83	-1.83191	9.12253	3.663817
84	-8.17452	4.761921	3.240586
85	-8.17452	-4.76192	3.240586
86	-8.84119	3.09017	3.504874
87	-8.84119	-3.09017	3.504874
88	-9.24213	-1.07677	3.663817
89	-9.24213	1.076769	3.663817
90	-7.05492	-6.30291	3.240586
91	2.002792	-9.24594	3.240586
92	-5.67101	-7.45356	3.504874
93	0.206847	-9.36339	3.504874
94	-1.83191	-9.12253	3.663817
95	-3.88004	-8.45705	3.663817
96	3.04235	9.36339	1.752437
97	9.845251	0	1.752437
98	3.04235	-9.36339	1.752437
99	-7.96498	-5.78689	1.752437
100	-7.96498	5.786893	1.752437

Table A.16: Geodesic gridshell: Node coordinates, Design Option 8 (1/2)

Rigid nodes			Splice joints				
	x [m]	y [m]	z [m]		x [m]	y [m]	z [m]
1	0	0	10	1	1.620293	0	9.867859
2	3.432786	0	9.392336	2	8.602163	1.54099	4.860879
3	6.865572	0	7.270758	3	4.123783	7.704951	4.860879
4	8.944272	0	4.472136	4	0.500698	1.54099	9.867859
5	7.926362	3.264774	5.149179	5	2.29397	1.666667	9.589574
6	5.554365	6.529547	5.149179	6	7.551281	1.666667	6.340377
7	2.763932	8.506508	4.472136	7	3.918568	6.666667	6.340377
8	2.121578	6.529547	7.270758	8	6.061816	1.742248	7.760088
9	1.060789	3.264774	9.392336	9	3.530181	5.226745	7.760088
10	4.911235	3.568221	7.946545	10	4.229907	1.742248	8.892269
11	-0.6556	8.547288	5.149179	11	2.96409	3.484496	8.892269
12	-4.49358	7.300256	5.149179	12	6.627906	3.484496	6.627906
13	-7.23607	5.257311	4.472136	13	5.362089	5.226745	6.627906
14	-5.55437	4.035482	7.270758	14	1.192646	8.657335	4.860879
15	-2.77718	2.017741	9.392336	15	-6.05353	6.302912	4.860879
16	-1.87593	5.773503	7.946545	16	-1.31085	0.952384	9.867859
17	-8.33155	2.017741	5.149179	17	-0.87622	2.696723	9.589574
18	-8.33155	-2.01774	5.149179	18	0.74838	7.696723	6.340377
19	-7.23607	-5.25731	4.472136	19	-5.12947	5.786893	6.340377
20	-5.55437	-4.03548	7.270758	20	0.216227	6.303513	7.760088
21	-2.77718	-2.01774	9.392336	21	-3.88004	4.972554	7.760088
22	-6.07062	0	7.946545	22	-0.34986	4.561265	8.892269
23	-4.49358	-7.30026	5.149179	23	-2.398	3.895785	8.892269
24	-0.6556	-8.54729	5.149179	24	-1.26582	7.380282	6.627906
25	2.763932	-8.50651	4.472136	25	-3.31395	6.714802	6.627906
26	2.121578	-6.52955	7.270758	26	-7.86507	3.809537	4.860879
27	1.060789	-3.26477	9.392336	27	-7.86507	-3.80954	4.860879
28	-1.87593	-5.7735	7.946545	28	-1.31085	-0.95238	9.867859
29	5.554365	-6.52955	5.149179	29	-2.8355	0	9.589574
30	7.926362	-3.26477	5.149179	30	-7.08876	3.09017	6.340377
31	4.911235	-3.56822	7.946545	31	-7.08876	-3.09017	6.340377
32	4.898761	-8.54729	1.716393	32	-5.92818	2.153537	7.760088
33	9.642755	-2.01774	1.716393	33	-5.92818	-2.15354	7.760088
34	7.946545	-5.7735	1.875925	34	-4.44614	1.076769	8.892269
35	9.642755	2.017741	1.716393	35	-4.44614	-1.07677	8.892269
36	4.898761	8.547288	1.716393	36	-7.41022	1.076769	6.627906
37	7.946545	5.773503	1.875925	37	-7.41022	-1.07677	6.627906
38	1.060789	9.794321	1.716393	38	-6.05353	-6.30291	4.860879
39	-6.61515	7.300256	1.716393	39	1.192646	-8.65734	4.860879
40	-3.03531	9.341724	1.875925	40	0.500698	-1.54099	9.867859
41	-8.98715	4.035482	1.716393	41	-0.87622	-2.69672	9.589574
42	-8.98715	-4.03548	1.716393	42	-5.12947	-5.78689	6.340377
43	-9.82247	0	1.875925	43	0.74838	-7.69672	6.340377
44	-6.61515	-7.30026	1.716393	44	-3.88004	-4.97255	7.760088
45	1.060789	-9.79432	1.716393	45	0.216227	-6.30351	7.760088
46	-3.03531	-9.34172	1.875925	46	-2.398	-3.89579	8.892269
				47	-0.34986	-4.56127	8.892269
				48	-3.31395	-6.7148	6.627906
				49	-1.26582	-7.38028	6.627906
				50	4.123783	-7.70495	4.860879

Table A.17: Geodesic gridshell: Node coordinates, Design Option 8 (2/2)**Splice joints**

	x [m]	y [m]	z [m]
51	8.602163	-1.54099	4.860879
52	2.29397	-1.66667	9.589574
53	3.918568	-6.66667	6.340377
54	7.551281	-1.66667	6.340377
55	3.530181	-5.22675	7.760088
56	6.061816	-1.74225	7.760088
57	2.96409	-3.4845	8.892269
58	4.229907	-1.74225	8.892269
59	5.362089	-5.22675	6.627906
60	6.627906	-3.4845	6.627906
61	3.814335	-8.65734	3.240586
62	9.412309	-0.95238	3.240586
63	8.969032	-2.69672	3.504874
64	5.33632	-7.69672	3.504874
65	6.844134	-6.30351	3.663817
66	8.109951	-4.56127	3.663817
67	9.412309	0.952384	3.240586
68	3.814335	8.657335	3.240586
69	8.969032	2.696723	3.504874
70	5.33632	7.696723	3.504874
71	6.844134	6.303513	3.663817
72	8.109951	4.561265	3.663817
73	2.002792	9.245941	3.240586
74	-7.05492	6.302912	3.240586
75	0.206847	9.36339	3.504874
76	-5.67101	7.45356	3.504874
77	-3.88004	8.457051	3.663817
78	-1.83191	9.12253	3.663817
79	-8.17452	4.761921	3.240586
80	-8.17452	-4.76192	3.240586
81	-8.84119	3.09017	3.504874
82	-8.84119	-3.09017	3.504874
83	-9.24213	-1.07677	3.663817
84	-9.24213	1.076769	3.663817
85	-7.05492	-6.30291	3.240586
86	2.002792	-9.24594	3.240586
87	-5.67101	-7.45356	3.504874
88	0.206847	-9.36339	3.504874
89	-1.83191	-9.12253	3.663817
90	-3.88004	-8.45705	3.663817
91	3.04235	9.36339	1.752437
92	9.845251	0	1.752437
93	3.04235	-9.36339	1.752437
94	-7.96498	-5.78689	1.752437
95	-7.96498	5.786893	1.752437

Cross section and material properties

One cross section is used for all beams and has a width (b) of 200 mm and a height (h) of 175 mm. The strength class is C30, which properties are presented in Table A.18.

Table A.18: Strength properties C30 timber

$E_{0,g,05}$	8000 N/mm ²
$f_{m,g,k}$	30 N/mm ²
$f_{t,0,g,k}$	19 N/mm ²
$f_{t,90,g,k}$	0.4 N/mm ²
$f_{c,0,g,k}$	24 N/mm ²
$f_{c,90,g,k}$	2.7 N/mm ²
$f_{v,g,k}$	4 N/mm ²

Boundary conditions and support

Table A.19 presents the coordinates of the supports in the structure and their boundary conditions are listed in Table A.20.

Table A.19: Geodesic Gridshell: Support coordinates

	x [m]	y [m]	z [m]
1	8.676042	-4.97255	0
2	7.410225	-6.7148	0
3	8.676042	4.972554	0
4	7.410225	6.714802	0
5	9.510565	-3.09017	0
6	9.510565	3.09017	0
7	9.941859	-1.07677	0
8	9.941859	1.076769	0
9	5.877853	8.09017	0
10	4.096271	9.12253	0
11	2.048136	9.78801	0
12	0	10	0
13	-2.04814	9.78801	0
14	-4.09627	9.12253	0
15	-5.87785	8.09017	0
16	-7.41023	6.714802	0
17	-8.67604	4.972554	0
18	-9.51057	3.09017	0
19	-9.94186	1.076769	0
20	-9.94186	-1.07677	0
21	-9.51057	-3.09017	0
22	-8.67604	-4.97255	0
23	-7.41023	-6.7148	0
24	-5.87785	-8.09017	0
25	-4.09627	-9.12253	0
26	-2.04814	-9.78801	0
27	0	-10	0
28	5.877853	-8.09017	0
29	2.048136	-9.78801	0
30	4.096271	-9.12253	0

Table A.20: Geodesic Gridshell: Support conditions

T_x	fixed
T_y	fixed
T_z	fixed
R_x	free
R_y	free
R_z	free

Joints

The pinned nodes in the classic geodesic gridshell have the following conditions:

Table A.21: Classic Geodesic Gridshell: Joint conditions, pinned nodes

T_x	fixed
T_y	fixed
T_z	fixed
R_x	fixed
R_y	free
R_z	fixed

Table A.22: Modular Geodesic Gridshell: Joint conditions, rigid nodes

T_x	fixed
T_y	fixed
T_z	fixed
R_x	fixed
R_y	fixed
R_z	fixed

Table A.23: Modular Geodesic Gridshell: Joint conditions, splice joints

T_x	fixed
T_y	fixed
T_z	fixed
R_x	fixed
R_y	free
R_z	fixed

Load conditions

The load combinations that are applied to the structure are as discussed in subsection 4.3.2. The structure is bending inactive, which means that it contains initially curved beams that are not actively bend to achieve their curvature.

A.2. Numerical results

Table A.24: Geodesic Gridshell: FEA results (1/2) (20 m span, C30, 200x175 mm)

	Classic	DO 1	DO 2	DO 3	DO 4	DO 5	DO 6	DO 7	DO 8	
Reaction force (Qualitative)										
Rx	12.89	14.37	13.93	13.22	13.96	14.86	13.14	13.20	12.95	kN
Ry	13.07	14.53	13.63	12.49	14.71	12.06	13.29	17.54	18.03	kN
Rz	16.18	13.60	13.86	21.79	12.23	18.07	16.65	16.36	14.84	kN
Nodal displacement (SLS)										
dx	0.008	0.015	0.008	0.008	0.008	0.008	0.008	0.009	0.007	m
dy	0.009	0.016	0.015	0.012	0.013	0.016	0.016	0.016	0.015	m
dz	0.015	0.030	0.027	0.021	0.023	0.027	0.027	0.027	0.026	m
Beam displacement (SLS)										
w (-)	-0.015	-0.030	-0.027	-0.021	-0.023	-0.027	-0.027	-0.027	-0.026	m
w (+)	0.005	0.018	0.013	0.010	0.009	0.013	0.013	0.013	0.013	m
Unity checks SLS										
Roof defl.	0.192	0.372	0.333	0.262	0.286	0.332	0.332	0.332	0.323	[-]
x-displ.	0.252	0.438	0.250	0.230	0.248	0.254	0.255	0.258	0.221	[-]
y-displ.	0.261	0.479	0.463	0.358	0.398	0.467	0.467	0.471	0.442	[-]
Deformation energy (Qualitative)										
U_axial	0.215	0.263	0.255	0.250	0.248	0.256	0.255	0.254	0.252	kNm
U_bending	0.976	0.924	0.760	0.637	0.656	0.739	0.743	0.726	0.687	kNm
U_ax/U_tot	0.181	0.222	0.251	0.282	0.275	0.257	0.255	0.259	0.269	[-]
Stress (ULS)										
σ_{max}	0.948	1.555	1.190	1.303	1.095	1.187	1.187	1.189	1.158	kN/cm ²
σ_{min}	-0.865	-1.550	-1.386	-1.350	-1.308	-1.386	-1.375	-1.369	-1.294	kN/cm ²
τ_{max}	0.036	0.116	0.091	0.075	0.083	0.092	0.092	0.092	0.085	kN/cm ²
Cross section force (ULS)										
Nx,c	-45.17	-54.89	-53.51	-51.32	-51.97	-53.64	-53.33	-53.38	-55.49	kN
Nx,t	46.09	57.04	54.70	49.77	52.36	54.07	54.71	54.76	53.76	kN
Vz	8.14	12.08	11.73	11.27	10.98	11.75	11.67	11.61	12.07	kN
Vy	6.07	5.82	6.45	6.25	6.40	6.46	6.45	6.45	6.60	kN
Mt	0.21	1.04	0.81	0.67	0.71	0.82	0.82	0.82	0.76	kNm
My,hog	-8.40	-13.66	-12.37	-11.32	-11.45	-12.37	-12.29	-12.26	-11.88	kNm
My,sag	6.57	12.52	9.61	10.96	9.35	9.64	9.57	9.57	9.94	kNm
Mz,hog	-5.58	-5.73	-5.02	-4.74	-5.18	-5.02	-5.02	-5.00	-5.49	kNm
Mz,sag	2.29	4.80	3.81	3.53	3.41	3.83	3.84	3.86	3.63	kNm

Table A.25: Geodesic Gridshell: FEA results (2/2) (20 m span, C30, 200x175 mm)

	Classic	DO 1	DO 2	DO 3	DO 4	DO 5	DO 6	DO 7	DO 8	
Unity checks ULS										
Axial tension	0.129	0.159	0.153	0.139	0.146	0.151	0.153	0.153	0.150	[-]
Axial compr.	0.100	0.121	0.118	0.113	0.115	0.119	0.118	0.118	0.123	[-]
Bending (y-axis)	0.683	0.968	0.870	0.802	0.828	0.870	0.865	0.863	0.863	[-]
Bending (z-axis)	0.650	0.855	0.764	0.708	0.740	0.764	0.761	0.759	0.774	[-]
Shear (par.)	0.108	0.160	0.156	0.149	0.146	0.156	0.155	0.154	0.160	[-]
Shear (perp.)	0.162	0.240	0.233	0.224	0.218	0.234	0.232	0.231	0.240	[-]
Torsion	0.021	0.104	0.081	0.067	0.071	0.082	0.082	0.082	0.076	[-]
Bending + ten. (y)	0.811	1.127	1.023	0.941	0.974	1.021	1.018	1.016	1.014	[-]
Bending + ten. (z)	0.779	1.014	0.917	0.847	0.886	0.915	0.913	0.912	0.925	[-]
Bending + com. (y)	0.693	0.982	0.884	0.815	0.841	0.884	0.879	0.877	0.879	[-]
Bending + com. (z)	0.660	0.869	0.778	0.721	0.753	0.778	0.775	0.773	0.789	[-]
Flex. buckling (y)	0.891	1.948	1.726	1.286	1.398	1.728	1.718	1.716	1.701	[-]
Flex. buckling (z)	0.980	2.498	2.197	1.510	1.688	2.201	2.187	2.187	2.175	[-]
LTS	0.528	2.169	1.863	1.163	1.317	1.868	1.852	1.852	1.798	[-]
Nodal force pinned joints (ULS)										
Nx,c	-45.17	-51.37	-53.48	-46.99	-51.11	-53.61	-53.31	-53.09	-48.68	kN
Nx,t	46.09	57.04	49.31	47.98	46.64	49.09	49.12	48.53	46.47	kN
Vy	6.07	2.26	1.66	1.58	1.62	1.67	1.67	1.68	1.64	kN
Vz	8.14	4.69	4.56	4.31	4.15	4.59	4.58	4.59	4.66	kN
Mx	0.11	0.55	0.38	0.33	0.26	0.38	0.38	0.39	0.36	kNm
Mz,hog	-5.58	-0.91	-0.69	-0.39	-0.58	-0.67	-0.67	-0.67	-0.67	kNm
Mz,sag	1.65	4.10	3.52	3.41	3.26	3.54	3.54	3.55	3.32	kNm
Nodal force rigid joints (ULS)										
Nx,c	-	-54.82	-53.15	-50.43	-51.92	-53.17	-53.22	-53.30	-54.48	kN
Nx,t	-	55.91	53.59	49.06	51.27	52.97	53.59	53.65	53.55	kN
Vy	-	-5.82	-6.45	-6.25	-6.40	-6.46	-6.45	-6.45	-6.60	kN
Vz	-	-11.31	-10.98	-9.89	-10.63	-10.85	-11.00	-10.99	-10.63	kN
Mx	-	1.04	0.81	0.67	0.71	0.82	0.82	0.82	0.76	kNm
My,hog	-	-13.66	-12.37	-11.32	-11.45	-12.37	-12.29	-12.26	-11.88	kNm
My,sag	-	12.52	9.61	10.96	9.35	9.64	9.57	9.57	9.94	kNm
Mz,hog	-	-5.73	-5.02	-4.74	-5.18	-5.02	-5.02	-5.00	-5.49	kNm
Mz,sag	-	4.80	3.81	3.27	3.37	3.83	3.84	3.86	3.63	kNm
Stability (2nd order, ULS)										
Buckling factor	12.48	-5.73	-5.02	-4.74	-5.18	-5.02	-5.02	-5.00	-5.49	[-]

A.3. Axial stress & displacement plots

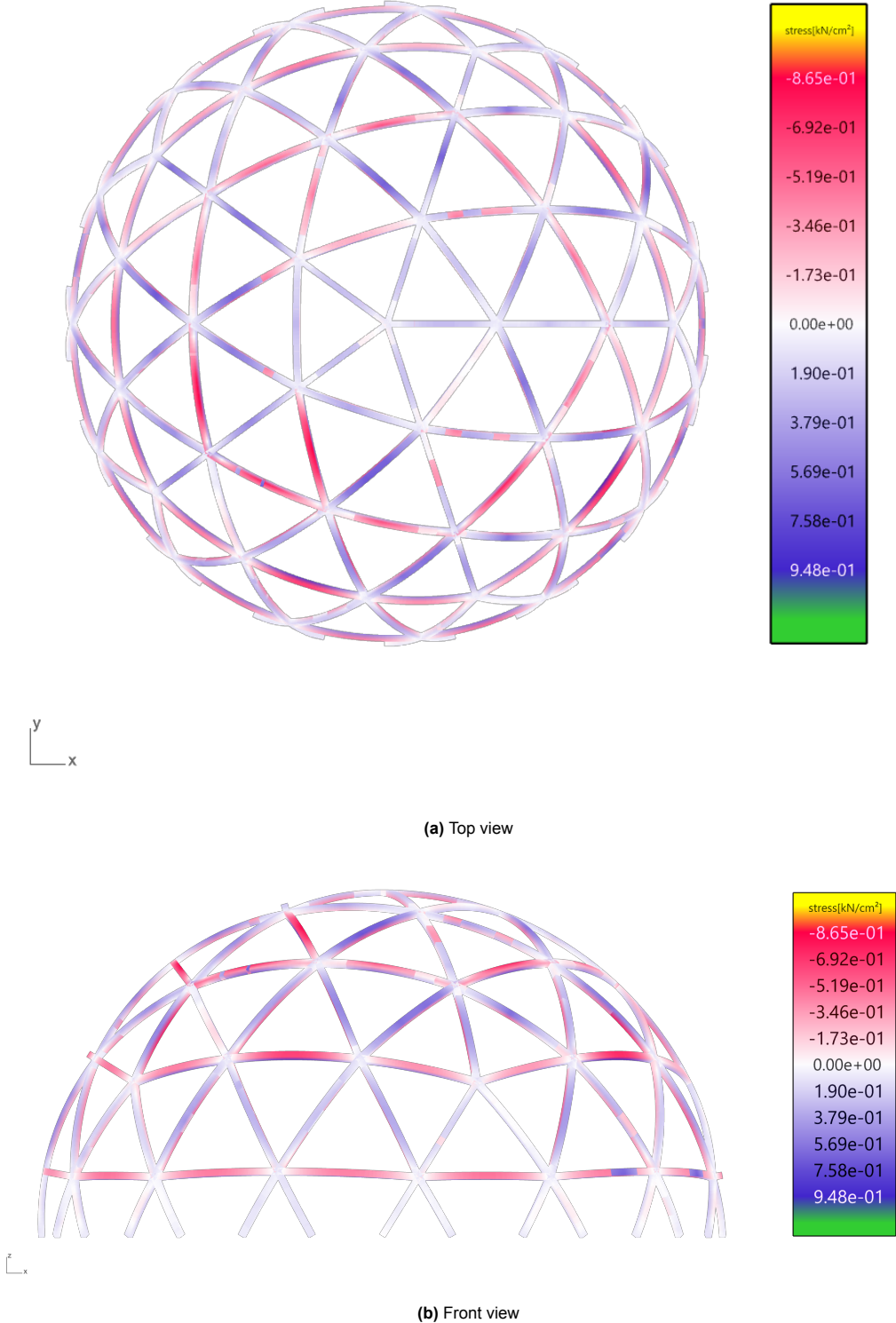


Figure A.3: Classic Geodesic Gridshell: Axial stress (ULS, 20 m span, C30, 200x175 mm)

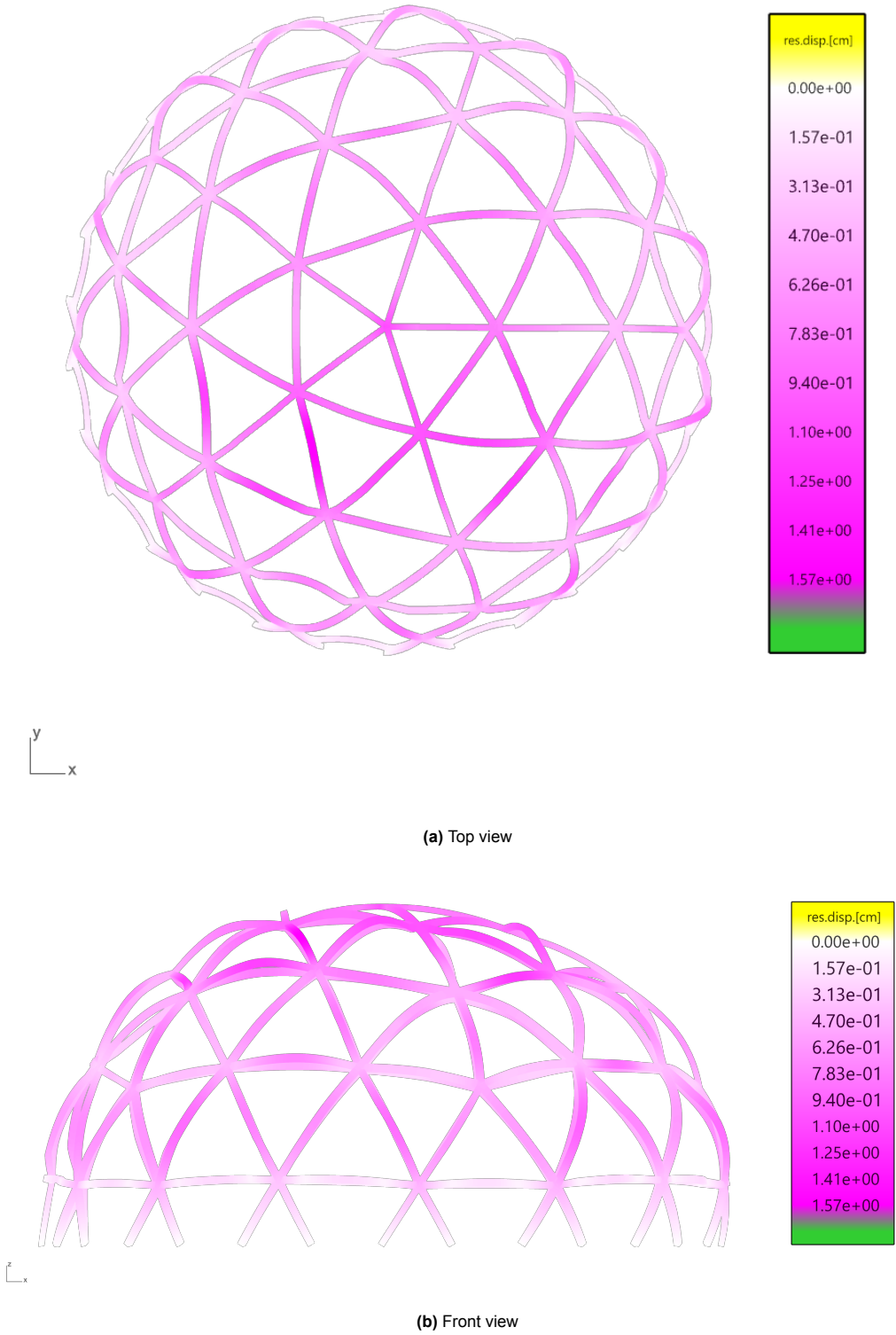


Figure A.4: Classic Geodesic Gridshell: Displacement (SLS, 20 m span, C30, 200x175 mm)

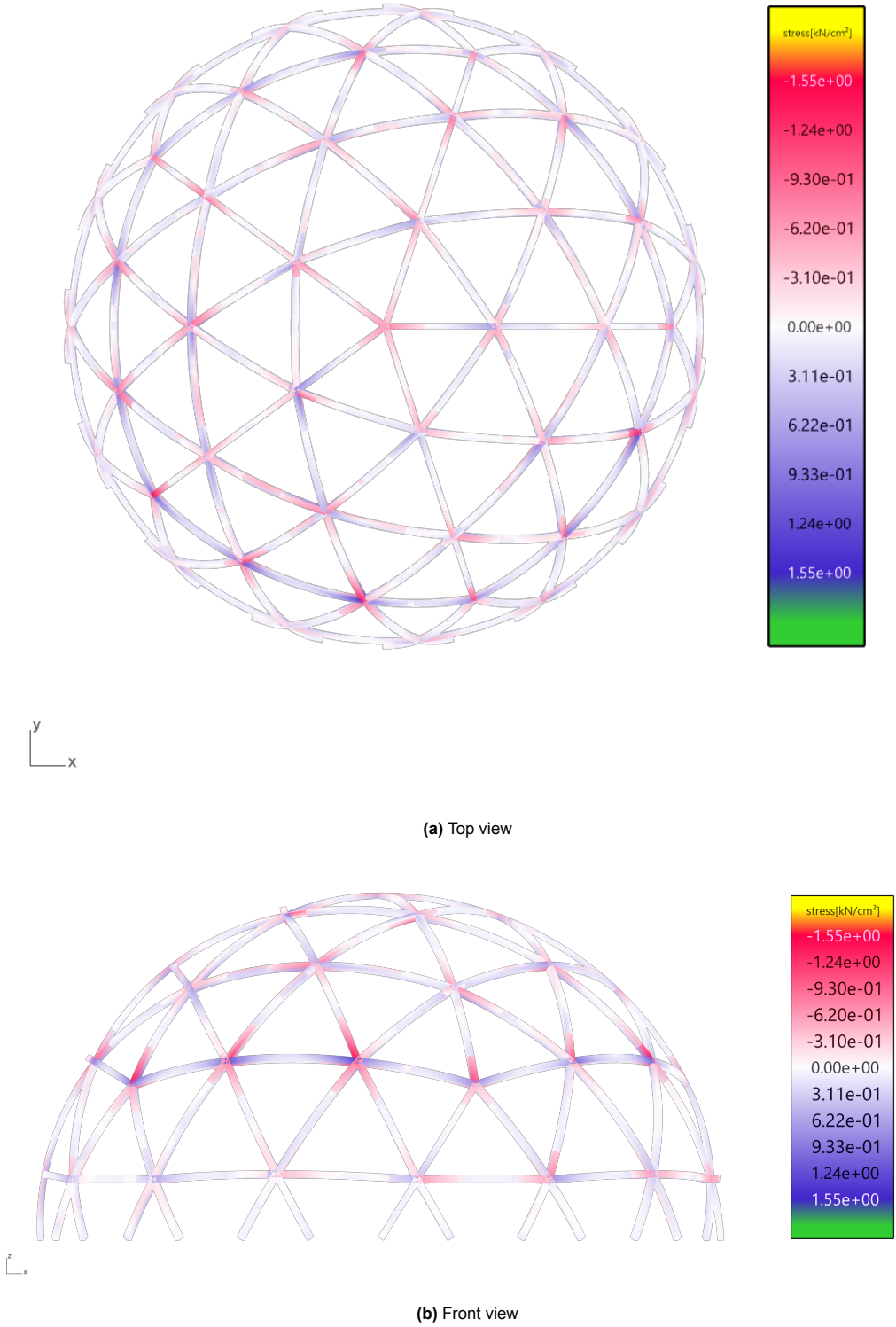


Figure A.5: Geodesic Gridshell: Axial stress, Design Option 1 (ULS, 20 m span, C30, 200x175 mm)

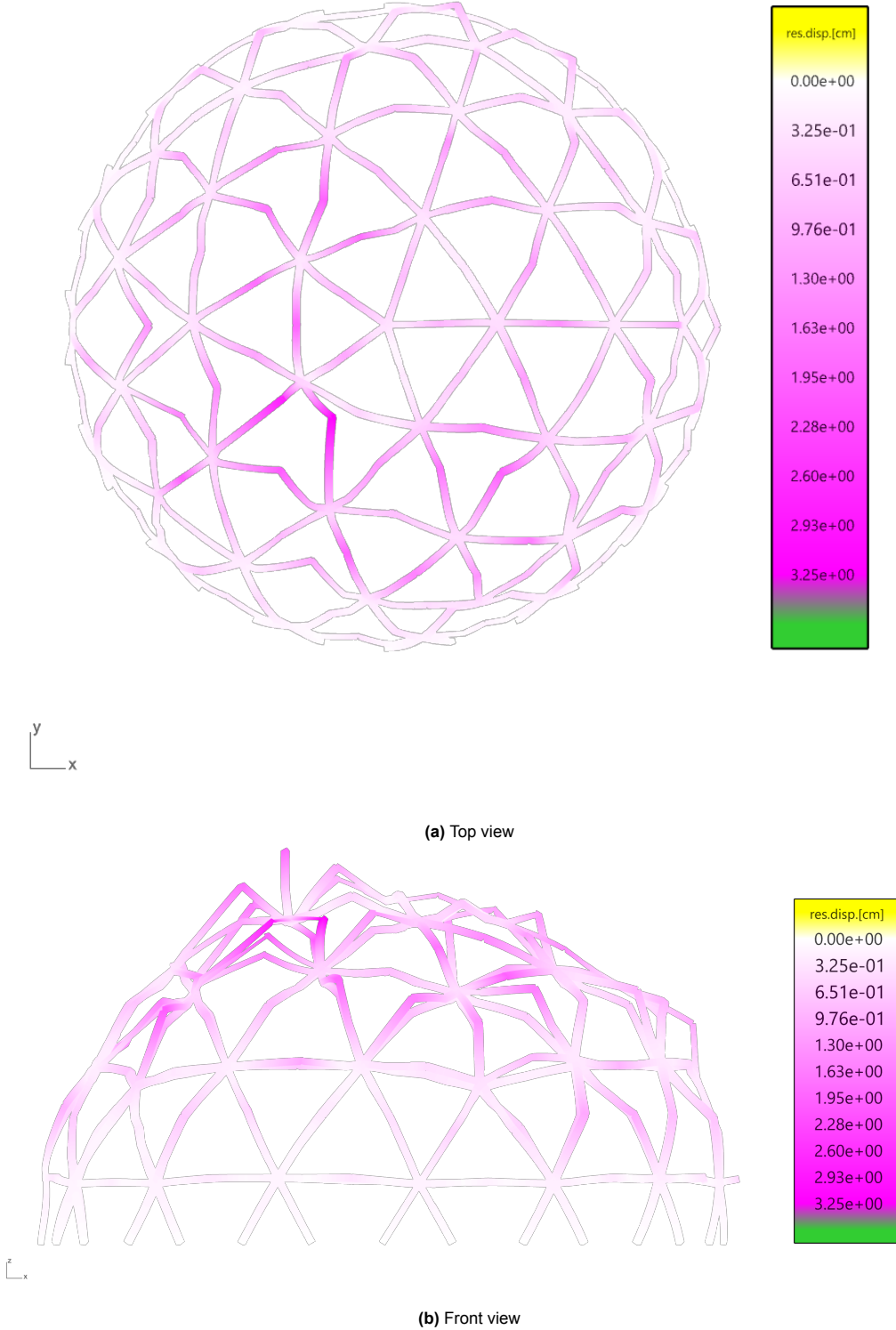


Figure A.6: Geodesic Gridshell: Displacement, Design Option 1 (SLS, 20 m span, C30, 200x175 mm)

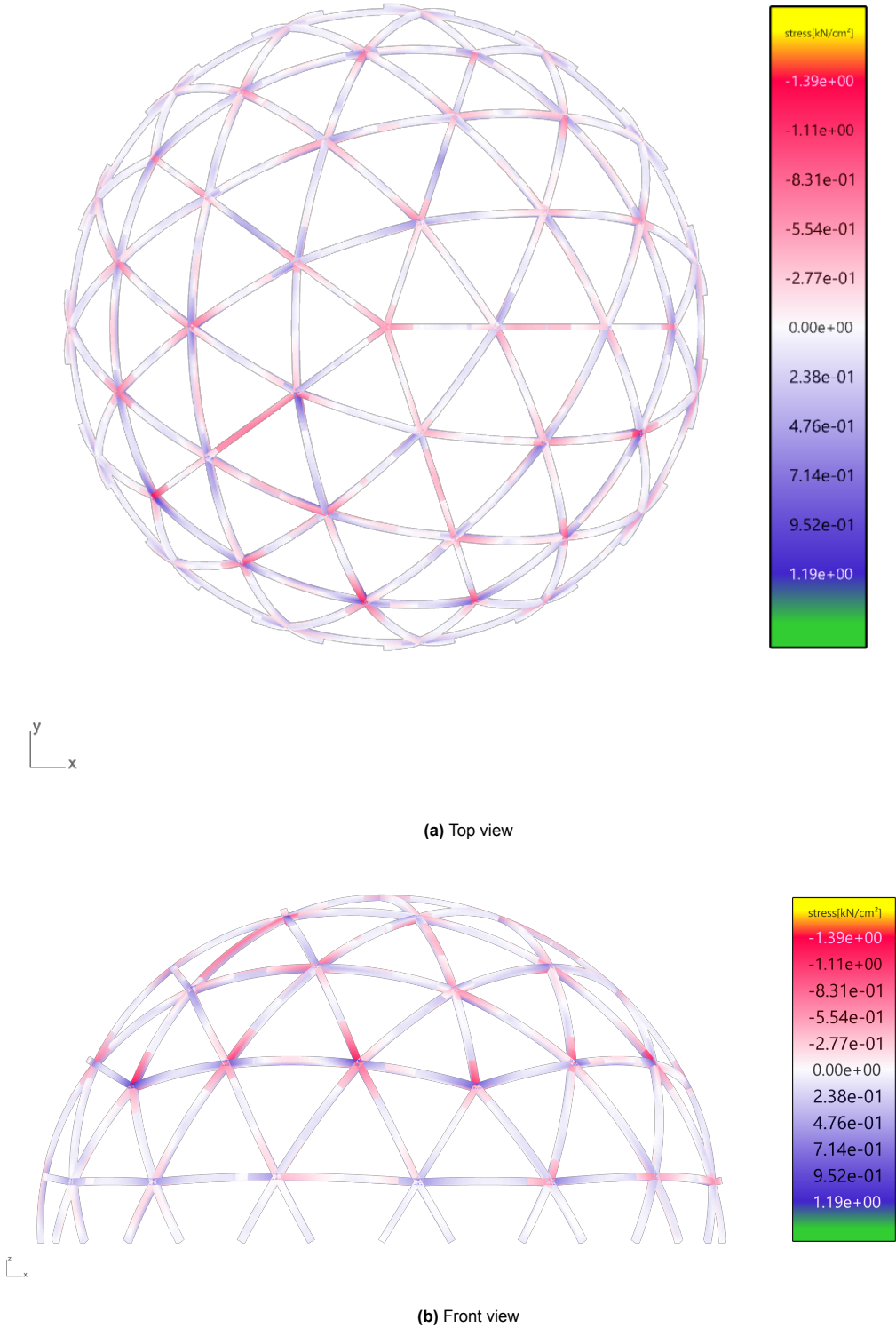


Figure A.7: Geodesic Gridshell: Axial stress, Design Option 2 (ULS, 20 m span, C30, 200x175 mm)

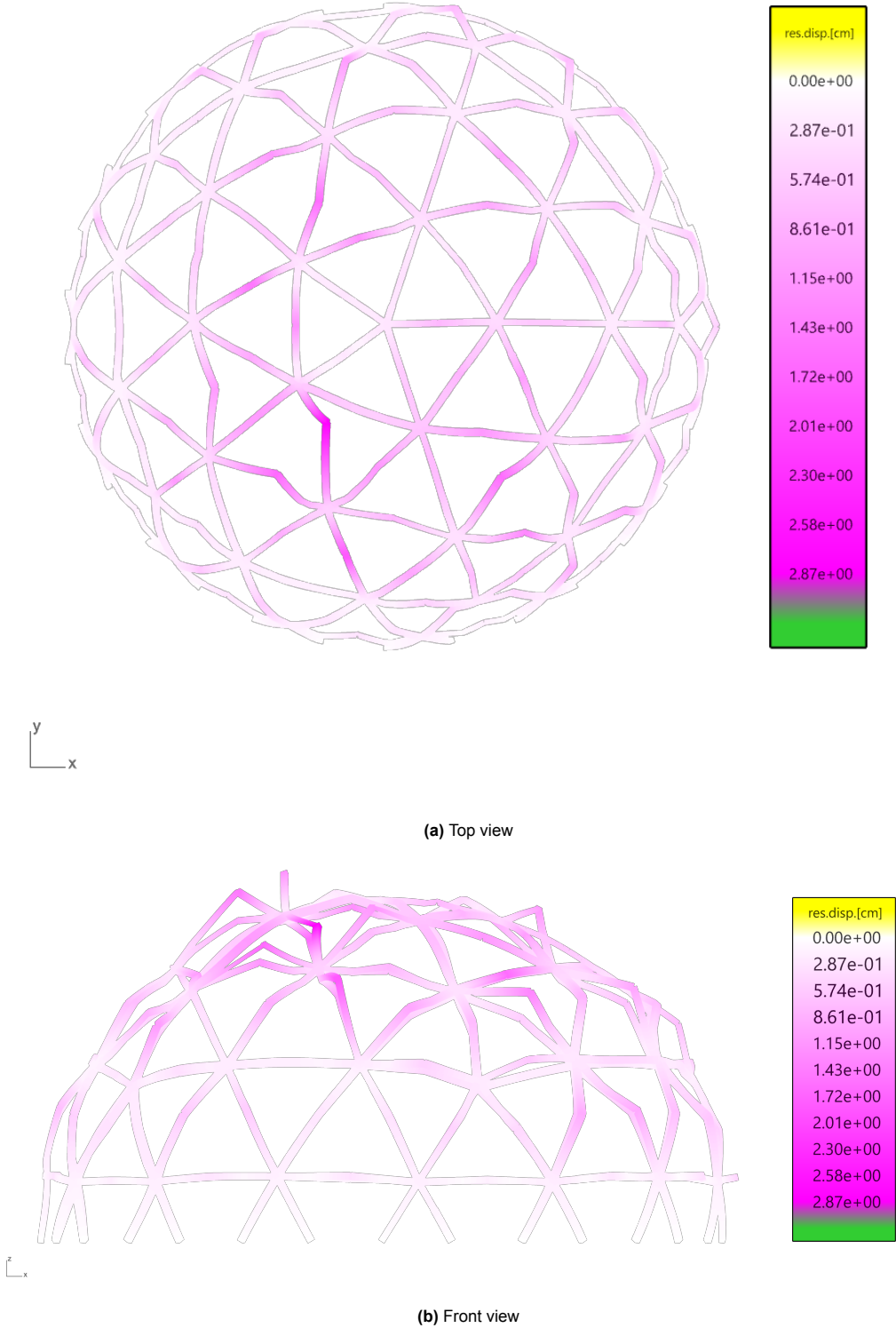


Figure A.8: Geodesic Gridshell: Displacement, Design Option 2 (SLS, 20 m span, C30, 200x175 mm)

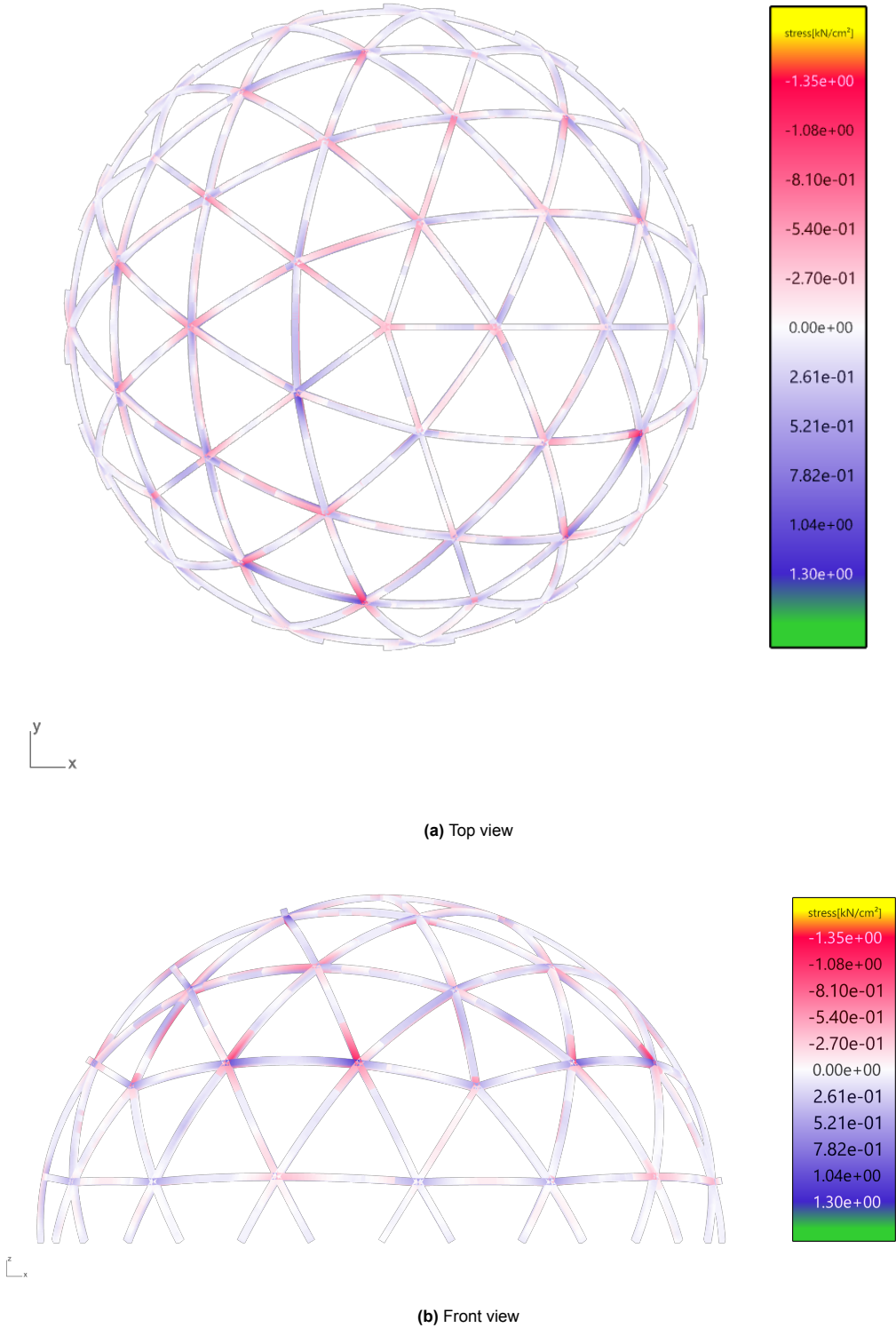


Figure A.9: Geodesic Gridshell: Axial stress, Design Option 3 (ULS, 20 m span, C30, 200x175 mm)

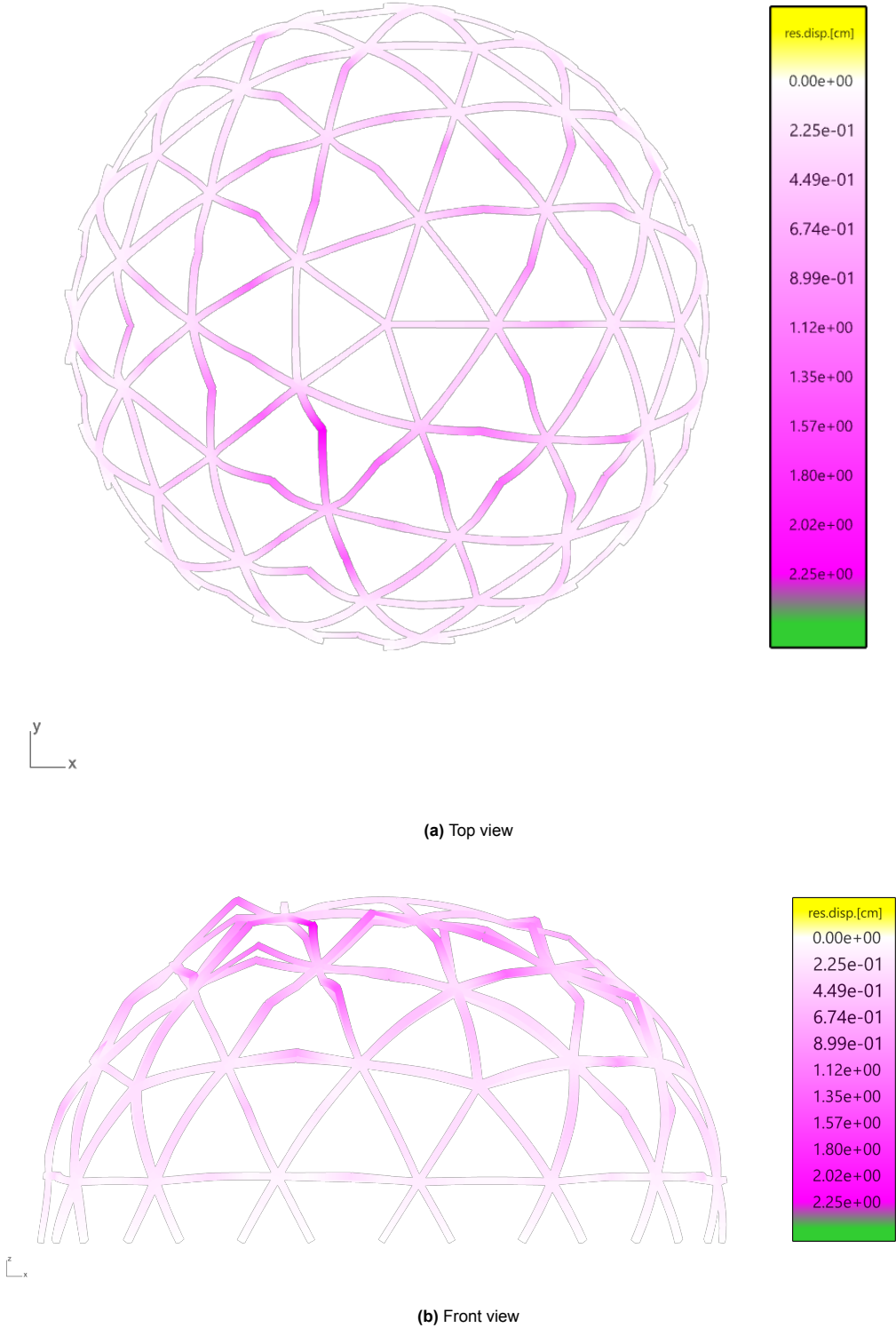


Figure A.10: Geodesic Gridshell: Displacement, Design Option 3 (SLS, 20 m span, C30, 200x175 mm)

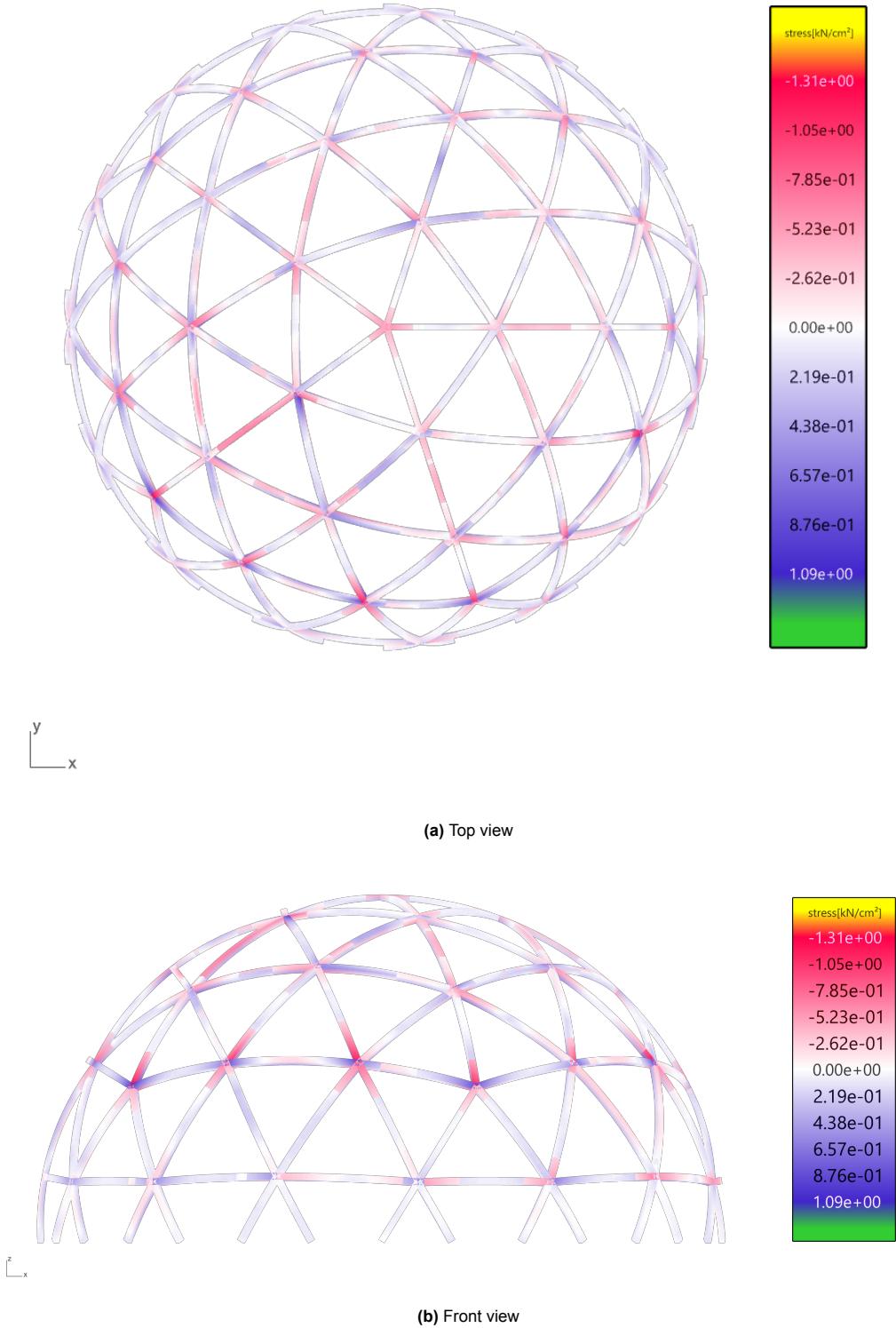


Figure A.11: Geodesic Gridshell: Axial stress, Design Option 4 (ULS, 20 m span, C30, 200x175 mm)

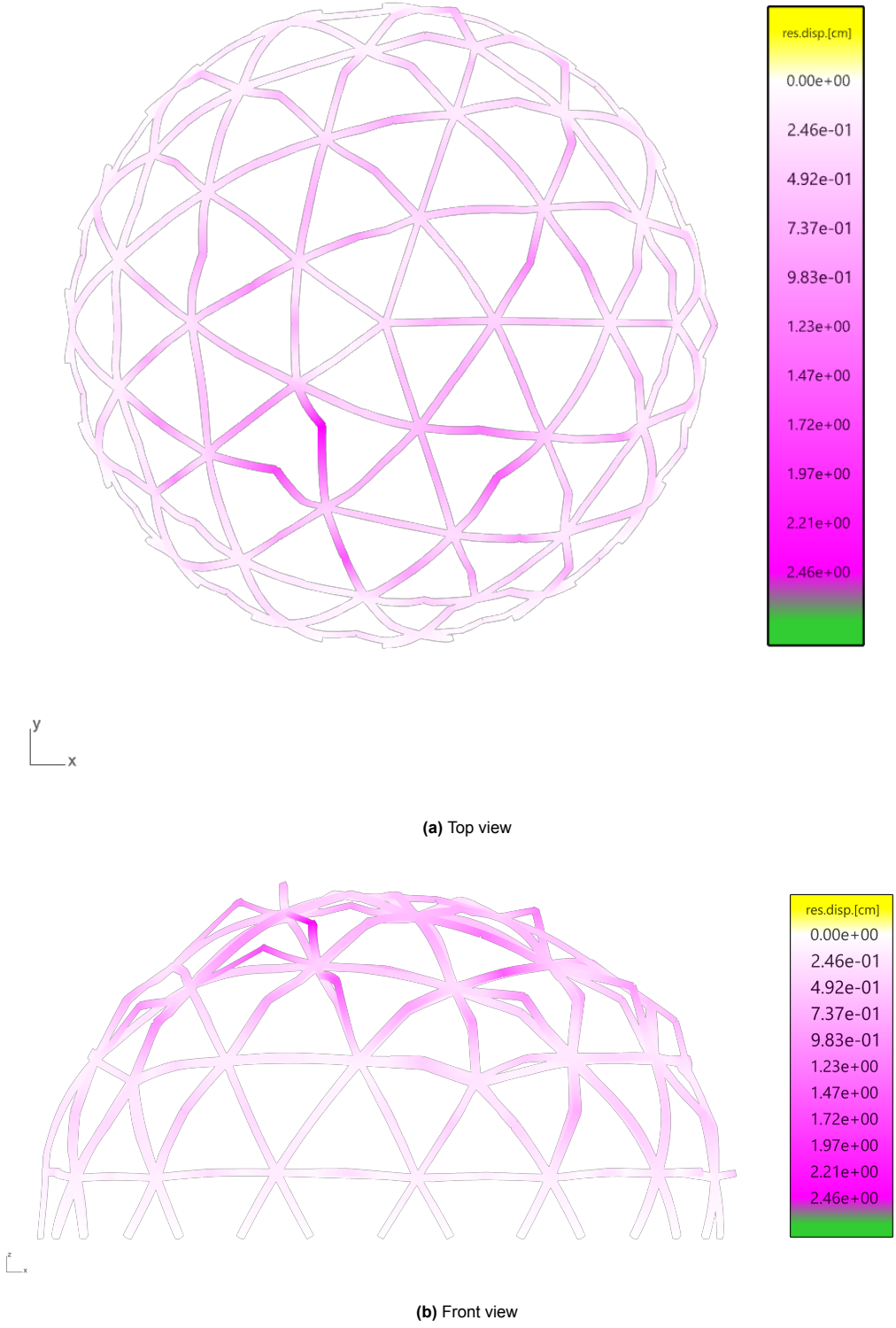


Figure A.12: Geodesic Gridshell: Displacement, Design Option 4 (SLS, 20 m span, C30, 200x175 mm)

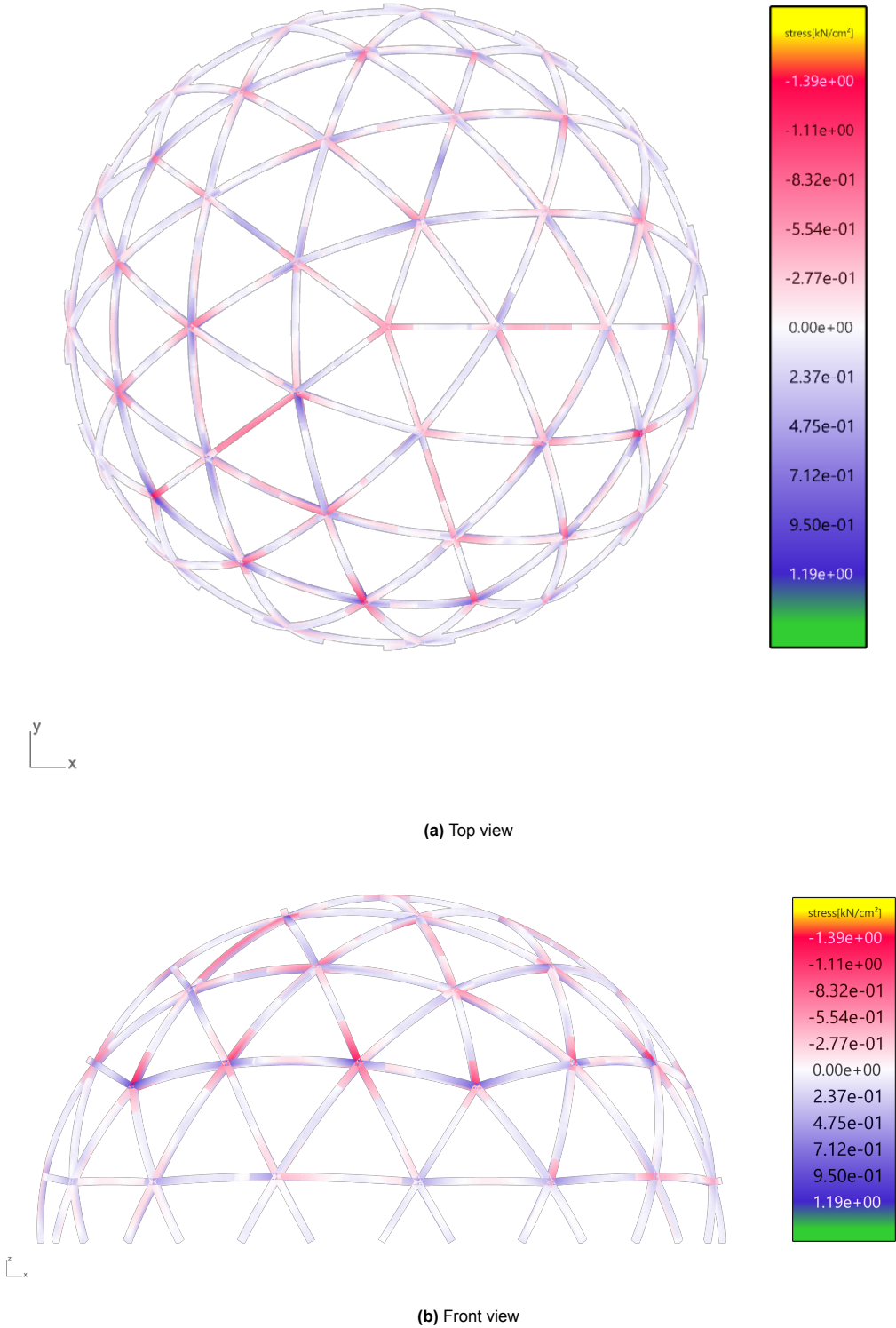


Figure A.13: Geodesic Gridshell: Axial stress, Design Option 5 (ULS, 20 m span, C30, 200x175 mm)

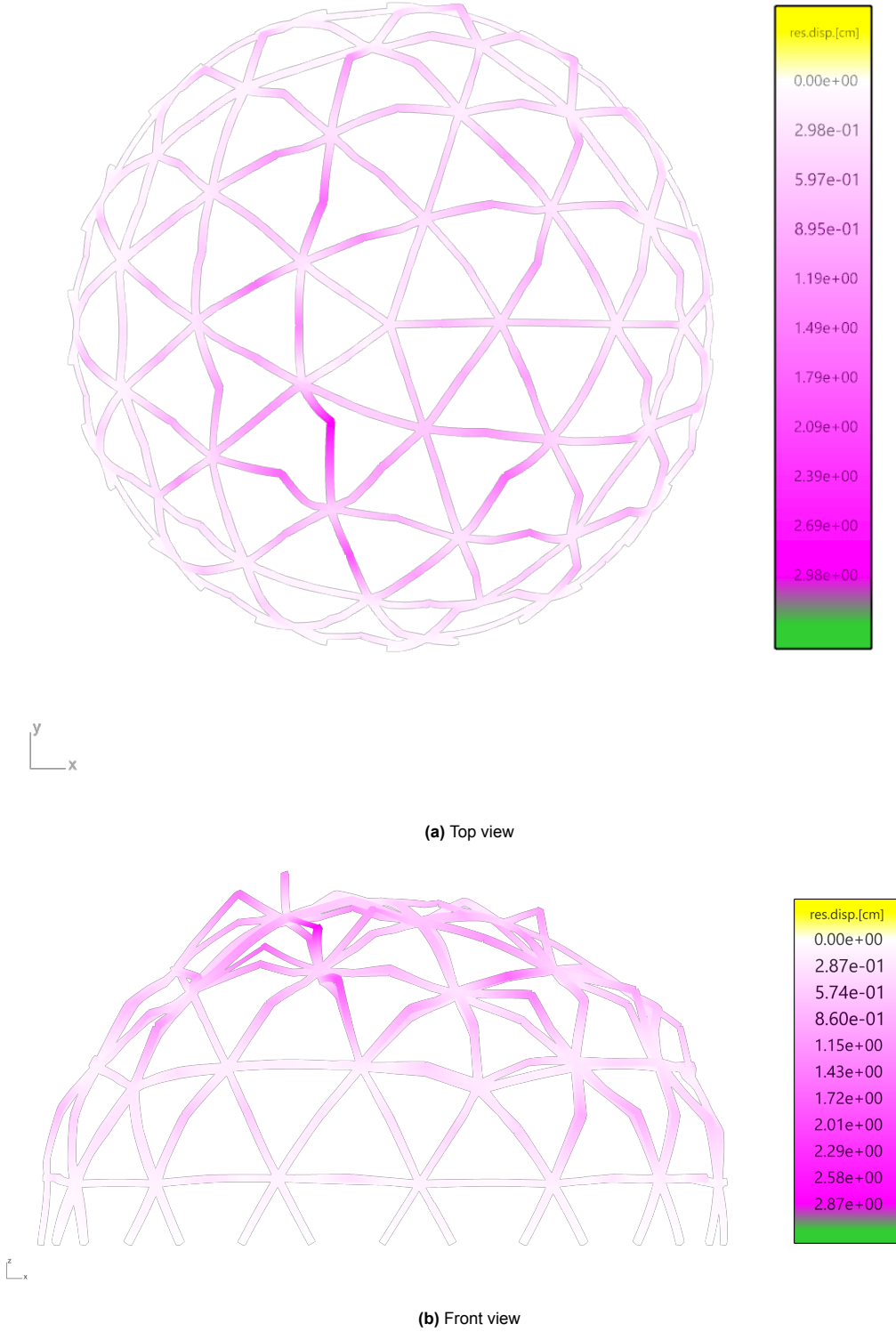


Figure A.14: Geodesic Gridshell: Displacement, Design Option 5 (SLS, 20 m span, C30, 200x175 mm)

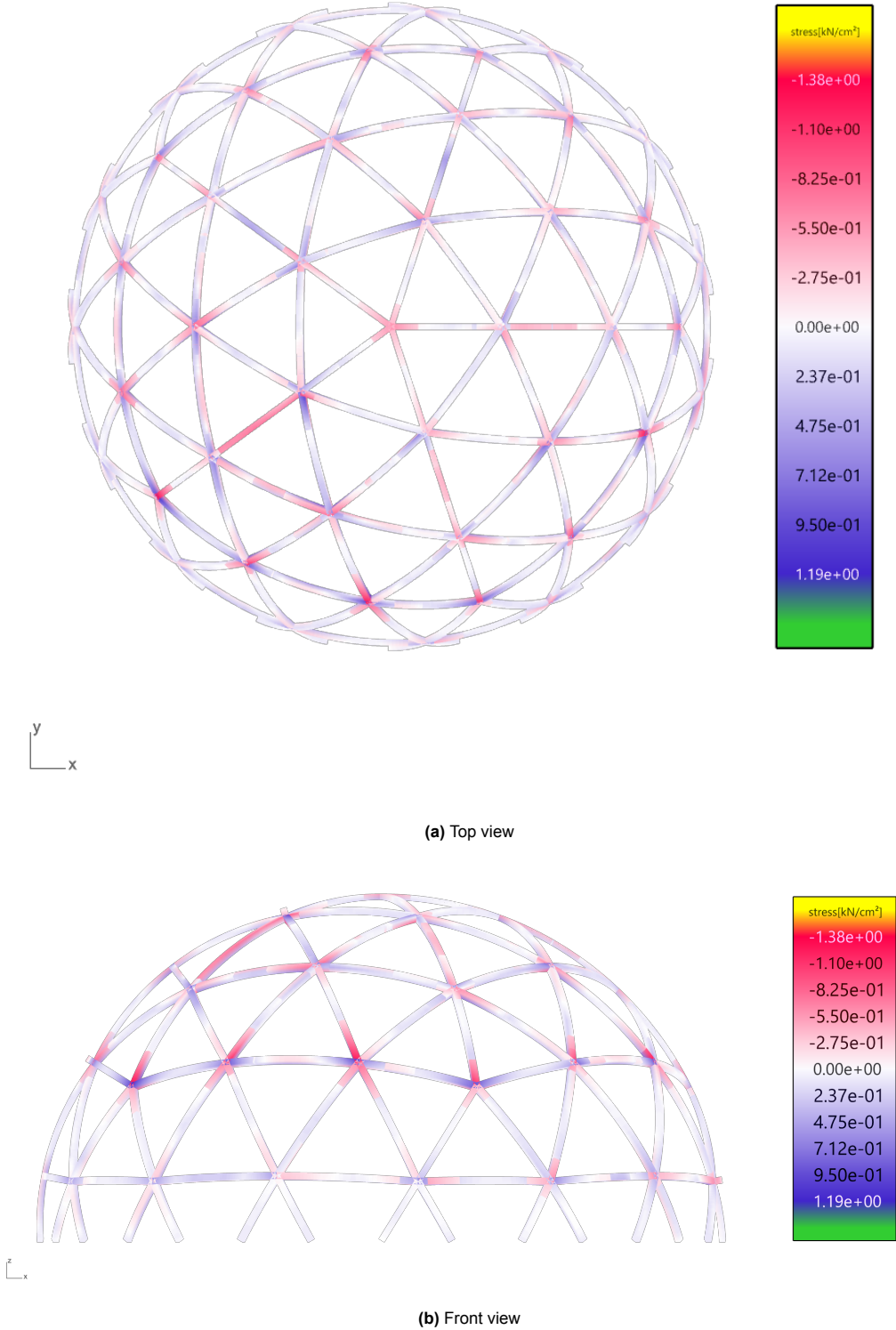


Figure A.15: Geodesic Gridshell: Axial stress, Design Option 6 (ULS, 20 m span, C30, 200x175 mm)

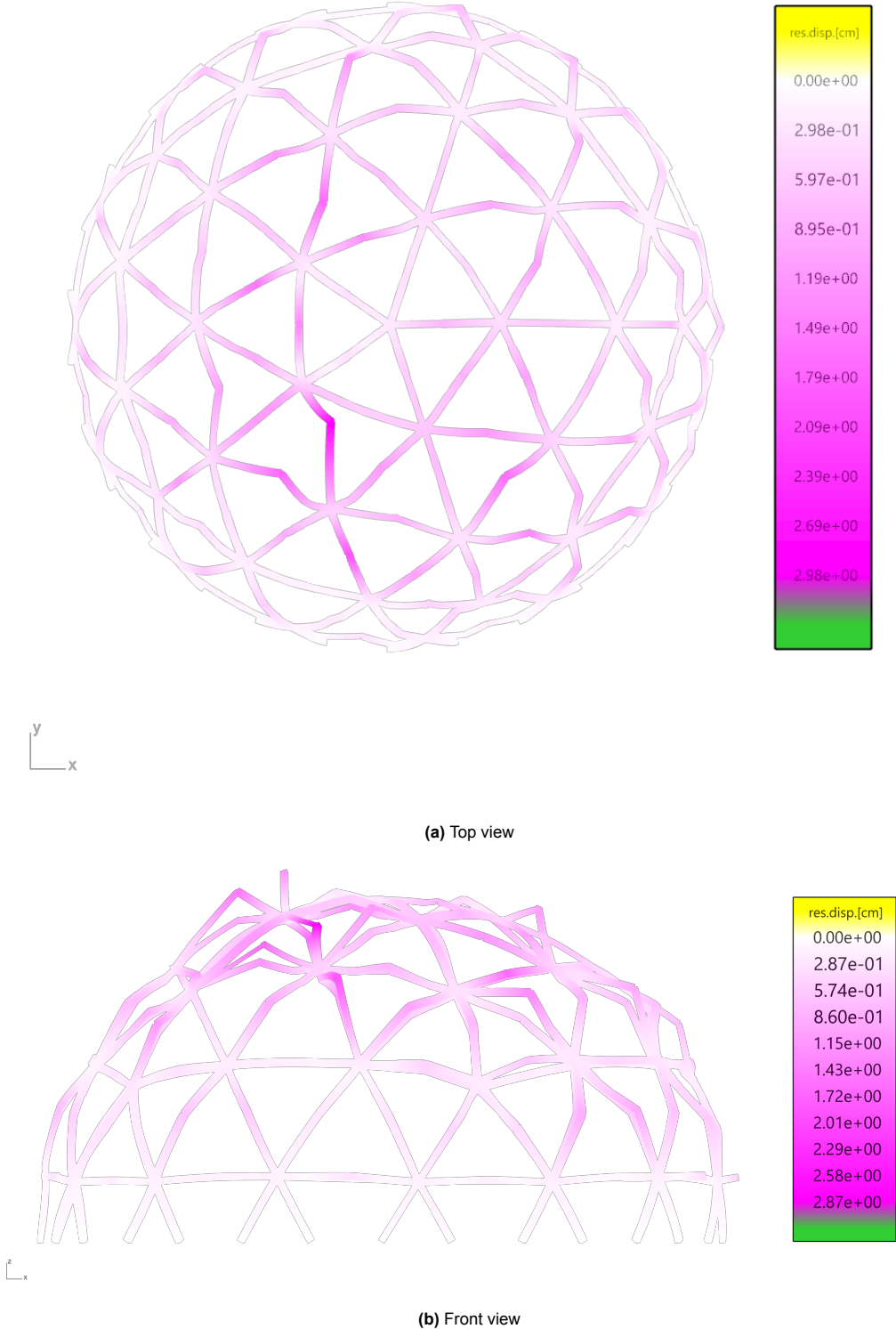


Figure A.16: Geodesic Gridshell: Displacement, Design Option 6 (SLS, 20 m span, C30, 200x175 mm)

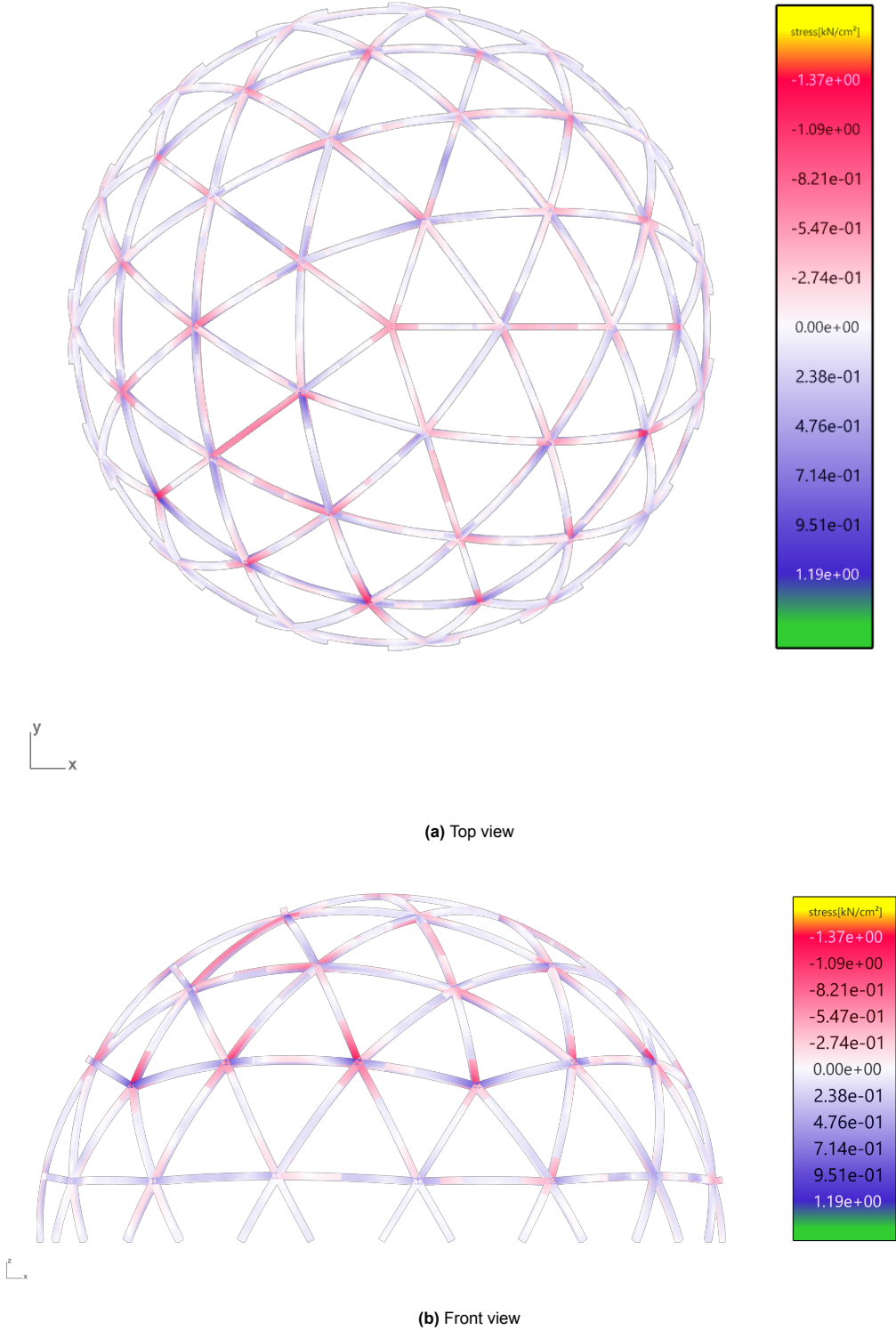


Figure A.17: Geodesic Gridshell: Axial stress, Design Option 7 (ULS, 20 m span, C30, 200x175 mm)

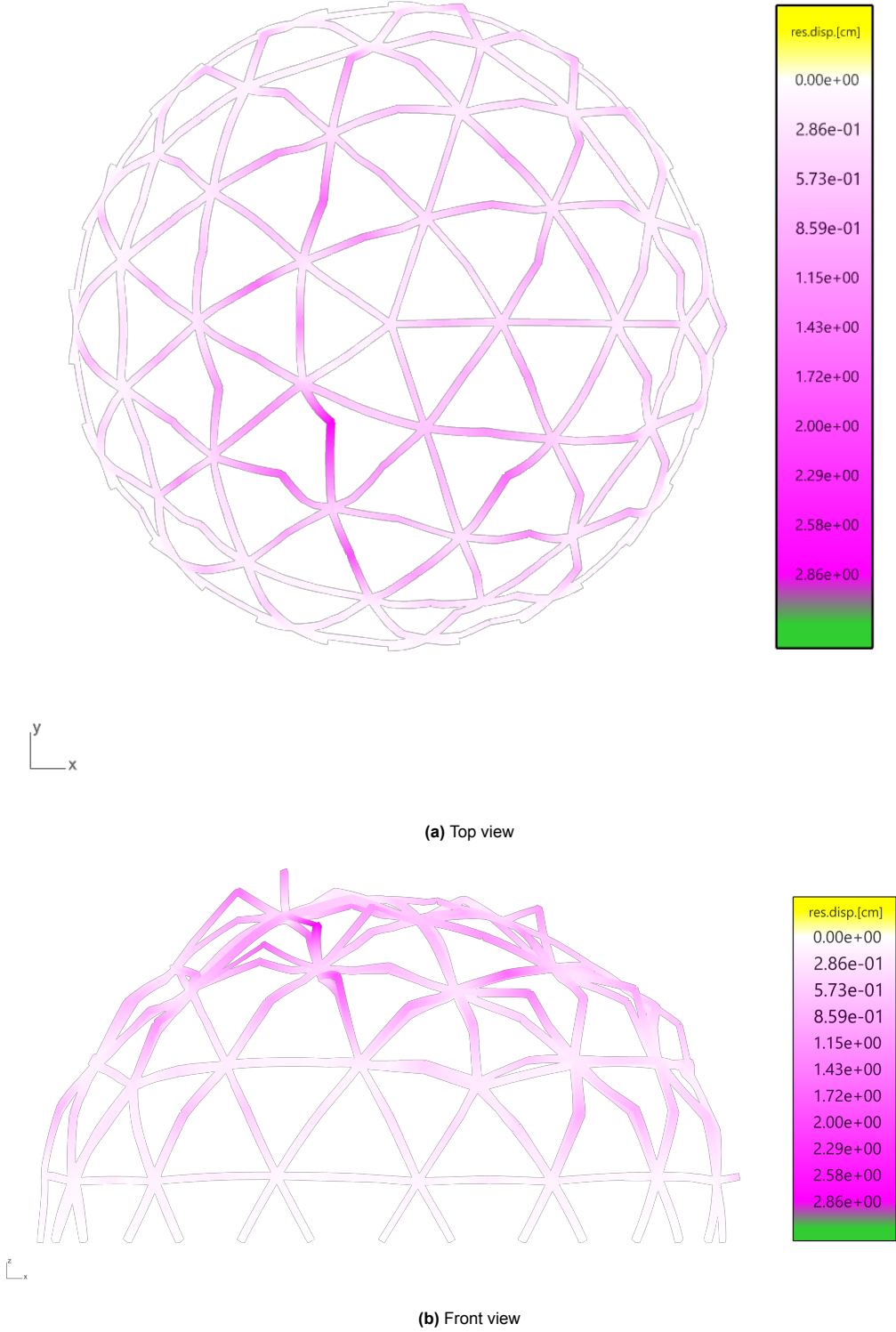


Figure A.18: Geodesic Gridshell: Displacement, Design Option 7 (SLS, 20 m span, C30, 200x175 mm)

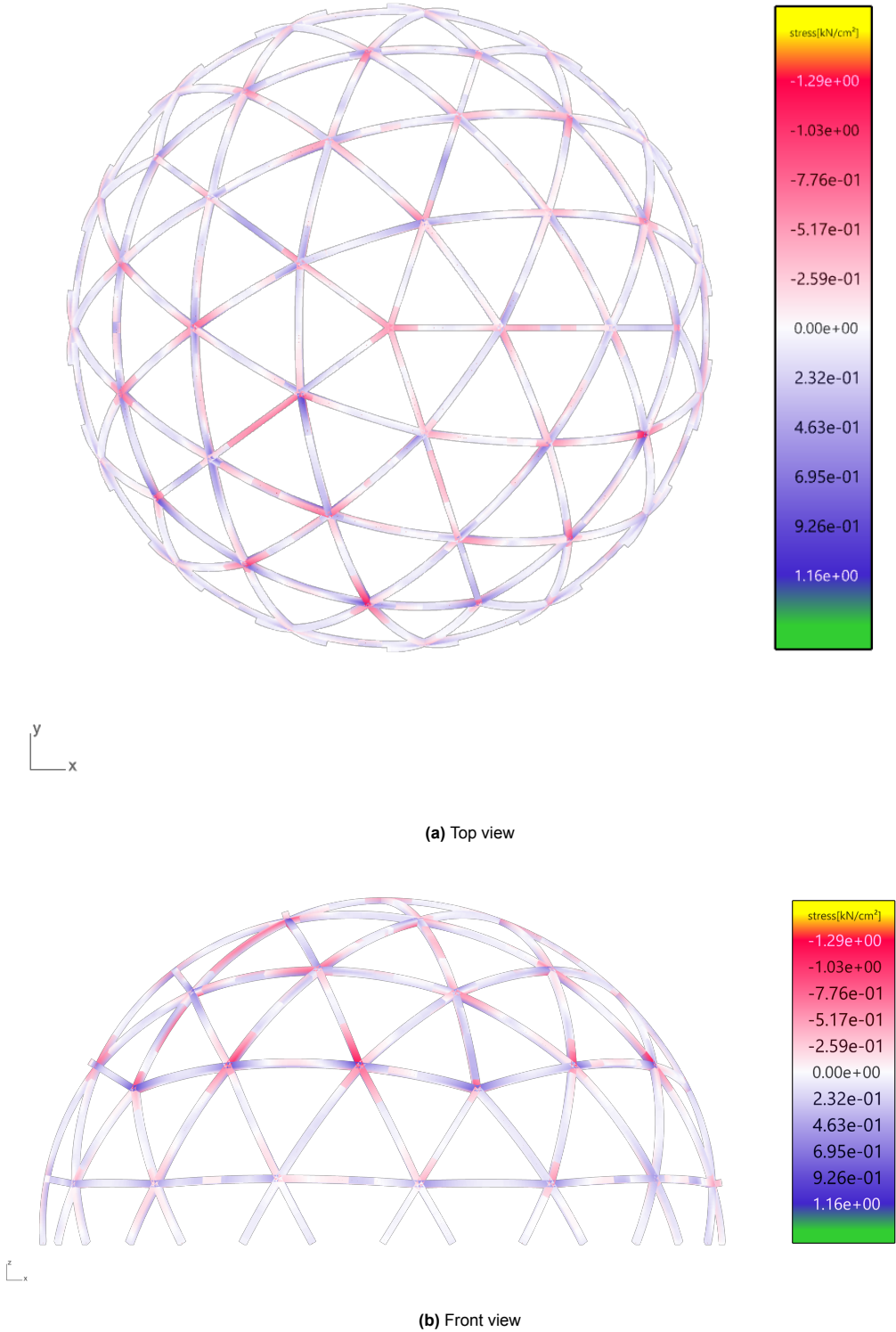


Figure A.19: Geodesic Gridshell: Axial stress, Design Option 8 (ULS, 20 m span, C30, 200x175 mm)

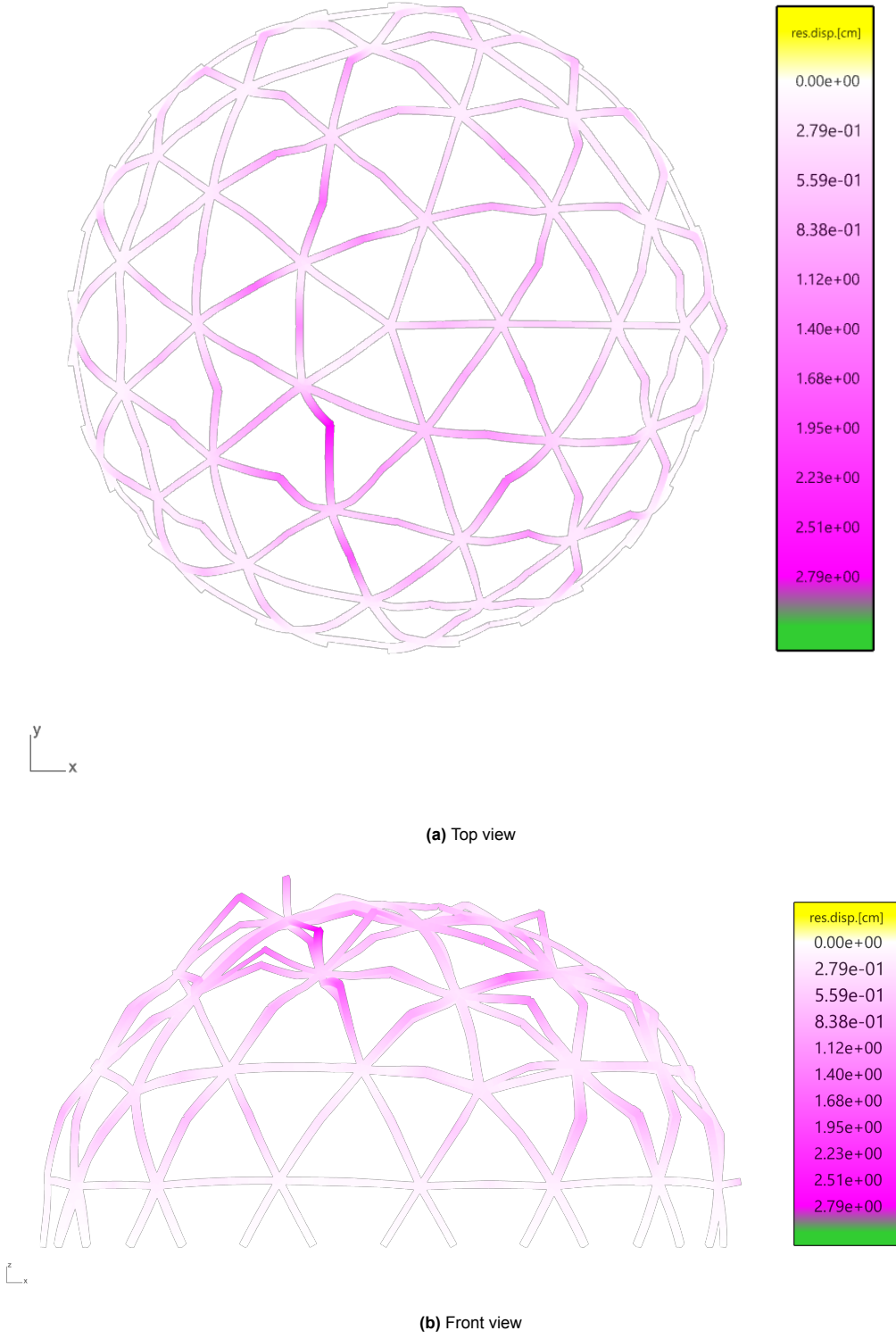


Figure A.20: Geodesic Gridshell: Displacement, Design Option 8 (SLS, 20 m span, C30, 200x175 mm)

A.4. Results bar charts

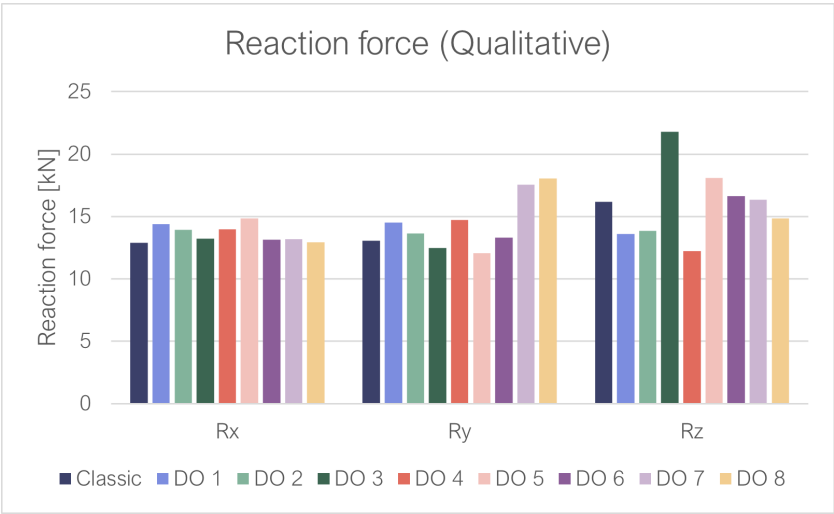


Figure A.21: Geodesic Gridshell: Reaction force results (Qualitative, 20 m span, C30, 200x175 mm)

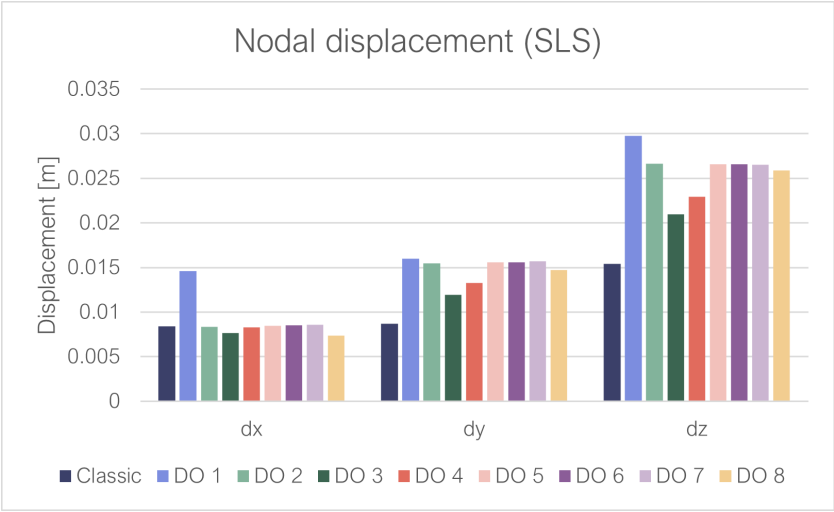


Figure A.22: Geodesic Gridshell: Nodal displacement results (SLS, 20 m span, C30, 200x175 mm)

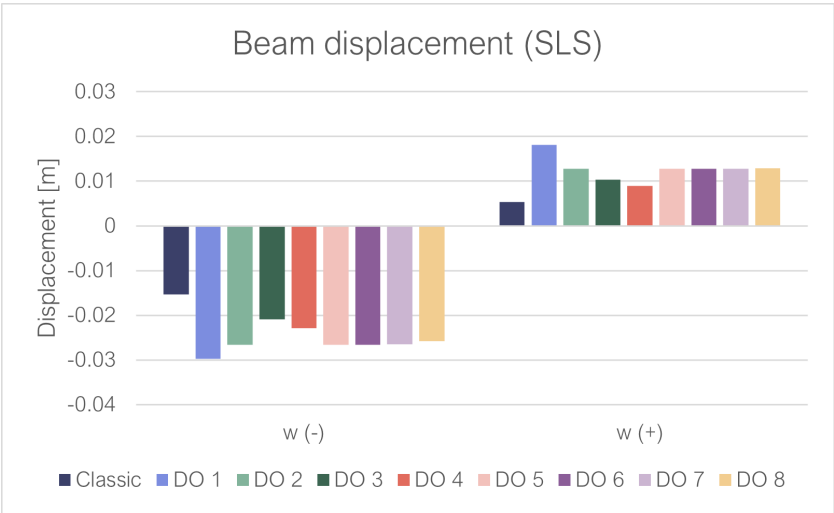


Figure A.23: Geodesic Gridshell: Beam displacement results (SLS, 20 m span, C30, 200x175 mm)

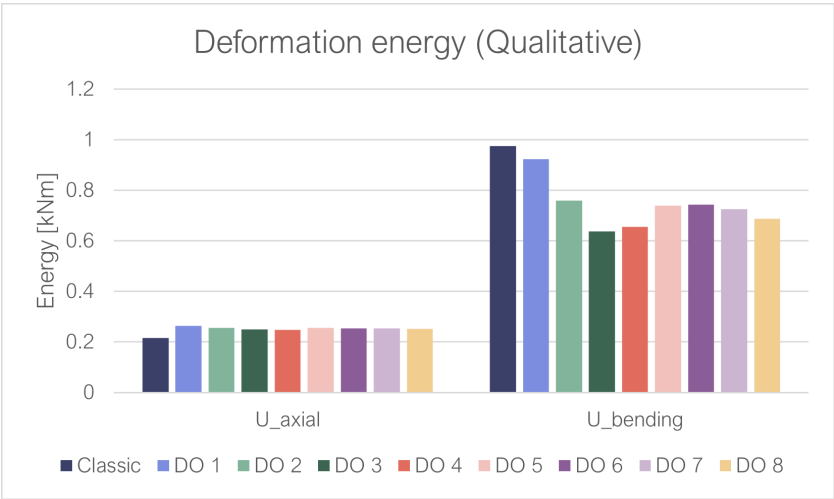


Figure A.24: Geodesic Gridshell: Deformation energy results (Qualitative, 20 m span, C30, 200x175 mm)

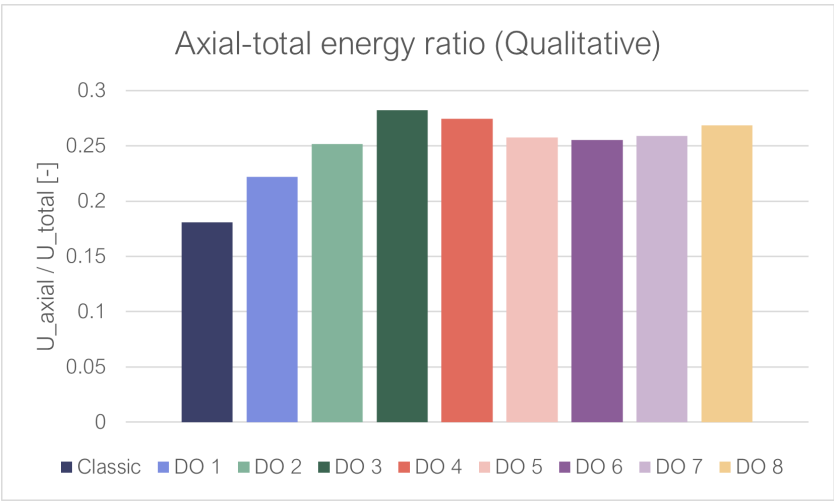


Figure A.25: Geodesic Gridshell: Axial-total deformation energy ratio results (Qualitative, 20 m span, C30, 200x175 mm)

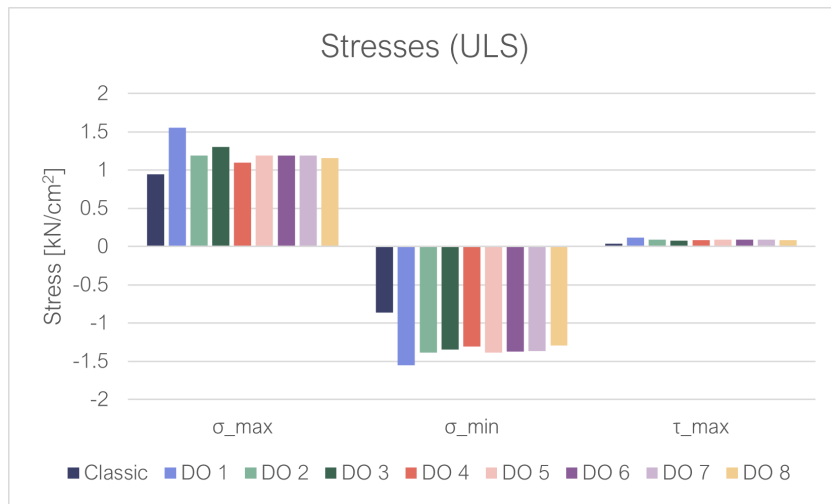


Figure A.26: Geodesic Gridshell: Stress results (ULS, 20 m span, C30, 200x175 mm)

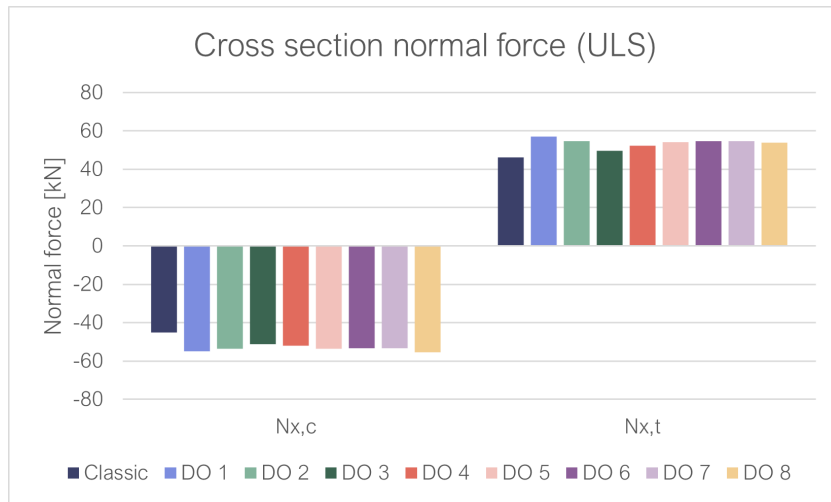


Figure A.27: Cross section normal force results: Geodesic Gridshell (ULS, 20 m span, C30, 200x175 mm)

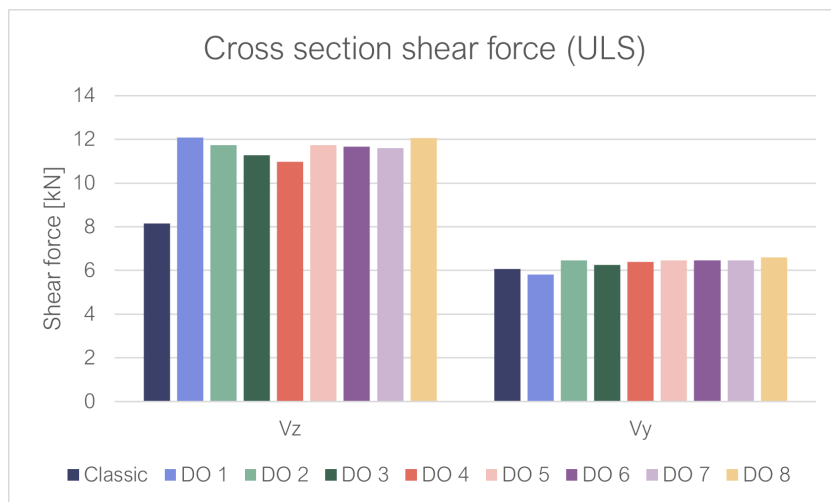


Figure A.28: Geodesic Gridshell: Cross section shear force results (ULS, 20 m span, C30, 200x175 mm)

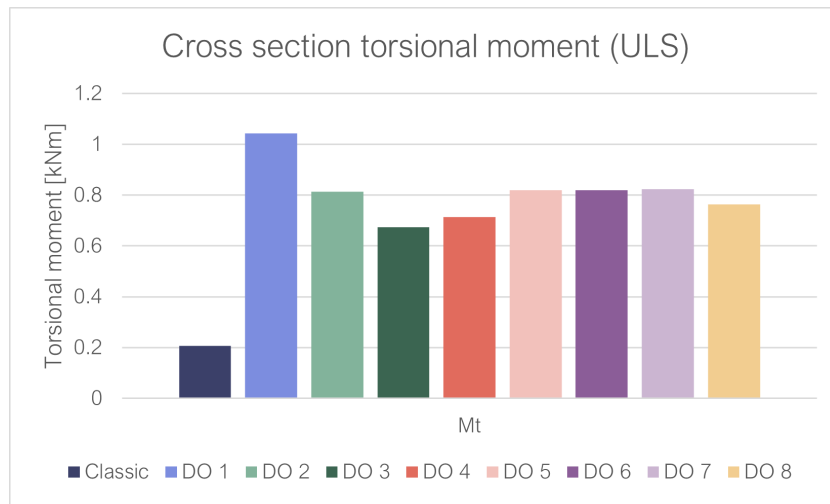


Figure A.29: Geodesic Gridshell: Cross section torsional moment results (ULS, 20 m span, C30, 200x175 mm)

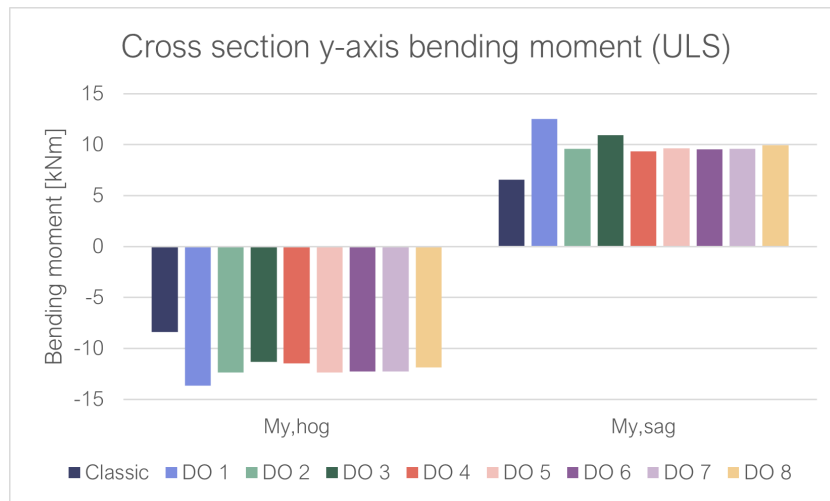


Figure A.30: Geodesic Gridshell: Cross section y-axis bending moment results (ULS, 20 m span, C30, 200x175 mm)

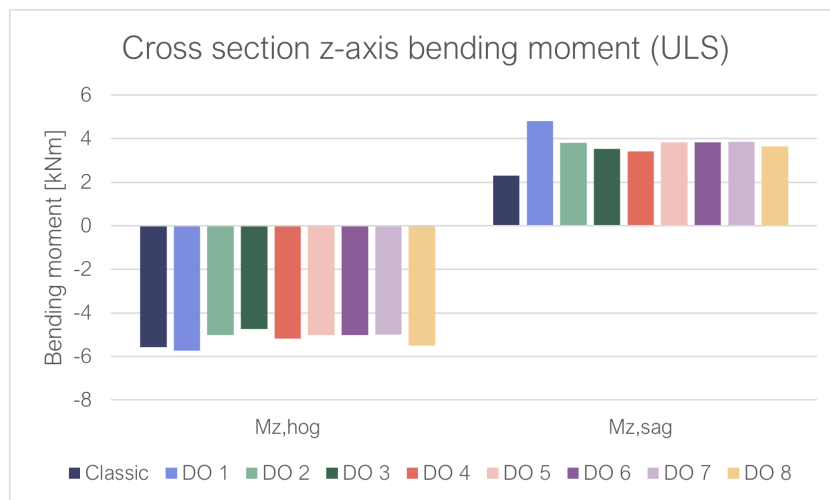


Figure A.31: Geodesic Gridshell: Cross section z-axis bending moment results (ULS, 20 m span, C30, 200x175 mm)

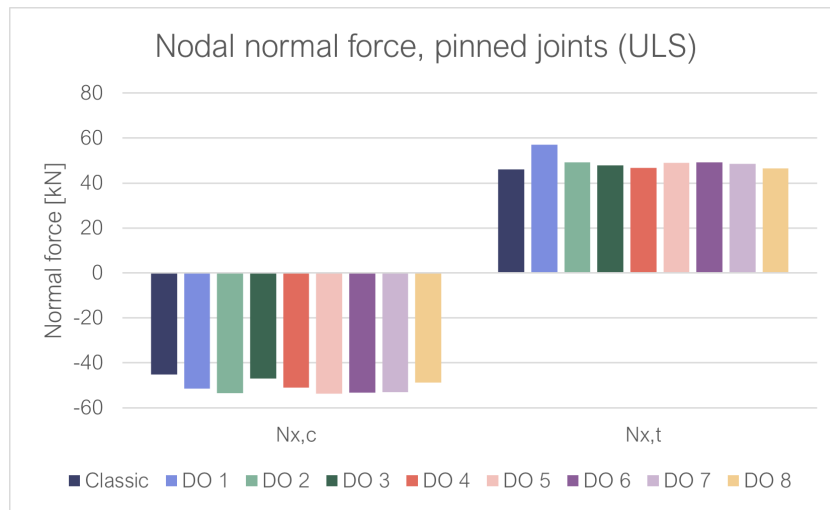


Figure A.32: Geodesic Gridshell: Nodal normal force, pinned joints results (ULS, 20 m span, C30, 200x175 mm)

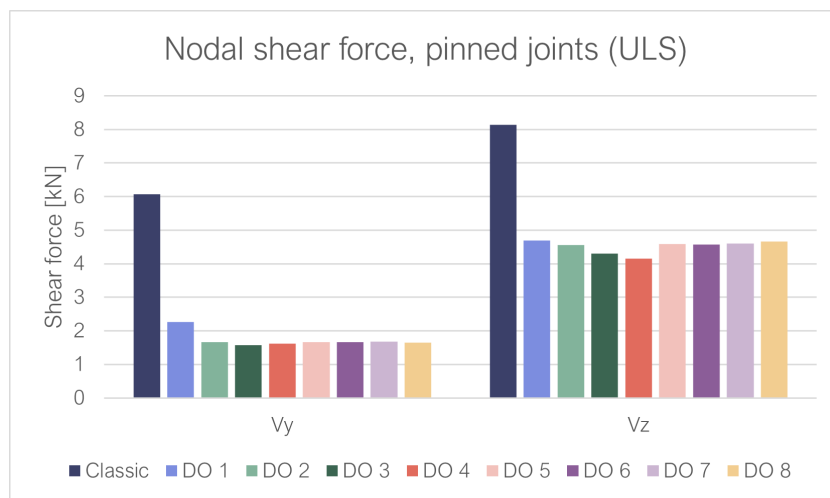


Figure A.33: Geodesic Gridshell: Nodal shear force, pinned joints results (ULS, 20 m span, C30, 200x175 mm)

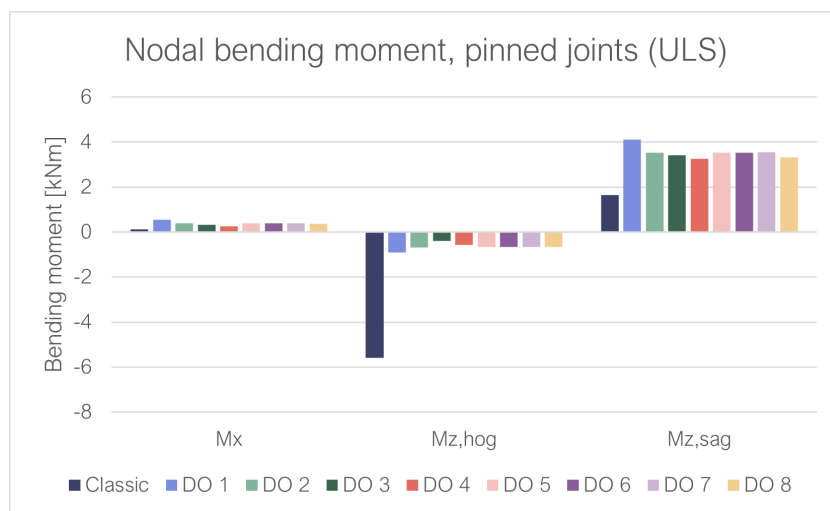


Figure A.34: Geodesic Gridshell: Nodal bending moment, pinned joints results (ULS, 20 m span, C30, 200x175 mm)

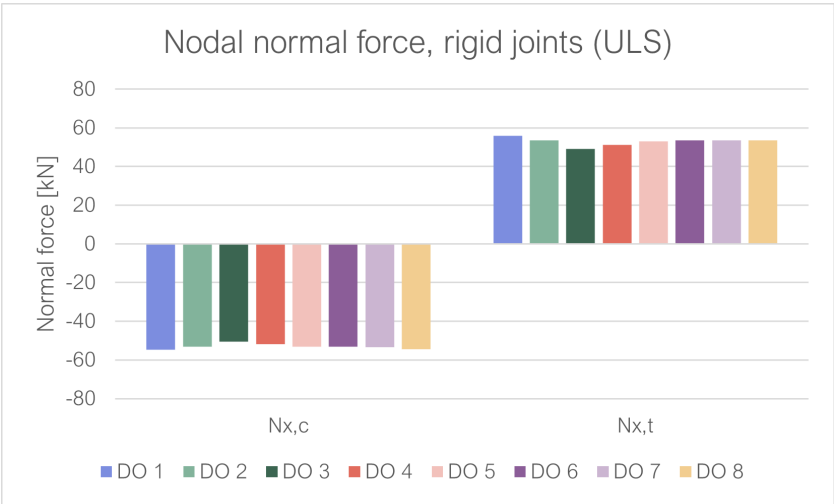


Figure A.35: Geodesic Gridshell: Nodal normal force, rigid joints results (ULS, 20 m span, C30, 200x175 mm)

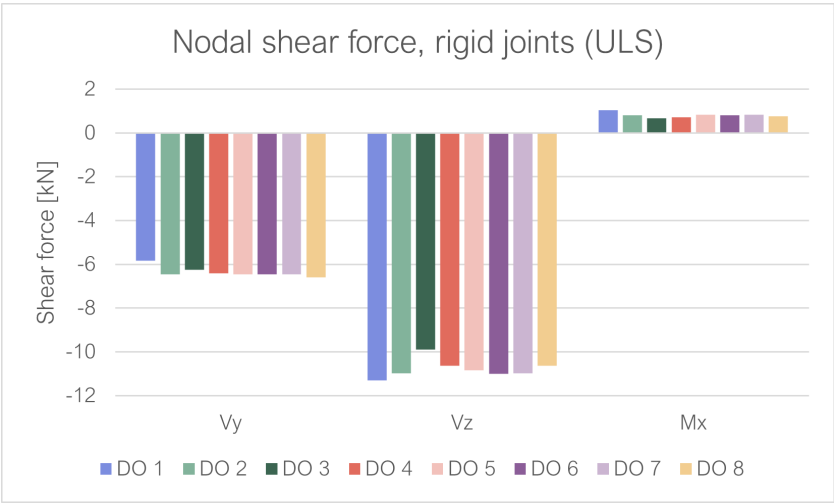


Figure A.36: Geodesic Gridshell: Nodal shear force, rigid joints results (ULS, 20 m span, C30, 200x175 mm)

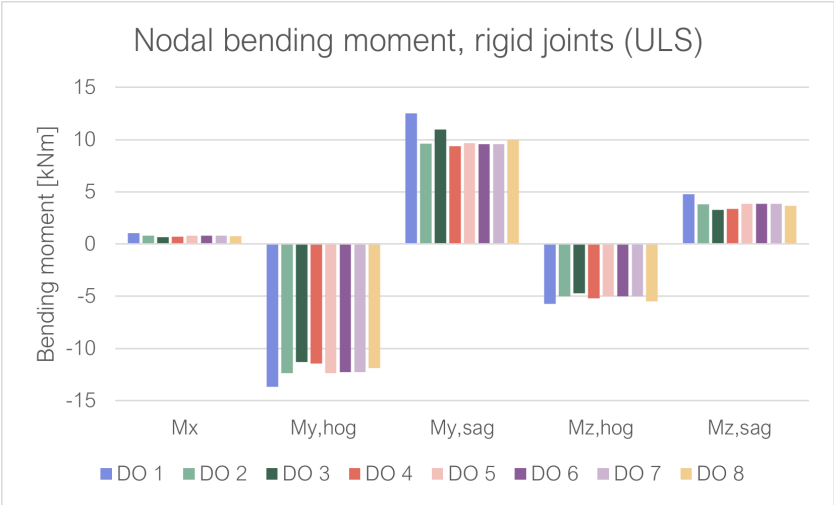


Figure A.37: Geodesic Gridshell: Nodal bending moment, rigid joints results (ULS, 20 m span, C30, 200x175 mm)

A.5. Utilisation results after cross section optimisation

Table A.26: Geodesic Gridshell: FEA utilisation results after cross section optimisation (20 m span)

	Classic	DO 1	DO 2	DO 3	DO 4	DO 5	DO 6	DO 7	DO 8		
Cross section											
Width	200	250	250	225	225	250	250	250	250	250	mm
Height	175	250	225	200	225	225	225	225	225	225	mm
Strength class	C30	C30	C30	C30	C30	C30	C30	C30	C30	C30	[-]
Unity checks SLS											
Roof defl.	0.192	0.121	0.138	0.164	0.134	0.138	0.138	0.137	0.134	0.134	[-]
x-displ.	0.252	0.136	0.098	0.141	0.111	0.099	0.100	0.101	0.098	0.098	[-]
y-displ.	0.261	0.149	0.184	0.220	0.181	0.186	0.186	0.187	0.176	0.176	[-]
Unity checks ULS											
Axial tension	0.129	0.093	0.097	0.109	0.103	0.096	0.097	0.097	0.093	0.093	[-]
Axial compr.	0.100	0.069	0.077	0.090	0.080	0.077	0.076	0.076	0.079	0.079	[-]
Bending (y-axis)	0.683	0.422	0.438	0.557	0.496	0.438	0.435	0.434	0.434	0.434	[-]
Bending (z-axis)	0.650	0.358	0.383	0.491	0.433	0.383	0.381	0.380	0.388	0.388	[-]
Shear (par.)	0.108	0.093	0.099	0.117	0.103	0.099	0.098	0.098	0.102	0.102	[-]
Shear (perp.)	0.162	0.139	0.148	0.176	0.155	0.149	0.148	0.147	0.152	0.152	[-]
Torsion	0.021	0.041	0.040	0.046	0.037	0.040	0.040	0.040	0.037	0.037	[-]
Bending + ten. (y)	0.811	0.514	0.534	0.666	0.599	0.534	0.532	0.531	0.527	0.527	[-]
Bending + ten. (z)	0.779	0.451	0.480	0.599	0.536	0.479	0.478	0.477	0.481	0.481	[-]
Bending + com. (y)	0.693	0.426	0.443	0.566	0.503	0.444	0.441	0.440	0.440	0.440	[-]
Bending + com. (z)	0.660	0.363	0.389	0.499	0.439	0.389	0.387	0.386	0.394	0.394	[-]
Flex. buckling (y)	0.891	0.840	0.812	0.869	0.839	0.813	0.810	0.810	0.798	0.798	[-]
Flex. buckling (z)	0.980	0.777	0.942	0.974	0.776	0.943	0.941	0.940	0.930	0.930	[-]
LTS	0.528	0.530	0.669	0.659	0.487	0.670	0.668	0.668	0.644	0.644	[-]
Stability (2nd order, ULS)											
Buckling factor	12.48	7.17	6.63	7.95	9.00	6.62	6.62	6.61	6.83	6.83	[-]

B

FEA results: Geodesic Gridshell with Denser Grid

This appendix presents the results of the Finite Element Analysis (FEA) of the geodesic gridshell with a denser grid. The structure of this appendix is similar to Appendix A.

B.1. Assumptions and input

The assumptions and input are similar to the geodesic gridshell, as discussed in section A.1. However, there are some differences, such as the geometry, the cross section, and the support locations. These aspects are discussed below.

Geometry

The geometry of the geodesic gridshell with a denser grid is shown in Figure B.1 and Figure B.2. This geometry is formed as explained in chapter 6. Because the beams have a curvature, they are subdivided in multiple small straight elements with a length of 0.047 m. These elements are rigidly connected to each other. This also explains why the figures consist of many small elements in every single beam.

The hemisphere has a radius of 10 meters. All beams have the same cross section of 150x125 millimeters and strength class C30.

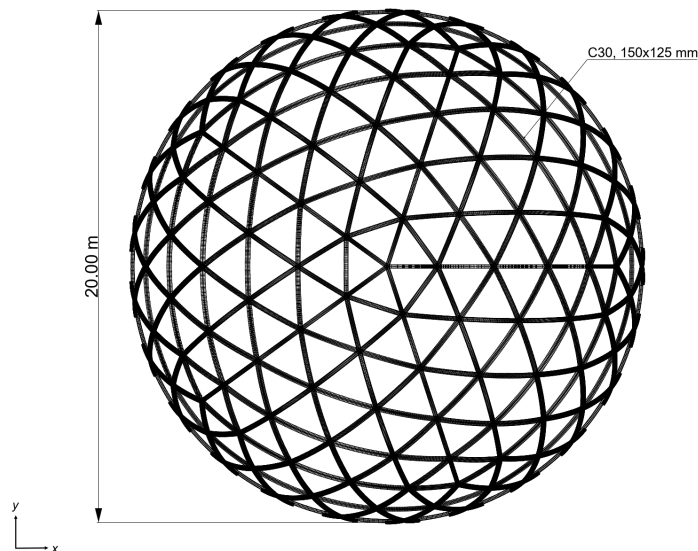


Figure B.1: Geodesic Gridshell with Denser Grid top view

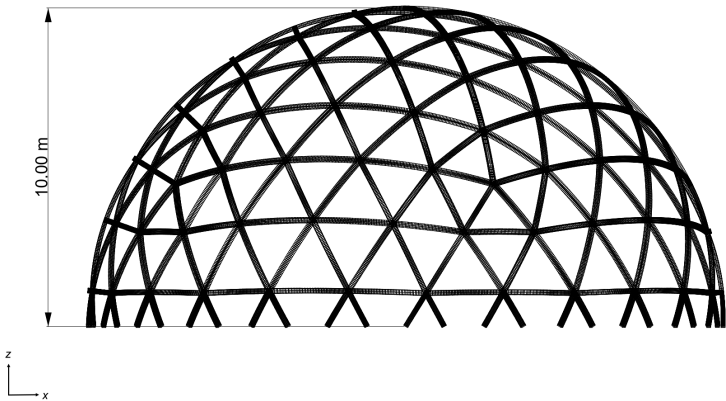


Figure B.2: Geodesic Gridshell with Denser Grid front view

The coordinates of all nodes are presented in Table B.1 to Table B.11.

Table B.1: Geodesic Gridshell with Denser Grid: Node coordinates, Classic (1/2)

Pinned nodes				Pinned nodes			
	x [m]	y [m]	z [m]		x [m]	y [m]	z [m]
1	0	0	10	51	-6.96674	-2.53082	6.712634
2	1.971726	0	9.803688	52	-5.77134	-6.51103	4.929314
3	4.174083	0	9.087191	53	-3.77549	-7.64999	5.217603
4	6.261124	0	7.797328	54	-1.44211	-8.40815	5.217603
5	7.886903	0	6.147908	55	0.842027	-8.65984	4.929314
6	8.944272	0	4.472136	56	2.763932	-8.50651	4.472136
7	8.496199	1.875222	4.929314	57	2.437187	-7.50089	6.147908
8	7.550986	3.969788	5.217603	58	1.934794	-5.95468	7.797328
9	6.108876	5.954683	5.217603	59	1.289862	-3.96979	9.087191
10	4.408913	7.50089	4.929314	60	0.609297	-1.87522	9.803688
11	2.763932	8.506508	4.472136	61	-1.07642	-3.31288	9.373693
12	2.437187	7.50089	6.147908	62	-2.91294	-4.73235	8.313821
13	1.934794	5.954683	7.797328	63	-0.42499	-5.54074	8.313821
14	1.289862	3.969788	9.087191	64	-4.55979	-5.8437	6.712634
15	0.609297	1.875222	9.803688	65	-2.22529	-6.84873	6.938519
16	2.818107	2.047474	9.373693	66	0.254109	-7.40783	6.712634
17	5.138224	2.116373	8.313821	67	4.408913	-7.50089	4.929314
18	3.600589	4.232746	8.313821	68	6.108876	-5.95468	5.217603
19	7.12379	2.047474	6.712634	69	7.550986	-3.96979	5.217603
20	5.825875	4.232746	6.938518	70	8.496199	-1.87522	4.929314
21	4.148636	6.142423	6.712634	71	2.818107	-2.04747	9.373693
22	0.842027	8.659841	4.929314	72	3.600589	-4.23275	8.313821
23	-1.44211	8.408147	5.217603	73	5.138224	-2.11637	8.313821
24	-3.77549	7.649985	5.217603	74	4.148636	-6.14242	6.712634
25	-5.77134	6.511027	4.929314	75	5.825875	-4.23275	6.938518
26	-7.23607	5.257311	4.472136	76	7.12379	-2.04747	6.712634
27	-6.38064	4.635805	6.147908	77	4.032347	-8.65984	2.957589
28	-5.06536	3.680196	7.797328	78	5.311698	-8.40815	1.043521
29	-3.3769	2.453464	9.087191	79	9.638028	-2.45346	1.043521
30	-1.59516	1.158951	9.803688	80	9.482062	-1.15895	2.957588
31	-1.07642	3.312883	9.373693	81	8.865476	-3.31288	3.229263
32	-0.42499	5.540736	8.313821	82	7.62617	-5.54074	3.33793
33	-2.91294	4.732354	8.313821	83	8.738813	-4.73235	1.112643
34	0.254109	7.407832	6.712634	84	5.890322	-7.40783	3.229263
35	-2.22529	6.848727	6.938519	85	7.201178	-6.84873	1.112643
36	-4.55979	5.8437	6.712634	86	9.482062	1.158951	2.957588
37	-7.9758	3.476854	4.929314	87	9.638028	2.453464	1.043521
38	-8.44226	1.226732	5.217603	88	5.311698	8.408147	1.043521
39	-8.44226	-1.22673	5.217603	89	4.032347	8.659841	2.957589
40	-7.9758	-3.47685	4.929314	90	8.865476	3.312883	3.229263
41	-7.23607	-5.25731	4.472136	91	8.738813	4.732354	1.112643
42	-6.38064	-4.63581	6.147908	92	7.62617	5.540736	3.33793
43	-5.06536	-3.6802	7.797328	93	7.201178	6.848727	1.112643
44	-3.3769	-2.45346	9.087191	94	5.890322	7.407832	3.229263
45	-1.59516	-1.15895	9.803688	95	9.941897	0	1.076421
46	-3.48337	0	9.373693	96	0.644931	9.924471	1.043521
47	-5.40088	1.30799	8.313821	97	1.82789	9.376113	2.957589
48	-5.40088	-1.30799	8.313821	98	3.072215	9.455306	1.076421
49	-6.96674	2.530817	6.712634	99	-6.35522	7.649985	1.043521
50	-7.20118	0	6.938519	100	-6.98994	6.511027	2.957589

Table B.2: Geodesic Gridshell with Denser Grid: Node coordinates, Classic (2/2)**Pinned nodes**

	x [m]	y [m]	z [m]
101	-0.41116	9.455306	3.229263
102	-1.80029	9.773483	1.112643
103	-2.91294	8.9651	3.33793
104	-4.28824	8.9651	1.112643
105	-5.22506	7.891175	3.229263
106	-9.23944	3.680196	1.043521
107	-8.35236	4.635805	2.957589
108	-8.04316	5.8437	1.076421
109	-9.23944	-3.6802	1.043521
110	-8.35236	-4.63581	2.957589
111	-9.11959	2.530817	3.229263
112	-9.85146	1.30799	1.112643
113	-9.42646	0	3.33793
114	-9.85146	-1.30799	1.112643
115	-9.11959	-2.53082	3.229263
116	-6.35522	-7.64999	1.043521
117	-6.98994	-6.51103	2.957589
118	-8.04316	-5.8437	1.076421
119	0.644931	-9.92447	1.043521
120	1.82789	-9.37611	2.957589
121	-5.22506	-7.89118	3.229263
122	-4.28824	-8.9651	1.112643
123	-2.91294	-8.9651	3.33793
124	-1.80029	-9.77348	1.112643
125	-0.41116	-9.45531	3.229263
126	3.072215	-9.45531	1.076421

Table B.3: Geodesic Gridshell with Denser Grid: Node coordinates, Design Option 1 (1/4)

Rigid nodes				Rigid nodes			
	x [m]	y [m]	z [m]		x [m]	y [m]	z [m]
1	0	0	10	51	-6.96674	-2.53082	6.712634
2	1.971726	0	9.803688	52	-5.77134	-6.51103	4.929314
3	4.174083	0	9.087191	53	-3.77549	-7.64999	5.217603
4	6.261124	0	7.797328	54	-1.44211	-8.40815	5.217603
5	7.886903	0	6.147908	55	0.842027	-8.65984	4.929314
6	8.944272	0	4.472136	56	2.763932	-8.50651	4.472136
7	8.496199	1.875222	4.929314	57	2.437187	-7.50089	6.147908
8	7.550986	3.969788	5.217603	58	1.934794	-5.95468	7.797328
9	6.108876	5.954683	5.217603	59	1.289862	-3.96979	9.087191
10	4.408913	7.50089	4.929314	60	0.609297	-1.87522	9.803688
11	2.763932	8.506508	4.472136	61	-1.07642	-3.31288	9.373693
12	2.437187	7.50089	6.147908	62	-2.91294	-4.73235	8.313821
13	1.934794	5.954683	7.797328	63	-0.42499	-5.54074	8.313821
14	1.289862	3.969788	9.087191	64	-4.55979	-5.8437	6.712634
15	0.609297	1.875222	9.803688	65	-2.22529	-6.84873	6.938519
16	2.818107	2.047474	9.373693	66	0.254109	-7.40783	6.712634
17	5.138224	2.116373	8.313821	67	4.408913	-7.50089	4.929314
18	3.600589	4.232746	8.313821	68	6.108876	-5.95468	5.217603
19	7.12379	2.047474	6.712634	69	7.550986	-3.96979	5.217603
20	5.825875	4.232746	6.938518	70	8.496199	-1.87522	4.929314
21	4.148636	6.142423	6.712634	71	2.818107	-2.04747	9.373693
22	0.842027	8.659841	4.929314	72	3.600589	-4.23275	8.313821
23	-1.44211	8.408147	5.217603	73	5.138224	-2.11637	8.313821
24	-3.77549	7.649985	5.217603	74	4.148636	-6.14242	6.712634
25	-5.77134	6.511027	4.929314	75	5.825875	-4.23275	6.938518
26	-7.23607	5.257311	4.472136	76	7.12379	-2.04747	6.712634
27	-6.38064	4.635805	6.147908	77	4.032347	-8.65984	2.957589
28	-5.06536	3.680196	7.797328	78	5.311698	-8.40815	1.043521
29	-3.3769	2.453464	9.087191	79	9.638028	-2.45346	1.043521
30	-1.59516	1.158951	9.803688	80	9.482062	-1.15895	2.957588
31	-1.07642	3.312883	9.373693	81	8.865476	-3.31288	3.229263
32	-0.42499	5.540736	8.313821	82	7.62617	-5.54074	3.33793
33	-2.91294	4.732354	8.313821	83	8.738813	-4.73235	1.112643
34	0.254109	7.407832	6.712634	84	5.890322	-7.40783	3.229263
35	-2.22529	6.848727	6.938519	85	7.201178	-6.84873	1.112643
36	-4.55979	5.8437	6.712634	86	9.482062	1.158951	2.957588
37	-7.9758	3.476854	4.929314	87	9.638028	2.453464	1.043521
38	-8.44226	1.226732	5.217603	88	5.311698	8.408147	1.043521
39	-8.44226	-1.22673	5.217603	89	4.032347	8.659841	2.957589
40	-7.9758	-3.47685	4.929314	90	8.865476	3.312883	3.229263
41	-7.23607	-5.25731	4.472136	91	8.738813	4.732354	1.112643
42	-6.38064	-4.63581	6.147908	92	7.62617	5.540736	3.33793
43	-5.06536	-3.6802	7.797328	93	7.201178	6.848727	1.112643
44	-3.3769	-2.45346	9.087191	94	5.890322	7.407832	3.229263
45	-1.59516	-1.15895	9.803688	95	9.941897	0	1.076421
46	-3.48337	0	9.373693	96	0.644931	9.924471	1.043521
47	-5.40088	1.30799	8.313821	97	1.82789	9.376113	2.957589
48	-5.40088	-1.30799	8.313821	98	3.072215	9.455306	1.076421
49	-6.96674	2.530817	6.712634	99	-6.35522	7.649985	1.043521
50	-7.20118	0	6.938519	100	-6.98994	6.511027	2.957589

Table B.4: Geodesic Gridshell with Denser Grid: Node coordinates, Design Option 1 (2/4)

Rigid nodes			Splice joints				
	x [m]	y [m]	z [m]		x [m]	y [m]	z [m]
101	-0.41116	9.455306	3.229263	1	1.299266	0.943972	9.870199
102	-1.80029	9.773483	1.112643	2	8.247125	0.943972	5.576186
103	-2.91294	8.9651	3.33793	3	3.446273	7.551778	5.576186
104	-4.28824	8.9651	1.112643	4	3.533716	1.015638	9.299534
105	-5.22506	7.891175	3.229263	5	5.761048	1.032033	8.108343
106	-9.23944	3.680196	1.043521	6	2.761784	5.160166	8.108344
107	-8.35236	4.635805	2.957589	7	7.570361	0.985063	6.459047
108	-8.04316	5.8437	1.076421	8	6.538994	3.147747	6.879916
109	-9.23944	-3.6802	1.043521	9	5.014346	5.246245	6.879916
110	-8.35236	-4.63581	2.957589	10	2.391579	0.985063	9.65971
111	-9.11959	2.530817	3.229263	11	4.675904	1.032033	8.778999
112	-9.85146	1.30799	1.112643	12	3.991581	2.098498	8.925446
113	-9.42646	0	3.33793	13	3.229257	3.147747	8.925446
114	-9.85146	-1.30799	1.112643	14	2.426456	4.128133	8.778999
115	-9.11959	-2.53082	3.229263	15	6.73743	1.015638	7.319529
116	-6.35522	-7.64999	1.043521	16	6.198072	2.098498	7.561759
117	-6.98994	-6.51103	2.957589	17	3.9111	5.246245	7.561759
118	-8.04316	-5.8437	1.076421	18	6.767032	4.128133	6.096376
119	0.644931	-9.92447	1.043521	19	6.017216	5.160166	6.096376
120	1.82789	-9.37611	2.957589	20	5.18372	6.093828	5.999526
121	-5.22506	-7.89118	3.229263	21	4.311977	6.89544	5.818915
122	-4.28824	-8.9651	1.112643	22	0.291263	0.896416	9.955481
123	-2.91294	-8.9651	3.33793	23	1.624598	5	8.506508
124	-1.80029	-9.77348	1.112643	24	2.62137	8.067748	5.295267
125	-0.41116	-9.45531	3.229263	25	-0.49628	1.527379	9.870199
126	3.072215	-9.45531	1.076421	26	1.650731	8.135185	5.576186
				27	-6.11721	5.611228	5.576186
				28	0.126049	3.674613	9.299534
				29	0.79874	5.797998	8.108344
				30	-4.05417	4.221191	8.108344
				31	1.40252	7.504242	6.459047
				32	-0.97303	7.19166	6.879916
				33	-3.43996	6.390105	6.879916
				34	-0.19781	2.578928	9.65971
				35	0.463412	4.765965	8.778999
				36	-0.76232	4.44469	8.925446
				37	-1.99579	4.043913	8.925446
				38	-3.17627	3.58336	8.778999
				39	1.116051	6.721526	7.31953
				40	-0.08048	6.543189	7.561759
				41	-3.78088	5.340856	7.561759
				42	-1.83496	7.711493	6.096376
				43	-3.04819	7.317291	6.096376
				44	-4.19372	6.813106	5.999526
				45	-5.22548	6.231742	5.818915
				46	-0.76254	0.554016	9.955481
				47	-4.25325	3.09017	8.506508
				48	-6.86284	4.986143	5.295267
				49	-1.60598	0	9.870199
				50	-7.22692	4.083848	5.576186

Table B.5: Geodesic Gridshell with Denser Grid: Node coordinates, Design Option 1 (3/4)

Splice joints				Splice joints			
	x [m]	y [m]	z [m]		x [m]	y [m]	z [m]
51	-7.22692	-4.08385	5.576186	101	3.446273	-7.55178	5.576186
52	-3.45581	1.255397	9.299534	102	8.247125	-0.94397	5.576186
53	-5.2674	2.551326	8.108344	103	2.057907	-3.04691	9.299534
54	-5.2674	-2.55133	8.108344	104	2.761784	-5.16017	8.108344
55	-6.70356	3.652814	6.459047	105	5.761048	-1.03203	8.108343
56	-7.14036	1.296943	6.879916	106	3.276221	-6.89544	6.459047
57	-7.14036	-1.29694	6.879916	107	5.014346	-5.24625	6.879916
58	-2.51383	0.608802	9.65971	108	6.538994	-3.14775	6.879916
59	-4.3895	1.913495	8.778999	109	1.675889	-1.97013	9.65971
60	-4.46272	0.648472	8.925446	110	2.426456	-4.12813	8.778999
61	-4.46272	-0.64847	8.925446	111	3.229257	-3.14775	8.925446
62	-4.3895	-1.9135	8.778999	112	3.991581	-2.0985	8.925446
63	-6.04767	3.138494	7.31953	113	4.675904	-1.03203	8.778999
64	-6.24781	1.945415	7.561759	114	3.04791	-6.09383	7.319529
65	-6.24781	-1.94542	7.561759	115	3.9111	-5.24625	7.561759
66	-7.9011	0.637832	6.096376	116	6.198072	-2.0985	7.561759
67	-7.9011	-0.63783	6.096376	117	6.017216	-5.16017	6.096376
68	-7.77558	-1.8831	5.999526	118	6.767032	-4.12813	6.096376
69	-7.5415	-3.04401	5.818915	119	7.397432	-3.04691	5.999526
70	-0.76254	-0.55402	9.955481	120	7.890427	-1.97013	5.818914
71	-4.25325	-3.09017	8.506508	121	8.774196	-0.89642	4.71274
72	-6.86284	-4.98614	5.295267	122	6.88191	-5	5.257311
73	-0.49628	-1.52738	9.870199	123	3.563918	-8.06775	4.71274
74	-6.11721	-5.61123	5.576186	124	9.050115	-1.52738	3.970205
75	1.650731	-8.13519	5.576186	125	4.249263	-8.13519	3.970205
76	-2.26186	-2.89873	9.299534	126	9.32929	-2.89873	2.13581
77	-4.05417	-4.22119	8.108344	127	6.895116	-5.798	4.340576
78	0.79874	-5.798	8.108344	128	5.149921	-7.50424	4.143026
79	-5.54555	-5.24668	6.459047	129	6.588734	-7.19166	2.206492
80	-3.43996	-6.39011	6.879916	130	9.24625	-2.20267	3.107269
81	-0.97303	-7.19166	6.879916	131	7.644932	-4.76597	4.340576
82	-1.35582	-2.20267	9.65971	132	8.324083	-4.44469	3.309737
83	-3.17627	-3.58336	8.778999	133	8.875706	-4.04391	2.206492
84	-1.99579	-4.04391	8.925446	134	9.272648	-3.58336	1.085144
85	-0.76232	-4.44469	8.925446	135	6.047673	-6.72153	4.27162
86	0.463412	-4.76597	8.778999	136	6.799435	-6.54319	3.309738
87	-4.85372	-4.78183	7.31953	137	6.273383	-7.71149	1.085144
88	-3.78088	-5.34086	7.561759	138	3.563918	8.067748	4.71274
89	-0.08048	-6.54319	7.561759	139	6.88191	5	5.257311
90	-3.04819	-7.31729	6.096376	140	8.774196	0.896416	4.71274
91	-1.83496	-7.71149	6.096376	141	9.050115	1.527379	3.970205
92	-0.61186	-7.97692	5.999526	142	4.249263	8.135185	3.970205
93	0.564575	-8.11304	5.818915	143	8.261385	3.674613	4.27162
94	0.291263	-0.89642	9.955481	144	6.895116	5.797998	4.340576
95	1.624598	-5	8.506508	145	6.588734	7.19166	2.206492
96	2.62137	-8.06775	5.295267	146	8.728372	2.578928	4.143025
97	8.482933	0	5.295267	147	9.272648	3.58336	1.085144
98	5.257311	0	8.506508	148	8.875706	4.043913	2.206492
99	0.942548	0	9.955481	149	8.324083	4.44469	3.309737
100	1.299266	-0.94397	9.870199	150	7.644932	4.765965	4.340576

Table B.6: Geodesic Gridshell with Denser Grid: Node coordinates, Design Option 1 (4/4)

Splice joints				Splice joints			
	x [m]	y [m]	z [m]		x [m]	y [m]	z [m]
151	6.799435	6.543189	3.309738	201	-9.60798	-2.55133	1.085144
152	6.273383	7.711493	1.085144	202	-9.25139	-3.13849	2.13581
153	5.639769	7.976924	2.13581	203	-8.77507	-3.65281	3.107269
154	4.95211	8.113044	3.107269	204	-7.80539	-4.98614	3.770192
155	9.24547	-0.55402	3.770192	205	-7.72319	-5.61123	2.977654
156	9.24547	0.554016	3.770192	206	-7.24163	-6.81311	1.067905
157	9.546391	0	2.977654	207	-7.5415	-6.23174	2.071513
158	9.863243	1.255397	1.067905	208	-7.1541	-5.88256	3.770192
159	9.764128	0.608802	2.071513	209	1.858833	-8.62176	4.712741
160	3.383908	8.621764	3.770192	210	-2.62866	-8.09017	5.257311
161	2.949997	9.079157	2.977654	211	-6.57157	-5.88256	4.712741
162	1.853956	9.76844	1.067905	212	-6.42393	-6.5552	3.970205
163	2.438276	9.474368	2.071513	213	1.344016	-9.07916	3.970205
164	2.330107	8.964165	3.770192	214	-4.52372	-7.82874	4.27162
165	-6.57157	5.882559	4.712741	215	-2.17029	-8.74353	4.340576
166	-2.62866	8.09017	5.257311	216	-1.10325	-9.69094	2.206492
167	1.858833	8.621764	4.712741	217	-5.54555	-7.21681	4.143026
168	1.344016	9.079157	3.970205	218	-5.39548	-8.34933	1.085144
169	-6.42393	6.5552	3.970205	219	-4.80365	-8.4886	2.206492
170	-0.94186	8.992562	4.27162	220	-4.1218	-8.4886	3.309738
171	-3.38352	8.349324	4.340576	221	-3.38352	-8.34932	4.340576
172	-4.80365	8.488604	2.206492	222	-1.65487	-9.29016	3.309738
173	0.244509	9.098107	4.143026	223	-0.54257	-9.92613	1.085144
174	-0.54257	9.926131	1.085144	224	0.126049	-9.76844	2.13581
175	-1.10325	9.690936	2.206492	225	0.762387	-9.47437	3.107269
176	-1.65487	9.290159	3.309738	226	2.330107	-8.96417	3.770192
177	-2.17029	8.743526	4.340576	227	3.383908	-8.62176	3.770192
178	-4.1218	8.488604	3.309738	228	2.949997	-9.07916	2.977654
179	-5.39548	8.349325	1.085144	229	4.241864	-8.99256	1.067905
180	-5.84372	7.828744	2.13581	230	3.596287	-9.09811	2.071513
181	-6.18568	7.216805	3.107269				
182	-7.1541	5.882559	3.770192				
183	-7.72319	5.611228	2.977654				
184	-8.71744	4.781831	1.067905				
185	-8.25719	5.246679	2.071513				
186	-7.80539	4.986143	3.770192				
187	-7.62537	-4.43213	4.712741				
188	-8.50651	0	5.257311				
189	-7.62537	4.432127	4.712741				
190	-8.21947	4.083848	3.970205				
191	-8.21947	-4.08385	3.970205				
192	-8.84348	1.883096	4.27162				
193	-8.98624	-0.63783	4.340576				
194	-9.55755	-1.94542	2.206492				
195	-8.57726	3.044011	4.143026				
196	-9.60798	2.551326	1.085144				
197	-9.55755	1.945415	2.206492				
198	-9.34685	1.296943	3.309738				
199	-8.98624	0.637832	4.340576				
200	-9.34685	-1.29694	3.309738				

Table B.7: Geodesic Gridshell with Denser Grid: Node coordinates, Design Option 2 (1/5)

Rigid nodes				Rigid nodes			
	x [m]	y [m]	z [m]		x [m]	y [m]	z [m]
1	0	0	10	51	-6.96674	-2.53082	6.712634
2	1.971726	0	9.803688	52	-5.77134	-6.51103	4.929314
3	4.174083	0	9.087191	53	-3.77549	-7.64999	5.217603
4	6.261124	0	7.797328	54	-1.44211	-8.40815	5.217603
5	7.886903	0	6.147908	55	0.842027	-8.65984	4.929314
6	8.944272	0	4.472136	56	2.763932	-8.50651	4.472136
7	8.496199	1.875222	4.929314	57	2.437187	-7.50089	6.147908
8	7.550986	3.969788	5.217603	58	1.934794	-5.95468	7.797328
9	6.108876	5.954683	5.217603	59	1.289862	-3.96979	9.087191
10	4.408913	7.50089	4.929314	60	0.609297	-1.87522	9.803688
11	2.763932	8.506508	4.472136	61	-1.07642	-3.31288	9.373693
12	2.437187	7.50089	6.147908	62	-2.91294	-4.73235	8.313821
13	1.934794	5.954683	7.797328	63	-0.42499	-5.54074	8.313821
14	1.289862	3.969788	9.087191	64	-4.55979	-5.8437	6.712634
15	0.609297	1.875222	9.803688	65	-2.22529	-6.84873	6.938519
16	2.818107	2.047474	9.373693	66	0.254109	-7.40783	6.712634
17	5.138224	2.116373	8.313821	67	4.408913	-7.50089	4.929314
18	3.600589	4.232746	8.313821	68	6.108876	-5.95468	5.217603
19	7.12379	2.047474	6.712634	69	7.550986	-3.96979	5.217603
20	5.825875	4.232746	6.938518	70	8.496199	-1.87522	4.929314
21	4.148636	6.142423	6.712634	71	2.818107	-2.04747	9.373693
22	0.842027	8.659841	4.929314	72	3.600589	-4.23275	8.313821
23	-1.44211	8.408147	5.217603	73	5.138224	-2.11637	8.313821
24	-3.77549	7.649985	5.217603	74	4.148636	-6.14242	6.712634
25	-5.77134	6.511027	4.929314	75	5.825875	-4.23275	6.938518
26	-7.23607	5.257311	4.472136	76	7.12379	-2.04747	6.712634
27	-6.38064	4.635805	6.147908	77	4.032347	-8.65984	2.957589
28	-5.06536	3.680196	7.797328	78	5.311698	-8.40815	1.043521
29	-3.3769	2.453464	9.087191	79	9.638028	-2.45346	1.043521
30	-1.59516	1.158951	9.803688	80	9.482062	-1.15895	2.957588
31	-1.07642	3.312883	9.373693	81	8.865476	-3.31288	3.229263
32	-0.42499	5.540736	8.313821	82	7.62617	-5.54074	3.33793
33	-2.91294	4.732354	8.313821	83	8.738813	-4.73235	1.112643
34	0.254109	7.407832	6.712634	84	5.890322	-7.40783	3.229263
35	-2.22529	6.848727	6.938519	85	7.201178	-6.84873	1.112643
36	-4.55979	5.8437	6.712634	86	9.482062	1.158951	2.957588
37	-7.9758	3.476854	4.929314	87	9.638028	2.453464	1.043521
38	-8.44226	1.226732	5.217603	88	5.311698	8.408147	1.043521
39	-8.44226	-1.22673	5.217603	89	4.032347	8.659841	2.957589
40	-7.9758	-3.47685	4.929314	90	8.865476	3.312883	3.229263
41	-7.23607	-5.25731	4.472136	91	8.738813	4.732354	1.112643
42	-6.38064	-4.63581	6.147908	92	7.62617	5.540736	3.33793
43	-5.06536	-3.6802	7.797328	93	7.201178	6.848727	1.112643
44	-3.3769	-2.45346	9.087191	94	5.890322	7.407832	3.229263
45	-1.59516	-1.15895	9.803688	95	9.941897	0	1.076421
46	-3.48337	0	9.373693	96	0.644931	9.924471	1.043521
47	-5.40088	1.30799	8.313821	97	1.82789	9.376113	2.957589
48	-5.40088	-1.30799	8.313821	98	3.072215	9.455306	1.076421
49	-6.96674	2.530817	6.712634	99	-6.35522	7.649985	1.043521
50	-7.20118	0	6.938519	100	-6.98994	6.511027	2.957589

Table B.8: Geodesic Gridshell with Denser Grid: Node coordinates, Design Option 2 (2/5)

Rigid nodes			Splice joints				
	x [m]	y [m]	z [m]		x [m]	y [m]	z [m]
101	-0.41116	9.455306	3.229263	1	0.942548	0	9.955481
102	-1.80029	9.773483	1.112643	2	5.257311	0	8.506508
103	-2.91294	8.9651	3.33793	3	8.482933	0	5.295267
104	-4.28824	8.9651	1.112643	4	8.774196	0.896416	4.71274
105	-5.22506	7.891175	3.229263	5	6.88191	5	5.257311
106	-9.23944	3.680196	1.043521	6	3.563918	8.067748	4.71274
107	-8.35236	4.635805	2.957589	7	2.62137	8.067748	5.295267
108	-8.04316	5.8437	1.076421	8	1.624598	5	8.506508
109	-9.23944	-3.6802	1.043521	9	0.291263	0.896416	9.955481
110	-8.35236	-4.63581	2.957589	10	1.299266	0.943972	9.870199
111	-9.11959	2.530817	3.229263	11	8.247125	0.943972	5.576186
112	-9.85146	1.30799	1.112643	12	3.446273	7.551778	5.576186
113	-9.42646	0	3.33793	13	3.533716	1.015638	9.299534
114	-9.85146	-1.30799	1.112643	14	2.057907	3.046914	9.299534
115	-9.11959	-2.53082	3.229263	15	5.761048	1.032033	8.108343
116	-6.35522	-7.64999	1.043521	16	4.40727	3.202069	8.385865
117	-6.98994	-6.51103	2.957589	17	2.761784	5.160166	8.108344
118	-8.04316	-5.8437	1.076421	18	7.570361	0.985063	6.459047
119	0.644931	-9.92447	1.043521	19	6.538994	3.147747	6.879916
120	1.82789	-9.37611	2.957589	20	5.014346	5.246245	6.879916
121	-5.22506	-7.89118	3.229263	21	3.276221	6.89544	6.459047
122	-4.28824	-8.9651	1.112643	22	2.391579	0.985063	9.65971
123	-2.91294	-8.9651	3.33793	23	1.675889	1.970126	9.65971
124	-1.80029	-9.77348	1.112643	24	4.675904	1.032033	8.778999
125	-0.41116	-9.45531	3.229263	25	3.991581	2.098498	8.925446
126	3.072215	-9.45531	1.076421	26	3.229257	3.147747	8.925446
				27	2.426456	4.128133	8.778999
				28	6.73743	1.015638	7.319529
				29	5.529555	3.202069	7.692255
				30	4.754075	4.269425	7.692255
				31	3.04791	6.093828	7.319529
				32	7.890427	1.970126	5.818914
				33	7.397432	3.046914	5.999526
				34	6.767032	4.128133	6.096376
				35	6.017216	5.160166	6.096376
				36	5.18372	6.093828	5.999526
				37	4.311977	6.89544	5.818915
				38	1.858833	8.621764	4.712741
				39	-2.62866	8.09017	5.257311
				40	-6.57157	5.882559	4.712741
				41	-6.86284	4.986143	5.295267
				42	-4.25325	3.09017	8.506508
				43	-0.76254	0.554016	9.955481
				44	-0.49628	1.527379	9.870199
				45	1.650731	8.135185	5.576186
				46	-6.11721	5.611228	5.576186
				47	0.126049	3.674613	9.299534
				48	-2.26186	2.898734	9.299534
				49	0.79874	5.797998	8.108344
				50	-1.68343	5.181056	8.385865

Table B.9: Geodesic Gridshell with Denser Grid: Node coordinates, Design Option 2 (3/5)

Splice joints			Splice joints				
	x [m]	y [m]	z [m]		x [m]	y [m]	z [m]
51	-4.05417	4.221191	8.108344	101	-7.77558	1.883096	5.999526
52	1.40252	7.504242	6.459047	102	-7.9011	0.637832	6.096376
53	-0.97303	7.19166	6.879916	103	-7.9011	-0.63783	6.096376
54	-3.43996	6.390105	6.879916	104	-7.77558	-1.8831	5.999526
55	-5.54555	5.246679	6.459047	105	-7.5415	-3.04401	5.818915
56	-0.19781	2.578928	9.65971	106	-6.57157	-5.88256	4.712741
57	-1.35582	2.202667	9.65971	107	-2.62866	-8.09017	5.257311
58	0.463412	4.765965	8.778999	108	1.858833	-8.62176	4.712741
59	-0.76232	4.44469	8.925446	109	2.62137	-8.06775	5.295267
60	-1.99579	4.043913	8.925446	110	1.624598	-5	8.506508
61	-3.17627	3.58336	8.778999	111	0.291263	-0.89642	9.955481
62	1.116051	6.721526	7.31953	112	-0.49628	-1.52738	9.870199
63	-1.33662	6.248412	7.692255	113	-6.11721	-5.61123	5.576186
64	-2.59138	5.840719	7.692255	114	1.650731	-8.13519	5.576186
65	-4.85372	4.78183	7.31953	115	-2.26186	-2.89873	9.299534
66	0.564575	8.113044	5.818915	116	0.126049	-3.67461	9.299534
67	-0.61186	7.976924	5.999526	117	-4.05417	-4.22119	8.108344
68	-1.83496	7.711493	6.096376	118	-1.68343	-5.18106	8.385865
69	-3.04819	7.317291	6.096376	119	0.79874	-5.798	8.108344
70	-4.19372	6.813106	5.999526	120	-5.54555	-5.24668	6.459047
71	-5.22548	6.231742	5.818915	121	-3.43996	-6.39011	6.879916
72	-7.62537	4.432127	4.712741	122	-0.97303	-7.19166	6.879916
73	-8.50651	0	5.257311	123	1.40252	-7.50424	6.459047
74	-7.62537	-4.43213	4.712741	124	-1.35582	-2.20267	9.65971
75	-6.86284	-4.98614	5.295267	125	-0.19781	-2.57893	9.65971
76	-4.25325	-3.09017	8.506508	126	-3.17627	-3.58336	8.778999
77	-0.76254	-0.55402	9.955481	127	-1.99579	-4.04391	8.925446
78	-1.60598	0	9.870199	128	-0.76232	-4.44469	8.925446
79	-7.22692	4.083848	5.576186	129	0.463412	-4.76597	8.778999
80	-7.22692	-4.08385	5.576186	130	-4.85372	-4.78183	7.31953
81	-3.45581	1.255397	9.299534	131	-2.59138	-5.84072	7.692255
82	-3.45581	-1.2554	9.299534	132	-1.33662	-6.24841	7.692255
83	-5.2674	2.551326	8.108344	133	1.116051	-6.72153	7.31953
84	-5.44769	0	8.385865	134	-5.22548	-6.23174	5.818915
85	-5.2674	-2.55133	8.108344	135	-4.19372	-6.81311	5.999526
86	-6.70356	3.652814	6.459047	136	-3.04819	-7.31729	6.096376
87	-7.14036	1.296943	6.879916	137	-1.83496	-7.71149	6.096376
88	-7.14036	-1.29694	6.879916	138	-0.61186	-7.97692	5.999526
89	-6.70356	-3.65281	6.459047	139	0.564575	-8.11304	5.818915
90	-2.51383	0.608802	9.65971	140	3.563918	-8.06775	4.71274
91	-2.51383	-0.6088	9.65971	141	6.88191	-5	5.257311
92	-4.3895	1.913495	8.778999	142	8.774196	-0.89642	4.71274
93	-4.46272	0.648472	8.925446	143	1.299266	-0.94397	9.870199
94	-4.46272	-0.64847	8.925446	144	3.446273	-7.55178	5.576186
95	-4.3895	-1.9135	8.778999	145	8.247125	-0.94397	5.576186
96	-6.04767	3.138494	7.31953	146	2.057907	-3.04691	9.299534
97	-6.35563	0.659662	7.692255	147	3.533716	-1.01564	9.299534
98	-6.35563	-0.65966	7.692255	148	2.761784	-5.16017	8.108344
99	-6.04767	-3.13849	7.31953	149	4.40727	-3.20207	8.385865
100	-7.5415	3.044011	5.818915	150	5.761048	-1.03203	8.108343

Table B.10: Geodesic Gridshell with Denser Grid: Node coordinates, Design Option 2 (4/5)

Splice joints				Splice joints			
	x [m]	y [m]	z [m]		x [m]	y [m]	z [m]
151	3.276221	-6.89544	6.459047	201	8.728372	2.578928	4.143025
152	5.014346	-5.24625	6.879916	202	9.272648	3.58336	1.085144
153	6.538994	-3.14775	6.879916	203	8.324083	4.44469	3.309737
154	7.570361	-0.98506	6.459047	204	7.644932	4.765965	4.340576
155	1.675889	-1.97013	9.65971	205	8.03906	5.840719	1.122285
156	2.391579	-0.98506	9.65971	206	7.477917	6.248412	2.24457
157	2.426456	-4.12813	8.778999	207	6.799435	6.543189	3.309738
158	3.229257	-3.14775	8.925446	208	6.047673	6.721526	4.27162
159	3.991581	-2.0985	8.925446	209	6.273383	7.711493	1.085144
160	4.675904	-1.03203	8.778999	210	5.639769	7.976924	2.13581
161	3.04791	-6.09383	7.319529	211	4.95211	8.113044	3.107269
162	4.754075	-4.26943	7.692255	212	9.546391	0	2.977654
163	5.529555	-3.20207	7.692255	213	9.863243	-1.2554	1.067905
164	6.73743	-1.01564	7.319529	214	9.863243	1.255397	1.067905
165	4.311977	-6.89544	5.818915	215	9.764128	-0.6088	2.071513
166	5.18372	-6.09383	5.999526	216	9.764128	0.608802	2.071513
167	6.017216	-5.16017	6.096376	217	2.330107	8.964165	3.770192
168	6.767032	-4.12813	6.096376	218	2.949997	9.079157	2.977654
169	7.397432	-3.04691	5.999526	219	4.241864	8.992562	1.067905
170	7.890427	-1.97013	5.818914	220	1.853956	9.76844	1.067905
171	3.383908	-8.62176	3.770192	221	3.596287	9.098107	2.071513
172	9.24547	-0.55402	3.770192	222	2.438276	9.474368	2.071513
173	9.050115	-1.52738	3.970205	223	-7.1541	5.882559	3.770192
174	4.249263	-8.13519	3.970205	224	1.344016	9.079157	3.970205
175	8.261385	-3.67461	4.27162	225	-6.42393	6.5552	3.970205
176	9.32929	-2.89873	2.13581	226	0.126049	9.76844	2.13581
177	6.895116	-5.798	4.340576	227	-0.94186	8.992562	4.27162
178	5.149921	-7.50424	4.143026	228	-2.37704	9.450481	2.24457
179	8.728372	-2.57893	4.143025	229	-3.38352	8.349324	4.340576
180	9.24625	-2.20267	3.107269	230	-5.54555	7.216805	4.143026
181	7.644932	-4.76597	4.340576	231	0.762387	9.474368	3.107269
182	8.324083	-4.44469	3.309737	232	0.244509	9.098107	4.143026
183	9.272648	-3.58336	1.085144	233	-0.54257	9.926131	1.085144
184	6.047673	-6.72153	4.27162	234	-1.65487	9.290159	3.309738
185	6.799435	-6.54319	3.309738	235	-2.17029	8.743526	4.340576
186	7.477917	-6.24841	2.24457	236	-3.07065	9.450481	1.122285
187	8.03906	-5.84072	1.122285	237	-3.63179	9.042788	2.24457
188	4.95211	-8.11304	3.107269	238	-4.1218	8.488604	3.309738
189	5.639769	-7.97692	2.13581	239	-4.52372	7.828744	4.27162
190	6.273383	-7.71149	1.085144	240	-5.39548	8.349325	1.085144
191	9.24547	0.554016	3.770192	241	-5.84372	7.828744	2.13581
192	3.383908	8.621764	3.770192	242	-6.18568	7.216805	3.107269
193	9.050115	1.527379	3.970205	243	-7.80539	4.986143	3.770192
194	4.249263	8.135185	3.970205	244	-7.72319	5.611228	2.977654
195	9.32929	2.898734	2.13581	245	-7.24163	6.813106	1.067905
196	8.261385	3.674613	4.27162	246	-8.71744	4.781831	1.067905
197	8.253397	5.181056	2.24457	247	-7.5415	6.231742	2.071513
198	6.895116	5.797998	4.340576	248	-8.25719	5.246679	2.071513
199	5.149921	7.504242	4.143026	249	-7.80539	-4.98614	3.770192
200	9.24625	2.202667	3.107269	250	-8.21947	4.083848	3.970205

Table B.11: Geodesic Gridshell with Denser Grid: Node coordinates, Design Option 2 (5/5)**Splice joints**

	x [m]	y [m]	z [m]
251	-8.21947	-4.08385	3.970205
252	-9.25139	3.138494	2.13581
253	-8.84348	1.883096	4.27162
254	-9.72249	0.659662	2.24457
255	-8.98624	-0.63783	4.340576
256	-8.57726	-3.04401	4.143026
257	-8.77507	3.652814	3.107269
258	-8.57726	3.044011	4.143026
259	-9.60798	2.551326	1.085144
260	-9.34685	1.296943	3.309738
261	-8.98624	0.637832	4.340576
262	-9.93682	0	1.122285
263	-9.72249	-0.65966	2.24457
264	-9.34685	-1.29694	3.309738
265	-8.84348	-1.8831	4.27162
266	-9.60798	-2.55133	1.085144
267	-9.25139	-3.13849	2.13581
268	-8.77507	-3.65281	3.107269
269	-7.1541	-5.88256	3.770192
270	-7.72319	-5.61123	2.977654
271	-8.71744	-4.78183	1.067905
272	-7.24163	-6.81311	1.067905
273	-8.25719	-5.24668	2.071513
274	-7.5415	-6.23174	2.071513
275	2.330107	-8.96417	3.770192
276	-6.42393	-6.5552	3.970205
277	1.344016	-9.07916	3.970205
278	-5.84372	-7.82874	2.13581
279	-4.52372	-7.82874	4.27162
280	-3.63179	-9.04279	2.24457
281	-2.17029	-8.74353	4.340576
282	0.244509	-9.09811	4.143026
283	-6.18568	-7.21681	3.107269
284	-5.54555	-7.21681	4.143026
285	-5.39548	-8.34933	1.085144
286	-4.1218	-8.4886	3.309738
287	-3.38352	-8.34932	4.340576
288	-3.07065	-9.45048	1.122285
289	-2.37704	-9.45048	2.24457
290	-1.65487	-9.29016	3.309738
291	-0.94186	-8.99256	4.27162
292	-0.54257	-9.92613	1.085144
293	0.126049	-9.76844	2.13581
294	0.762387	-9.47437	3.107269
295	2.949997	-9.07916	2.977654
296	1.853956	-9.76844	1.067905
297	4.241864	-8.99256	1.067905
298	2.438276	-9.47437	2.071513
299	3.596287	-9.09811	2.071513
300	8.253397	-5.18106	2.24457

Cross section and material properties

The cross section that is used for all beams has a width (b) of 150 mm and a height (h) of 125 mm. The beams have a strength class of C30.

Boundary conditions and support

Table B.12 presents the coordinates of the supports in the structure. Their boundary conditions are equivalent to the geodesic gridshell (Table A.20).

Table B.12: Geodesic Gridshell with Denser Grid: Support coordinates

	x [m]	y [m]	z [m]
1	9.065404	-4.22119	0
2	7.69198	-6.39011	0
3	8.454304	-5.34086	0
4	6.815955	-7.31729	0
5	9.065404	4.221191	0
6	7.69198	6.390105	0
7	8.454304	5.340856	0
8	6.815955	7.317291	0
9	9.510565	-3.09017	0
10	9.510565	3.09017	0
11	9.81522	-1.9135	0
12	9.978952	-0.64847	0
13	9.978952	0.648472	0
14	9.81522	1.913495	0
15	5.877853	8.09017	0
16	4.852912	8.743526	0
17	3.700399	9.290159	0
18	2.466933	9.690936	0
19	1.213228	9.926131	0
20	0	10	0
21	-1.21323	9.926131	0
22	-3.7004	9.290159	0
23	-2.46693	9.690936	0
24	-4.85291	8.743526	0
25	-5.87785	8.09017	0
26	-6.81596	7.317291	0
27	-7.69198	6.390105	0
28	-8.4543	5.340856	0
29	-9.0654	4.221191	0
30	-9.51057	3.09017	0
31	-9.81522	1.913495	0
32	-9.97895	-0.64847	0
33	-9.97895	0.648472	0
34	-9.81522	-1.9135	0
35	-9.51057	-3.09017	0
36	-9.0654	-4.22119	0
37	-8.4543	-5.34086	0
38	-7.69198	-6.39011	0
39	-6.81596	-7.31729	0
40	-5.87785	-8.09017	0
41	-4.85291	-8.74353	0
42	-2.46693	-9.69094	0
43	-3.7004	-9.29016	0
44	-1.21323	-9.92613	0
45	0	-10	0
46	5.877853	-8.09017	0
47	1.213228	-9.92613	0
48	2.466933	-9.69094	0
49	3.700399	-9.29016	0
50	4.852912	-8.74353	0

B.2. Numerical results

Table B.13: Geodesic Gridshell with Denser Grid: FEA results (1/2) (20 m span, C30, 150x125 mm)

	Classic	DO 1	DO 2	
Reaction force (Qualitative)				
Rx	9.76	11.12	11.09	kN
Ry	9.65	9.38	11.28	kN
Rz	8.47	8.32	7.75	kN
Nodal displacement (SLS)				
dx	0.003	0.006	0.006	m
dy	0.003	0.006	0.007	m
dz	0.010	0.009	0.010	m
Beam displacement (SLS)				
w (-)	-0.010	-0.009	-0.010	m
w (+)	0.004	0.007	0.010	m
Unity checks SLS				
Roof defl.	0.129	0.118	0.128	[-]
x-displ.	0.104	0.177	0.181	[-]
y-displ.	0.094	0.177	0.221	[-]
Deformation energy (Qualitative)				
U_axial	0.287	0.296	0.305	kNm
U_bending	0.506	0.403	0.469	kNm
U_ax/U_tot	0.362	0.423	0.394	[-]
Stress (ULS)				
σ_{max}	0.986	1.097	1.190	kN/cm ²
σ_{min}	-0.842	-1.052	-1.196	kN/cm ²
τ_{max}	0.041	0.060	0.083	kN/cm ²
Cross section force (ULS)				
Nx,c	-39.96	-37.16	-40.38	kN
Nx,t	33.58	33.71	40.31	kN
Vz	6.33	7.44	7.59	kN
Vy	2.40	2.27	2.41	kN
Mt	0.04	0.16	0.24	kNm
My,hog	-2.85	-3.75	-4.13	kNm
My,sag	3.42	3.42	3.95	kNm
Mz,hog	-1.13	-1.04	-1.24	kNm
Mz,sag	0.64	0.80	0.85	kNm

Table B.14: Geodesic Gridshell with Denser Grid: FEA results (2/2) (20 m span, C30, 150x125 mm)

	Classic	DO 1	DO 2	
Unity checks ULS				
Axial tension	0.175	0.176	0.210	[-]
Axial compr.	0.165	0.153	0.167	[-]
Bending (y-axis)	0.577	0.611	0.683	[-]
Bending (z-axis)	0.495	0.512	0.578	[-]
Shear (par.)	0.157	0.184	0.188	[-]
Shear (perp.)	0.235	0.276	0.282	[-]
Torsion	0.010	0.040	0.061	[-]
Bending + ten. (y)	0.752	0.787	0.893	[-]
Bending + ten. (z)	0.671	0.688	0.788	[-]
Bending + com. (y)	0.604	0.635	0.711	[-]
Bending + com. (z)	0.523	0.535	0.606	[-]
Flex. buckling (y)	0.852	1.108	1.698	[-]
Flex. buckling (z)	0.992	1.492	2.625	[-]
LTS	0.700	1.225	2.344	[-]
Nodal force pinned joints (ULS)				
Nx,c	-39.79	-34.29	-36.54	kN
Nx,t	33.50	33.46	36.41	kN
Vy	2.40	1.14	1.21	kN
Vz	5.87	3.93	3.96	kN
Mx	0.02	0.12	0.17	kNm
Mz,hog	-1.13	-0.18	-0.27	kNm
Mz,sag	0.43	0.60	0.75	kNm
Nodal force rigid joints (ULS)				
Nx,c	-	-37.08	-40.28	kN
Nx,t	-	33.71	40.31	kN
Vy	-	-2.22	-2.19	kN
Vz	-	-7.08	-7.30	kN
Mx	-	0.16	0.24	kNm
My,hog	-	-3.75	-4.13	kNm
My,sag	-	3.42	3.95	kNm
Mz,hog	-	-1.04	-1.24	kNm
Mz,sag	-	0.59	0.85	kNm
Stability (2nd order, ULS)				
Buckling factor	8.61	4.41	2.03	[-]

B.3. Axial stress & displacement plots

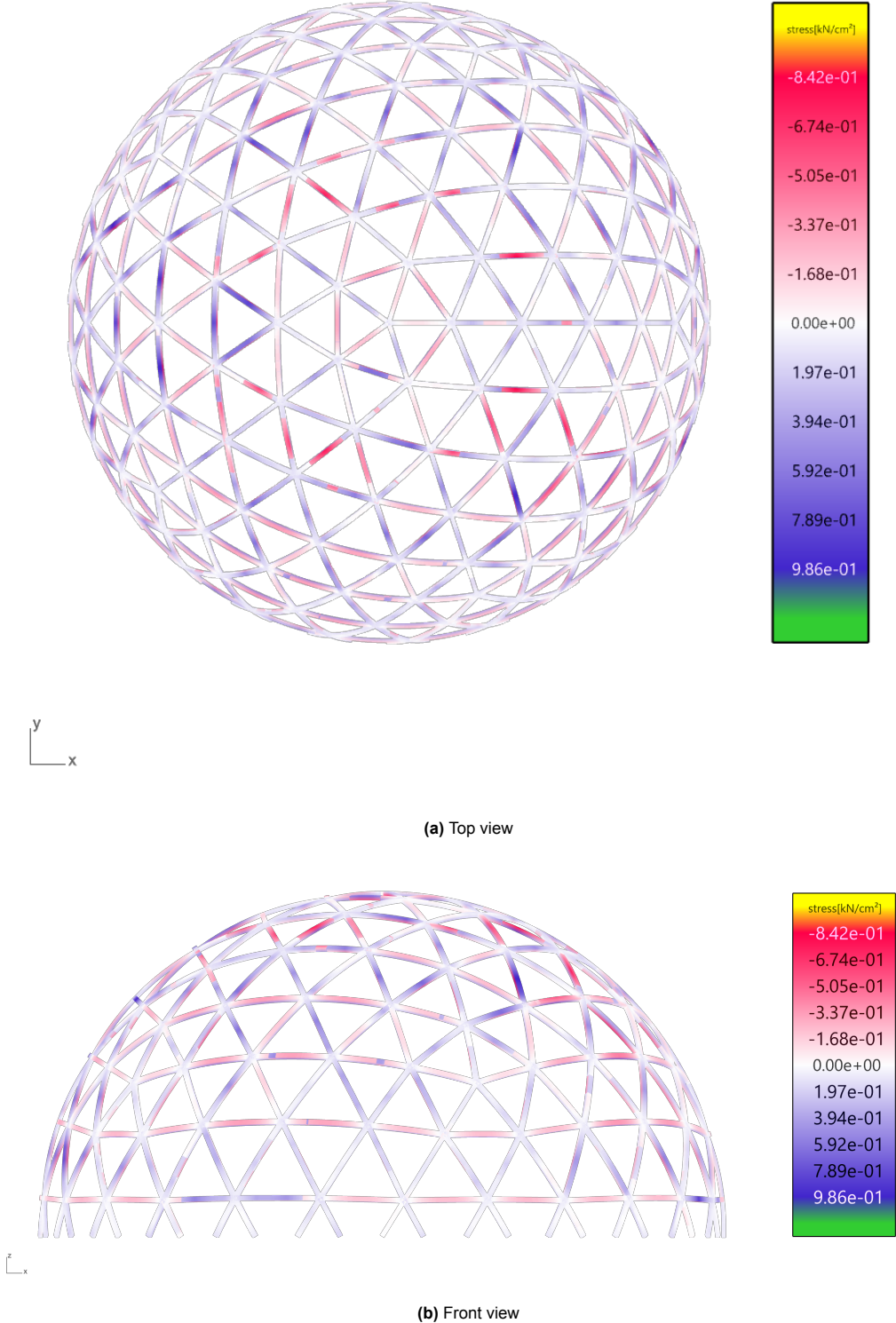


Figure B.3: Classic Geodesic Gridshell with Denser Grid: Axial stress (ULS, 20 m span, C30, 150x125 mm)

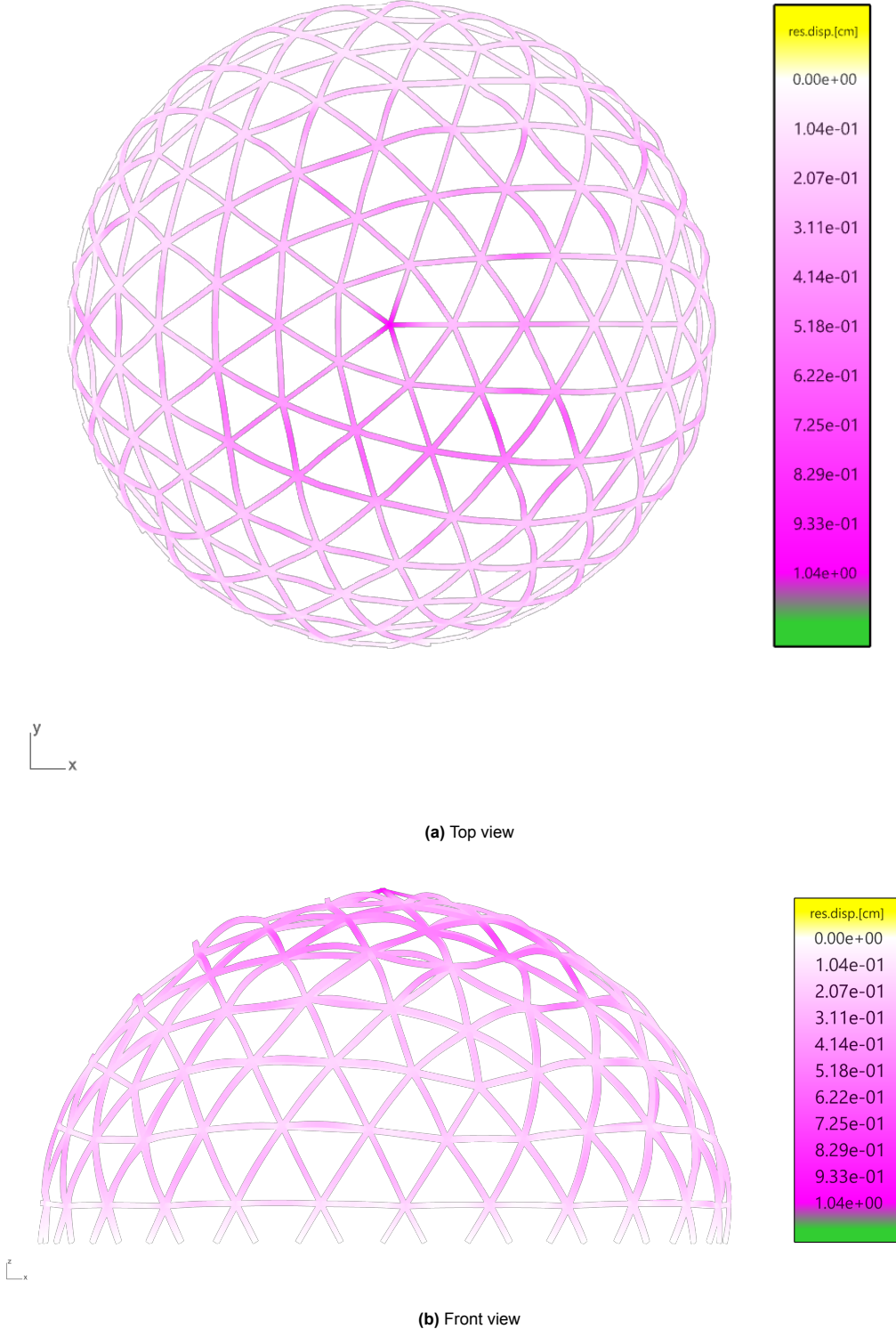


Figure B.4: Classic Geodesic Gridshell with Denser Grid: Displacement (SLS, 20 m span, C30, 150x125 mm)

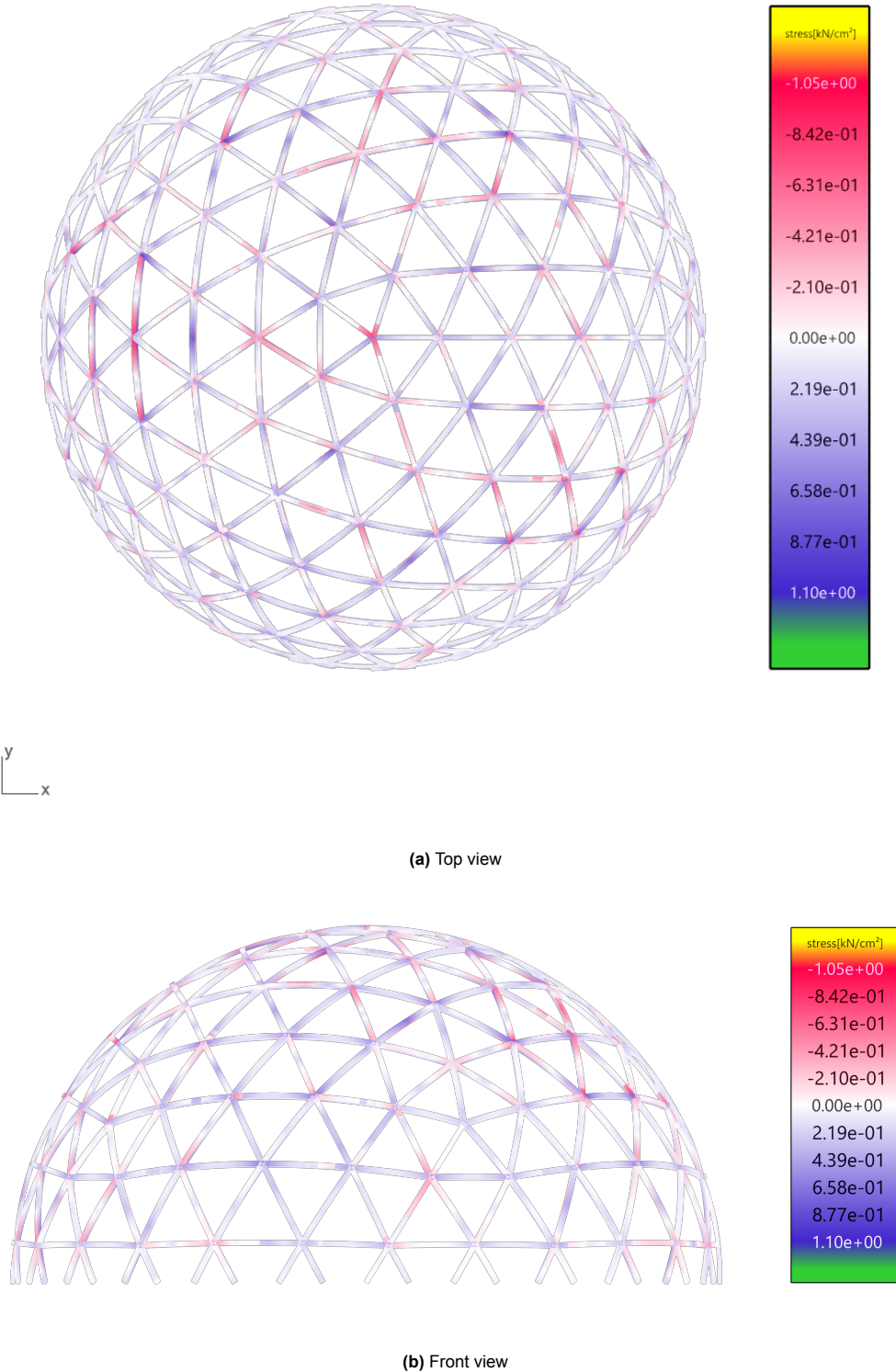


Figure B.5: Geodesic Gridshell with Denser Grid: Axial stress, Design Option 1 (ULS, 20 m span, C30, 150x125 mm)

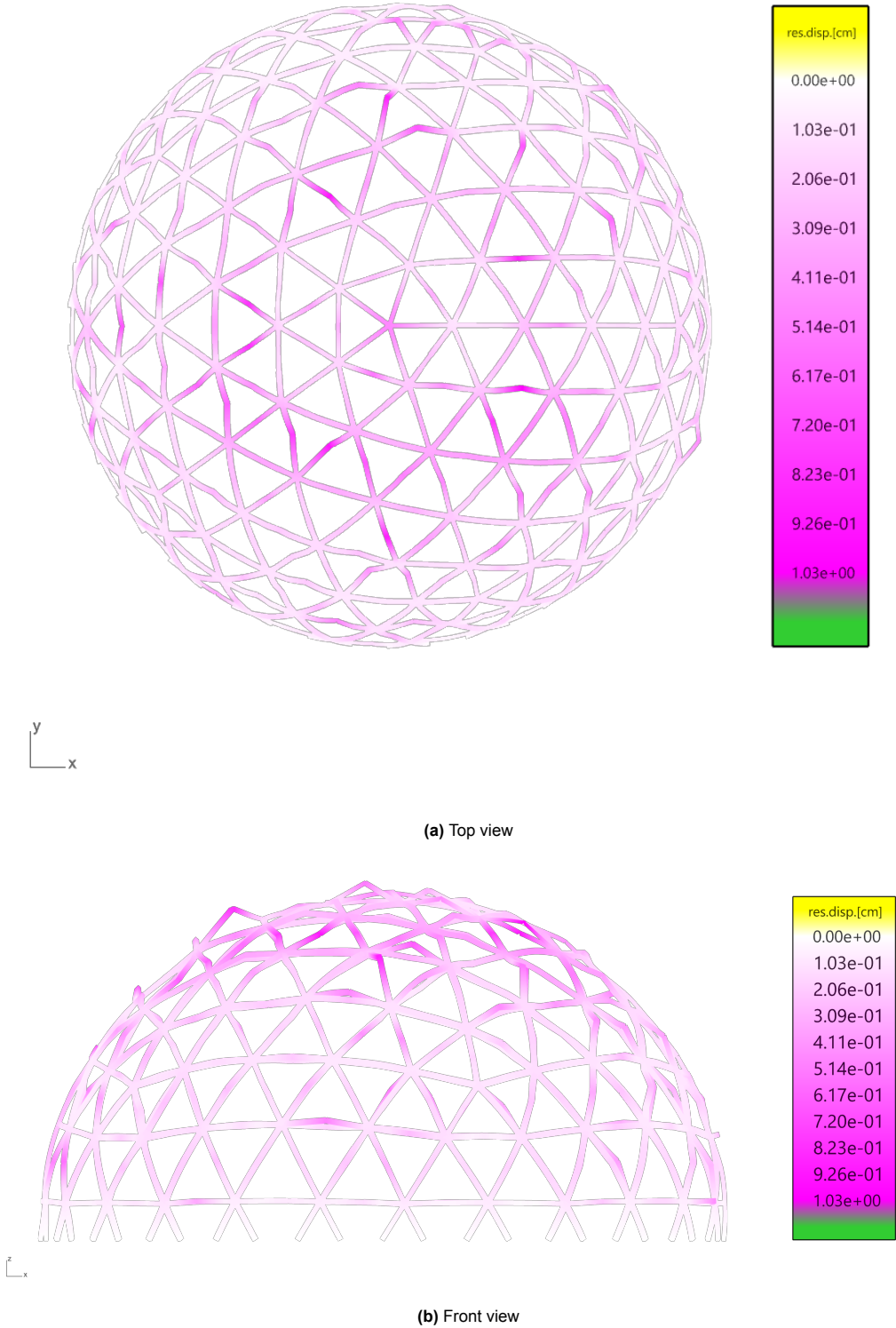


Figure B.6: Geodesic Gridshell with Denser Grid: Displacement, Design Option 1 (SLS, 20 m span, C30, 150x125 mm)

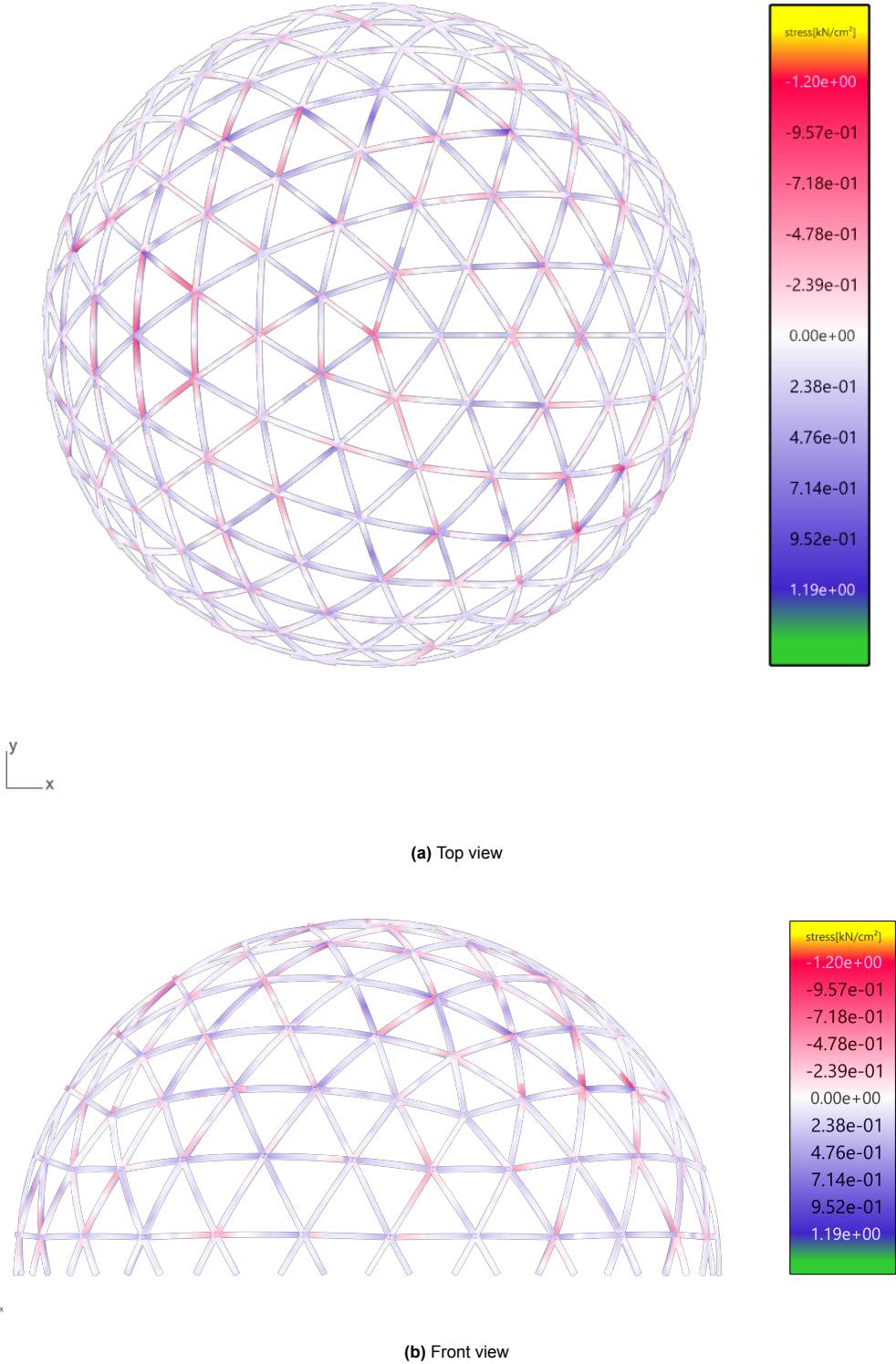


Figure B.7: Geodesic Gridshell with Denser Grid: Axial stress, Design Option 2 (ULS, 20 m span, C30, 150x125 mm)

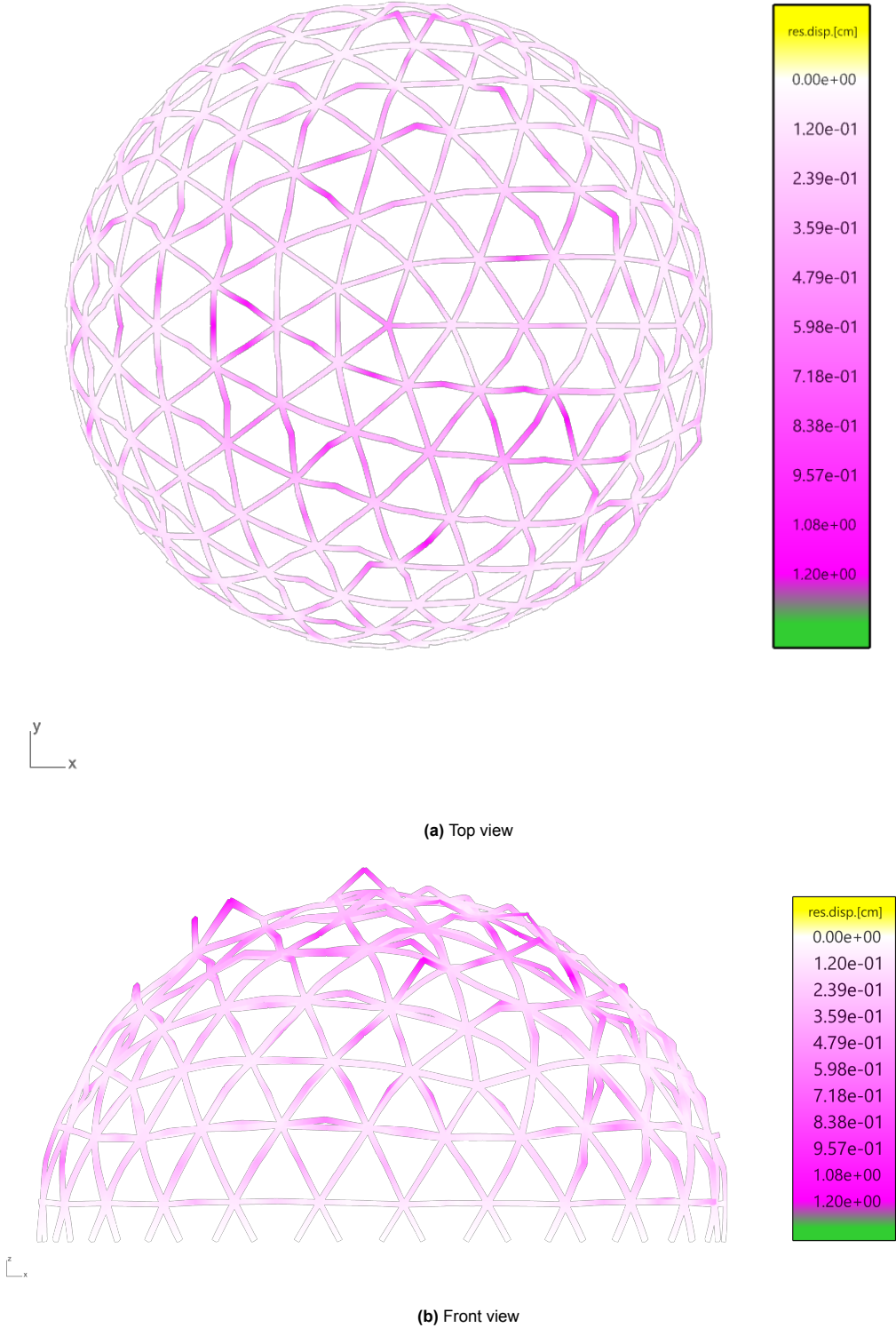


Figure B.8: Geodesic Gridshell with Denser Grid: Displacement, Design Option 2 (SLS, 20 m span, C30, 150x125 mm)

B.4. Results bar charts

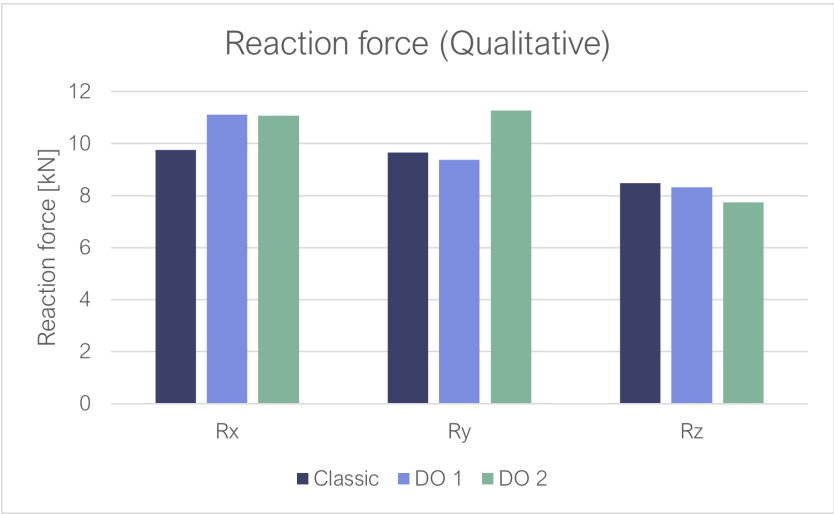


Figure B.9: Geodesic Gridshell with Denser Grid: Reaction force results (Qualitative, 20 m span, C30, 150x125 mm)

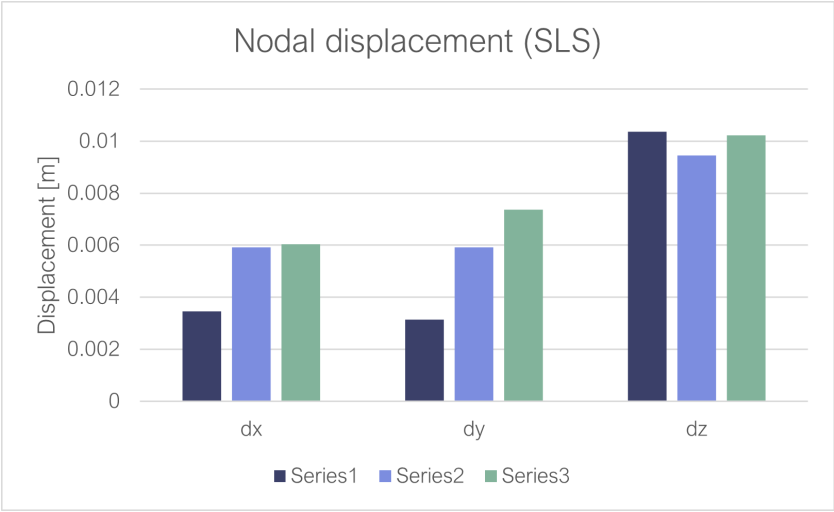


Figure B.10: Geodesic Gridshell with Denser Grid: Nodal displacement results (SLS, 20 m span, C30, 150x125 mm)

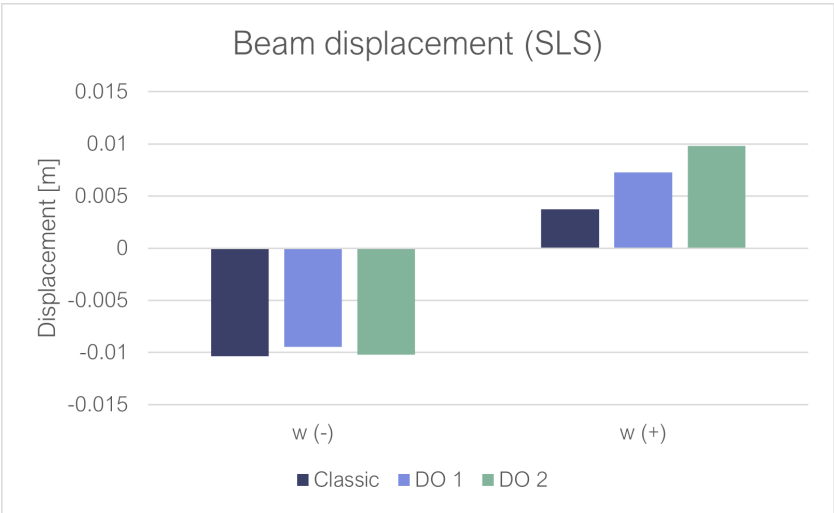


Figure B.11: Geodesic Gridshell with Denser Grid: Beam displacement results (SLS, 20 m span, C30, 150x125 mm)

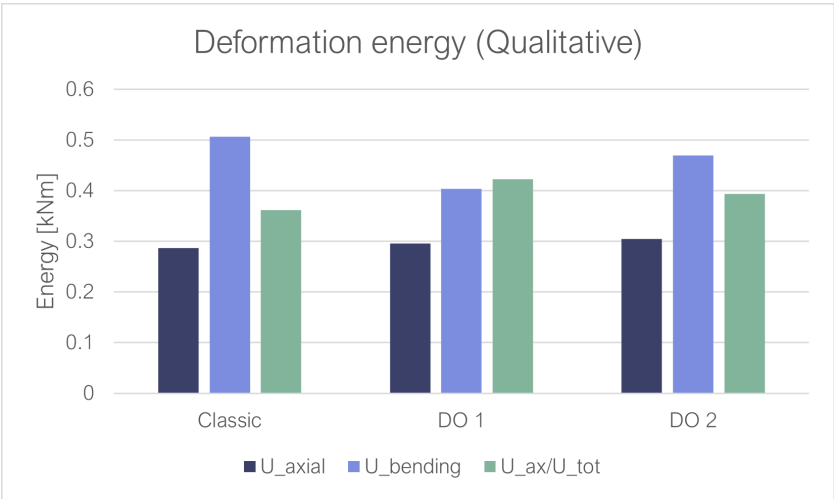


Figure B.12: Geodesic Gridshell with Denser Grid: Deformation energy results (Qualitative, 20 m span, C30, 150x125 mm)

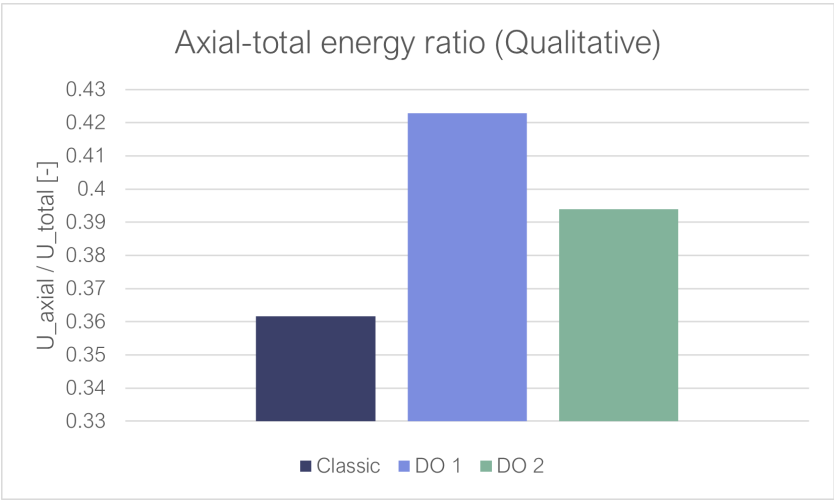


Figure B.13: Geodesic Gridshell with Denser Grid: Axial-total deformation energy ratio results (Qualitative, 20 m span, C30, 150x125 mm)

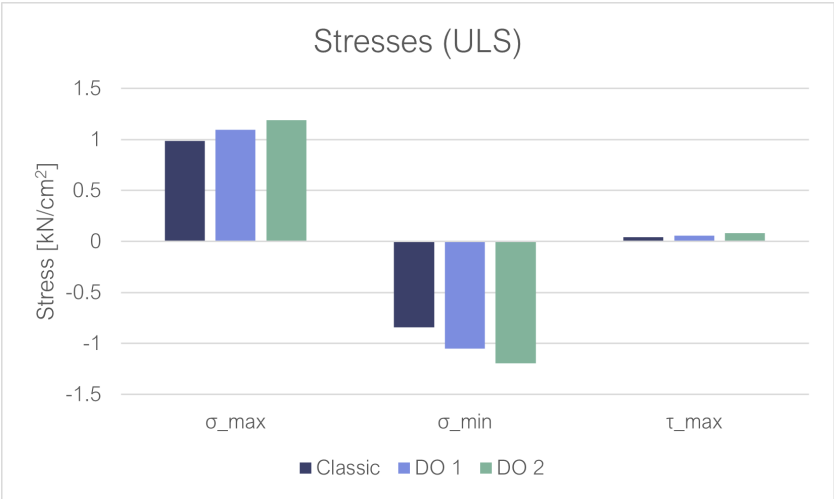


Figure B.14: Geodesic Gridshell with Denser Grid: Stress results (ULS, 20 m span, C30, 150x125 mm)

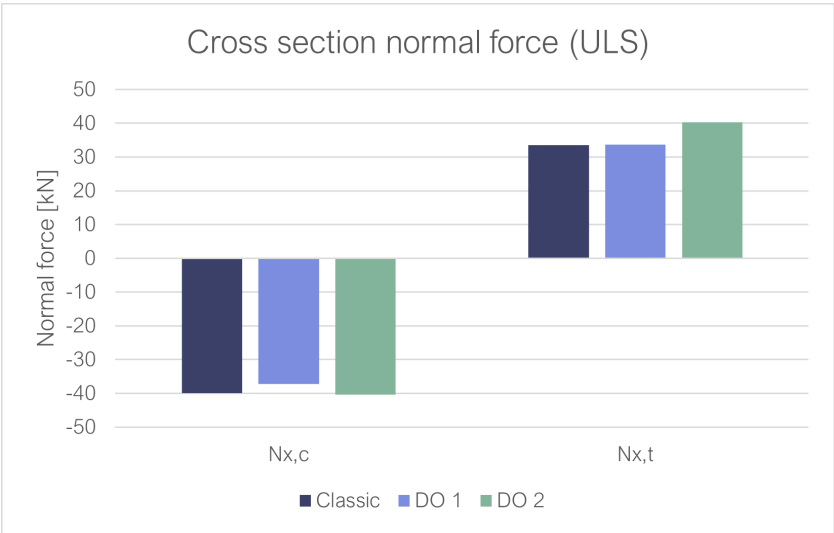


Figure B.15: Geodesic Gridshell with Denser Grid: Cross section normal force results (ULS, 20 m span, C30, 150x125 mm)

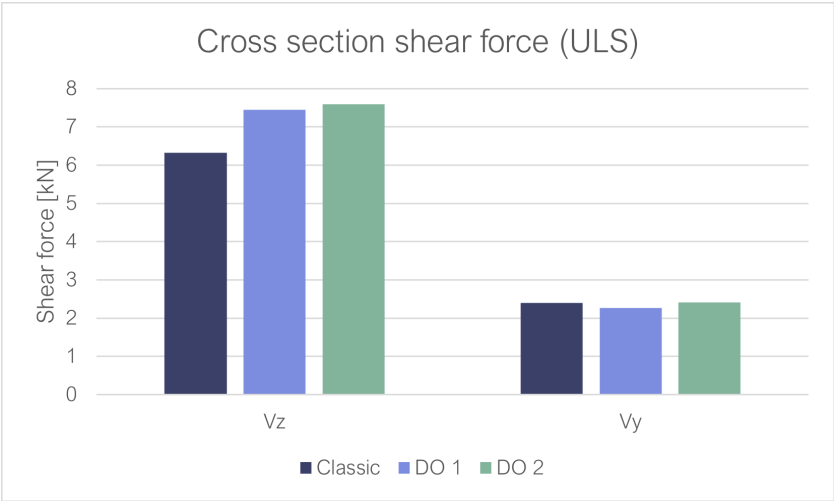


Figure B.16: Geodesic Gridshell with Denser Grid: Cross section shear force results (ULS, 20 m span, C30, 150x125 mm)

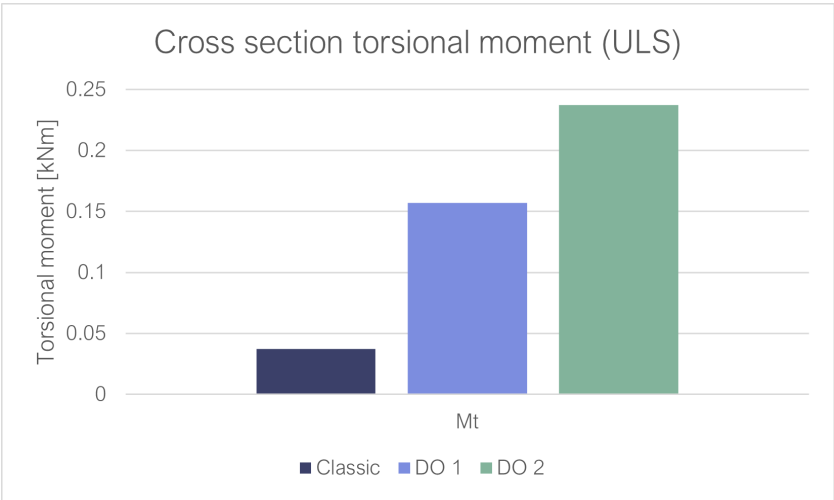


Figure B.17: Geodesic Gridshell with Denser Grid: Cross section torsional moment results (ULS, 20 m span, C30, 150x125 mm)

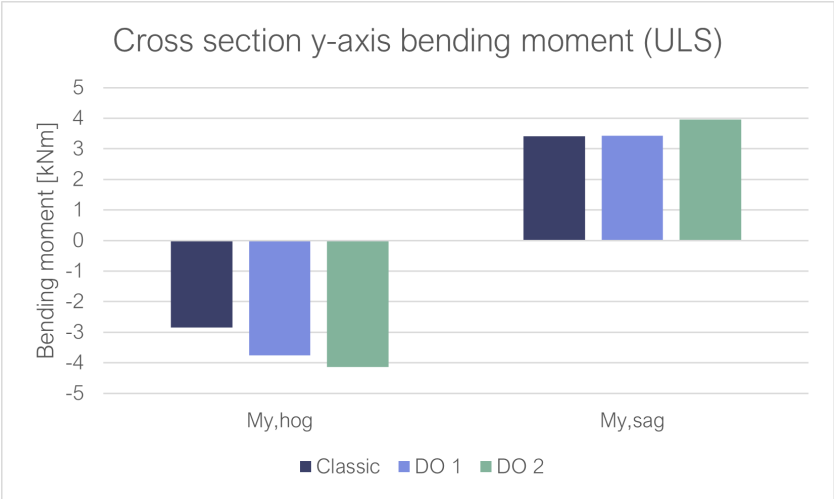


Figure B.18: Geodesic Gridshell with Denser Grid: Cross section y-axis bending moment results (ULS, 20 m span, C30, 150x125 mm)

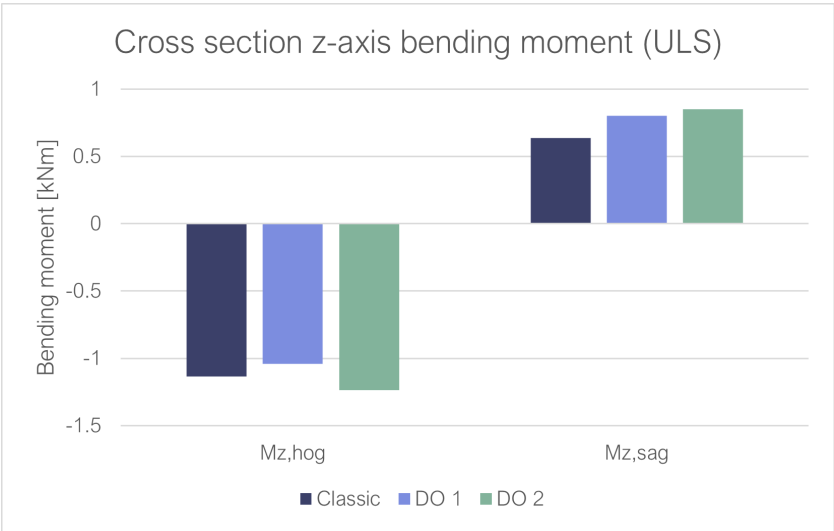


Figure B.19: Geodesic Gridshell with Denser Grid: Cross section z-axis bending moment results (ULS, 20 m span, C30, 150x125 mm)

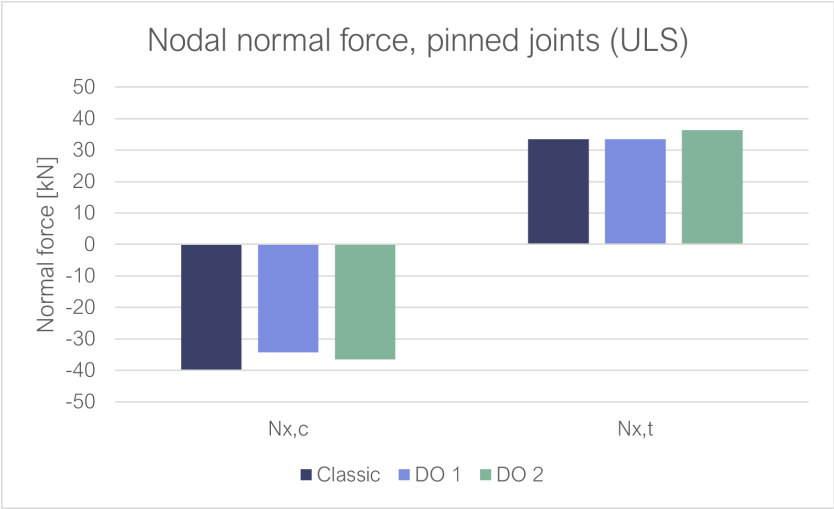


Figure B.20: Geodesic Gridshell with Denser Grid: Nodal normal force, pinned joints results (ULS, 20 m span, C30, 150x125 mm)

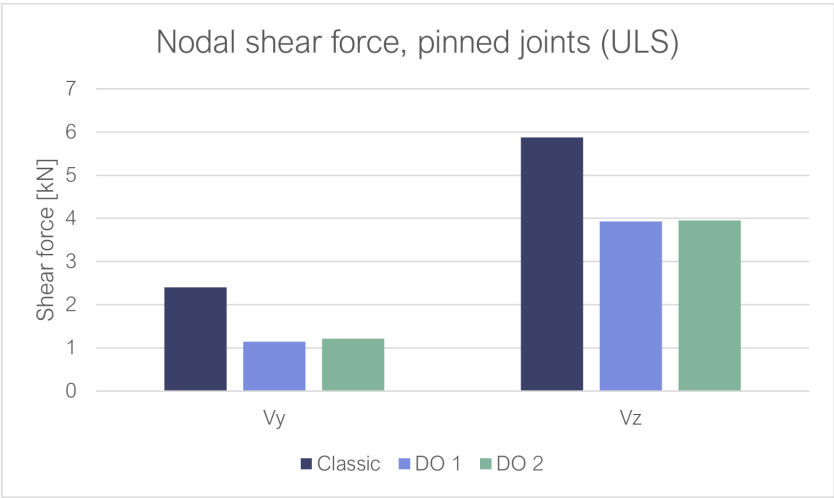


Figure B.21: Geodesic Gridshell with Denser Grid: Nodal shear force, pinned joints results (ULS, 20 m span, C30, 150x125 mm)

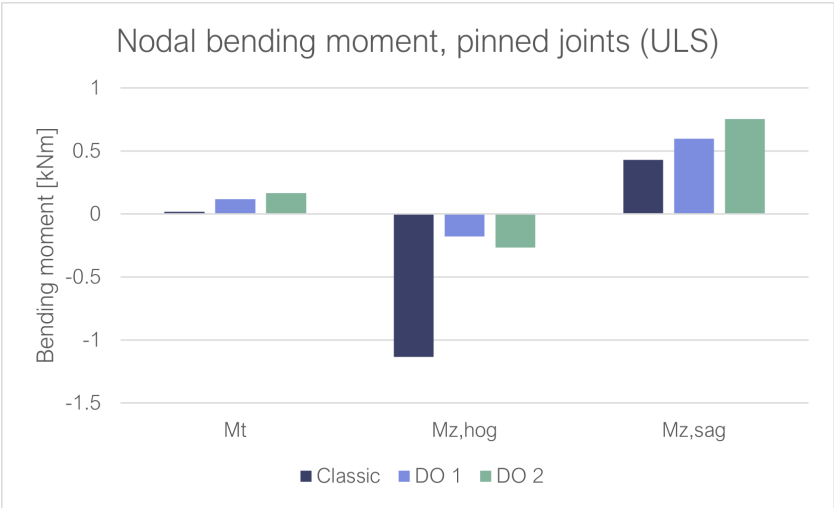


Figure B.22: Geodesic Gridshell with Denser Grid: Nodal bending moment, pinned joints results (ULS, 20 m span, C30, 150x125 mm)

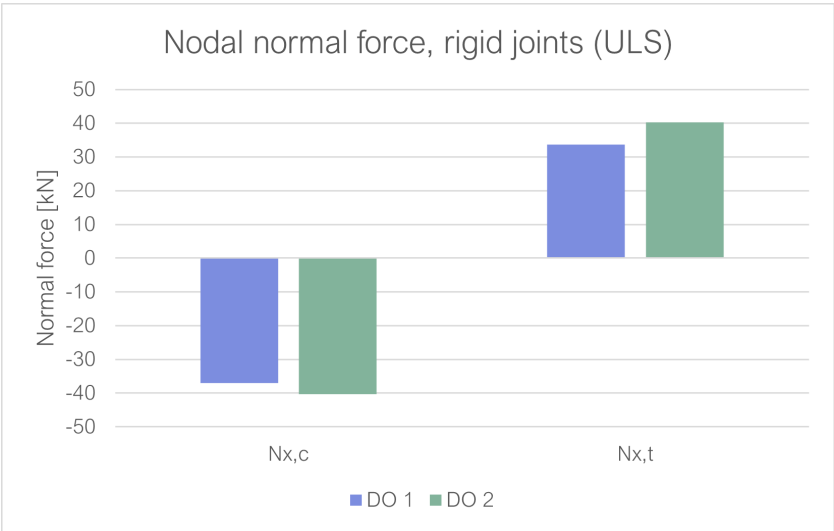


Figure B.23: Geodesic Gridshell with Denser Grid: Nodal normal force, rigid joints results (ULS, 20 m span, C30, 150x125 mm)

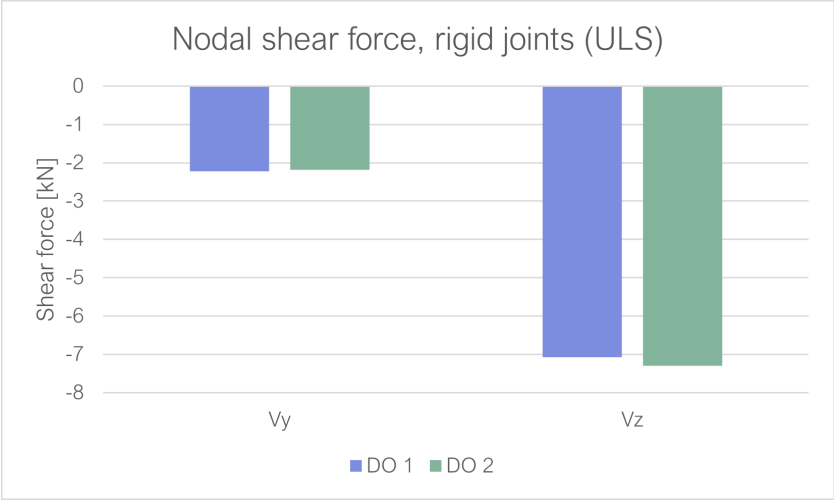


Figure B.24: Geodesic Gridshell with Denser Grid: Nodal shear force, rigid joints results (ULS, 20 m span, C30, 150x125 mm)

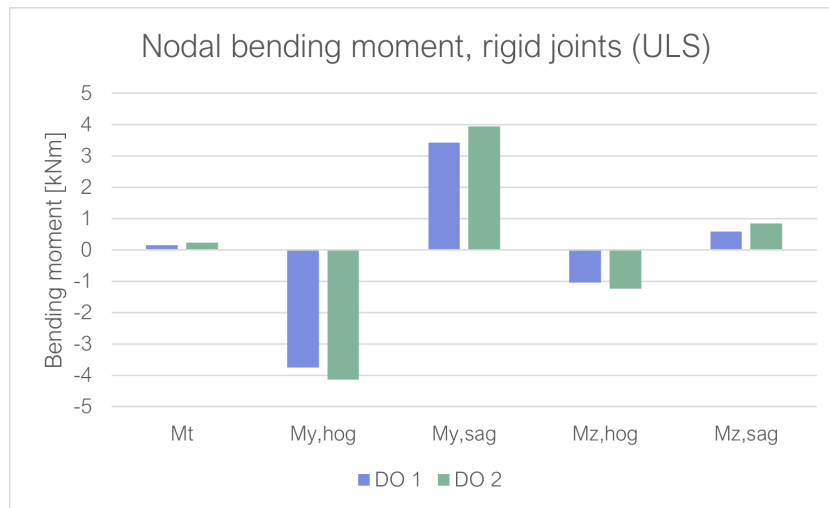


Figure B.25: Geodesic Gridshell with Denser Grid: Nodal bending moment, rigid joints results (ULS, 20 m span, C30, 150x125 mm)

B.5. Utilisation results after cross section optimisation

Table B.15: Geodesic Gridshell with Denser Grid: FEA utilisation results after cross section optimisation (20 m span)

	Classic	DO 1	DO 2	
Cross section				
Width	150	150	175	[mm]
Height	125	150	175	[mm]
Strength class	C30	C30	C30	[-]
Unity checks SLS				
Roof defl.	0.129	0.076	0.053	[-]
x-displ.	0.104	0.110	0.067	[-]
y-displ.	0.094	0.111	0.079	[-]
Unity checks ULS				
Axial tension	0.175	0.145	0.117	[-]
Axial compr.	0.165	0.128	0.104	[-]
Bending (y-axis)	0.577	0.488	0.349	[-]
Bending (z-axis)	0.495	0.397	0.285	[-]
Shear (par.)	0.157	0.154	0.115	[-]
Shear (perp.)	0.235	0.230	0.172	[-]
Torsion	0.010	0.029	0.027	[-]
Bending + ten. (y)	0.752	0.633	0.465	[-]
Bending + ten. (z)	0.671	0.542	0.402	[-]
Bending + com. (y)	0.604	0.504	0.359	[-]
Bending + com. (z)	0.523	0.413	0.296	[-]
Flexural buckling (y)	0.852	0.923	0.879	[-]
Flexural buckling (z)	0.992	0.832	0.816	[-]
LTS	0.700	0.605	0.616	[-]
Stability (2nd order, ULS)				
Buckling factor	8.61	7.24	5.73	[-]



ULS & SLS verification

This appendix discusses the verification of the structure in both the ultimate limit state (ULS) and the serviceability limit state (SLS) according to Eurocode 5 (Nederlands Normalisatie-instituut, 2011b). The verifications discussed in this appendix are performed on the classic geodesic gridshell of the preliminary study. All other designs in this thesis are verified in the same way.

C.1. ULS verification

The properties of the cross-section of the classic geodesic gridshell are presented in Table C.1, including the moments of resistance ($W_y = \frac{1}{6}hb^2$ and $W_z = \frac{1}{6}bh^2$) and moments of inertia ($I_y = \frac{1}{12}hb^3$ and $I_z = \frac{1}{12}bh^3$), which are all based on the coordinate system of Karamba3D.

The design values of the strength properties of all members are determined according to the following equation, with X_k the characteristic value.

$$X_d = k_{mod} \frac{X_k}{\gamma_M} \quad (C.1)$$

k_{mod} is determined according to EN 1995-1-1 (Nederlands Normalisatie-instituut, 2011b). Because of the different load-duration classes (permanent and short term), k_{mod} is chosen corresponding to the load with the shortest duration, in this case snow and wind actions, which are short term actions. The structure has service class 3 because of the high moisture contents, due to a high humidity in The Netherlands (AirSain, n.d.). Therefore $k_{mod} = 0.7$ for solid timber. γ_M is equal to 1.3 for solid timber. The characteristic and design values of the strength properties of all used strength classes are listed in Table C.2.

Table C.1: Classic Geodesic Gridshell: Cross-sectional properties

b	200 mm
h	175 mm
W_y	$1.17 \cdot 10^6 \text{ mm}^3$
W_z	$1.02 \cdot 10^6 \text{ mm}^3$
I_y	$1.17 \cdot 10^8 \text{ mm}^4$
I_z	$8.93 \cdot 10^7 \text{ mm}^4$

Table C.2: Strength properties C30 timber

$E_{0,g,05}$	8000 N/mm ²	$f_{m,d}$	16.15 N/mm ²
$f_{m,g,k}$	30 N/mm ²	$f_{t,0,d}$	10.23 N/mm ²
$f_{t,0,g,k}$	19 N/mm ²	$f_{t,90,d}$	0.2154 N/mm ²
$f_{t,90,g,k}$	0.4 N/mm ²	$f_{c,0,d}$	12.92 N/mm ²
$f_{c,0,g,k}$	24 N/mm ²	$f_{c,90,d}$	1.454 N/mm ²
$f_{c,90,g,k}$	2.7 N/mm ²	$f_{v,d}$	2.154 N/mm ²
$f_{v,g,k}$	4 N/mm ²		

The ULS verification is performed on one beam using the most critical values of the cross-section forces. These results are listed in Table C.3.

Table C.3: Classic Geodesic Gridshell: Resulting forces

N_t	46.09 kN
N_c	-45.17 kN
V_y	6.07 kN
V_z	8.14 kN
$M_{y,sag}$	6.57 kNm
$M_{y,hog}$	-8.40 kNm
$M_{z,sag}$	2.29 kNm
$M_{z,hog}$	-5.58 kNm
M_t	0.21 kNm

Tension parallel to the grain

The design tensile stress is calculated using N_t :

$$\sigma_{t,0,d} = \frac{N_t}{bh} = \frac{46.09 \cdot 10^3}{200 \cdot 175} = 1.317 \text{ N/mm}^2 \quad (\text{C.2})$$

The following unity check is performed to satisfy $\sigma_{t,0,d} \leq f_{t,0,d}$:

$$U.C. = \frac{\sigma_{t,0,d}}{f_{t,0,d}} = \frac{1.317}{10.23} = \mathbf{0.13} \quad (\text{C.3})$$

Compression parallel to the grain

The design compression stress is calculated using N_c :

$$\sigma_{c,0,d} = \frac{N_c}{bh} = \frac{-45.17 \cdot 10^3}{200 \cdot 175} = -1.291 \text{ N/mm}^2 \quad (\text{C.4})$$

The following unity check is performed to satisfy $\sigma_{c,0,d} \leq f_{c,0,d}$:

$$U.C. = \frac{-\sigma_{c,0,d}}{f_{c,0,d}} = \frac{1.291}{12.92} = \mathbf{0.10} \quad (\text{C.5})$$

Bending

The design bending stresses about the y- and z-axis are both calculated using the largest absolute value of the hogging and sagging moment.

$$\sigma_{m,y,d} = \frac{\max(M_{y,sag}; |M_{y,hog}|)}{W_y} = \frac{8.40 \cdot 10^6}{1.17 \cdot 10^6} = 7.197 \text{ N/mm}^2 \quad (\text{C.6})$$

$$\sigma_{m,z,d} = \frac{\max(M_{z,sag}; |M_{z,hog}|)}{W_z} = \frac{5.58 \cdot 10^6}{1.02 \cdot 10^6} = 5.469 \text{ N/mm}^2 \quad (\text{C.7})$$

k_m is equal to 0.7 for rectangular cross-sections. The following two unity checks are performed:

$$U.C. = \frac{\sigma_{m,y,d}}{f_{m,y,d}} + k_m \cdot \frac{\sigma_{m,z,d}}{f_{m,z,d}} = \frac{7.197}{16.15} + 0.7 \cdot \frac{5.469}{16.15} = \mathbf{0.68} \quad (\text{C.8})$$

$$U.C. = k_m \cdot \frac{\sigma_{m,y,d}}{f_{m,y,d}} + \frac{\sigma_{m,z,d}}{f_{m,z,d}} = 0.7 \cdot \frac{7.197}{16.15} + \frac{5.469}{16.15} = \mathbf{0.65} \quad (\text{C.9})$$

Shear

Both the shear stress parallel and perpendicular to the grain are observed. The design shear stress parallel to the grain is calculated with the maximum value of τ_{xy} and τ_{xz} :

$$\tau_{xy} = \frac{V_y}{bh} = \frac{6.07 \cdot 10^3}{200 \cdot 175} = 0.173 \text{ N/mm}^2 \quad (\text{C.10})$$

$$\tau_{xz} = \frac{V_z}{bh} = \frac{8.14 \cdot 10^3}{200 \cdot 175} = 0.233 \text{ N/mm}^2 \quad (\text{C.11})$$

$$\tau_d = \tau_{max} = \max(\tau_{xy}; \tau_{xz}) = 0.233 \text{ N/mm}^2 \quad (\text{C.12})$$

A unity check is performed to satisfy $\tau_d \leq f_{v,d}$:

$$U.C. = \frac{\tau_d}{f_{v,d}} = \frac{0.233}{2.154} = \mathbf{0.11} \quad (\text{C.13})$$

The design shear stress perpendicular to the grain is calculated with the maximum value of τ_{zy} and τ_{yz} using V_y and V_z :

$$\tau_{zy} = \frac{3V_y}{2bh} = \frac{3 \cdot 6.07 \cdot 10^3}{2 \cdot 200 \cdot 175} = 0.260 \text{ N/mm}^2 \quad (\text{C.14})$$

$$\tau_{yz} = \frac{3V_z}{2bh} = \frac{3 \cdot 8.14 \cdot 10^3}{2 \cdot 200 \cdot 175} = 0.349 \text{ N/mm}^2 \quad (\text{C.15})$$

$$\tau_d = \tau_{max} = \max(\tau_{zy}; \tau_{yz}) = 0.349 \text{ N/mm}^2 \quad (\text{C.16})$$

A unity check is performed to satisfy $\tau_d \leq f_{v,d}$:

$$U.C. = \frac{\tau_d}{f_{v,d}} = \frac{0.349}{2.154} = \mathbf{0.16} \quad (\text{C.17})$$

Torsion

The torsional stress is calculated using the torsional bending moment, M_t . The maximum torsional stress in rectangular sections is calculated using the formula:

$$\tau_{max} = \frac{3M_t}{8AB^2} \left(1 + 0.6095 \frac{B}{A} + 0.8865 \frac{B^2}{A^2} - 1.8023 \frac{B^3}{A^3} + 0.9100 \frac{B^4}{A^4} \right) \quad (\text{C.18})$$

, in which A and B represent the cross section dimensions, divided by 2. $A \geq B$, so in this case: $A = \frac{b}{2} = 100 \text{ mm}$ and $B = \frac{h}{2} = 87.5 \text{ mm}$. This leads to the following calculation for the torsional stress:

$$\begin{aligned} \tau_{tor,d} = \tau_{max} &= \frac{3 \cdot 0.21 \cdot 10^6}{8 \cdot 100 \cdot 87.5^2} \cdot \left(1 + 0.6095 \cdot \frac{87.5}{100} + 0.8865 \cdot \frac{87.5^2}{100^2} \right. \\ &\quad \left. - 1.8023 \cdot \frac{87.5^3}{100^3} + 0.9100 \cdot \frac{87.5^4}{100^4} \right) = 0.052 \text{ N/mm}^2 \end{aligned} \quad (\text{C.19})$$

The shape factor k_{shape} for torsion is calculated for a rectangular cross-section:

$$k_{shape} = \min \left(1 + 0.15 \frac{b}{h}; 2.0 \right) = \min \left(1 + 0.15 \cdot \frac{200}{175}; 2.0 \right) = 1.171 \quad (\text{C.20})$$

To satisfy $\tau_{tor,d} \leq k_{shape} f_{v,d}$, the following unity check is performed:

$$U.C. = \frac{\tau_{tor,d}}{k_{shape} f_{v,d}} = \frac{0.052}{1.171 \cdot 2.154} = \mathbf{0.02} \quad (\text{C.21})$$

Combined bending and axial tension

To verify the combination of bending and axial tension, $\sigma_{t,0,d}$, $\sigma_{m,y,d}$ and $\sigma_{m,z,d}$ are used. k_m is equal to 0.7 for rectangular cross-sections. The following two unity checks are performed:

$$U.C. = \frac{\sigma_{t,0,d}}{f_{t,0,d}} + \frac{\sigma_{m,y,d}}{f_{m,y,d}} + k_m \frac{\sigma_{m,z,d}}{f_{m,z,d}} = \frac{1.317}{10.23} + \frac{7.197}{16.15} + 0.7 \cdot \frac{5.469}{16.15} = \mathbf{0.81} \quad (\text{C.22})$$

$$U.C. = \frac{\sigma_{t,0,d}}{f_{t,0,d}} + k_m \frac{\sigma_{m,y,d}}{f_{m,y,d}} + \frac{\sigma_{m,z,d}}{f_{m,z,d}} = \frac{1.317}{10.23} + 0.7 \cdot \frac{7.197}{16.15} + \frac{5.469}{16.15} = \mathbf{0.78} \quad (C.23)$$

Combined bending and axial compression

To verify the combination of bending and axial compression, $\sigma_{c,0,d}$, $\sigma_{m,y,d}$ and $\sigma_{m,z,d}$, that are calculated previously, are used. k_m is equal to 0.7 for rectangular cross-sections. The following two unity checks are performed:

$$U.C. = \left(\frac{\sigma_{c,0,d}}{f_{c,0,d}} \right)^2 + \frac{\sigma_{m,y,d}}{f_{m,y,d}} + k_m \frac{\sigma_{m,z,d}}{f_{m,z,d}} = \left(\frac{1.291}{12.92} \right)^2 + \frac{7.197}{16.15} + 0.7 \cdot \frac{5.469}{16.15} = \mathbf{0.69} \quad (C.24)$$

$$U.C. = \left(\frac{\sigma_{c,0,d}}{f_{c,0,d}} \right)^2 + k_m \frac{\sigma_{m,y,d}}{f_{m,y,d}} + \frac{\sigma_{m,z,d}}{f_{m,z,d}} = \left(\frac{1.291}{12.92} \right)^2 + 0.7 \cdot \frac{7.197}{16.15} + \frac{5.469}{16.15} = \mathbf{0.66} \quad (C.25)$$

Stability (flexural buckling) - Compression or combined compression and bending

As discussed in subsection 4.3.5, Karamba3D provides the buckling factor of the most critical buckling mode, when performing a second order analysis. This buckling factor refers to global buckling of the structure, rather than local buckling of the individual beams. However, because the buckling length of individual beams cannot be computed by Karamba3D, an estimation of the buckling lengths is made using the buckling factor for global buckling.

This is done, using using both formulas below of the buckling force, N_{cr} , in which λ is assumed to be the buckling factor. N_c^{II} refers to the second order normal compression force.

$$N_{cr} = \lambda \cdot N_c^{II} \quad (C.26)$$

$$N_{cr} = \frac{\pi^2 EI}{L_{cr}^2} \quad (C.27)$$

Therefore, the critical buckling length can be calculated as follows:

$$L_{cr} = \sqrt{\frac{\pi^2 EI}{\lambda N_c^{II}}} \quad (C.28)$$

Using this formula in Karamba3D, the critical buckling length in both y- and z-direction is extracted: $L_y = 3981.5$ mm, $L_z = 4550.3$ mm.

The slenderness in y-direction is calculated as follows:

$$\lambda_y = L_y \sqrt{\frac{bh}{I_y}} = 3981.5 \cdot \sqrt{\frac{200 \cdot 175}{1.17 \cdot 10^8}} = 68.96 \quad (C.29)$$

$$\lambda_z = L_z \sqrt{\frac{bh}{I_z}} = 4550.3 \cdot \sqrt{\frac{200 \cdot 175}{8.93 \cdot 10^7}} = 90.07 \quad (C.30)$$

Subsequently, the relative slenderness is calculated in the following way:

$$\lambda_{rel,y} = \frac{\lambda_y}{\pi} \sqrt{\frac{f_{c,0,k}}{E_{0.05}}} = \frac{68.96}{\pi} \sqrt{\frac{24}{8000}} = 1.202 \quad (C.31)$$

$$\lambda_{rel,z} = \frac{\lambda_z}{\pi} \sqrt{\frac{f_{c,0,k}}{E_{0.05}}} = \frac{90.07}{\pi} \sqrt{\frac{24}{8000}} = 1.570 \quad (C.32)$$

k_m is again equal to 0.7 and β_c is equal to 0.2 for solid timber. $k_{c,y}$ and $k_{c,z}$ are calculated in the following way:

$$k_y = 0.5 \cdot (1 + \beta_c \cdot (\lambda_{rel,y} - 0.3)) + \lambda_{rel,y}^2 = 0.5 \cdot (1 + 0.2 \cdot (1.202 - 0.3)) + 1.202^2 = 1.313 \quad (C.33)$$

$$k_z = 0.5 \cdot (1 + \beta_c \cdot (\lambda_{rel,z} - 0.3) + \lambda_{rel,z}^2) = 0.5 \cdot (1 + 0.2 \cdot (1.570 - 0.3) + 1.570^2) = 1.860 \quad (C.34)$$

$$k_{c,y} = \frac{1}{k_y + \sqrt{k_y^2 - \lambda_{rel,y}^2}} = \frac{1}{1.313 + \sqrt{1.313^2 - 1.202^2}} = 0.543 \quad (C.35)$$

$$k_{c,z} = \frac{1}{k_z + \sqrt{k_z^2 - \lambda_{rel,z}^2}} = \frac{1}{1.860 + \sqrt{1.860^2 - 1.570^2}} = 0.350 \quad (C.36)$$

The following two unity checks are performed:

$$U.C. = \frac{\sigma_{c,0,d}}{k_{c,y} f_{c,0,d}} + \frac{\sigma_{m,y,d}}{f_{m,y,d}} + k_m \frac{\sigma_{m,z,d}}{f_{m,z,d}} = \frac{1.291}{0.543 \cdot 12.92} + \frac{7.197}{16.15} + 0.7 \cdot \frac{5.469}{16.15} = \mathbf{0.89} \quad (C.37)$$

$$U.C. = \frac{\sigma_{c,0,d}}{k_{c,z} f_{c,0,d}} + k_m \frac{\sigma_{m,y,d}}{f_{m,y,d}} + \frac{\sigma_{m,z,d}}{f_{m,z,d}} = \frac{1.291}{0.350 \cdot 12.92} + 0.7 \cdot \frac{7.197}{16.15} + \frac{5.469}{16.15} = \mathbf{0.98} \quad (C.38)$$

Lateral torsional stability - Bending or combined compression and bending

Lastly, the verification for lateral torsional stability is performed. The effective length l_{ef} is equal to the smallest of L_y and L_z , which is in this case 3981.5 mm. The critical bending stress for a rectangular cross-section and the relative slenderness are calculated as follows:

$$\sigma_{m,crit} = \frac{0.78b^2}{hl_{ef}} E_{0.05} = \frac{0.78 \cdot 200^2}{175 \cdot 3981.5} \cdot 8000 = 240.0 \text{ N/mm}^2 \quad (C.39)$$

$$\lambda_{rel,m} = \sqrt{\frac{f_{m,k}}{\sigma_{m,crit}}} = \sqrt{\frac{30}{240.0}} = 0.354 \quad (C.40)$$

Because $\lambda_{rel,m} \leq 0.75$, k_{crit} should be taken equal to 1. The following unity check is performed:

$$U.C. = \left(\frac{\sigma_{m,y,d}}{k_{crit} f_{m,d}} \right)^2 + \frac{\sigma_{c,0,d}}{k_{c,z} f_{c,0,d}} = \left(\frac{7.197}{1 \cdot 16.15} \right)^2 + \frac{1.291}{0.350 \cdot 12.92} = \mathbf{0.52} \quad (C.41)$$

C.2. SLS verification

The SLS verification is performed on one beam using the most critical values of the displacement. These results are listed in Table C.4.

Table C.4: Classic Geodesic Gridshell: Resulting displacement

dx	0.00839 m
dy	0.00870 m
dz	0.01539 m

Roof deflection

According to the National Annex of Eurocode 0 (Koninklijk Nederlands Normalisatie-instituut, 2019), for the serviceability limit state of roofs, it is required that the displacement in z-direction has a maximum of $l_{rep}/250$. l_{rep} is the length of the span. The displacement in z-direction is equal to the nodal z-displacement: $u_z = dz$. The span length l_{rep} is equal to 20 m. This leads to the following upper limit of the beam deflection in z-direction, followed by a unity check.

$$u_{z,max} = \frac{l_{rep}}{250} = \frac{20 \cdot 10^3}{250} = 80.0 \text{ mm} \quad (C.42)$$

$$U.C. = \frac{u_z}{u_{z,max}} = \frac{0.01539 \cdot 10^3}{80} = \mathbf{0.19} \quad (C.43)$$

Horizontal displacement

According to the National Annex of Eurocode 0 (Koninklijk Nederlands Normalisatie-instituut, 2019), for the serviceability limit state the total horizontal displacement of buildings with only one storey has

a maximum of $h/300$ for buildings other than industry buildings. The horizontal displacement in x- and y-direction are equal to the nodal x- and y-displacements: $u_x = dx$ and $u_y = dy$. h is in this case the radius of the hemisphere, which is equal to 10 m. This leads to the following upper limit of the horizontal nodal displacement, followed by a unity check for both the x- and y-direction.

$$u_{hoz,max} = \frac{h}{300} = \frac{10 \cdot 10^3}{300} = 33.3 \text{ mm} \quad (\text{C.44})$$

$$U.C. = \frac{u_x}{u_{hoz,max}} = \frac{0.00839 \cdot 10^3}{33.3} = \mathbf{0.25} \quad (\text{C.45})$$

$$U.C. = \frac{u_y}{u_{hoz,max}} = \frac{0.00870 \cdot 10^3}{33.3} = \mathbf{0.26} \quad (\text{C.46})$$

D

Transport analysis: Geodesic Gridshell

This appendix shows the results of the transport analysis of the geodesic gridshell, as explained in subsection 4.4.1.

D.1. Preliminary Study: Classic Geodesic Gridshell

Table D.1: Classic Geodesic Gridshell: Transport sizes

Beam	n	Bounding box curves			Bounding box + b		
		l [m]	w [m]	h [m]	l [m]	w [m]	h [m]
1	30	3.486	0.000	0.153	3.686	0.200	0.353
2	40	4.035	0.000	0.206	4.235	0.200	0.406
3	50	4.124	0.000	0.215	4.324	0.200	0.415
4	10	1.980	0.000	0.049	2.180	0.200	0.249
5	10	2.166	0.000	0.059	2.366	0.200	0.259
6	10	2.028	0.000	0.053	2.228	0.200	0.253

Table D.2: Classic Geodesic Gridshell: Transport truck capacity

Beam	Vertical stacking	Horizontal placement	Element/truck
1	34	7	238
2	11	7	77
3	11	7	77
4	34	10	340
5	34	11	374
6	34	11	374

Table D.3: Classic Geodesic Gridshell: Transport arrangement

Trucks	Beam	n	Beam	n	Beam	n	Beam	n
1	1	30	4	10	5	10	6	10
2	2	40						
3	3	50						

D.2. Design Option 1

Table D.4: Geodesic Gridshell: Transport sizes, Design Option 1

Module	n	Bounding box curves			Bounding box + b		
		l [m]	w [m]	h [m]	l [m]	w [m]	h [m]
1	30	3.981	3.558	0.216	4.231	3.808	0.466
2	10	4.307	3.730	0.235	4.557	3.980	0.485
3	6	3.082	2.931	0.132	3.332	3.181	0.382

Table D.5: Geodesic Gridshell: Transport truck capacity, Design Option 1

Module	Vertical stacking	Horizontal placement	Element/truck
1	6	2	12
2	6	2	12
3	6	3	18

Table D.6: Geodesic Gridshell: Transport arrangement, Design Option 1

Trucks	Module	n	Module	n
1	1	12		
2	1	12		
3	2	10		
4	3	6	1	6

D.3. Design Option 2

Table D.7: Geodesic Gridshell: Transport sizes, Design Option 2

Module	n	Bounding box curves			Bounding box + b		
		l [m]	w [m]	h [m]	l [m]	w [m]	h [m]
1	10	4.307	3.73	0.235	4.557	3.980	0.485
2	10	7.619	3.484	0.754	7.869	3.734	1.004
3	10	3.981	3.558	0.215	4.231	3.808	0.465
4	6	3.082	2.931	0.132	3.332	3.181	0.382

Table D.8: Geodesic Gridshell: Transport truck capacity, Design Option 2

Module	Vertical stacking	Horizontal placement	Element/truck
1	6	2	12
2	4	1	4
3	6	2	12
4	6	3	18

Table D.9: Geodesic Gridshell: Transport arrangement, Design Option 2

Trucks	Module	n	Module	n
1	1	10	2	1
2	2	4	4	6
3	2	4		
4	3	10	2	1

D.4. Design Option 3

Table D.10: Geodesic Gridshell: Transport sizes, Design Option 3

Module	n	Bounding box curves			Bounding box + b		
		l [m]	w [m]	h [m]	l [m]	w [m]	h [m]
1	10	4.307	3.73	0.235	4.532	3.955	0.460
2	6	10	9.703	1.493	10.225	9.928	1.718

The bounding box of module 2 implies that the dimensions of this module are too large to fit in either a general transport truck or a special transport truck. Therefore, the elements of Design Option 3 cannot be transported.

D.5. Design Option 4

Table D.11: Geodesic Gridshell: Transport sizes, Design Option 4

Module	n	Bounding box curves			Bounding box + b		
		l [m]	w [m]	h [m]	l [m]	w [m]	h [m]
1	10	8.09	7.017	0.881	8.315	7.242	1.106
2	10	3.981	3.558	0.215	4.206	3.783	0.440
3	6	3.082	2.931	0.132	3.307	3.156	0.357

The bounding box of module 1 implies that the dimensions of this module are too large to fit in either a general transport truck or a special transport truck. Therefore, the elements of Design Option 4 cannot be transported.

D.6. Design Option 5

Table D.12: Geodesic Gridshell: Transport sizes, Design Option 5

Module	n	Bounding box curves			Bounding box + b		
		l [m]	w [m]	h [m]	l [m]	w [m]	h [m]
1	15	7.619	3.484	0.754	7.869	3.734	1.004
2	10	4.307	3.73	0.235	4.557	3.980	0.485
3	6	3.082	2.931	0.132	3.332	3.181	0.382

Table D.13: Geodesic Gridshell: Transport truck capacity, Design Option 5

Module	Vertical stacking	Horizontal placement	Element/truck
1	4	1	4
2	6	2	12
3	6	3	18

Table D.14: Geodesic Gridshell: Transport arrangement, Design Option 5

Trucks	Module	n	Module	n
1	1	4	3	6
2	1	4		
3	1	4		
4	1	4		
5	2	10		

D.7. Design Option 6

Table D.15: Geodesic Gridshell: Transport sizes, Design Option 6

Module	n	Bounding box curves			Bounding box + b		
		l [m]	w [m]	h [m]	l [m]	w [m]	h [m]
1	10	7.619	3.484	0.754	7.869	3.734	1.004
2	6	3.082	2.931	0.132	3.332	3.181	0.382
3	5	4.307	3.73	0.235	4.557	3.980	0.485
4	5	8.106	3.708	0.884	8.356	3.958	1.134
5	5	3.981	3.558	0.215	4.231	3.808	0.465

Table D.16: Geodesic Gridshell: Transport truck capacity, Design Option 6

Module	Vertical stacking	Horizontal placement	Element/truck
1	4	1	4
2	6	3	18
3	6	2	12
4	4	1	4
5	6	2	12

Table D.17: Geodesic Gridshell: Transport arrangement, Design Option 6

Trucks	Module	n	Module	n
1	1	4	2	6
2	1	4		
3	1	2	4	1
4	3	5	5	5
5	4	4		

D.8. Design Option 7

Table D.18: Geodesic Gridshell: Transport sizes, Design Option 7

Module	n	Bounding box curves			Bounding box + b		
		l [m]	w [m]	h [m]	l [m]	w [m]	h [m]
1	10	7.619	3.484	0.754	7.869	3.734	1.004
2	6	3.082	2.931	0.132	3.28332	3.181	0.382
3	5	4.307	3.73	0.235	4.55	3.980	0.485
4	5	11.574	3.664	1.991	11.824	3.914	2.241

Table D.19: Geodesic Gridshell: Transport truck capacity, Design Option 7

Module	Vertical stacking	Horizontal placement	Element/truck
1	4	1	4
2	6	3	18
3	6	2	12
4	1	1	1

Table D.20: Geodesic Gridshell: Transport arrangement, Design Option 7

Trucks	Module	n	Module	n
1	1	4	2	6
2	1	4		
3	1	2	3	5
4	4	1		
5	4	1		
6	4	1		
7	4	1		
8	4	1		

D.9. Design Option 8

Table D.21: Geodesic Gridshell: Transport sizes, Design Option 8

Module	n	Bounding box curves			Bounding box + b		
		l [m]	w [m]	h [m]	l [m]	w [m]	h [m]
1	5	4.307	3.73	0.235	4.557	3.980	0.485
2	5	10.229	3.484	1.433	10.4729	3.734	1.683
3	5	7.619	3.484	0.754	7.869	3.734	1.004
4	5	11.574	3.664	1.991	11.824	3.914	2.241
5	1	3.082	2.931	0.132	3.332	3.181	0.3382

Table D.22: Geodesic Gridshell: Transport truck capacity, Design Option 8

Module	Vertical stacking	Horizontal placement	Element/truck
1	6	2	12
2	3	1	3
3	4	1	4
4	1	1	1
5	6	3	18

Table D.23: Geodesic Gridshell: Transport arrangement, Design Option 8

Trucks	Module	n	Module	n
1	1	5	3	1
2	2	3		
3	2	2		
4	3	4	5	1
5	4	1		
6	4	1		
7	4	1		
8	4	1		
9	4	1		

E

Transport analysis: Geodesic Gridshell with Denser Grid

This appendix shows the results of the transport analysis of the geodesic gridshell with a denser grid, as explained in subsection 4.4.1.

E.1. Preliminary Study: Classic Geodesic Gridshell

Table E.1: Classic Geodesic Gridshell with Denser Grid: Transport sizes

Beam	n	Bounding box curves			Bounding box + b		
		l [m]	w [m]	h [m]	l [m]	w [m]	h [m]
1	60	2.472	0.000	0.077	2.622	0.150	0.227
2	60	2.257	0.000	0.064	2.407	0.150	0.214
3	50	2.451	0.000	0.075	2.601	0.150	0.225
4	50	2.552	0.000	0.082	2.702	0.150	0.232
5	30	1.981	0.000	0.049	2.131	0.150	0.199
6	30	2.316	0.000	0.067	2.466	0.150	0.217
7	30	2.318	0.000	0.067	2.468	0.150	0.217
8	30	2.616	0.000	0.086	2.766	0.150	0.236
9	10	2.453	0.000	0.076	2.603	0.150	0.226
10	10	1.229	0.000	0.019	1.379	0.150	0.169
11	10	1.267	0.000	0.020	1.417	0.150	0.170
12	10	1.300	0.000	0.021	1.450	0.150	0.171
13	10	1.188	0.000	0.018	1.338	0.150	0.168
14	10	1.257	0.000	0.020	1.407	0.150	0.170

Table E.2: Classic Geodesic Gridshell with Denser Grid: Transport truck capacity

Beam	Vertical stacking	Horizontal placement	Element/truck
1	40	9	360
2	40	9	360
3	40	9	360
4	40	9	360
5	40	9	360
6	40	9	360
7	40	9	360
8	40	9	360
9	40	9	360
10	40	13	520
11	40	13	520
12	40	13	520
13	40	13	520
14	40	13	520

Table E.3: Classic Geodesic Gridshell with Denser Grid: Transport arrangement

Trucks	Beam	n
1	1 to 10	360
2	11 to 14	40

E.2. Design Option 1

Table E.4: Geodesic Gridshell with Denser Grid: Transport sizes, Design Option 1

Module	n	Bounding box curves			Bounding box + b		
		l [m]	w [m]	h [m]	l [m]	w [m]	h [m]
1	30	4.604	4.229	0.347	4.754	4.379	0.497
2	10	5.103	4.450	0.330	5.253	4.600	0.480
3	10	1.793	1.705	0.045	1.943	1.855	0.195

The bounding box of module 2 implies that the dimensions of this module are too large to fit in either a general transport truck or a special transport truck. Therefore, the elements of Design Option 1 cannot be transported.

E.3. Design Option 2

Table E.5: Geodesic Gridshell with Denser Grid: Transport sizes, Design Option 2

Module	n	Bounding box curves			Bounding box + b		
		l [m]	w [m]	h [m]	l [m]	w [m]	h [m]
1	30	4.550	2.077	0.289	4.725	2.252	0.464
2	20	4.987	2.239	0.316	5.162	2.414	0.491
3	10	2.432	2.186	0.079	2.607	2.361	0.254
4	10	2.594	2.222	0.085	2.769	2.397	0.260
5	6	1.793	1.705	0.045	1.968	1.880	0.220

Table E.6: Geodesic Gridshell with Denser Grid: Transport truck capacity, Design Option 2

Module	Vertical stacking	Horizontal placement	Element/truck
1	11	2	22
2	11	2	22
3	37	1	37
4	37	1	37
5	37	1	37

Table E.7: Geodesic Gridshell with Denser Grid: Transport arrangement, Design Option 2

Trucks	Module	n	Module	n	Module	n	Module	n
1	1	22						
2	1	8	3	10	4	10	5	6
3	2	20						

F

Discarded Design Options: Geodesic Gridshell

This Appendix shows the design options of the geodesic gridshell that have been discarded during the iteration process.

F.1. Design Option 9

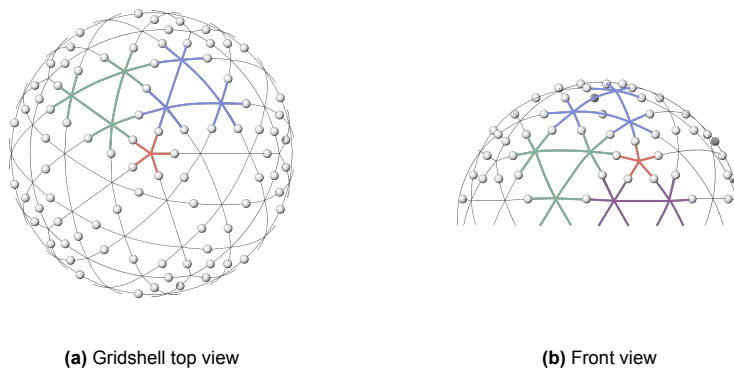


Figure F.1: Geodesic Gridshell: Design Option 9

F.2. Design Option 10

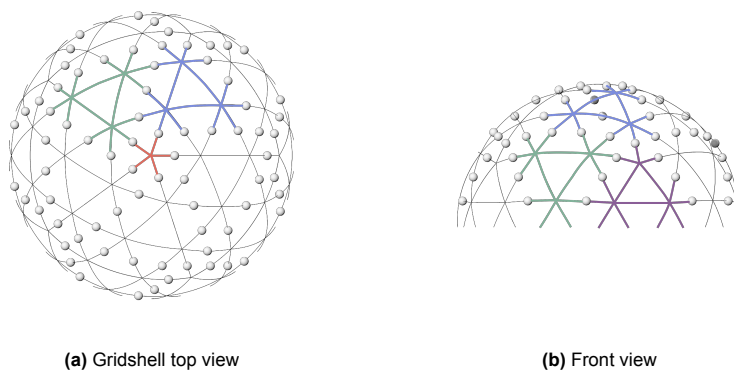
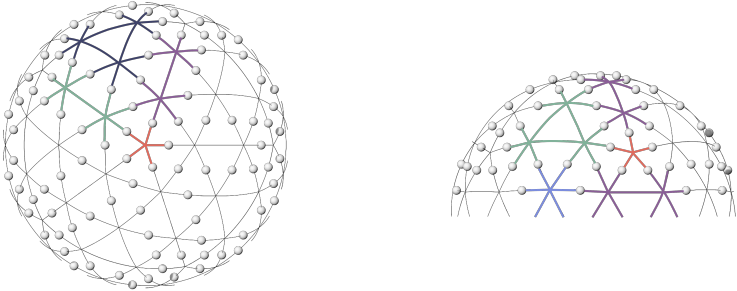


Figure F.2: Geodesic Gridshell: Design Option 10

F.3. Design Option 11

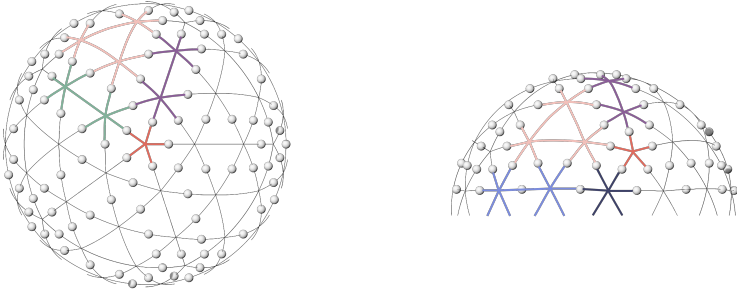


(a) Gridshell top view

(b) Front view

Figure F.3: Geodesic Gridshell: Design Option 11

F.4. Design Option 12

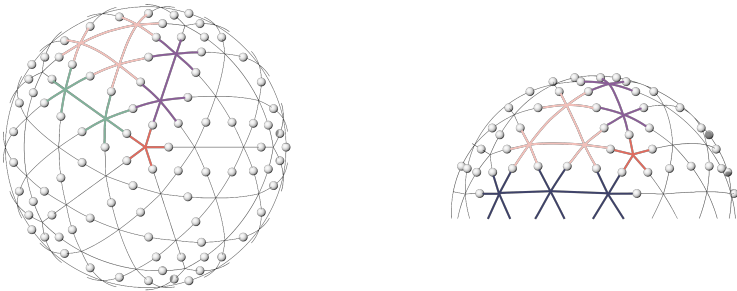


(a) Gridshell top view

(b) Front view

Figure F.4: Geodesic Gridshell: Design Option 12

F.5. Design Option 13

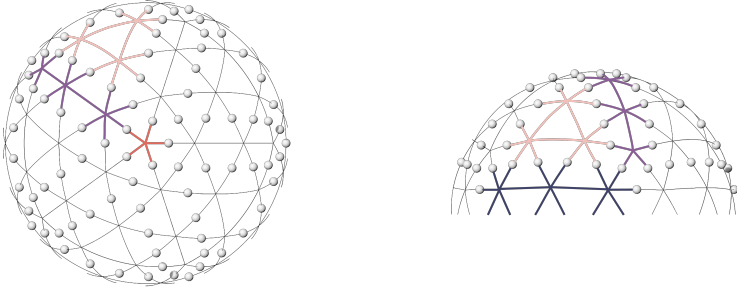


(a) Gridshell top view

(b) Front view

Figure F.5: Geodesic Gridshell: Design Option 13

F.6. Design Option 14



(a) Gridshell top view

(b) Front view

Figure F.6: Geodesic Gridshell: Design Option 14